Marine microbial community dynamics and responses to ocean acidification

Ro Allen

A thesis submitted for the degree of
Doctor of Philosophy
University of Otago

Dunedin, New Zealand

January 2019

For my parents, Keith and Denise.

Abstract

Marine microbes, including both eukaryotes and prokaryotes, are the basal components of marine food webs and play a fundamental role in global biogeochemical cycling. Marine phytoplankton are responsible for approximately 50% of Earth's primary production, while heterotrophic bacteria and archaea modulate carbon and nutrient cycling in the marine environment. The structure and function of marine microbial communities are closely coupled. Consequently, understanding the factors which govern the distribution of marine microbes through space and time has key implications for food webs and biogeochemical cycling. The development of high-throughput sequencing technologies has revolutionised marine microbial ecology by facilitating the profiling of microbial communities in high taxonomic resolution. In this thesis high-throughput sequencing of the 16S and 18S rRNA genes was used to achieve two major aims. The first aim was to investigate the ecological processes which underpin microbial community assembly in the marine environment. The second aim was to investigate the responses of marine microbial communities to near-future ocean acidification.

Two studies were performed towards the first aim of this thesis. In the first study, the microbial biogeography of the South Pacific Gyre was characterised across three depths at 22 stations along a 2,000 km longitudinal transect of the region. Microbial community composition was homogenous across horizontal spatial scales in the surface waters of the South Pacific Gyre, but varied significantly between surface waters and the deep chlorophyll maximum. A null model approach was used to unveil the ecological processes driving microbial community assembly in the region. Microbial communities in the surface waters were assembled primarily through the deterministic process of homogeneous selection, indicating that selection pressures were sufficient to overwhelm the influence of dispersal effects and ecological drift across vast horizontal spatial distances in the region. Dispersal limitation was comparatively more influential in the assembly of microbial communities between the surface waters and the deep chlorophyll maximum, indicating that stochastic processes play a significant role in microbial community assembly between these contiguous water masses.

In the second study, the bacterioplankton and protist biogeography of the Southland Front system was characterised in surface waters at 24 stations spanning four water masses. Both bacterioplankton and protist communities displayed significant structuring according to water mass, although this effect was most pronounced in bacterioplankton communities. A null model approach revealed that bacterioplankton communities were primarily assembled through homogeneous selection, while protist communities were primarily assembled through dispersal limitation and ecological drift across the Southland Front system. These findings highlight that distinct ecological processes can underpin the assembly of co-occurring bacterioplankton and protist communities, and that hydrographic features such as oceanic fronts play an important role in structuring both bacterioplankton and protist communities.

Two studies were conducted towards the second aim of this thesis. In the first study, the effect of ocean acidification and warming on bacterioplankton communities was investigated at the fringe and ultra-oligotrophic centre of the South Pacific Gyre using trace-metal clean deckboard incubation experiments. Bacterioplankton community composition and function were resistant to ocean acidification alone, and combined with warming, at the fringe of the South Pacific Gyre. Subtle but significant responses of bacterioplankton community composition to ocean acidification were observed at the ultra-oligotrophic centre of the South Pacific Gyre. These results suggest that bacterioplankton community responses to ocean acidification may be modulated by nutrient regimes. Nonetheless, the findings of this study did not diverge substantially from the narrative that bacterioplankton communities are resistant to near-future acidification.

In the second study, the effect of ocean acidification on both prokaryotic and eukaryotic biofilm communities was investigated at the Shikine-Jima CO_2 seep system in Japan. The composition of both prokaryotic and eukaryotic communities was profoundly affected by ocean acidification through early successional stages, though these responses were not associated with shifts in community diversity or evenness. Notably, the relative abundance of the nuisance algae *Prymnesium sp.* and *Biddulphia biddulphiana* were enhanced under high CO_2 conditions. These findings suggest that benthic biofilm communities may be vulnerable to near-future ocean acidification, and that changes in biofilm community composition may contribute to the reorganisation of coastal ecosystem observed at CO_2 seeps globally.

In its entirety, this thesis significantly contributes to our understanding of the spatial dynamics of marine microbial communities by revealing the highly deterministic nature of bacterioplankton community assembly in the coastal waters and central gyre of the South

Pacific Ocean. Furthermore, the findings of this thesis highlight the dominance of stochastic processes in structuring marine protist communities across short spatial scales, which may contribute to challenges in correlating abiotic environmental variables with marine protist community composition through space. The resistance of bacterioplankton communities to ocean acidification at the fringe of the South Pacific Gyre, and subtle responses to ocean acidification at the ultra-oligotrophic centre of the South Pacific Gyre broadly support the notion that bacterioplankton communities are resilient to near-future ocean acidification. In contrast, the composition of both prokaryotic and eukaryotic biofilm communities was profoundly affected by ocean acidification, leading to the proliferation of harmful algae with potentially severe consequences for coastal marine environments.

Acknowledgements

The most important acknowledgement of this thesis is to my two supervisors, Dr. Linn Hoffmann and Dr. Tina Summerfield. Thank you for all of your guidance over the past three years. Thank you for investing in my ideas and for allowing me to explore a range of research avenues as part of this project. I have been incredibly lucky to have you as supervisors. Furthermore, I am grateful to all the members of the Hoffmann lab and Summerfield lab with whom I have shared this experience. In particular, to Andy Nilsen for sharing his encyclopaedic knowledge of the lab protocols with me when I arrived.

I would like to thank Dr. Matt Larcombe for entertaining my poorly drawn whiteboard diagrams and guiding me in the exploration of wider ecological theories. I always thoroughly enjoyed our conversations.

Thank you to Dr. Kim Currie for your guidance and support during cruises of the Munida Transect aboard the *RV Polaris II*, and to Morgan Meyers, Nadjejda Espinel-Velasco, Blair Thomson, and Jess Wenley for sharing many long and entertaining days on the sampling deck. I would like to thank Dr. Ben Harvey and Dr. Sylvain Agostini for being great hosts and mentors during the Shikine-Jima research expedition, and to Prof. Jason Hall-Spencer for initiating the collaboration. Thank you to Dr. Andres Gutierrez-Rodriguez for fantastic mentorship during the *RV Tangaroa* cruise and CARIM mesocosm experiment, which tremendously benefitted my development as a scientist.

Thank you to Dr. Joshua Neale, Dr. Adam Denny, and Dr. Lorna Daniels. Our conversations about academia and life over coffee will always be among my best memories. Thanks to Adeel Akmal and Wayne Dillon for indulging me in many long lunch breaks and bad movies. Finally, thank you to Mum, Dad, Tara, and Wendy for your endless support.

This project was supported by a University of Otago Doctoral Scholarship and seed funding grants awarded by the University of Otago Ocean Acidification Research Theme and University of Otago Polar Environments Research Theme.

Table of Contents

List of Figures

List of Tables

Chapter 1: Introduction

Chapter 1: Introduction

1.1 Marine microbial community structure and function

1.1.1 Microbial diversity

Microbes dominate marine ecosystems by both abundance and biomass (Whitman *et al.*, 1998; Biard *et al.*, 2016). A single microliter of surface seawater can contain up to 10 heterotrophic protists, 10 photosynthetic protists, 100 cyanobacteria, and 1000 heterotrophic bacteria (Azam and Malfatti, 2007). The vast microbial diversity of the marine environment has long been recognised, yet estimates of taxonomic richness continue to increase with progressive surveying and technological developments (Pedrós-Alió, 2006; de Vargas *et al.*, 2015; Sunagawa *et al.*, 2015).

On a global scale, the phototrophic component of protist communities in the marine environment is dominated by diatoms, haptophytes (including coccolithophores), and chlorophytes (de Vargas *et al.*, 2015; Malviya *et al.*, 2016; Piredda *et al.*, 2018), while the heterotrophic component of protist communities is dominated by radiolarians, excavata, ciliates, and other marine alveolates (de Vargas *et al.*, 2015; Biard *et al.*, 2017). Dinoflagellates are a highly abundant and diverse component of marine protist communities, and possess a range of trophic strategies, including phototrophy, mixotrophy, heterotrophy, parasitism, and mutualism (Le Bescot *et al.*, 2016; Faure *et al.*, 2019). An estimated 150,000 distinct protist operational taxonomic units (OTUs) occupy the photic ocean (de Vargas *et al.*, 2015).

Prokaryotic communities (bacteria and archaea) in the marine environment are dominated by Alphaproteobacteria and Gammaproteobacteria (Sunagawa *et al.*, 2015). The genomically streamlined alphaproteobacterial SAR11 clade and gammaproteobacterial SAR86 clade are amongst the most abundant free-living marine bacteria and have a cosmopolitan distribution in the marine environment (Dupont *et al.*, 2012; Sunagawa *et al.*, 2015; Giovannoni, 2017). Bacteroidetes are the most abundant heterotrophic bacteria following Alphaproteobacteria and Gammaproteobacteira (Sunagawa *et al.*, 2015), and are associated with productive marine environments suited to their predominantly particle

attached lifestyle (Fernández-Gómez *et al.*, 2013). Cyanobacteria are the only phylum of prokaryotic oxygenic photoautotrophs, and represent a substantial component of prokaryotic communities in the marine environment (Sunagawa *et al.*, 2015; Farrant *et al.*, 2016). The cyanobacterial genera *Synechococcus* and *Prochlorococcus* are cosmopolitan in their distribution, excluding polar environments, but are particularly concentrated at tropical and subtropical latitudes (Flombaum *et al.*, 2013). Marine archaea represent a consistent minor component of prokaryotic communities in the photic ocean, though ammonia-oxidising Thaumarchaeota represent a larger component of prokaryotic communities in the mesopelagic zone (Sunagawa *et al.*, 2015; Santoro *et al.*, 2019). An estimated 37,470 distinct prokaryotic OTUs occupy the epipelagic and mesopelagic ocean (Sunagawa *et al.*, 2015).

1.1.2 Microbial primary production

Phytoplankton (including photosynthetic protists and prokaryotes) account for an estimated 0.2% of the total photosynthetically active carbon biomass on Earth (Field, 1998). However, as a result of their rapid turnover rates, these organisms are responsible for approximately 46-50% of global primary production (Field, 1998; Behrenfeld *et al.*, 2001), equating to the fixation of ~39-50 Pg C yr^{-1} (Field, 1998; Rousseaux and Gregg, 2013). Phytoplankton primary production is greatest in high-latitude and upwelling regions, yet subtropical and tropical regions are major contributors to total primary production due to their vast area (Rousseaux and Gregg, 2013).

Rousseaux & Gregg (2013) coupled satellite-derived ocean colour data with the NASA Ocean Biogeochemical Model to partition marine primary production between major phytoplankton groups. On a global scale, they estimated that diatoms accounted for over 50% (20.3 Pg C yr^{-1}), coccolithophores accounted for 21% (8.0 Pg C yr^{-1}), chlorophytes accounted for 17% (6.8 Pg C yr^{-1}), and cyanobacteria accounted for 10% (4.0 Pg C yr^{-1}) of phytoplankton primary production. The contribution of each phytoplankton group to total primary production varied substantially between regions. Diatoms were the dominant primary producers in high-latitude regions, accounting for ~89% of carbon fixation in the Southern Ocean. Coccolithophores were important primary producers in temperate and subtropical ocean basins, accounting for ~29% of carbon fixation in the South Pacific. Chlorophytes played a large role in equatorial regions, accounting for ~42% of carbon fixation in the equatorial Atlantic Ocean. Finally, cyanobacteria contributed significantly

to primary production in subtropical and equatorial regions, where they accounted for up to 19% of carbon fixation (Rousseaux and Gregg, 2013).

Remote sensing techniques provide key insights into phytoplankton carbon fixation on a global scale. However, estimates of phytoplankton carbon fixation vary according to the specific methods employed, highlighting that substantial uncertainty surrounds these estimates (Blondeau-Patissier *et al.*, 2014; Lee *et al.*, 2015). For example, Flombaum *et al.* (2013) estimate that cyanobacteria account for approximately 25% of marine primary production based on direct measurements of carbon fixation rates, in comparison to 10% as estimated by Rousseaux & Gregg (2013) using remote sensing techniques. Nonetheless, these data demonstrate the enormous contribution of marine phytoplankton to global carbon fixation and outline the relative contributions of major phytoplankton groups.

1.1.3 Marine carbon cycling

Phytoplankton primary production is classically transferred to higher trophic level through direct zooplankton grazing, and the subsequent consumption of zooplankton by fish and other large marine organisms (Pomeroy, 1974). However, a large fraction of phytoplankton-derived organic carbon is ultimately converted to dissolved organic matter (DOM) through exudation, cell lysis, and the breakdown of dead cells by extracellular enzymes (Azam and Malfatti, 2007). This DOM, only accessible to heterotrophic bacteria and archaea (Azam and Malfatti, 2007), is either remineralised or transferred to higher trophic levels through the marine microbial loop (Azam *et al.* 1983; Fig. 1.1).

The marine microbial loop commences with the uptake of phytoplankton-derived DOM by heterotrophic bacteria and archaea, which act as a food source for protist grazers. Protist grazers are consumed by zooplankton, facilitating the transfer of organic carbon to higher trophic levels. Between 60 and 99% of DOM assimilated by heterotrophic bacteria and archaea is respired (Del Giorgio and Cole, 1998; Reinthaler and Herndl, 2005; Reinthaler *et al.*, 2005; Alonso-Sáez *et al.*, 2007), though these values can be substantially lower under certain circumstances (Baltar *et al.,* 2015b). Thus, phytoplankton-derived organic carbon has multiple routes of transfer to higher trophic levels, but respiratory carbon loss is greatest through the marine microbial loop.

A minor proportion of phytoplankton-derived organic carbon escapes the marine microbial loop (Azam and Malfatti, 2007), primarily through the formation and sinking of aggregates (Turley and Stutt, 2000). Between 15 and 20% of phytoplankton-derived organic carbon is

exported to the oceans' interior, where it remains for hundreds to thousands of years based on deep water residence time (Siegel *et al.*, 2016). Approximately 0.3% of phytoplankton-derived organic carbon is exported to deep sea sediments, where it is sequestered on geological timescales (Dunne *et al.*, 2007). The efficiency of the marine microbial loop plays a key role in modulating oceanic carbon flux, and consequently the global carbon cycle (Azam and Malfatti, 2007).

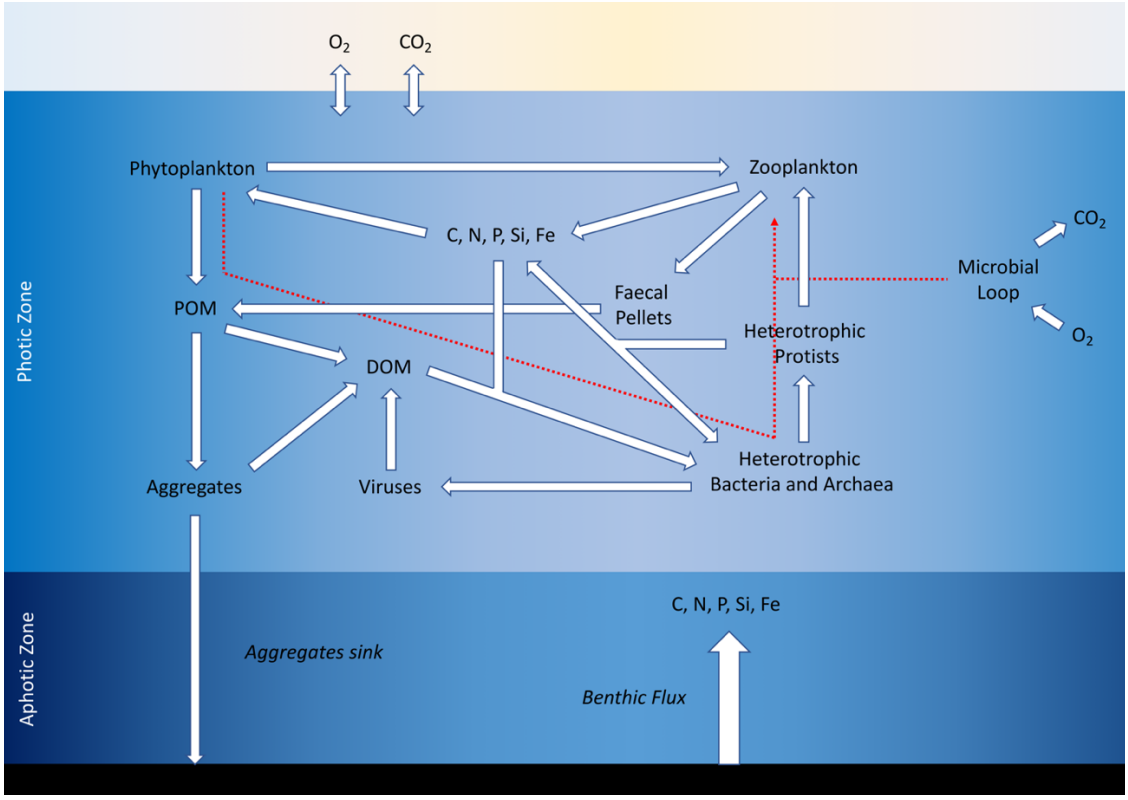

Figure 1.1 The marine microbial food web. Most carbon fixed through phytoplankton primary production becomes DOM, which is utilised by marine bacteria and archaea. The majority of assimilated DOM is remineralised through respiration by bacteria and archaea, but a small proportion is returned to the marine food web through protist grazing on heterotrophic bacteria and archaea, and subsequent zooplankton grazing on heterotrophic protists. The red dotted line indicates the route of phytoplankton-derived organic carbon through the marine microbial loop. Adapted from Azam & Malfatti (2007).

1.1.4 The relationship between marine microbial community structure and function

Marine protists are highly diverse, illustrated by the 150,000 protist operational taxonomic units identified in a global survey of the sunlit ocean (de Vargas *et al.*, 2015). Vast morphological, physiological, and behavioural diversity exists in marine protists, often below the species level (Worden *et al.*, 2015; Keeling and del Campo, 2017). Consequently, the taxonomic structure of marine protist communities influences community function, including primary production and carbon cycling (Dutkiewicz *et al.*, 2015; Worden *et al.*, 2015). For example, carbon export can be expedited by the presence of diatoms (Leblanc *et al.*, 2018; Tréguer *et al.*, 2018), radiolarians (Gutierrez-Rodriguez *et al.*, 2018), and coccolithophores (Iversen and Ploug, 2010), which form heavy biogenic structures that increase the sinking velocity of aggregates. The specific composition of diatom communities influences their contribution to carbon export, due to the morphological and physiological distinctions between species (Kemp and Villareal, 2018; Tréguer *et al.*, 2018). Furthermore, nutrient acquisition strategies differ between phytoplankton taxa (Beltrán-Heredia *et al.*, 2017; Berthelot *et al.*, 2018) which can influence overall ecosystem productivity. Ecosystem level investigations demonstrate that phytoplankton productivity is linked with community structure in marine environments (Blais *et al.*, 2017; Mayot *et al.*, 2017; Talaber *et al.*, 2018). Advances in single-cell genomic techniques have revealed high levels of functional diversity amongst closely related heterotrophic protists (Seeleuthner *et al.*, 2018; Strassert *et al.*, 2018), suggesting that the specific composition of heterotrophic protist communities may influence the flow of carbon through marine food webs. Indeed, protist community structure has been demonstrated as an excellent proxy of community function in freshwater systems (Grossmann *et al.*, 2016).

Marine prokaryotes are also highly diverse (Sunagawa *et al.*, 2015). The structure of prokaryotic communities in the marine environment is often predictable based on environmental conditions, which is likely to result from narrow niches and low levels of functional redundancy within these communities (Fuhrman, 2009). Heterotrophic marine bacteria possess a diverse range of mechanisms for the acquisition and utilisation of organic carbon (Reintjes *et al.*, 2018; Zhang *et al.*, 2018) and other resources (Bryson *et al.*, 2017). Galand *et al.* (2018) show that the taxonomic diversity of prokaryotic communities in the marine environment is well correlated with functional diversity, based on metagenomic profiling of microbial communities in the Mediterranean Sea. These data indicate that minimal functional redundancy exists in marine prokaryotic communities. These findings contrast with evidence of functional redundancy in marine prokaryotic communities from

global surveys (Louca *et al.*, 2016). However, Louca *et al.* (2016) screened prokaryotic communities for a predefined set of functional traits rather than surveying the broader functional diversity of these communities, and consequently their data are limited to indicating the ubiquitous nature of key metabolic functions in marine prokaryotic communities. Nonetheless, evidence of functional redundancy in prokaryotic communities has been established across a range of environments (Martiny, 2015; Louca, Polz, *et al.*, 2018) though the extent of function redundancy in marine prokaryotic communities remains a key area of investigation. Guidi *et al.* (2016) show that the composition of prokaryotic communities has a strong influence on carbon export in the oligotrophic ocean, and Landa *et al.* (2015) show that prokaryotic community composition influences carbon cycling during phytoplankton blooms, highlighting the important functional implications of prokaryotic community composition in the marine environment.

The structure and function of prokaryotic and protist communities in the marine environment are fundamentally linked and have implications for marine food webs and global biogeochemical cycling (Nemergut *et al.*, 2014). Consequently, understanding the factors which govern the structure of these communities through space and time is of paramount importance, as the structure of microbial communities inevitably impacts key functions such as primary production and carbon cycling.

1.2 Marine microbial community assembly

Community ecology aims to unravel the factors which underpin the abundance and distribution of species through space and time. Classical theories have characterised community assembly as either niche-based (exclusively deterministic) or neutral (exclusively stochastic) (Hubbell 2001). Niche-based community assembly theories posit that the community composition and diversity is deterministically controlled by interactions between species and their environment, and interactions between species themselves (Vellend, 2010). In contrast, neutral community assembly theories posit that the community composition and diversity is stochastically controlled through demographic processes, independent of species traits (Hubbell, 2001). More recently, it has been accepted that communities assemble through a combination of deterministic and stochastic processes, and investigating the relative importance of these processes has become a central focus in community ecology (Chase and Myers, 2011; Vellend *et al.*, 2014).

Vellend (2010) highlighted that community ecology was becoming an increasingly convoluted field of research and provided a conceptual framework to facilitate hypothesis driven lines of investigation incorporating both stochastic and deterministic processes. Borrowing from the four major processes in population genetics (selection, gene flow, drift, mutation), Vellend proposed that communities are assembled through a combination of selection, dispersal, drift, and speciation (Table 1.1). While this framework is very general, it has the potential to serve the same function as analogous theory in population genetics and has been widely adopted by community ecologists (830 citations as of 17.01.2019).

Table 1.1 Microbial community assembly processes according to Vellend's conceptual framework (Vellend, 2010), adapted from Zhou & Ning (2017).

Process	Definition
Selection	Deterministic process which shapes community structure due to fitness differences between organisms, including both abiotic conditions and biotic interactions
Dispersal	Movement and colonization of individual organisms from one location to another location, through active or passive mechanisms
Drift	Random changes in the relative abundance of different organisms within a community due to stochastic demographic processes
Speciation (Diversification)	The emergence of new genetic variation through evolutionary processes

The value of Vellend's conceptual framework, with minor adaptations, was quickly recognised by microbial ecologists (Hanson *et al.*, 2012; Stegen *et al.*, 2013; Zhou and Ning, 2017). The most prominent adaptation was the replacement of speciation with diversification, to avoid complexities associated with microbial species definitions and to acknowledge the ecological relevance of genetic diversity below species resolution (Zhou and Ning, 2017; Caron and Hu, 2018). Methods to partition the relative influence of selection, dispersal, drift, and diversification on microbial community assembly have recently emerged (Stegen *et al.*, 2013, 2015; Wang *et al.*, 2013; Dini-Andreote *et al.*, 2015). These methods, combined with the vast availability of high-throughput amplicon sequencing derived profiles of microbial community composition, have significantly advanced our understanding of microbial community assembly across a range of systems

(Nemergut *et al.*, 2013; Zhou and Ning, 2017). For example, Valverde *et al.* (2014) and Tripathi *et al.* (2018) showed that deterministic processes become increasingly important in microbial communities under abiotic stress. Liao *et al.* (2016) demonstrated that deterministic processes have a greater influence on habitat specialists, while stochastic processes have a greater influence on habitat generalists. Graham *et al.* (2017) found that deterministic processes are able to overwhelm the influence of dispersal in highly connected aquatic environments, and Graham and Stegen (2017) illustrated that communities assembled primarily through deterministic processes are more biogeochemically efficient.

Despite the rapid increase in published studies investigating microbial community assembly processes (Zhou and Ning, 2017), few studies have been conducted in the marine environment. Investigations of marine sediments consistently show that deterministic processes dominate prokaryotic community assembly (Meyerhof *et al.*, 2016; Petro *et al.*, 2017; Starnawski *et al.*, 2017). However, investigations of pelagic environments show that prokaryotic community assembly can vary from highly deterministic (Logares *et al.*, 2018), to a more even balance between stochastic and deterministic processes (Wu *et al.*, 2017a; Mo *et al.*, 2018). Comparisons of community assembly processes between prokaryotes and protists also display contrasting results in the marine environment. Logares *et al.* (2018) showed that while prokaryotic community assembly is highly deterministic, stochastic processes dominate protist community assembly in marine and freshwater Antarctic lakes. Conversely, Wu *et al.* (2017a) showed that the ratio of deterministic to stochastic processes is greater in protists than in prokaryotes in the East China Sea. Consequently, substantial further investigation is necessary to advance our understanding of the ecological processes which underpin microbial community assembly in the marine environment. This knowledge will significantly contribute to our ability to predict how microbial communities are likely to respond to environmental change (Stegen *et al.*, 2018).

1.3 Marine microbial community profiling using high-throughput sequencing

Victor Smetacek commented that while terrestrial ecologists studying macroorganisms can immerse themselves in habitats and directly observe the organisms which they study, marine microbial ecologists cannot, adding a degree of abstraction to our understanding of

these systems (Smetacek, 2018). Traditionally, investigations of prokaryotic communities have relied on the generation of bacterial 16S rRNA gene clone libraries followed by Sanger sequencing, which only succeeds in capturing a small proportion of the diversity present in these communities (Lovejoy *et al.*, 2006). Investigations of protist community composition traditionally rely on taxonomy-based light microscopy analyses, but these techniques require expert taxonomists and are prone to observer effects (Moreira and López-García, 2002; Silva, 2008). Furthermore, light microscopy is not always sufficient to distinguish between ecologically relevant protists, as cryptical species are pervasive (Smayda, 2011). More recently, molecular tools have been employed for profiling both prokaryotic and protist communities (Hugerth and Andersson, 2017). Denaturing gradient gel electrophoresis (Muyzer *et al.*, 1993), terminal restriction fragment length polymorphism (Liu *et al.*, 1997), and automated ribosomal intergenic space analysis (Fisher and Triplett, 1999) allow the comparison of general patterns in microbial community composition but offer limited insights into the precise taxonomic composition of these communities. Microarrays offer greater taxonomic insights in the context of microbial community profiling but are limited to screening for a predefined cohort of taxa (Ehrenreich, 2006). The arrival of high-throughput sequencing technologies revolutionised our ability to profile microbial communities in high depth and taxonomic resolution (Sogin *et al.*, 2006; Caporaso *et al.*, 2011).

High-throughput amplicon sequencing profiles of microbial communities are based on polymerase chain reaction (PCR) amplified marker gene fragments originating from genomic DNA extracted from environmental samples. The small subunit (SSU) ribosomal RNA (rRNA) gene (prokaryotes: 16S rRNA gene, eukaryotes: 18S rRNA gene) has been adopted as a universal marker gene for both prokaryotic and protist communities due to its presence across all taxa, lack of horizontal gene transfer, and the presence of hypervariable regions flanked by highly conserved regions providing reliable binding sites for universal PCR primers (Hugerth and Andersson, 2017). Assigning taxonomic identities to resulting SSU rRNA gene sequences relies on cross-referencing with sequence databases which are available for both prokaryotes (DeSantis *et al.*, 2006; Quast *et al.*, 2013; Cole *et al.*, 2014) and protists (Guillou *et al.*, 2013; Quast *et al.*, 2013; Cole *et al.*, 2014; Decelle *et al.*, 2015). The selection of primers, library preparation protocols, and sequencing analysis protocols in high-throughput sequencing studies can impact the profile of microbial communities obtained, and consequently universal guidelines have been developed to allow comparisons to be drawn between studies on a global scale (Caporaso *et al.*, 2012; Thompson *et al.*, 2017; Knight *et al.*, 2018).

Marine microbial ecologists were among the first to implement high-throughput amplicon sequencing for profiling microbial communities (Sogin *et al.*, 2006). These techniques have provided novel insights into the global diversity and distribution of marine prokaryotes (Sunagawa *et al.*, 2015; Santoro *et al.*, 2019) and protists (de Vargas *et al.*, 2015; Malviya *et al.*, 2016; Biard *et al.*, 2017; Faure *et al.*, 2019). Moreover, these techniques have revealed the temporal dynamics of marine microbial communities across multiple scales, from daily succession during phytoplankton bloom events (Needham and Fuhrman, 2016) to interannual cycles in community composition (Ward *et al.*, 2017). High-throughput amplicon sequencing studies have also begun to unveil the complex nature of microbial interactions in the marine environment (Lima-Mendez *et al.*, 2015) and the influence of microbial community structure on marine carbon cycling (Guidi *et al.*, 2016).

1.4 Ocean acidification

Anthropogenic CO_2 emissions have driven atmospheric CO_2 concentrations from preindustrial levels of 280 ppm, to present day levels exceeding 400 ppm (Stocker, 2014). Present day atmospheric CO_2 concentrations are at their highest level in the past 800,000 years (Lüthi *et al.*, 2008). Under the intergovernmental panel on climate change (IPCC) representative concentration pathway (RCP) 8.5 'business as usual' emissions scenario, atmospheric CO_2 concentrations are projected to reach 1,000 ppm by 2100 (Stocker, 2014). The accumulation of anthropogenic CO_2 in the atmosphere has contributed to the definition of the Anthropocene, a new geological epoch characterised by anthropogenic remodelling of the biosphere (Lewis and Maslin, 2015).

Approximately 30% of anthropogenic CO_2 emissions are taken up by the ocean (Sabine *et al.*, 2004), reducing surface ocean pH and shifting the marine carbonate system through a process termed 'ocean acidification' (Fig. 1.2; Caldeira & Wickett 2003, Doney *et al.* 2009). Mean surface ocean pH has decreased by 0.1 units from 8.2 to 8.1 since the pre-industrial era and is projected to decrease by a further 0.3 units by the end of this century (Hoegh-Guldberg *et al.*, 2014), corresponding to a 150% increase in H^+ ion concentration (Doney *et al.*, 2009). Atmospheric CO_2 reacts with water altering the marine carbonate system according to the following equation:

$$CO_{2\,(atmos)} \leftrightharpoons CO_{2\,(aq)} + H_2O \leftrightharpoons HCO_3^- + H^+ \leftrightharpoons CO_3^{2-} + 2H^+$$

The dissolution of CO_2 into the surface ocean leads to an increase in the concentration of CO_2 and bicarbonate ions (HCO_3^-), and a decrease in the concentration of carbonate ions (CO_3^{2-}) in seawater (Fig. 1.2). The projected mean surface ocean pH decrease of 0.3 units by the end of the century corresponds with a 50% decrease of CO_3^{2-} ion concentrations (Orr *et al.*, 2005). This decrease in CO_3^{2-} ion concentration will reduce the availability of calcium carbonate in the marine environment, which has important implications for organisms that form calcareous structures (Hoegh-Guldberg *et al.*, 2014).

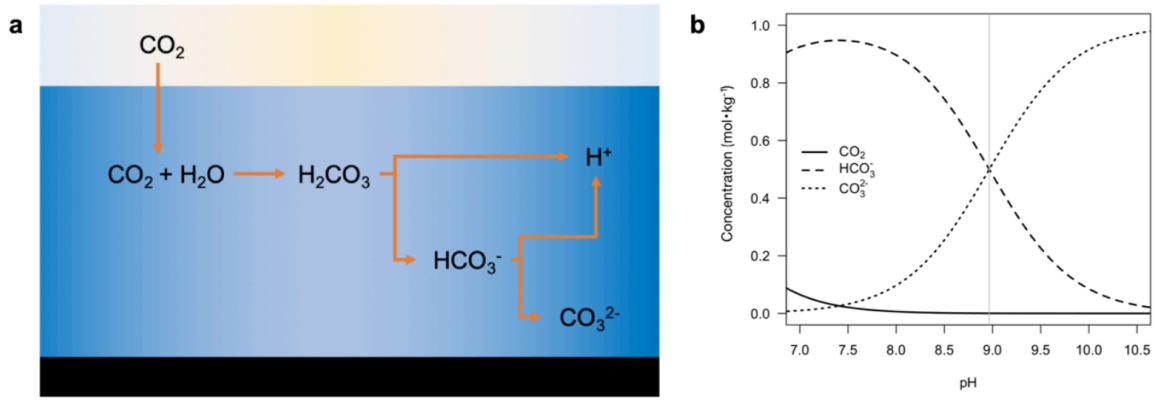

Figure 1.2 (a) The dissolution of atmospheric carbon dioxide into the surface ocean leads to the formation of carbonic acid, which dissociates to form bicarbonate ions, carbonate ions, and hydrogen ions. (b) Bjerrum plot showing the concentration of different inorganic carbon species as a function of pH (adapted from Mccoy, 2013).

Ocean acidification is not occurring in isolation, but rather within a wider framework of oceanic climate change. The increased concentration of atmospheric CO_2 and other greenhouse gases has driven a temperature increase of 0.11ºC per decade in the surface ocean (Hoegh-Guldberg *et al.*, 2014). This warming leads to increased stratification of pelagic environments, reducing vertical nutrient supply to the surface ocean and reducing the concentration of dissolved oxygen in the ocean interior (Hoegh-Guldberg *et al.*, 2014). Thus, it is important to consider how these complex environmental changes will interact (Boyd *et al.*, 2016).

1.5 Marine microbial responses to ocean acidification

The responses of marine microbes to ocean acidification will have profound implications for marine carbon cycling, as the magnitude of carbon fixation and export is linked to the structure of microbial communities in the marine environment. Significant research effort has been dedicated to understanding how marine microbial communities, including both photoautotrophic and heterotrophic components, will respond to ocean acidification.

Joint *et al.* (2011) hypothesised that marine prokaryotic communities may be resilient to ocean acidification as these organisms already experience large fluctuations in pH across a range of spatiotemporal scales, and consequently possess sufficient physiological plasticity to tolerate projected decreases in mean surface ocean pH. Liu *et al.* (2010) conducted a meta-analysis of prokaryotic community responses to ocean acidification, reporting significant effects of ocean acidification on prokaryotic community diversity and structure in some studies and no effects in others. Since these seminal papers, studies investigating the impact of ocean acidification on prokaryotic community diversity and composition employing CO_2 manipulation experiments have reported minimal effects in the Arctic Ocean (Newbold *et al.*, 2012; Roy *et al.*, 2013; Zhang *et al.*, 2013; Oliver *et al.*, 2014; Hartmann *et al.*, 2016; Wang *et al.*, 2016), Southern Ocean (Maas *et al.*, 2013; Donahue *et al.*, 2019), Pacific Ocean (Burrell *et al.*, 2017), Mediterranean Sea (Baltar *et al.* 2015a), and Baltic Sea (Lindh *et al.*, 2013; Bergen *et al.*, 2016). While these studies report little to no effect of ocean acidification on prokaryotic community diversity and composition, there is a growing body of evidence demonstrating that ocean acidification can interact with temperature, nutrient availability, dissolved organic carbon supply, and other environmental variables to restructure prokaryotic communities in the marine environment (Lindh *et al.*, 2013; Bergen *et al.*, 2016; Sala *et al.*, 2016).

The effect of ocean acidification on phytoplankton is challenging to predict, as different species employ distinct carbon concentrating mechanisms (CCMs; Reinfelder 2011, Mackey *et al.* 2015). These molecular mechanisms concentrate CO_2 around RuBisCO for carbon fixation, typically by employing carbonic anhydrases to convert HCO_3^- to CO_2 (Hopkinson *et al.*, 2011). The increased availability of dissolved CO_2 projected by the end of the century may reduce the necessity of CCMs, leading to downregulation of their activity (e.g. reduced expression of carbonic anhydrases; Li *et al.* 2015). Downregulation of CCMs reduces the energetic cost of carbon fixation, leading to the reorganisation of species energy budgets (Mackey *et al.*, 2015). The distinct inorganic carbon utilization

strategies and CCMs of different phytoplankton species may lead to shifts in competitive interactions under elevated CO_2 conditions, with the potential to restructure phytoplankton communities (Mackey *et al.*, 2015). Indeed, meta-analyses reveal a diverse range of physiological responses to ocean acidification across major phytoplankton groups (Dutkiewicz *et al.*, 2015). In addition to these photophysiological effects, calcifying phytoplankton such as coccolithophores are expected to be physiologically vulnerable to ocean acidification as the reduced availability of calcium carbonate can alter the energetic cost of producing and maintaining their calcareous structures (Beaufort *et al.*, 2011; Bach *et al.*, 2013). However, physiological responses of coccolithophores to ocean acidification vary between species (Meyer and Riebesell, 2014) and between different strains of conspecifics (Langer *et al.*, 2009; Müller *et al.*, 2015).

Incubation experiments indicate that high CO_2 conditions can lead to an increased abundance of large centric diatoms in the Southern Ocean (Feng *et al.*, 2010; Hoppe *et al.*, 2013; Trimborn *et al.*, 2017) and Atlantic Ocean (Eggers *et al.*, 2014). These findings align with physiological studies which indicate that large diatoms are able to capitalise on increased CO_2 concentrations more effectively than smaller diatoms (Wu *et al.*, 2014). In contrast, incubation experiments in the Arctic Ocean indicate subtle shifts in community structure from large diatoms and coccolithophores, to smaller diatoms and picoeukaryotes (Newbold *et al.*, 2012; Schulz *et al.*, 2013, 2017; Hoppe *et al.*, 2018). Comparable enhancement of picoeukaryote abundance under elevated CO_2 conditions has been demonstrated in the Baltic Sea (Bach *et al.*, 2016; Crawfurd *et al.*, 2017). Regional differences in phytoplankton community responses to ocean acidification may originate from differences in the composition of communities at the beginning of each experiment (Eggers *et al.*, 2014) or the interactions between ocean acidification and other environmental variables including temperature and iron availability (Hoppe *et al.*, 2013, 2018; Trimborn *et al.*, 2017).

Investigations of the effect of ocean acidification on heterotrophic protists are less common than studies investigating phytoplankton. Early studies report no significant effect of CO_2 on heterotrophic protist community composition (Suffrian *et al.*, 2008; Aberle *et al.*, 2013). However, Hancock *et al.* (2018) demonstrated species-specific responses of choanoflagellates to elevated CO_2 conditions in a Southern Ocean mesocosm experiment. Further investigation of the responses of heterotrophic protists to ocean acidification are warranted due to the important role these organisms play in the marine microbial loop (Worden *et al.*, 2015).

1.6 Thesis Outline

This thesis has two major aims. The first aim is to investigate the ecological processes which underpin microbial community assembly in the marine environment, as this knowledge predicates our ability to understand microbial community responses to environmental change (Stegen *et al.*, 2018). The second aim is to investigate the responses of marine microbial communities to ocean acidification employing high-throughput amplicon sequencing techniques. To this end, the proceeding chapters are organised as outlined below.

Chapter 2 describes the microbial biogeography of the oligotrophic South Pacific Gyre, which is under-sampled in global surveys of marine microbial communities (Sunagawa *et al.*, 2015). The ecological processes which underpin microbial community assembly in the region are unveiled using an ecological null model approach (Stegen *et al.*, 2013), and the effects of key environmental parameters on the balance between deterministic and stochastic processes are quantified. Moreover, I discuss potential mechanisms leading to the enhanced taxonomic richness of the deep chlorophyll maximum when compared with surface waters.

Chapter 3 describes the distribution of both prokaryotes and protists across the dynamic Southland Front System, a compression of the Subtropical Frontal Zone located east of New Zealand's South Island. Employing high-spatial resolution sampling, the ecological processes which structure prokaryotic and protist communities across the region are investigated and differences between prokaryotic and protist community assembly are discussed.

Chapter 4 investigates the response of prokaryotic communities to ocean acidification and warming at the fringe and at the centre of the South Pacific Gyre. These oligotrophic regions have been understudied in the context of ocean acidification despite their key role in marine carbon cycling. Profiles of prokaryotic community composition are complemented with flow-cytometry and bacterial production data to predict how prokaryotic community structure and function may respond to future conditions in the region.

Chapter 5 determines the responses of marine biofilm communities to ocean acidification at a volcanic CO_2 seep system located in Shikine-Jima, Japan. Trends in biofilm diversity, evenness, and composition are presented, and discussed in the context of previous studies at CO_2 seeps. The ecological mechanisms which underpin differences in biofilm

community composition between control and high CO_2 sites and the potential enhancement of toxin-producing protists under high CO_2 conditions are discussed.

Chapter 6 summarises the findings of the preceding four chapters and discusses these findings in relation to one another and in the wider context of both marine microbial community assembly and marine microbial community responses of ocean acidification, before areas for further investigation are outlined.

1.7 Author Contributions

Table 1.2 Summary of author contributions to each chapter (RA = Ro Allen, LJH = Linn J. Hoffmann, TCS = Tina C. Summerfield, MJL = Matthew J. Larcombe, CL = Cliff Law, KC = Kim Currie, ZL = Ziva Louisson).

Chapter	Writing	Editing	Sample Collection	Sequencing	Sequence Processing	Statistical Design	Statistical Analyses
Chapter 1	RA	RA, LJH, TCS	-	-	-	-	-
Chapter 2	RA	RA, LJH, TCS, MJL	TCS	RA, ZL	RA	RA	RA
Chapter 3	RA	RA, LJH, TCS	RA, KC	RA	RA	RA	RA
Chapter 4	RA	RA, LJH, TCS, CL	LJH, TCS	TCS	RA	RA	RA
Chapter 5	RA	RA, LJH, TCS	RA	RA	RA	RA	RA
Chapter 6	RA	RA, LJH, TCS	-	-	-	-	-

Additional co-authors of Chapter 5 are included for provision of logistical support and site access at the Shikine-Jima CO_2 seep system.

Chapter 2: Selection dominates microbial community assembly in the oligotrophic ocean

Co-authors of the manuscript: Linn Hoffmann, Matt Larcombe, Ziva Louisson, Tina Summerfield

Chapter 2: Selection dominates microbial community assembly in the oligotrophic ocean

2.1 Abstract

Oligotrophic subtropical gyres play a key role in global biogeochemical cycles. In these regions microbial communities govern primary production and carbon and nutrient cycling, yet little is known about the ecological processes which underpin assembly of these microbial communities. I investigated microbial biogeography and community assembly processes at three depths over a ~2,000 km longitudinal transect of the South Pacific Gyre. Microbial communities in the surface waters (15 m and 50 m) were homogeneous across the transect, whilst communities at the deep chlorophyll maximum were distinct from the surface waters and displayed greater compositional variability. Homogeneous selection was the dominant community assembly process in both the surface waters (100%) and at the deep chlorophyll maximum (85.96%), though variable selection (6.43%) and stochastic processes (7.60%) had a minor influence at the deep chlorophyll maximum. Homogeneous selection (55.89-57.11%), dispersal limitation (33.42-33.58%), and variable selection (9.47-9.77%) influenced community assembly between the surface waters and the deep chlorophyll maximum. Temperature was the most important environmental modulator of the balance between stochastic and deterministic assembly processes. These findings demonstrate that microbial community assembly in the oligotrophic ocean is highly deterministic, suggesting that these communities may respond predictably to environmental change.

2.2 Introduction

Oligotrophic subtropical gyres cover approximately 40% of Earth's surface by area, and are expanding globally (Polovina *et al.*, 2008). These regions represent the largest continuous biomes on Earth (Raimbault *et al.*, 2008), and have been described as ocean deserts due to their characteristically low nutrient concentrations and productivity (Irwin and Oliver, 2009). Nonetheless, these regions account for ~20% of total marine primary production due to their vast size (Hoegh-Guldberg and Poloczanska, 2017). Oligotrophic subtropical gyres are microbially dominated systems; cyanobacteria are the major primary producers (Grob *et al.*, 2007; Flombaum *et al.*, 2013), whilst heterotrophic bacteria and archaea modulate carbon and nutrient cycling (Azam and Malfatti, 2007). Carbon export in oligotrophic subtropical gyres is closely related to microbial community composition (Guidi *et al.*, 2016), supporting recent evidence that microbial community function is strongly correlated with taxonomic composition in the marine environment (Galand *et al.*, 2018). Consequently, understanding the ecological processes which underpin microbial community assembly through space and time in the oligotrophic ocean is of great importance.

Ecological theories describing community assembly have classically been categorised as stochastic (neutral) (Hubbell, 2001) or deterministic (niche-based) (Chase and Leibold, 2003). This dichotomy has been studied extensively in the macroecological context, and has polarised ecologists (Vellend *et al.*, 2014). However, stochastic and deterministic processes are not mutually exclusive, and the relative balance between these processes has received increased attention (Vellend *et al.*, 2014; Zhou and Ning, 2017). Vellend proposed the partitioning of community assembly into four major processes (selection, dispersal, drift, and speciation), considering both stochastic and deterministic elements (Vellend, 2010). Under this framework, selection refers to deterministic changes in local community composition due to differences in fitness between species. Dispersal refers to the movement of individuals between local communities, and is not an entirely stochastic processes, as species traits can affect dispersal ability (Hanson *et al.*, 2012). However, in this study dispersal is considered to be a primarily stochastic process, as microbial dispersal is predominantly passive (Nemergut *et al.*, 2013). Drift refers to stochastic changes in the abundance of species within a local community. Speciation refers to the emergence of new species within a local community, through evolutionary processes. Importantly, speciation is expected to have minimal influence on the structuring of local communities between

which dispersal is possible (i.e. metacommunities) (Leibold *et al.*, 2004; Stegen *et al.*, 2013). Vellend's partitioning of community assembly processes (Vellend, 2010) lends itself well to microbial ecology and provides a suitable framework for investigating the balance between stochastic and deterministic processes (Nemergut *et al.*, 2013; Stegen *et al.*, 2013).

Advances in high-throughput sequencing technologies have facilitated global-scale surveying of microbial diversity (Sunagawa *et al.*, 2015; Thompson *et al.*, 2017). Concurrently, emergent macroecological patterns in microbial communities (Shade *et al.*, 2018), and the ecological processes which underpin microbial community assembly (Hanson *et al.*, 2012; Nemergut *et al.*, 2013; Zhou and Ning, 2017), have become focal topics in microbial ecology. The balance between stochastic and deterministic processes in microbial community assembly has been investigated across a range of free-living and host-associated systems, with contrasting results (Stegen *et al.*, 2013; Dini-Andreote *et al.*, 2015; Martínez *et al.*, 2015; Graham *et al.*, 2017; Griffin and Wells, 2017; Logares *et al.*, 2018; Tripathi *et al.*, 2018). Subsequently, debate still remains about the relative importance of these processes, and defining general rules of microbial community assembly remains a major challenge. In the marine environment, analysis of metacommunity structure through time in the Sargasso Sea shows deviation from purely stochastic community assembly in the surface waters but not at 200 m (Vergin *et al.*, 2017). In Chinese coastal bays and the East China Sea, respectively, stochastic processes outweigh deterministic processes in microbial community assembly (Wu *et al.*, 2017a; Mo *et al.*, 2018). These studies highlight that microbial community assembly processes are not conserved between different marine ecosystems.

The South Pacific Gyre is the largest oligotrophic subtropical gyre (Polovina *et al.*, 2008), yet little is known about the microbial biogeography of the region, as it has been under-sampled relative to other marine biomes (Sunagawa *et al.*, 2015; Walsh *et al.*, 2015). Moreover, the ecological processes which underpin microbial community assembly in the South Pacific Gyre have not been investigated, limiting our ability to predict how these communities may respond to oceanic climate change (Stegen *et al.*, 2018). Environmental conditions, and therefore selective regimes, in the South Pacific Gyre are homogeneous across large horizontal spatial scales and heterogeneous across short vertical spatial scales (Ellwood *et al.*, 2018), offering an ideal system in which to investigate microbial community assembly processes.

The microbial biogeography of the oligotrophic South Pacific Gyre was surveyed across horizontal (longitude) and vertical (depth) spatial scales during the New Zealand leg of the

GP13 GEOTRACES transect (Ellwood *et al.*, 2018; Schlitzer *et al.*, 2018). I then used a null model approach (Stegen *et al.*, 2013, 2015) to investigate the relative contribution of stochastic and deterministic processes to microbial community assembly.

Table 2.1 Definitions of microbial community assembly processes partitioned according to Stegen *et al.*, (2013). ß-nearest-taxon-index (ßNTI) and the modified Raup-Crick metric based on Bray-Curtis dissimilarity (RC_{bray}).

Class	Process	Definition	ßNTI	RC_{Bray}
Deterministic	Homogeneous Selection	Consistent selective pressure resulting from consistent environmental conditions is the primary cause of compositional turnover between a pair of local communities	< -2	-
Deterministic	Variable Selection	Divergent selective pressure resulting from divergent environmental conditions is the primary cause of compositional turnover between a pair of local communities	> +2	-
Stochastic	Homogenising Dispersal	High dispersal rates between a pair of local communities is the primary cause of compositional turnover between a pair of local communities	< |2|	< -0.95
Stochastic	Dispersal Limitation	Low dispersal rates between a pair of local communities, acting in concert with ecological drift, is the primary cause of compositional turnover between a pair of local communities	< |2|	> +0.95
Stochastic	Undominated	Stochastic dispersal and drift are the primary cause of compositional turnover between a pair of local communities	< |2|	< |0.95|

2.3 Methods

2.3.1 Study area and sampling

During June 2011, samples were collected from the surface waters (15 m and 50 m) and the deep chlorophyll maximum (DCM; 109 m – 154 m) at 22 stations spanning a 2 000 km longitudinal transect of the oligotrophic South Pacific Gyre (32°S-32°S, 172°W-150°W; Fig. 2.1). The oceanic biogeochemistry of the region is described in detail by Ellwood *et al.* (Ellwood *et al.*, 2018), and these data are available through the *GEOTRACES Intermediate Data Product 2017* (Schlitzer *et al.*, 2018) (TAN1109 GP13). In brief, environmental conditions were horizontally consistent across the transect, but varied

substantially between depths (Fig. A.1). Surface waters (0-50 m) were characterised by extremely low nitrate concentrations (< 20 nmol L^{-1}), which are likely to have limited phytoplankton productivity. Phosphate concentrations in the surface waters ranged between 30 and 110 nmol L^{-1} and exceeded concentrations typically considered limiting (< 15 nmol L^{-1}) (Moore *et al.*, 2013). Iron concentrations in the surface waters were consistently low, ranging between 0.05 and 0.29 nmol L^{-1}. Vertical diffusion was the dominant mode of nitrate, phosphate, and iron supply to the surface waters. The DCM received greater vertical diffusive supply of nitrate, phosphate, and iron, than the surface waters. Phytoplankton communities at the DCM removed the vast majority of nitrate from the water, severely limiting nitrate supply to the surface waters (Ellwood *et al.*, 2018).

A total of 60 samples were collected from 15 m (n = 20), 50 m (n = 21), and the DCM (n = 19), using a winch-lowered SBE 32 Carousel water sampler (Sea-Bird Scientific, Bellevue, WA, USA). For bacterial community analyses, 2 l seawater samples were immediately filtered through 0.2 µm polyethersulfone filters (Sterlitech, Kent, WA, USA) and stored at -80ºC until DNA extraction in 2018. Temperature, salinity, oxygen, and depth profile data were recorded from an SBE 911plus CTD (Sea-Bird Scientific, Bellevue, WA, USA) integrated into the SBE 32 Carousel water sampler. Nitrate, phosphate, and silicate concentrations were sampled from the SBE 32 Carousel water sampler according to methods described in Ellwood *et al.* (Ellwood *et al.*, 2018) (Fig. A.1).

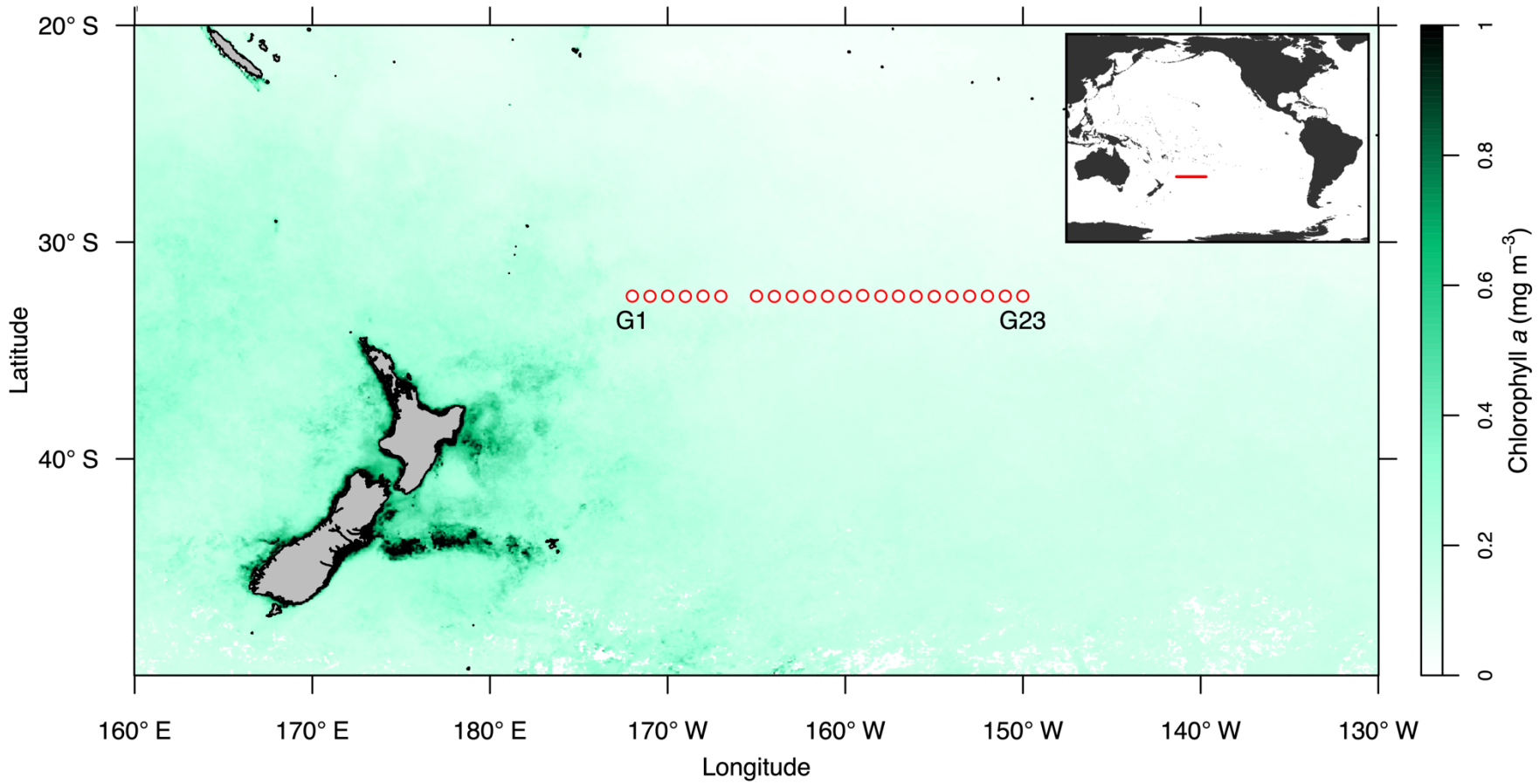

Figure 2.1 MODIS-Aqua satellite derived Chlorophyll *a* concentrations (4 km resolution; Hu *et al.*, 2012) in the oligotrophic South Pacific Gyre, averaged over Austral Winter 2011 (doi: 10.5067/AQUA/MODIS/L3B/CHL/2018). Locations of sampling stations are indicated by white-filled red circles. Inset displays a world map, with the cruise path indicated by the red line.

2.3.2 DNA extraction, PCR, and sequencing

Genomic DNA was extracted from each polyethersulfone filter using the DNEasy Plant Mini kit (Qiagen, Valencia, CA, USA) according to the manufacturer's instructions. The hypervariable V4 region of the 16S ribosomal RNA gene was amplified by PCR using universal 16S primers 515F (5′ GTGYCAGCMGCCGCGGTAA) (Parada *et al.*, 2016) and 806R (5' GGACTACNVGGGTWTCTAAT) (Apprill *et al.*, 2015) modified with an overhang region complementary to Illumina sequencing adapters (Griffith *et al.*, 2017). PCR amplifications were performed in triplicate for each sample using the HiFi Hotstart PCR kit (KAPA Biosystems, Boston, MA, USA) according to the manufacturer's instructions. The first round PCR protocol consisted of an initial denaturation at 95°C for 120 s, 25 cycles of denaturation at 98°C for 20 s, annealing at 50°C for 30 s, and extension at 72°C for 30 s, with a final extension at 72°C for 60 s. Following first round PCR, triplicate PCR products were pooled and purified using the Mag-bind TotalPure NGS kit (OMEGA Bio-tek, Norcross, GA, USA) according to the manufacturer's instructions. Purified PCR products were quantified using a Qubit dsDNA High Sensitivity Assay (Thermo Fisher Scientific, Waltham, MA, USA) and diluted to 1 ng ul^{-1}. A second round of PCR was performed to attach Illumina sequence adapters and indexes. The second round PCR protocol consisted of an initial denaturation at 95°C for 120 s, 10 cycles of denaturation at 98°C for 20 s, annealing at 60°C for 20 s, and extension at 72°C for 20 s, with a final extension at 72°C for 60 s. Finally, second round PCR products were purified, quantified, and pooled for sequencing on a single Illumina MiSeq run, returning 2 x 250 bp paired-end reads (Illumina, San Diego, CA, USA). Sequence data are accessible through the EMBL database under accession number PRJEB30061.

2.3.3 Sequence processing

Paired-end reads were processed in the R environment (R Core Team, 2013) according to the Bioconductor workflow (Callahan *et al.*, 2016). First, sequences were trimmed and truncated to remove primers and low-quality reads, respectively. Amplicon sequence variants (ASVs) were then resolved at single nucleotide resolution using DADA2 (Callahan *et al.*, 2016), which provides higher accuracy and reproducibility in 16S rRNA gene sequencing studies when compared with traditional operational taxonomic units (Callahan *et al.*, 2017). The *removeBimeraDenovo* function implemented through the 'DADA2' R

package was used to remove chimeric sequences. Taxonomy was assigned to sequences using the RDP naïve Bayesian classifier (Wang *et al.*, 2007) against the SILVA release 132 database (Quast *et al.*, 2013). Sequences which were not classified as bacteria or archaea, or were classified as chloroplasts or mitochondria, were excluded. A maximum-likelihood phylogenetic tree was then constructed, based on 16S rRNA gene sequences, using the R package 'phangorn' (Schliep, 2011). Sequence read counts, taxonomic assignments, the phylogenetic tree, and associated metadata were assembled as a phyloseq object for downstream analyses (McMurdie and Holmes, 2013). Sequence reads were randomly subsampled to an even depth of 29,280 reads per sample prior to analysis. Sequence processing R scripts are available at https://github.com/ro-allen/geotraces_transect.

2.3.4 Microbial biogeography

Shannon diversity (H') was compared between depths using a one-way ANOVA with Tukey's HSD ($\alpha = 0.05$). Differences in local community composition were tested between depths based on Bray-Curtis dissimilarity using PERMANOVA (Anderson, 2001) implemented using the *adonis* function in the R package 'vegan' (Oksanen *et al.*, 2016) ($\alpha = 0.05$). To investigate variability in local community composition at each depth, within-depth Bray-Curtis dissimilarity was compared between depths using a one-way ANOVA and Tukey's HSD ($\alpha = 0.05$). Distance-decay relationships between depths were quantified using a linear model, based on pairwise Bray-Curtis dissimilarity and the geographic distance separating each pair of local communities. Finally, trends in the distribution of ASVs across vertical scales were investigated by quantifying the proportion of shared and unique ASVs between depths using methods adapted from Schmidt *et al.* (Schmidt *et al.*, 2016).

2.3.5 Microbial Community Assembly

Patterns in microbial community assembly across horizontal (longitude) and vertical (depth) spatial scales in the South Pacific Gyre were examined using a null model approach described by Stegen *et al.* (Stegen *et al.*, 2013, 2015). The approach relies on phylogenetic signal in environmental optima, such that close phylogenetic relatives share similar environmental optima (validated using the Mantel Correlogram; Fig. A.2) and uses

measures of phylogenetic and compositional turnover between pairs of local communities to parse community assembly processes between homogeneous selection, variable selection, homogenising dispersal, dispersal limitation, and an undominated scenario (Table 2.1).

First, observed phylogenetic turnover between each pair of local communities was calculated as ß-mean-nearest-taxon-distance (ßMNTD) (Webb *et al.*, 2008; Stegen *et al.*, 2013) using the *comdistnt* function in the R package 'picante' (Kembel *et al.*, 2010):

$$\text{ßMNTD} = 0.5\left[\sum_{i_k=1}^{n_k} f_{i_k} \min\left(\Delta_{i_k j_m}\right) + \sum_{i_m=1}^{n_m} f_{i_m} \min\left(\Delta_{i_m j_k}\right)\right]$$

Where n_k is the total number of ASVs in local community k, f_{i_k} is the proportion of ASV i in local community k, and $\min\left(\Delta_{i_k j_m}\right)$ is the minimum phylogenetic distance observed between ASV i in community k and all ASVs j in local community m. A null model distribution of ßMNTD values was calculated by shuffling the tips of the phylogenetic tree, and recalculating ßMNTD over 999 randomizations (Stegen *et al.*, 2013). This simulates ßMNTD values expected under stochastic (neutral) community assembly.

For each pair of local communities, observed ßMNTD was compared with the null model distribution of ßMNTD using the ß-nearest-taxon-index (ßNTI) metric (Stegen *et al.*, 2013; Dini-Andreote *et al.*, 2015):

$$\text{ßNTI} = \frac{(\text{ßMNTD}_{obs} - \overline{\text{ßMNTD}_{null}})}{\sigma(\text{ßMNTD}_{null})}$$

ßNTI > +2 indicated greater than expected phylogenetic turnover and that variable selection was the primary assembly process (Table 2.1). ßNTI < -2 indicated less than expected phylogenetic turnover and that homogeneous selection was the primary assembly process. ßNTI < |2| indicated that phylogenetic turnover did not significantly deviate from the mean of the null model distribution (i.e. selection is not the primary community assembly process).

Pairs of local communities where selection was not the primary community assembly process (ßNTI < |2|) were further analysed to partition stochastic processes between dispersal limitation, homogenising dispersal, and an undominated scenario (Table 2.1), by comparing observed Bray-Curtis dissimilarity to a null model distribution of Bray-Curtis

dissimilarity (Stegen *et al.*, 2015). The null model distribution of Bray-Curtis dissimilarity was calculated by randomly drawing ASVs into a local community until the observed richness of that community is reached. The probability of drawing a particular ASV was proportional to the number of local communities in which the ASV was observed. Reads (individuals) were then randomly drawn into each drawn ASV until the total number of reads in the sample was reached (29,280 in all samples). The probability of drawing a read of a particular ASV was proportional to the sum of reads represented by that ASV across all local communities. Bray-Curtis dissimilarity was then re-calculated, and this randomization process was repeated 999 times to generate a null model distribution. Observed Bray-Curtis dissimilarity was compared to the null model distribution of Bray-Curtis dissimilarity using the RC_{bray} metric (Chase *et al.*, 2011; Stegen *et al.*, 2015):

$$RC_{bray} = 2\left\{\left[p(BC_{null} > BC_{obs}) + \frac{p(BC_{null} = BC_{obs})}{2}\right] - 0.5\right\}$$

Where $p(BC_{null} > BC_{obs})$ is the proportion of Bray-Curtis null model distribution values greater than the observed value, and $p(BC_{null} = BC_{obs})$ is the proportion equal to the observed value. For each pair of local communities, $RC_{bray} > +0.95$ indicated greater than expected community dissimilarity and that dispersal limitation was the primary assembly process. $RC_{bray} < -0.95$ indicated less than expected community dissimilarity and that homogenising dispersal was the primary assembly process. $RC_{bray} < |0.95|$ indicated that community assembly was not dominated by either selection or dispersal, and that stochastic dispersal and drift were the primary assembly processes (undominated) (Stegen *et al.*, 2015).

Importantly, the null model approaches described are used to infer the most influential process between pairs of local communities, but do not imply the absence of other processes (Stegen *et al.*, 2013). The efficacy of ßNTI and RC_{bray} metrics to infer patterns in microbial community assembly has been validated in previous studies (Dini-Andreote *et al.*, 2015; Stegen *et al.*, 2015).

To investigate the influence of environmental variables on microbial community assembly processes, pairwise differences in z-score transformed temperature, oxygen, salinity, nitrate, phosphate, silicate, and depth between samples were calculated. ßNTI scores were then regressed against z-score transformed pairwise differences in each environmental variable using linear models.

All null model analyses were conducted in the R environment, using the R package 'picante' (Kembel *et al.*, 2010) and code adapted from Stegen *et al.* (Stegen *et al.*, 2013). R scripts for these analyses are available at https://github.com/ro-allen/geotraces_transect.

2.4 Results

2.4.1 Microbial biogeography

Microbial communities at the DCM (H': 5.05 ± 0.15) were more diverse than at 15 m (H': 4.43 ± 0.10) and 50 m (H': 4.32 ± 0.09; Tukey's HSD, both $p < 0.001$), whilst diversity did not differ between 15 m and 50 m (Tukey's HSD, $p > 0.05$). Microbial community composition was profoundly different between both 15 m and the DCM (PERMANOVA, $R^2 = 0.66$, $p = 0.001$; Fig. 2.2a), and 50 m and the DCM (PERMANOVA, $R^2 = 0.67$, $p = 0.001$). Whilst microbial community composition also differed between 15 m and 50 m, the effect was much subtler (PERMANOVA, $R^2 = 0.09$, $p = 0.001$) and separation between these depths was difficult to distinguish through principal coordinates analysis (Fig. 2.2a). This reflects similar patterns in the abundance of dominant taxa at 15 m and 50 m, but not at the DCM (Fig. A.3). Microbial communities at the DCM were more variable than communities at 15 m and 50 m (Tukey's HSD, both $p < 0.001$; Fig. 2.2b), whilst there was no difference in variability between communities at 15 m and 50 m (Tukey's HSD, $p > 0.05$). Distance-decay in Bray-Curtis dissimilarity was weak but significant at 15 m (slope = 3.23×10^{-5}, $R^2 = 0.18$, $p < 0.001$), 50 m (slope = 4.55×10^{-5}, $R^2 = 0.30$, $p < 0.001$), and the DCM (slope = 1.36×10^{-4}, $R^2 = 0.20$, $p < 0.001$). However, the distance-decay slope was approximately three-fold steeper at the DCM (Fig. 2.2c), indicating that microbial communities became more dissimilar as the distance between them increased at the DCM than in the surface waters.

A total of 1826 ASVs were identified at the DCM, of which 63.20% were not found in the surface waters (Fig. 2.3a). Fewer ASVs were identified at 15 m (1253) and 50 m (1059), and a smaller fraction of these ASVs were not found at the DCM (i.e. unique to the surface waters; 15 m: 51.00%, 50 m: 48.16%). ASVs unique to the DCM represented 14.99% of 16S rRNA gene reads at that depth (Fig. 2.3b). ASVs unique to the surface waters represented a smaller proportion of 16S rRNA gene reads at 15 m (7.38%) and 50 m (6.59%), respectively.

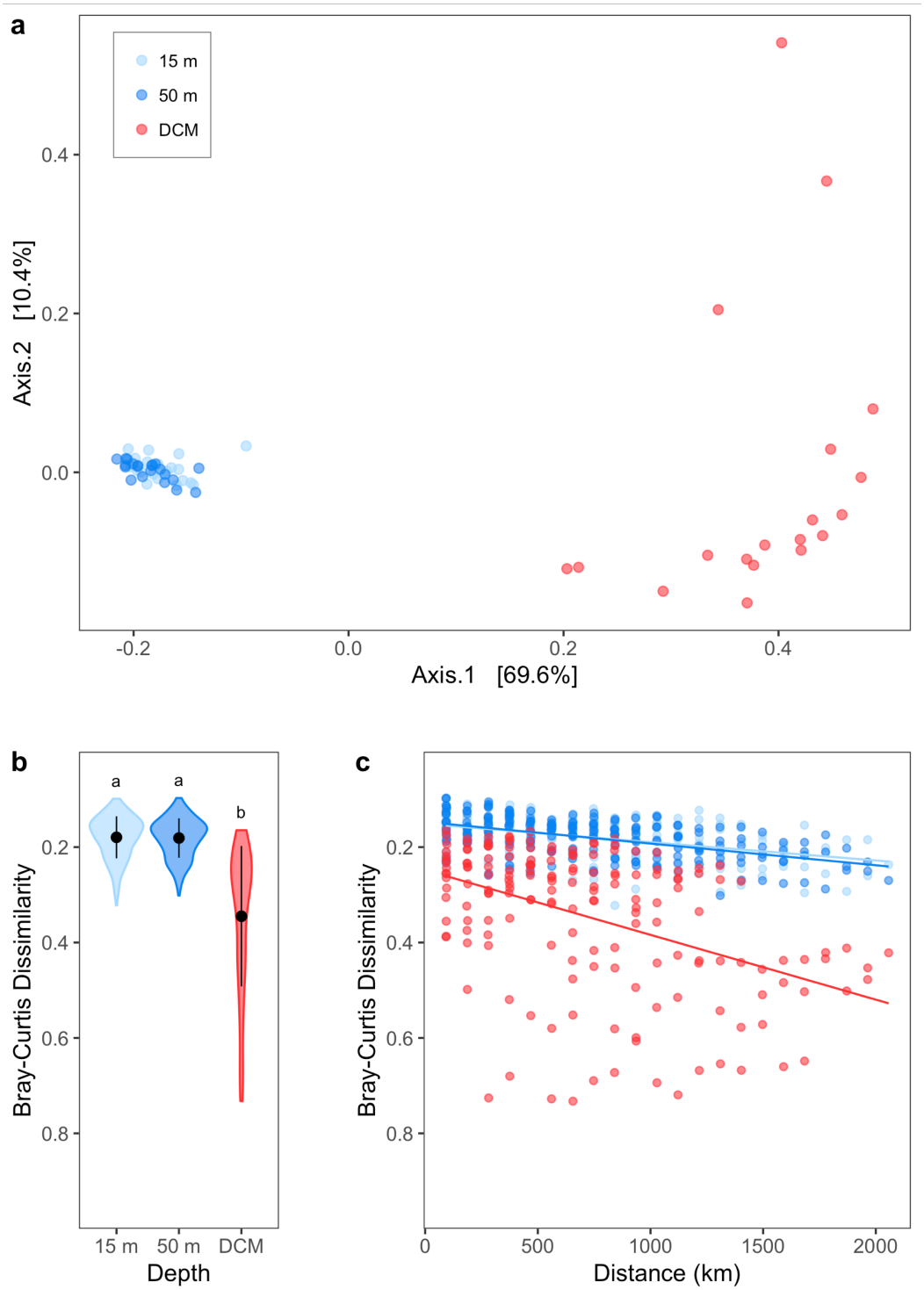

Figure 2.2 (a) Principal coordinates analysis (PCoA) based on Bray-Curtis dissimilarity between microbial communities at 15 m, 50 m, and the DCM of the oligotrophic South Pacific Gyre. 80% of variation is explained by the first two axes. (b) Violin plot of Bray-Curtis dissimilarity (inverse scale) between microbial communities within each depth. Black points represent the mean value, bars represent ±1 standard deviation, and letters represent significantly different groups (Tukey's HSD, $\alpha = 0.05$). (c) Distance-decay plot of Bray-Curtis dissimilarity (inverse scale) and geographic distance (km) between pairs of communities at each depth (15 m, 50 m, DCM). Lines represent significant relationships based on linear model fit ($p < 0.05$).

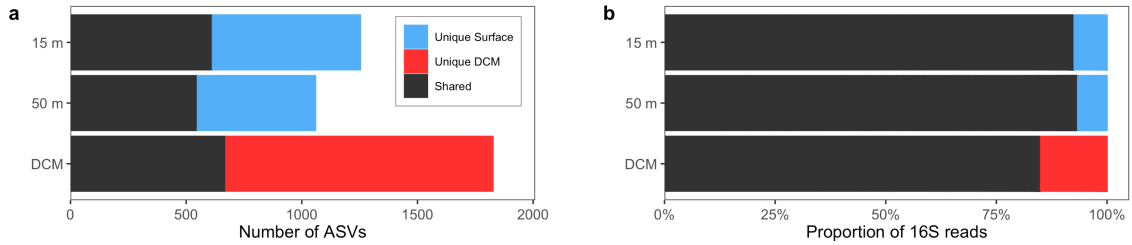

Figure 2.3 (a) The cumulative number of ASVs unique to the surface waters, unique to the DCM, and shared between the surface waters and the DCM, at each depth for all samples in the oligotrophic South Pacific Gyre after subsampling sequence reads to an even depth of 29,280 reads per sample. (b) The relative abundance of ASVs unique to the surface waters, unique to the DCM, and shared between the surface waters and the DCM, based on summed read counts from all samples at each depth.

2.4.2 Microbial community assembly

Microbial community assembly was investigated on large-scale horizontal (longitude) and vertical (depth) axes in the oligotrophic South Pacific Gyre (Table 2.2). Deterministic processes (homogeneous selection and variable selection) were consistently more important than stochastic processes (homogeneous dispersal, dispersal limitation, and undominated) along both axes, and homogeneous selection was the primary driver of community assembly. Across horizontal space, homogenous selection accounted for 100% of assembly in the surface waters (both 15 m and 50 m). At the DCM, homogenous selection accounted for 85.96% of assembly, whilst variable selection accounted for 6.43%. Stochastic processes had a minor influence at the DCM, where dispersal limitation and the undominated scenario accounted for 1.75% and 5.85% of assembly, respectively. Across vertical space, homogenous selection accounted for 100% of assembly between 15 m and 50 m. Stochastic processes were more influential when comparing surface waters to the DCM, as dispersal limitation accounted for 33.42% and 33.58% of assembly when comparing 15 m to the DCM and 50 m to the DCM, respectively.

Table 2.2 Microbial community assembly processes across horizontal and vertical spatial scales in the oligotrophic South Pacific Gyre. Values represent the percentage of local community pairs within each category which were primarily assembled by each process.

	Variable selection	Homogeneous selection	Total deterministic	Dispersal limitation	Homogenising dispersal	Undominated	Total stochastic
15 m	0	100	100	0	0	0	0
50 m	0	100	100	0	0	0	0
DCM	6.43	85.96	92.39	1.75	0	5.85	7.60
15 m to 50 m	0	100	100	0	0	0	0
15 m to DCM	9.47	57.11	66.58	33.42	0	0	33.42
50 m to DCM	9.77	55.89	65.66	33.58	0	0.75	34.33

Linear models were used to investigate the influence of environmental variables on microbial community assembly processes, revealing a strong relationship between temperature and ßNTI (slope = 1.64, R^2 = 0.46, $p < 0.001$). These results indicate that homogeneous selection was the primary community assembly process when temperature conditions between pairs of local communities were similar, and that the role of stochastic processes, and finally variable selection, increased as differences in temperature increased (Fig. 2.4). There was a moderate relationship between depth and ßNTI (slope = 1.41, R^2 = 0.31, $p < 0.001$), and a weak relationship between both phosphate and ßNTI (slope = 0.87, R^2 = 0.17, $p < 0.001$) and oxygen and ßNTI (slope = 0.74, R^2 = 0.12, $p < 0.001$). Nitrate, silicate, and salinity were not meaningfully related to ßNTI (all $R^2 < |0.01|$).

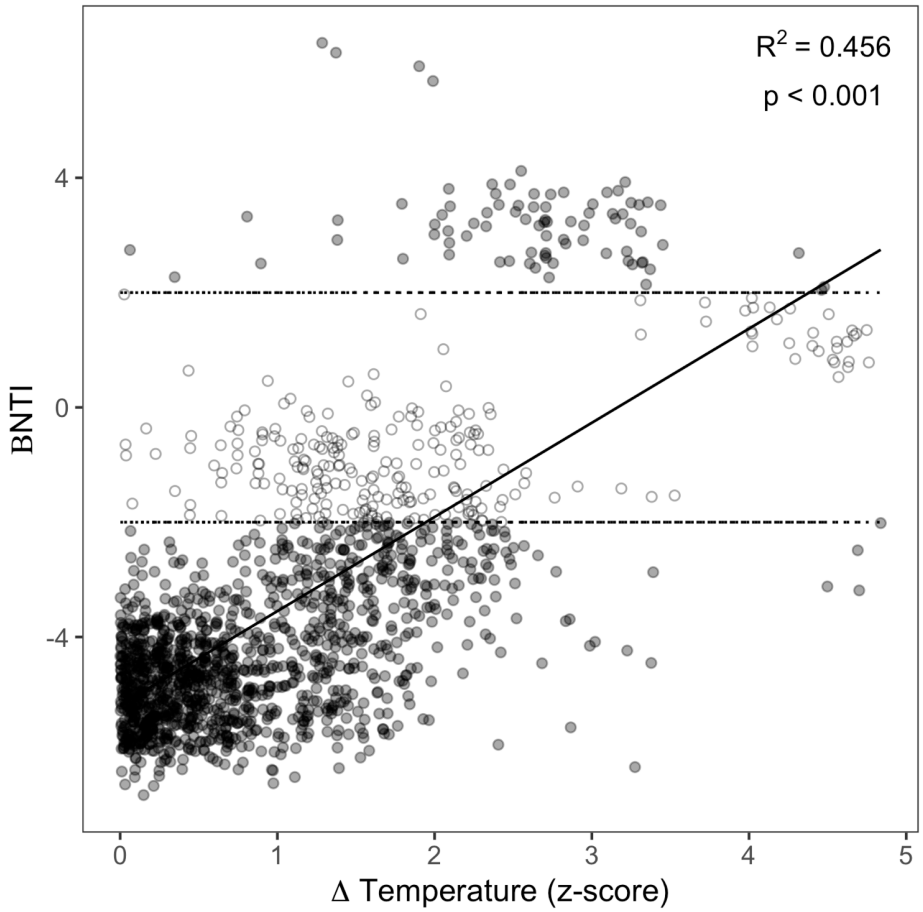

Figure 2.4 The relationship between ßNTI and differences in temperature (z-score) for each pair of samples in the oligotrophic South Pacific Gyre, based on linear model fit. Closed circles represent pairs of samples where deterministic processes dominated community assembly (ßNTI < -2: homogeneous selection, ßNTI > +2: variable selection). Open circles represent pairs of samples where stochastic processes dominated community assembly (ßNTI < |2|).

2.5 Discussion

2.5.1 Horizontal metacommunity structure and assembly

Horizontal metacommunity structure in the nutrient-limited surface waters (15 m and 50 m) of the South Pacific Gyre was remarkably consistent (Fig. 2.2). All local communities were dominated by Prochlorococcus and SAR11 ASVs (Fig. A.3), which are highly adapted to oligotrophic conditions (Biller *et al.*, 2014; Giovannoni, 2017). This likely reflects harsh nitrate limitation, combined with low concentrations of phosphate and iron (Ellwood *et al.*, 2018), which create a strong selective environment in the surface waters of the South Pacific Gyre. In line with this, homogeneous selection was the dominant community assembly process through horizontal space across the region (Table 2.2). Suboptimal environments can impose strong selection pressure by limiting the number of species in the regional pool which can tolerate local conditions (Chase, 2007), and by creating intense competition for limiting resources (e.g. nitrate). Strong selection minimises the role of stochasticity in community assembly, resulting in highly similar local community composition (Evans *et al.*, 2017) (Fig. 2.2a) and shallow distance-decay relationships (Hanson *et al.*, 2012) (Fig. 2.2c). The surface waters of the South Pacific Gyre are regarded amongst the most temporally stable environments on Earth (Raimbault *et al.*, 2008), which may contribute to the overwhelming role of homogeneous selection in the region. Temperature variation is low on decadal scales (Roemmich *et al.*, 2016) and productivity is consistently low due to nutrient-limitation (Dandonneau *et al.*, 2004). As a result, selection pressures act on microbial communities consistently through both space and time, which may enhance the influence of selection on local community composition (Dini-Andreote *et al.*, 2015). Computational models predict that microbial communities assembled primarily through selection should be biogeochemically efficient, as the probability of maladapted taxa being present in the community is low (Graham and Stegen, 2017). The findings of the current study support this notion, as previous reports demonstrate that microbial recycling of carbon and nutrients in the surface waters of the oligotrophic ocean is exceptionally efficient, leading to very low rates of vertical carbon export (Guidi *et al.*, 2016).

Horizontal metacommunity structure at the DCM was more variable than in the surface waters (Fig. 2.2). The DCM received greater vertical nutrient supply, was more productive, and was more environmentally variable than the surface waters (Ellwood *et al.*, 2018) (Fig.

A.1). As a result, variable selection was more important at the DCM than the surface waters (Table 2.2), aligning with the greater variation observed in local community composition (Evans *et al.*, 2017) (Fig. 2.2b). Stochastic processes were comparatively more influential at the DCM than the surface waters (Table 2.2), which is likely explained by two factors. First, horizontal dispersal between local communities at the DCM may be lower than in the surface waters as a result of reduced wind-driven mixing, which decreases as a function of depth (Wu *et al.*, 2017a). Second, macroecological theory suggests that stochasticity has a greater influence on community assembly in more productive environments, when other physicochemical parameters do not exert overwhelming selection pressure (Chase and Leibold, 2003; Chase, 2010). The greater influence of stochastic processes may also contribute to the higher diversity (Chase, 2010) and the steeper distance-decay relationship observed at the DCM (Hanson *et al.*, 2012) (Fig. 2.2c). Despite the greater influence of stochastic processes at the DCM relative to the surface waters, community assembly at the DCM was predominantly deterministic (Table 2.2).

2.5.2 Vertical metacommunity structure and assembly

Vertical metacommunity structure was consistent between 15 m and 50 m in the surface waters of the South Pacific Gyre (Fig. 2.2a). Environmental conditions were similar between these depths (Fig. A.1). Homogeneous selection was the primary assembly process, indicating that consistent selection pressures driven by consistent environmental conditions underpin the similarity in local community composition between these depths (Fig. 2.2a). Both 15 m and 50 m were located within the mixed layer at most sampling stations (Ellwood *et al.*, 2018), and consequently, rates of dispersal between the two depths are likely to be high. Even in a strong selective environment, sufficient dispersal is necessary to allow selection to overwhelm the potential effects of ecological drift (Evans *et al.*, 2017). These findings suggest that the surface waters of the oligotrophic South Pacific Gyre act as a continuous microbial habitat, due to a consistent selective regime and sufficient rates of dispersal.

Local communities at the DCM were distinct from the surface waters (Fig. 2.2a). The cooler deep waters of the DCM are separated from the warmer nutrient-limited surface waters of the South Pacific Gyre by a pycnocline (density gradient) (Ellwood *et al.*, 2018), across which there is minimal physical mixing. As a result, dispersal limitation accounted for over one third of microbial community assembly between the surface waters and the

DCM (Table 2.2). Temperature-related stratification of oceanic waters, as is observed here, has previously been shown to increase the influence of dispersal limitation on microbial community assembly (Vergin *et al.*, 2017). Furthermore, the dispersal limitation has previously been shown to substantially influence community assembly in contiguous aquifer and hyporheic environments (Stegen *et al.*, 2013; Graham *et al.*, 2017).

Though dispersal limitation plays an important role in microbial community assembly between the surface waters and the DCM, selection remains the most influential assembly process (Table 2.2). Variable selection accounted for approximately one tenth of community assembly between the surface waters and the DCM, reflecting the large environmental differences between these depths at particular stations (Fig. A.1). Interestingly, homogeneous selection accounted for over half of community assembly between the surface waters and the DCM.

Thus, despite environmental differences, it appears that selection pressure is at least partially conserved between these depths. These findings suggest that both deterministic and stochastic processes influence community assembly between contiguous water masses in the oligotrophic ocean.

2.5.3 Environmental features and community assembly

The role of deterministic assembly processes was closely related to temperature in the South Pacific Gyre (Fig. 2.4). Where temperature was similar between communities, homogeneous selection was the primary assembly process. As temperature diverged, stochastic processes, and finally variable selection, became more influential. Temperature controls the rate of metabolic processes in bacteria (Davidson and Janssens, 2006) and marine bacteria display highly specialised thermal niches (Yung *et al.*, 2015). The thermal niche of bacteria can interact with nutrient use efficiency (Hall *et al.*, 2009) and competition for limiting resources (Hall *et al.*, 2008), which is pertinent to consider in the nitrate-limited oligotrophic South Pacific Gyre (Ellwood *et al.*, 2018). The data reported in this study suggest that temperature exerts selection pressure on marine microbes. These findings align with evidence that temperature is the most influential driver of variation in marine microbial community composition on a global scale (Sunagawa *et al.*, 2015).

Phosphate concentrations were similarly related to microbial community assembly processes but explained a smaller proportion of variation and had a shallower slope than

temperature, suggesting that temperature exerted stronger selection pressure. This is likely to be because phosphate concentrations in the South Pacific Gyre were greater than those typically considered to be limiting (Moore *et al.*, 2013; Ellwood *et al.*, 2018).

Interestingly, nitrate concentrations were not meaningfully related to community assembly processes in the South Pacific Gyre. The explanation for this is two-fold. First, nitrate concentrations were consistently around the limit of detection (Ellwood *et al.*, 2018) (Fig. A.1), offering minimal variation in the dataset to analyse. Second, the measurements in this study quantified background nitrate concentrations, rather than nitrate supply. Nitrate supply to the DCM is greater than to the surface ocean in the South Pacific Gyre (Ellwood *et al.*, 2018), but higher rates of nitrate turnover at the DCM mean that background nitrate concentrations may appear similar between the two environments. Subsequently, the linear model approach used in this study is likely to have quantitatively under-estimated the influence of nitrate on microbial community assembly processes. Nonetheless, the relative abundance of highly adapted oligotrophs (Biller *et al.*, 2014; Giovannoni, 2017) (Fig. A.3) and the overwhelming influence of homogeneous selection in the oligotrophic surface waters (Table 2.2) suggest that nitrate concentrations are likely to exert selection pressure on microbial communities in the South Pacific Gyre.

2.5.4 ASV accumulation at the DCM

Vertical connectivity between local communities in the oligotrophic ocean is predominantly mediated by two processes. First, through particle sinking, where microbial colonisation of sinking particles in the surface waters can affect the structure of local communities in deeper waters (Mestre *et al.*, 2018). Second, through advection, where physical mixing of contiguous water masses leads to the dispersal of microbes between environments (Wilkins *et al.*, 2013). Advective dispersal of microbes between the surface waters and the DCM in the South Pacific Gyre is limited due to the stratified nature of the water column (Ellwood *et al.*, 2018). Wilkins *et al.* (2013) demonstrate that in areas of limited physical mixing, dispersal primarily affects metacommunity structure by providing opportunities for microbes to cross-colonise contiguous water masses. Colonisation success is determined by the selective landscape of the new environment, and this selection pressure can readily overwhelm the effects of advective dispersal between contiguous water masses (Graham *et al.*, 2017) (Table 2.2). Consequently, microbes which are distributed throughout both the surface waters and the DCM are inferred to be able to

successfully colonise both environments (Wilkins *et al.*, 2013) (that is, to be able to survive and reproduce in both environments). I propose the presence of a biased environmental filter between the surface waters and the DCM in the South Pacific Gyre, whereby microbes dispersed form the surface waters to the less environmentally restrictive DCM have a greater probability of colonisation success than microbes dispersed in the opposite direction (Fig. 2.5). In other words, a larger proportion of the regional species pool is capable of colonising the DCM than the surface waters. This proposal is supported by the greater absolute number of ASVs at the DCM, the larger fraction of unique ASVs at the DCM, and the larger proportion of reads represented by unique ASVs at the DCM, when compared with the surface waters (Fig. 2.3). Indeed, similar patterns of species accumulation in nutrient replete environments have been observed in freshwater systems (Schmidt *et al.*, 2016). Furthermore, this proposal aligns with the distinct life-history strategies of marine microbes (Lauro *et al.*, 2009). For example, oligotrophs such as SAR11 maintain growth rates and show minimal physiological responses to the increased availability of organic matter or nutrients, and possess a range of mechanisms to avoid direct competition with copiotrophic strategists (Giovannoni, 2017). Consequently, oligotrophs are likely to display high colonisation success of more nutrient-replete environments such as the DCM (Fig. 2.3). In contrast, copiotrophs have higher nutrient requirements and a life-history strategy focussed on exploiting transient resource availability (Vergin *et al.*, 2013), thus are less likely to be able to successfully colonise oligotrophic environments such as the surface waters of the South Pacific Gyre. I propose this biased environmental filter as a mechanism contributing to species accumulation observed at the DCM across oligotrophic oceans globally (Sunagawa *et al.*, 2015).

2.5.5 Summary

Here, I show that microbial community assembly is highly deterministic across horizontal scales of thousands of kilometres in the oligotrophic South Pacific Gyre. These findings support niche-based community assembly (Chase and Leibold, 2003) and contribute to a growing body of evidence supporting the dominance of determinism in shaping marine microbial communities (Vergin *et al.*, 2017; Wu *et al.*, 2017a; Mo *et al.*, 2018). Though deterministic processes remained the most influential microbial community assembly processes across vertical scales, dispersal limitation plays a substantial role in community assembly between contiguous water masses in the oligotrophic ocean. This highlights the

relevance of stochastic processes in structuring microbial communities, which is often debated (Zhou and Ning, 2017). I identified temperature as an environmental modulator of the balance between stochastic and deterministic community assembly processes in the South Pacific Gyre, aligning with evidence that temperature is the key determinant of microbial community composition on a global scale (Sunagawa *et al.*, 2015). Nutrient limitation is also likely to impose selection pressure on microbial communities in the South Pacific Gyre and may interact with temperature (Hall *et al.*, 2008, 2009), though these effects are likely to have been quantitatively underestimated in this study. Macroecological theory states that stochastic processes have a greater influence on community assembly in more productive environments (Chase, 2010). The findings of this study support this notion, demonstrating that microbial community assembly in the least productive oceanic waters on Earth (Claustre and Maritorena, 2003) is overwhelmingly deterministic. The findings of this study inform a conceptual model of microbial community assembly the oligotrophic ocean (Fig. 2.5) and suggest that microbial communities may respond predictably to oceanic climate change in these biogeochemically important regions (Stegen *et al.*, 2018).

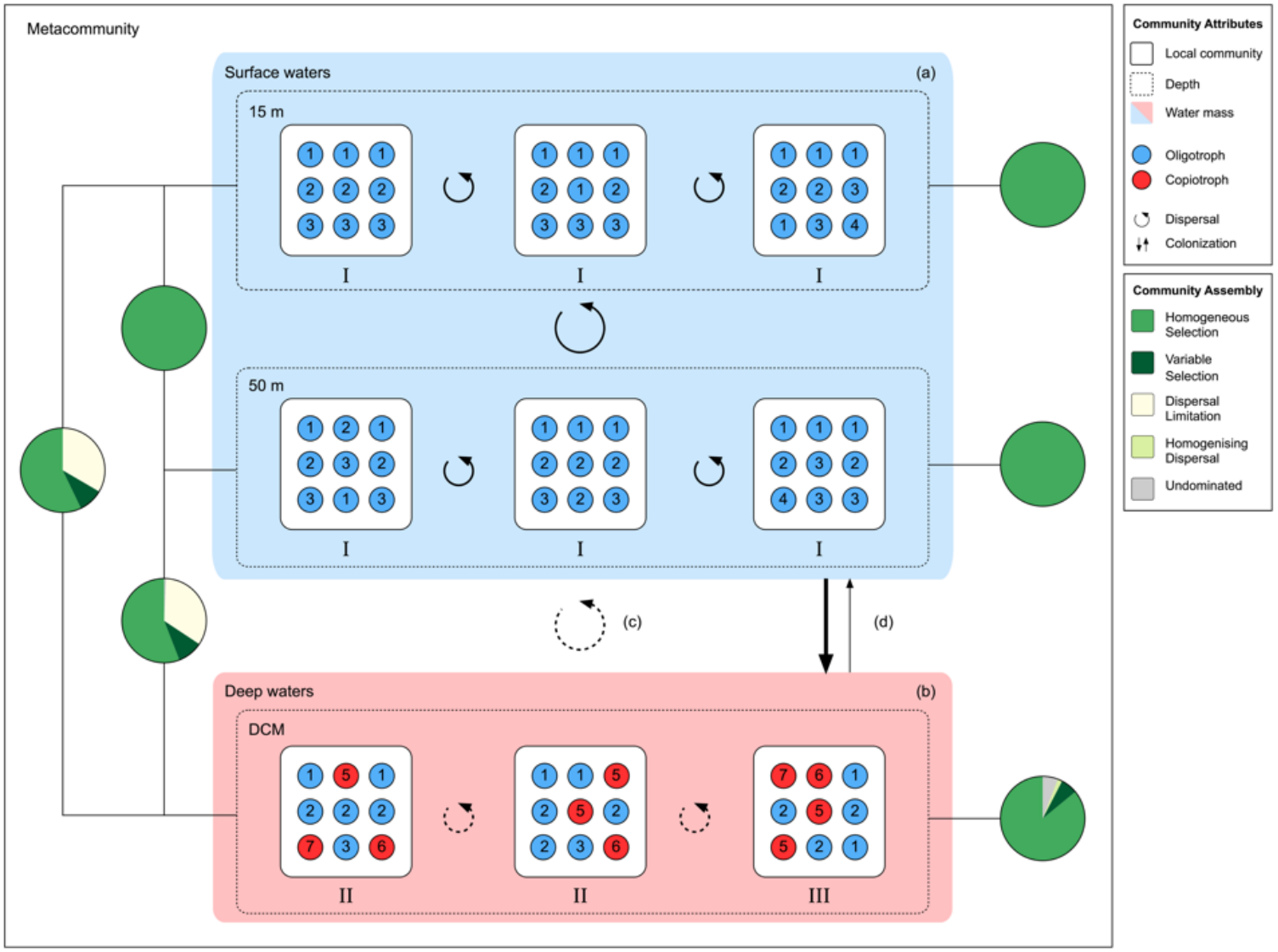
Metacommunity
Surface waters
(a)
15 m
I
I
I
50 m
I
I
I
(c)
(d)
Deep waters
(b)
DCM
II
II
III
Community Attributes
Local community
Depth
Water mass
Oligotroph
Copiotroph
Dispersal
Colonization
Community Assembly
Homogeneous Selection
Variable Selection
Dispersal Limitation
Homogenising Dispersal
Undominated

Figure 2.5 A conceptual model of microbial community assembly in the oligotrophic ocean. Coloured circles represent individuals in each local community (blue: oligotrophic strategists; red: copiotrophic strategists), numbers within each circle represent ASV identity. Local environmental conditions are represented by roman numerals below each local community. Sufficient dispersal to overwhelm the effects of ecological drift, and the occurrence of dispersal limitation, are indicated by solid and dashed curved arrows, respectively. Cross-colonization is represented by straight arrows, and arrow thickness indicates the probability of colonization success. Pie charts represent the community assembly processes within (right) and between (left) each depth. (a) Microbial communities in the surface waters display low alpha diversity, low beta diversity, and shallow distance-decay, as these communities are assembled through homogeneous selection driven by consistent environmental conditions across large horizontal spatial scales. Horizontal and vertical dispersal are sufficient to allow homogeneous selection to overwhelm the influence of drift. (b) Microbial communities in at the DCM display higher alpha diversity, higher beta diversity, and a steeper distance-decay, as variable selection and stochastic processes are more influential than in the surface waters. (c) The exchange of microbes between surface waters and the DCM is limited by low rates of physical mixing. Dispersal limitation and variable selection drive community divergence between the contiguous water masses of the surface waters and the DCM. (d) A biased environmental filter impacts the colonisation success of microbes dispersed between the surface waters and the DCM. Microbes dispersed from the surface waters to the DCM have a greater probability of successful colonization than microbes dispersed in the opposite direction, leading to ASV accumulation at the DCM.

Chapter 3: Distinct processes structure bacterioplankton and protist communities across an oceanic front

Co-authors of the manuscript: Tina Summerfield, Kim Currie, Linn Hoffmann

Chapter 3: Distinct processes structure bacterioplankton and protist communities across an oceanic front

3.1 Abstract

Bacterioplankton and protists fulfil key roles in the marine ecosystem. Understanding the abundance and distribution of these organisms through space and time is a key focus of biological oceanographers. The role of oceanographic features, in addition to environmental conditions, in structuring bacterioplankton and protist communities has been increasingly recognised. Here, patterns in bacterioplankton and protist diversity and community structure are investigated across the Southland Front system, a compaction of the subtropical front zone, to the east of New Zealand's South Island. Frontal waters are identified as a minor diversity hotspot for bacterioplankton, but not protists. Bacterioplankton show a high degree of spatial structuring across the front, with communities closely tracking water mass identity through the region. Protist communities also tracked water mass identity through the region, though this effect was less pronounced. An ecological null model approach was used to demonstrate that protist communities are primarily assembled through stochastic processes, whilst bacterioplankton are primarily assembled through deterministic processes across the Southland Front system. I suggest that these differences emerge from fundamental differences in the characteristics of bacterioplankton and protist communities. These findings add to a growing body of literature highlighting the importance of oceanographic features in shaping bacterioplankton and protist communities, promoting the necessity for such features to be considered more explicitly in the future.

3.2 Introduction

Bacterioplankton (bacteria and archaea) and protists form the fundamental basis of marine food webs and biogeochemical cycling (Chassot *et al.*, 2010; Passow and Carlson, 2012). Marine phytoplankton, including both cyanobacteria and photosynthetic protists, are responsible for approximately 50% of global primary production (Field, 1998). Protists are key components of marine environments due to their abundance, taxonomic diversity, and functional diversity, fulfilling roles are producers, consumers, decomposers, and parasites (de Vargas *et al.*, 2015). The vast majority of phytoplankton-derived organic carbon is routed through the marine microbial loop, where heterotrophic bacterioplankton remineralise organic matter, modulating the cycling of carbon and nutrients (Azam and Malfatti, 2007). The structure of marine bacterioplankton and protist communities is closely coupled to their function (Arrigo *et al.*, 1999; Guidi *et al.*, 2016; Galand *et al.*, 2018). Consequently, it is crucial to unravel the factors which determine the abundance and distribution of these organisms through space and time. Historically, efforts to understand the abundance and distribution of bacterioplankton and protists have focussed on the influence of environmental conditions, however, emerging evidence indicates that oceanographic features and hydrodynamics may play a significant role in structuring these communities (Clayton *et al.*, 2017; Djurhuus *et al.*, 2017; Lévy *et al.*, 2018).

Oceanic fronts are regions where environmentally distinct water masses meet, creating sharp physicochemical gradients over fine spatial scales (Belkin *et al.*, 2009). These regions vary in their spatial and temporal extent (Belkin *et al.*, 2009) and are frequently associated with enhanced productivity (Belkin *et al.*, 2009; Taylor *et al.*, 2012). Flow between water masses separated by oceanic fronts is limited, therefore fronts can act as soft dispersal barriers for passively drifting organisms such as bacterioplankton and protists (Gildor *et al.*, 2009). These regions may be considered as the marine analogues of terrestrial 'ecotones'; interfaces between habitat types which often harbour enhanced species richness (Smith, 1997; Ribalet *et al.*, 2010).

A latitudinal transect of the South Pacific basin found that bacterioplankton and protist diversity are enhanced at the mesoscale (> 50 km) Subtropical Frontal Zone (Raes *et al.*, 2018). However, this relationship does not emerge in bacterioplankton communities at a sub-mesoscale (< 50 km) compaction of the Subtropical Frontal Zone (Morales *et al.*, 2018). In contrast, sub-mesoscale oceanic fronts act as diversity hotspots for photosynthetic protists in the North Pacific (Ribalet *et al.*, 2010; Clayton *et al.*, 2013, 2017). These diversity hotspots are hypothesised to result from a combination of physical and biological

processes (Clayton *et al.*, 2013), such as physical mixing of communities and the relief of nutrient limitation (Clayton *et al.*, 2017). Further research is needed to understand the effect of sub-mesoscale oceanic fronts on bacterioplankton and protist diversity, with a particular consideration of heterotrophic protist which have often been overlooked by previous studies.

In addition to affecting diversity, oceanic fronts and other sub-mesoscale oceanographic features can influence the structure of bacterioplankton and protist communities (Lévy *et al.*, 2018). Both bacterioplankton and protist communities display biogeographic patterns across the South Pacific basin according to mesoscale oceanic front delimited biomes (Raes *et al.*, 2018). Moreover, sub-mesoscale oceanic fronts act as transition zones for bacterioplankton community structure in both surface (Baltar *et al.*, 2016) and deep waters (Baltar and Arístegui, 2017). Bacterioplankton communities track water masses closely across sub-mesoscale oceanic fronts in the Indian and Southern Oceans, as each water mass constrains a distinct bacterioplankton assemblage (Wilkins *et al.*, 2013; Djurhuus *et al.*, 2017; Hernando-Morales *et al.*, 2017). Intuitively, the structuring of bacterioplankton communities across sub-mesoscale oceanic fronts is associated with equally distinct functional shifts affecting bacterial respiration rates (Baltar *et al.*, 2015b) and extracellular enzyme activity (Baltar and Arístegui, 2017), highlighting the influence these features on marine biogeochemical cycling. Protist communities display similar biogeographic patterns to bacterioplankton communities across the South Pacific basin (Raes *et al.*, 2018), and photosynthetic protists also display structuring across sub-mesoscale oceanic fronts (Taylor *et al.*, 2012; Clayton *et al.*, 2014).

Although the structure of bacterioplankton and protist communities across oceanic fronts have been investigated independently, integrated studies are required to resolve differences in how these oceanographic features affect each community. Bacterioplankton and protist communities are assembled through the balance between stochastic process (neutral), such as dispersal limitation and ecological drift, and deterministic processes (niche-based), such as selection (Vellend, 2010). Recent evidence indicates that the balance between stochastic and deterministic processes can differ between co-occurring bacterioplankton and protist communities (Wu *et al.*, 2017a; Logares *et al.*, 2018). This suggests that oceanographic features, such as fronts, may affect bacterioplankton and protist communities differently.

Here, patterns in bacterioplankton and protist diversity and community structure are investigated in high spatial resolution across the Southland Front system, a local compaction of the Subtropical Frontal Zone which results in four environmentally distinct water masses occurring over a 65 km transect east of New Zealand's South Island.

Bacterioplankton and protist community composition was determined using high-throughput sequencing of the 16S and 18S rRNA gene, respectively, to investigate the following hypotheses: oceanic fronts act as diversity hotspots for bacterioplankton and protist communities, bacterioplankton and protist communities at oceanic fronts display water mass specificity, stochastic processes are comparatively more influential in protist community assembly than bacterioplankton community assembly.

3.3 Methods

3.3.1 Study area and sampling

Samples were collected across a longitudinal transect of the Southland Front system, a local manifestation of the larger Subtropical Frontal Zone hydrographic boundary which separates warm, high salinity subtropical waters from cooler, less saline subantarctic surface waters. In the Southland Front system, the Subtropical Frontal Zone narrows to a range of ~10 km, as it is constrained by the continental shelf break (Sutton, 2003; Fig. 3.1). The Southland Front system is characterised by abrupt transitions between four key water masses (coastal waters, subtropical waters, frontal waters, and subantarctic surface waters) over a fine spatial scale (< 65 km). Coastal waters are characterised by variable environmental conditions, due to transient riverine inputs of freshwater and nutrients (Jones *et al.*, 2013). Subtropical waters are more saline and warmer than their neighbouring water masses, and are modified from typical subtropical waters due to nutrient inputs from adjacent coastal waters (Jones *et al.*, 2013). Frontal waters represent the transition zone between subtropical and subantarctic waters. Subantarctic waters are cooler and less saline than the other water masses, and represent a classical high-nutrient low-chlorophyll environment (Jones *et al.*, 2013). Transitions in salinity and temperature have previously been used to distinguish these water masses (Jillett, 1969; Currie *et al.*, 2011; Jones *et al.*, 2013) (Fig. A.4).

Sampling of the Southland Front system was conducted during the *RV Polaris II* voyage of the Munida Time Series Transect on November 28th, 2017. Seawater samples were collected from ~2 m depth using a continuous underway pump at 24 stations along the transect, targeting the four constituent water masses of the Southland Front system (Fig. 3.1) which were differentiated according to temperature and salinity profiles (Jillett, 1969).

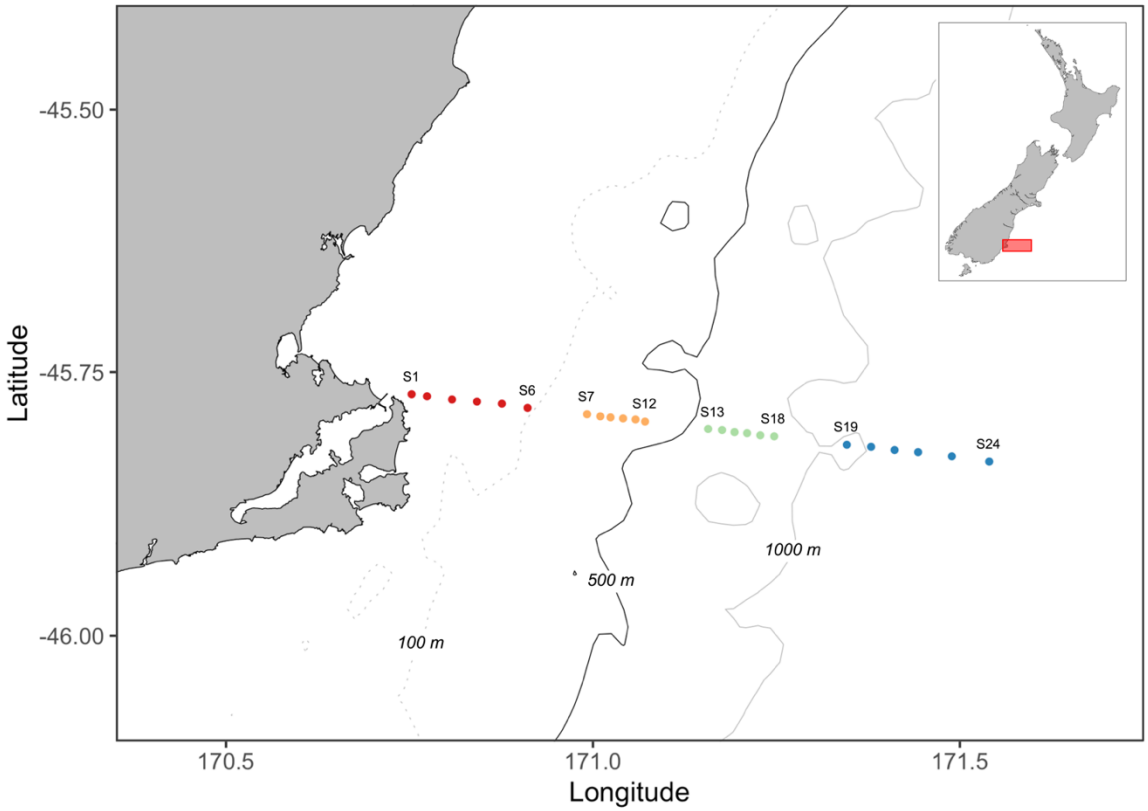

Figure 3.1 Map of the Southland Front system to the east of Tairoa Head, Dunedin, New Zealand. Solid circles represent the location sampling stations, colours indicate the water mass identity of each sampling station (red: coastal waters, orange: subtropical waters, green: frontal waters, blue: subantarctic waters). Contours indicate the major bathymetric features of the region. Inset map shows the sampled region of the Southland Front system, in the context of New Zealand.

3.3.2 Environmental measurements

Sea surface temperature and salinity data were recorded continuously throughout the voyage from the *RV Polaris II* continuous underway pump using a Sea Bird SBE45 thermosalinograph (Sea-Bird Scientific, Bellevue, WA, USA) associated with the vessel's GPS system. To quantify chlorophyll *a* concentrations, 500 ml seawater samples were collected from the continuous underway pump and filtered through 0.7 µm glass-fibre filters (GF/F) using a peristaltic pump. Following filtration, each GF/F was transferred to an opaque cryovial to prevent photodegradation of chlorophyll *a* and frozen at -20°C until further laboratory analysis. Chlorophyll *a* was extracted from each GF/F in 96% ethanol

through an incubation period of 24 hours at -20°C. Following the incubation period, cryovials were centrifuged at 6,000 rpm for 5 minutes to remove fibres and particulate matter. Chlorophyll *a* concentration was then determined using spectrophotometric methods described in Jeffery and Humphrey (Jeffrey and Humphrey, 1975). To quantify inorganic nutrient concentrations (nitrate, phosphate, silicate, ammonia), triplicate 50 ml seawater samples were collected from the continuous underway pump and syringe filtered through 0.22 µm polycarbonate filters. The filtrate was collected in 50 ml falcon tubes, and frozen at -20°C prior to laboratory analysis. Inorganic nutrient concentrations were determined using a Lachat FIA auto analyzer (Lachat Instruments, Loveland, CO, USA).

3.3.3 DNA sampling, extraction, and library preparation

At each station (Fig. 3.1), 2 l seawater samples were collected from the continuous underway pump and filtered through 0.2 µm polyethersulfone filters. Filters were frozen in liquid nitrogen for the duration of the voyage before being transferred to a -80°C freezer. Each filter was snap-frozen in liquid nitrogen and manually crushed using a sterile glass rod in preparation for DNA extraction. Genomic DNA was extracted using a DNEasy Plant Mini kit (Qiagen, Valencia, CA, USA) according to the manufacturer's instructions. To investigate the composition of bacterioplankton communities, the V4 region of the 16S rRNA gene was amplified using the 515F (5' GTGYCAGCMGCCGCGGTAA) and 806R primers (5' GGACTACNVGGGTWTCTAAT) (Apprill *et al.*, 2015; Parada *et al.*, 2016), modified to allow the downstream attachment of Illumina sequencing adapters (Griffith *et al.*, 2017). Triplicate PCR mixtures were prepared using the HiFi Hotstart PCR kit (KAPA Biosystems, Boston, MA, USA), and each contained 1 X KAPA HiFi buffer (2 mM $MgCl_2$), 0.3 mM KAPA dNTP Mix, 0.3 µM of forward and reverse primers, and 0.5 U of KAPA HiFi Hotstart DNA Polymerase. The PCR thermocycler program consisted of an initial denaturation step at 95°C for 120 s before 25 cycles of 98°C for 20 s, 60°C for 30 s, and 72°C for 30 s, followed by a final extension period of 60 s at 72°C. To investigate the composition of protist communities, the 18S rRNA gene was amplified using the TAReuk454FWD1 (5' CCAGCASCYGCGGTAATTCC) and TAReukREV3 (5' ACTTTCGTTCTTGATYRA) primers (Stoeck *et al.*, 2010), modified to allow the downstream attachment of Illumina sequencing adapters (Griffith *et al.*, 2017). Triplicate PCR mixtures were prepared according to protocols described above. The PCR thermocycler program consisted of an initial denaturation step at 95°C for 30 s before 10

cycles of 95°C for 30 s, 53°C for 30 s, and 72°C for 30 s, followed by 15 cycles of 95°C for 30 s, 48 °C for 30 s, and 72°C for 30 s, with a final extension period of 300 s at 72°C (adapted from Massana *et al.*, 2015). Following first round PCR, triplicate PCR products were pooled and purified using the Mag-bind TotalPure NGS kit (OMEGA Bio-tek, Norcross, GA, USA) according to the manufacturer's instructions. Purified PCR products were quantified using the Qubit dsDNA High Sensitivity Assay (Thermo Fisher Scientific, Waltham, MA, USA) according to the manufacturer's instructions. Once quantified, purified PCR products were diluted to a uniform concentration of 1 ng μl^{-1}. In order to attach Illumina sequence adapters and indexes, a second round of PCR was performed using 1 µl of diluted first round PCR products. The PCR thermocycler program for second round PCR consisted of an initial denaturation step at 95°C for 120 s before 10 cycles of 98°C for 20 s, 60°C for 20 s, and 72°C for 30 s, followed by a final extension period of 60 s at 72°C. Second round PCR products for 16S rRNA gene and 18S rRNA gene libraries were purified, quantified, and pooled independently. Pooled 16S rRNA gene libraries were sequenced on the Illumina MiSeq platform (Illumina, San Diego, CA, USA) using the V2 reagent kit, yielding 2 x 250 bp reads. Pooled 18S rRNA gene libraries were sequenced on the Illumina MiSeq platform using the V3 reagent kit, yielding 2 x 300 bp reads.

3.3.4 Sequence processing

All sequence processing was performed in the R environment (R Core Team, 2013), according to the Bioconductor workflow (Callahan *et al.*, 2016). The first step of the workflow is to trim and truncate reads to remove primers and low-quality sequences, respectively. Amplicon sequence variants (ASVs) were then resolved at single nucleotide resolution using the 'DADA2' R package (Callahan *et al.*, 2016). The resolution of exact ASVs improves the accuracy and reproducibility of high-throughput sequencing studies (Callahan *et al.*, 2017). Chimeric ASVs were identified and removed using the *removeBimeraDenovo* function in the 'DADA2' R package. Taxonomy was assigned against the SILVA database (release 132; Quast *et al.*, 2013) and the PR2 database (version 4.10.0; Guillou *et al.*, 2013) for 16S rRNA gene ASVs and 18S rRNA gene ASVs, respectively, using the RDP naïve Bayesian classifier (Wang *et al.*, 2007). 16S rRNA gene ASVs classified as bacteria or archaea were retained, and sequences classified as chloroplasts or mitochondria were removed prior to downstream analysis. 18S rRNA gene sequences classified as metazoan were removed prior to downstream analyses, resulting in

the exclusion of four 18S rRNA gene samples which were dominated by metazoan sequences (stations: S7, S8, S9, S12). Maximum-likelihood phylogenetic trees were constructed based on 16S rRNA gene sequences and 18S rRNA gene sequences, respectively, using the R package 'phangorn' (Schliep, 2011; Callahan *et al.*, 2016). ASV tables, taxonomic assignments, maximum likelihood trees, and environmental metadata were compiled as a phyloseq object (McMurdie and Holmes, 2013) for 16S rRNA gene ASVs and 18S rRNA gene ASVs, respectively. Sequence reads were randomly subsampled to an even depth prior to downstream analyses (16S rRNA gene: 51,121 reads, 18S rRNA gene: 17,340 reads).

3.3.5 Statistical analyses

The Chao1 index (Chao, 1984), implemented through the *estimate_richness* function in the R package 'phyloseq' (McMurdie and Holmes, 2013), was used to estimate ASV richness at each sampling station. The Chao1 index estimates ASV richness based on the observed number of ASVs, the observed number of ASVs occurring only once, and the observed number of ASVs occurring only twice (Chao, 1984). The index is well-suited to data sets with a high number of low-abundance ASVs, as is the case with high-throughput amplicon sequencing datasets (Hughes *et al.*, 2001). ASV richness was compared between water masses using a one-way ANOVA with Tukey's HSD. The relationship between ASV richness and environmental variables were investigated using linear models, for bacterioplankton and protist communities, respectively. The relationship between bacterioplankton and protist ASV richness was investigated using a linear model.

Bray-Curtis dissimilarity was used to quantify compositional differences between pairs of samples for both bacterioplankton and protist communities. PERMANOVA analysis (Anderson, 2001), based on Bray-Curtis dissimilarity and implemented through the *adonis* function in the R package 'vegan' (Oksanen *et al.*, 2016), was used to test the differences in community composition between water masses for both bacterioplankton and protist communities. Due to the spatially structured nature of environmental conditions across the Southland Front system, the multivariate regression tree (MRT) method was used to investigate the environmental and spatial features structuring bacterioplankton and protist communities across the region (De'ath, 2002). The MRT method, based on Bray-Curtis dissimilarity between pairs of samples and implemented through the 'mvpart' R package (De'ath, 2002), clusters groups of samples through a series of hierarchical binary splits

based on environmental or spatial features in order to minimize the sum of squared dissimilarity between samples in each resulting cluster. Where multiple parameters could delimit an identical binary split, spatial parameters were given priority. Cross-validation is used to select optimal tree size (minimum cross-validated relative error), and trees are summarized by their size (number of binary splits) and the proportion of variance in community dissimilarity explained (De'ath, 2002). All measured physicochemical variables, and longitude as a spatial variable, were included in the MRT analyses. The technique aims to characterise clusters of similar communities, defined by a series of binary environmental and spatial rules. Finally, the relationship between bacterioplankton and protist community dissimilarity was compared using the mantel test.

The influence of stochastic and deterministic processes on bacterioplankton and protist community assembly was investigated using a null model approach (Stegen *et al.*, 2013, 2015). The approach leverages phylogenetic signal, whereby organisms with close phylogenetic relationships occupy similar environmental niches. In brief, the approach compares observed phylogenetic turnover between pairs of communities to phylogenetic turnover expected under purely stochastic (i.e. null model) community assembly to generate the ßNTI metric. ßNTI > 2 indicates that pairs of communities are less phylogenetically clustered than expected under null model assembly, and that variable selection is the dominant community assembly processes. ßNTI < -2 indicates that pairs of communities are more phylogenetically clustered than expected under null model assembly, and that homogeneous selection is the dominant community assembly process. ßNTI < |2| indicates that phylogenetic clustering between pairs of communities does not deviate from null model expectations, and selection is not the dominant community assembly process. For pairs of communities where ßNTI < |2|, further analysis was performed to partition the influence of dispersal limitation, homogenising dispersal, and an undominated scenario indicating a combination of ecological drift, weak selection, and weak dispersal (Stegen *et al.*, 2015). For these pairs of communities, ASV turnover was quantified using a modified Raup-Crick metric based on Bray-Curtis dissimilarity (RC_{bray}; (Stegen *et al.*, 2013)) and compared to ASV turnover expected under purely stochastic community assembly. $RC_{bray} > 0.95$ indicates that communities had greater ASV turnover than expected, indicating that dispersal limitation was the dominant community assembly process. $RC_{bray} < -0.95$ indicates that communities had less ASV turnover than expected under purely stochastic community assembly, indicating that homogeneous dispersal was the dominant community assembly process. $RC_{bray} < |0.95|$ indicates that ASV turnover does not deviate from null model expectations, and communities are primarily assembled

under the undominated scenario. The relative contribution of variable selection, homogeneous selection, dispersal limitation, homogenising dispersal, and the undominated scenario to overall community assembly was quantified as the proportion of pairwise community comparisons dominated by each process (Stegen *et al.*, 2013). The efficacy of this approach to infer community assembly processes has been demonstrated in previous investigations (Dini-Andreote *et al.*, 2015; Stegen *et al.*, 2015). Whilst the approach identifies the most influential process in shaping communities, the described ecological processes are not mutually exclusive, and it is important to consider that identifying one process as dominant does not indicate the absence of other processes (Stegen *et al.*, 2015).

3.4 Results

3.4.1 Alpha diversity

Bacterioplankton communities displayed greater Chao1 estimated ASV richness in the frontal waters and coastal waters than neighbouring subtropical and subantarctic waters (Tukey's HSD < 0.05; Fig. 3.2a). Bacterioplankton ASV richness did not differ between frontal waters and coastal waters, or between subtropical and subantarctic waters (Tukey's HSD > 0.05). In contrast, protist ASV richness did not significantly differ between water masses (Tukey's HSD > 0.05; Fig. 3.2b). However, protist communities in the subtropical waters were excluded from this analysis due to an insufficient sample size (n = 2). Linear models were used to analyse the relationship between ASV richness and environmental variables in bacterioplankton and protist communities. Bacterioplankton ASV richness was moderately related to salinity (R^2: 0.27, $p < 0.01$), but no other environmental variables. Protist ASV richness was not significant related to any environmental variable ($p > 0.05$). Linear model analysis revealed no significant relationship between bacterioplankton and protist ASV richness across the Southland Front system ($p > 0.05$; Fig. A.5b).

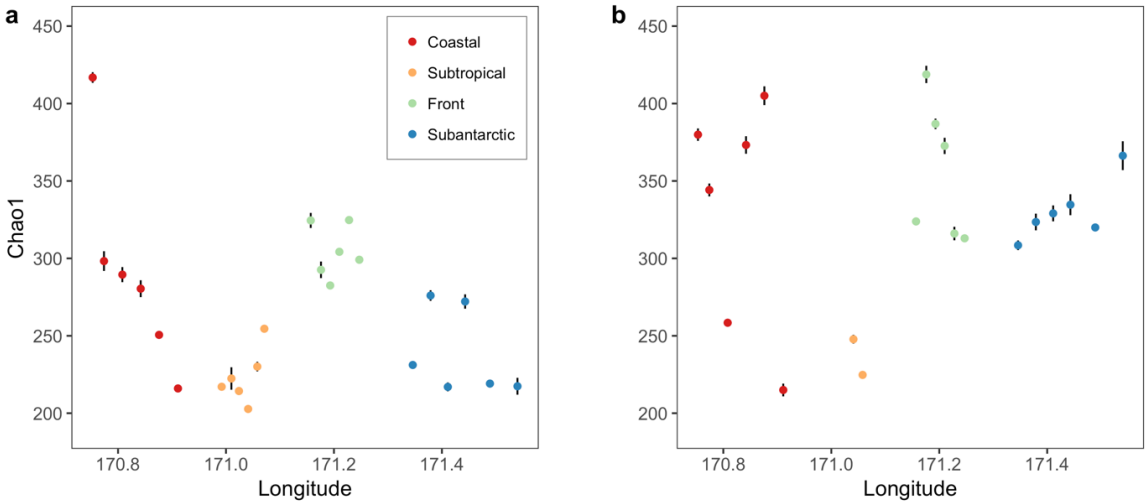

Figure 3.2 (a) Bacterioplankton Chao1 estimated ASV richness and longitudinal position of sampling stations. Error bars indicate error in Chao1 estimated ASV richness. Colours indicate water mass identity. (b) Protist Chao1 estimated ASV richness and longitudinal position of sampling stations.

3.4.2 Community structure

PERMANOVA analysis revealed that bacterioplankton communities significantly differed between all water masses, with the greatest difference being observed between subtropical and subantarctic waters (R^2: 0.95, p = 0.005; Fig. 3.3a; Fig. 3.4a) and the subtlest differences being observed between coastal and subtropical waters (R^2: 0.68, p = 0.005). Similarly, protist communities significantly differed between all water masses, though comparisons with subtropical waters should be interpreted with caution due a limited sample size (n = 2). The magnitude of differences in protist communities (R^2: 0.42-0.62) between water masses was lower than in bacterioplankton communities (R^2: 0.68-0.95). The greatest differences were observed between coastal and subantarctic waters (R^2: 0.62; p = 0.012; Fig. 3.3b; Fig. 3.4c), which are the water masses separated by the greatest geographic distance in the Southland Front system. The subtlest differences were observed between neighbouring coastal and subtropical waters (R^2: 0.42; p = 0.046).

Multivariate regression tree (MRT) analysis revealed the environmental and spatial features structuring bacterioplankton and protist communities across the Southland Front system. The main feature explaining variance in bacterioplankton community composition was longitude, which divided samples east and west of 171.1° longitude, corresponding to the separation of coastal and subtropical waters from front and subantarctic waters (Fig.

3.4b). This division also aligned with the clear division in environmental conditions at this longitude (Fig. 3.3c). Samples west of 171.1° longitude were further divided east and west of 170.8° longitude, corresponding to the separation of coastal and subtropical waters. Samples east of 171.1° longitude were further divided east and west of 171.3° longitude, distinguishing frontal waters from subantarctic waters. MRT analysis explained 93.2% of variance in bacterioplankton community composition, indicating that bacterioplankton community composition closely tracks water masses across the Southland Front system. Similar to bacterioplankton communities, the main feature explaining variance in protist communities was longitude, which divided samples east and west of 171.1° longitude (Fig. 3.4d). Samples of west 171.1° longitude were further divided east and west of 170.9° longitude, whilst samples east of 171.1° longitude were further divided east and west of 171.4° longitude. These binary divisions diverged from trends in bacterioplankton community structure and did not correspond to the complete separation of water masses. MRT analysis explained 77.2% of variance in protist community composition.

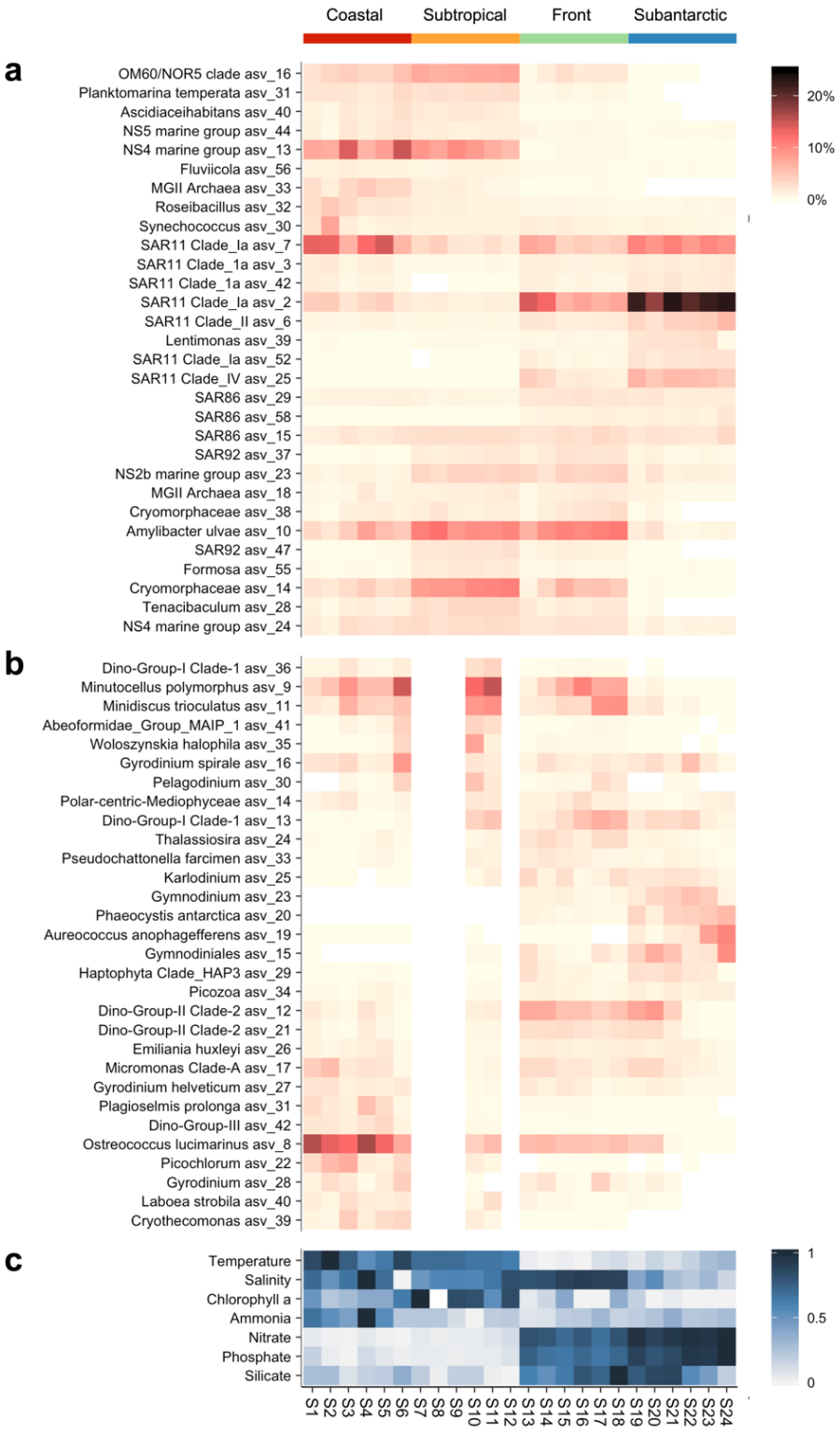

Figure 3.3 Heatmaps showing the structure of (a) the 30 most abundant bacterioplankton taxa, (b) the 30 most abundant protist taxa, and (c) environmental conditions across the Southland Front system. Taxa order is determined according to the neatmap algorithm (Rajaram and Oono, 2010), implemented through phyloseq. (b) Heatmap showing the structure of the 30 most abundant protist taxa. (c) Heatmap displaying variance in environmental conditions across the Southland Front system, using values normalized to 0-1.

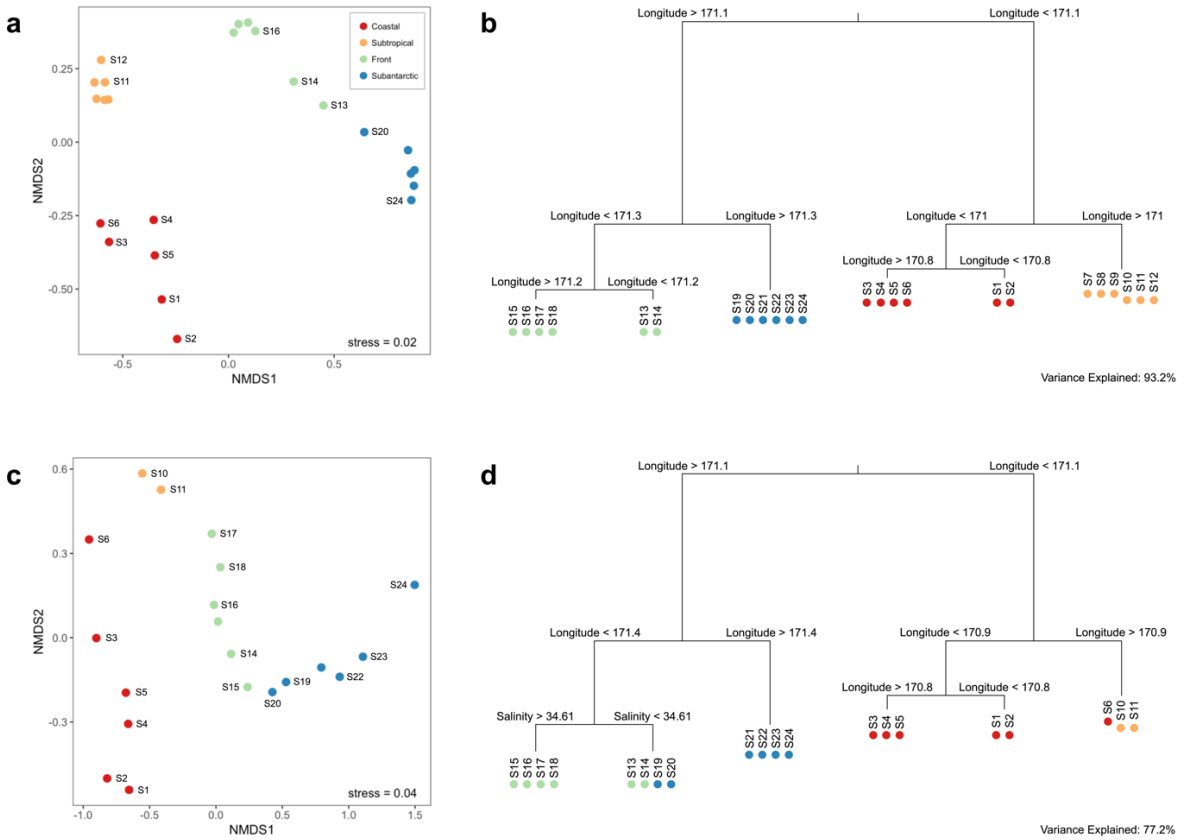

Figure 3.4 (a) Non-metric multidimensional scaling plot of bacterioplankton community composition across the Southland Front system. Labels indicate sampling station, colours indicate water mass identity. (b) Multivariate regression tree analysis indicating hierarchical binary splitting to explain bacterioplankton community structure across the Southland Front system. The depth of each branch is proportional to the variance explained by the preceding split. (c) Non-metric multidimensional scale plot of protist community composition across the Southland Front system. (d) Multivariate regression tree analysis indicating hierarchical binary splitting to explain protist community structure across the Southland Front system.

Linear models based on Bray-Curtis dissimilarity and geographic distance were used to investigate distance-decay relationships in bacterioplankton and protist communities. Both bacterioplankton communities ($R^2 = 0.60$, $p < 0.001$; Fig. 3.5a) and protist communities ($R^2 = 0.76$, $p < 0.001$; Fig. 3.5b) displayed a significant distance-decay relationship, though geographic distance explained a substantially larger proportion of variance in protist community composition than in bacterioplankton community composition.

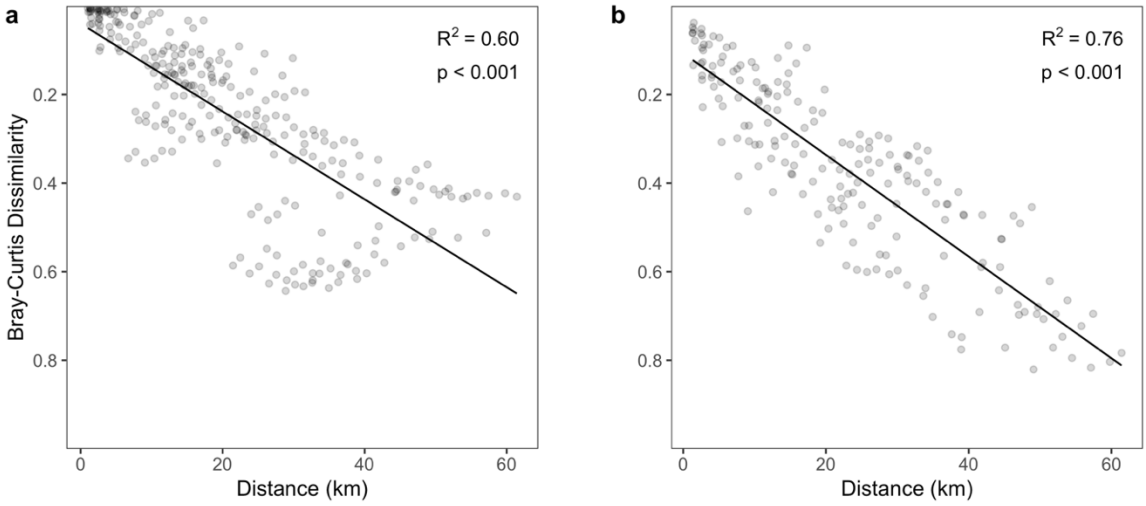

Figure 3.5 (a) Distance-decay relationship of bacterioplankton community composition across the Southland Front system determined by Bray-Curtis dissimilarity (inverse scale). Linear model fit and significance are displayed. (b) Distance-decay relationship of protist community composition across the Southland Front system.

The mantel test was used to quantify the relationship between bacterioplankton and protist community composition across the Southland Front system. There was a significant relationship between bacterioplankton and protist community composition ($r = 0.88$, $p < 0.001$; Fig. A.5a), demonstrating that these groups show broadly similar community structure across the Southland Front system, supporting the findings of non-metric multidimensional scaling and MRT analysis (Fig. 3.4).

3.4.3 Community assembly

A null model approach revealed that homogeneous selection (90.58%; Fig. 3.6) was the dominant bacterioplankton community assembly processes across the Southland Front system, whilst the undominated scenario (6.16%), homogenising dispersal (2.90%), and dispersal limitation (0.36%) were minor influences. In protist communities, dispersal limitation (58.42%) and the undominated scenario (37.37%) were the most influential assembly processes, whilst homogenising dispersal (3.68%) and homogeneous selection (0.53%) were minor influences. Thus, bacterioplankton community assembly was primarily deterministic, and protist community assembly was primarily stochastic, across the Southland Front system.

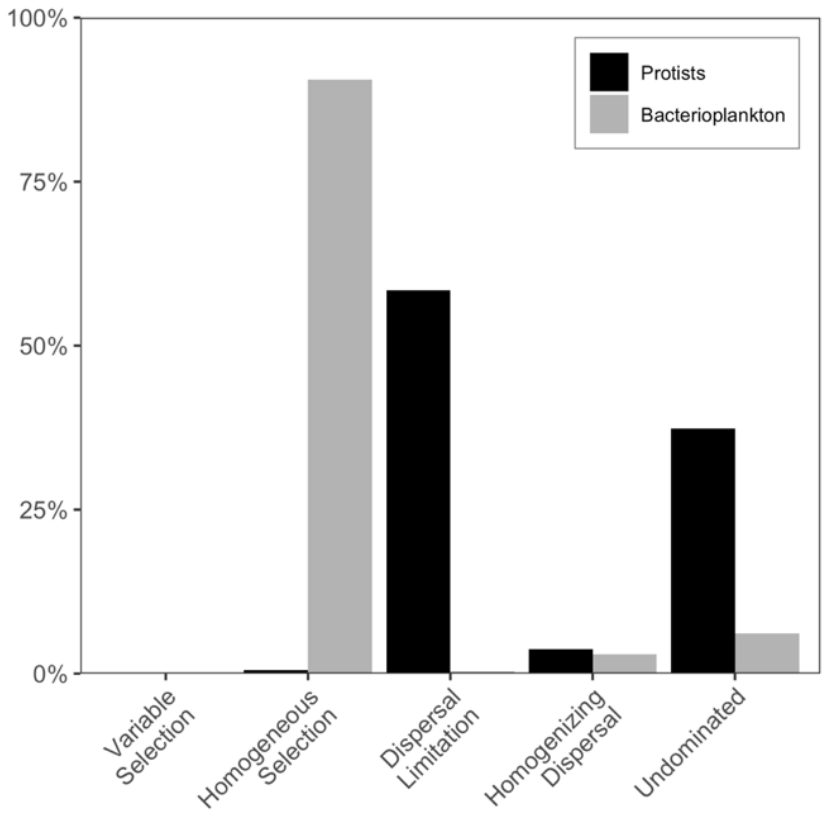

Figure 3.6 Bacterioplankton and protist community assembly processes across the Southland Front system inferred using a null model approach (Stegen *et al.* 2013).

3.5 Discussion

3.5.1 Alpha diversity

Several reports have suggested that oceanic fronts can act as diversity hotspots for both bacterioplankton (Raes *et al.*, 2018) and protist communities (Ribalet *et al.*, 2010; Clayton *et al.*, 2013; Mousing *et al.*, 2016; Raes *et al.*, 2018). However, the magnitude and presence of such effects are not consistent (Mousing *et al.*, 2016; Morales *et al.*, 2018). Two major mechanisms have been suggested to underpin observations of enhanced diversity at oceanic fronts. First, oceanic fronts act as regions where distinct water masses converge, and subsequently distinct bacterioplankton and protist communities have the potential to be physically mixed, enhancing diversity (Mousing *et al.*, 2016; Clayton *et al.*, 2017; Morales *et al.*, 2018). Second, oceanic fronts are frequently associated with increased nutrient concentrations and subsequently enhanced primary production, which may support higher bacterioplankton and protist diversity (Clayton *et al.*, 2014; Raes *et al.*, 2018). In this study, bacterioplankton ASV richness was higher in the frontal waters than in the neighbouring subtropical and subantarctic waters but was not significantly different from ASV richness in the coastal waters (Fig. 3.3a). These findings contrast with previous reports from the Southland Front system, which found no evidence of enhanced bacterioplankton diversity in frontal waters over a long-term time series study (Morales *et al.*, 2018). Two factors are likely to be responsible for the contrasting findings of these studies. First, this study employed a higher spatial resolution, which may have allowed the identification of a bacterioplankton diversity hotspot in the dynamic frontal waters that may have been missed by the long-term time series study. Second, this study used updated Earth Microbiome Project primers to survey bacterioplankton diversity, which more accurately capture the relative abundance and diversity of SAR11 clade Alphaproteobacteria in marine environments (Apprill *et al.*, 2015). SAR11 are important components of bacterioplankton communities across the Southland Front system and are likely to contribute to observed differences between studies. It remains uncertain whether the bacterioplankton diversity hotspot observed in this study persists seasonally, tracking shifts in the strength and position of the front (Morales *et al.*, 2018).

Protist ASV richness did not significantly differ between surveyed water masses (Fig. 3.3b), though subtropical waters were excluded from this analysis. These findings demonstrate that the frontal waters do not harbour enhanced protist diversity, contrasting

with the findings of previous reports from oceanic fronts in other regions (Clayton *et al.*, 2013, 2017; Raes *et al.*, 2018). Enhanced diversity of photosynthetic protists at oceanic fronts reported in previous studies is associated with increased primary production, aligning with global-scale correlations between these parameters (Vallina *et al.*, 2014). However, in this study no evidence of increased primary production in frontal waters was found using chlorophyll *a* as a proxy (Table A.1). Although chlorophyll *a* is frequently used as a proxy of primary production in marine environments, it is not always a good indicator due to the influence of grazing pressure on standing stocks of photosynthetic protists. Nonetheless, these findings suggest that oceanic fronts alone do not enhance protist community diversity, but that previously observed protist diversity hotspots at oceanic fronts may result from specific environmental conditions such as higher nutrient concentrations which can increase primary production.

Interestingly, bacterioplankton and protist diversity are positively correlated across the South Pacific basin, displaying similar trends in tracking oceanic fronts and features (Raes *et al.*, 2018). Moreover, both bacterioplankton and protist diversity were well correlated with chlorophyll *a* concentration (Raes *et al.*, 2018). In this study, no significant relationship between bacterioplankton and protist diversity was found across the Southland Front system (Fig. A.5b). Moreover, neither bacterioplankton or protist diversity were correlated with chlorophyll *a.*

Overall, these findings demonstrate the capacity of oceanic fronts to act as diversity hotspots for bacterioplankton communities, though further investigation is necessary to elucidate whether these trends persist through time. In contrast to previous studies, no evidence of oceanic fronts acting as diversity hotspots for protist communities was found. Differences in environmental conditions and productivity between fronts in different regions and at different spatial scales may underpin differences in observed results.

3.5.2 Community structure

Alphaproteobacteria and Bacteroidetes represented the largest component of bacterioplankton communities in the coastal and subtropical waters (Fig. A.6), where the greatest chlorophyll *a* concentrations were observed (Table A.1). Bacteroidetes are associated with high-productivity marine environments (Buchan *et al.*, 2014) and are important decomposers of algal-derived organic matter (Teeling *et al.*, 2012; Fernández-Gómez *et al.*, 2013). Alphaproteobacteria dominates bacterioplankton communities in the

subantarctic waters, whilst the relative abundance of Bacteroidetes was markedly lower in the subantarctic waters compared with other water masses. These findings may reflect the lower productivity of these environments (Table A.1). Alphaprotebacteria SAR11 Clade Ia ASVs dominated subantarctic waters (Fig. 3.3a). These free-living bacteria are well-adapted to low-productivity environments and are efficient scavengers of dissolved organic substrates (Giovannoni, 2017). Interestingly, the alphaproteobacterial *Amylibacter ulvae* displayed a high relative abundance in subtropical and frontal waters. These recently described bacteria are associated with the macroalgae *Ulva fenestrata* (Nedashkovskaya *et al.*, 2016), but the analysis in this study suggests that they may also play an important role in the surface waters of near-shore marine environments.

Bacterioplankton communities displayed structuring according to water mass across the Southland Front system (Fig. 3.3a), corroborating the findings of previous reports from the region which demonstrate that oceanic fronts act as transition zones, or ecotones, for bacterioplankton communities (Baltar *et al.*, 2016; Morales *et al.*, 2018). Bacterioplankton communities were highly similar within each water mass, but distinct between water masses (Fig. 3.2a, Fig. 3.3a), indicating that each water mass harbours a characteristic bacterioplankton community. The high degree of water mass specificity aligns with the findings of previous studies demonstrating that bacterioplankton communities track water masses across oceanic fronts (Djurhuus *et al.*, 2017; Hernando-Morales *et al.*, 2017), and highlights the important role of sub-mesoscale oceanographic features in structuring bacterioplankton communities.

Chlorophytes were a major component of protist communities in the coastal waters but decreased in relative abundance with increasing distance from the shore (Fig. A.6). In contrast, haptophytes represented a relatively minor component of protist communities in the near-shore coastal and subtropical waters but increased in relative abundance with increasing distance from the shore. Dinoflagellates represented a smaller component of protist communities in the coastal waters than in the subtropical, frontal, and subantarctic waters. Trends in other protist divisions were less pronounced, reflecting significant variation within each water mass (Fig. A.6). *Minutocellus polymorphus* and *Minidiscus trioculatus*, both centric diatom species, were prevalent in the coastal, subtropical, and frontal waters but had a much lower relative abundance in subantarctic waters (Fig. 3.3b). The bloom-forming prymnesiophyte, *Phaeocystis antarctica*, was absent from coastal and subtropical waters but represented a significant component of the protist communities in frontal and subantarctic waters. *Phaeocystis antarctica* is a major contributor to carbon export in the Southern Ocean (Arrigo *et al.*, 1999; Bender *et al.*, 2018). Finally,

Ostreococcus lucimarinus, one of the smallest eukaryotes on earth (Palenik *et al.*, 2007), dominated communities in the coastal waters, explaining the enhanced relative abundance of chlorophytes in these waters, but decreased in relative abundance with increased distance from the shore (Fig. 3.3b). Previous studies have shown *Osterococcus* to be well correlated with chlorophyll *a* concentrations across oceanic fronts, in agreement with the findings of this study (Clayton *et al.*, 2017). Overall, these findings demonstrate transitions between the dominant phytoplankton taxa across the Southland Front system.

Protist communities displayed structuring according to water mass across the Southland Front system. Though communities in each water mass were distinguishable based on PERMANOVA analysis, this effect was much less pronounced than in bacterioplankton communities (Fig. 3.3b; Fig. 3.4c; Fig. 3.4d). These findings build on previous evidence that distinct protist assemblages are separated by oceanic fronts (Ribalet *et al.*, 2010; Taylor *et al.*, 2012; Clayton *et al.*, 2014, 2017) by demonstrating the influence of water masses on protist community structure.

Protist communities displayed a stronger distance-decay relationship than bacterioplankton communities (Fig. 3.5). Distance-decay relationships are classical biogeographic patterns, which are associated with the influence of stochastic processes (i.e. dispersal limitation and ecological drift) on community assembly (Hanson *et al.*, 2012). Stronger distance-decay relationships indicate that communities become more dissimilar with increasing distance, as a result of dispersal limitation and ecological drift. However, the use of distance-decay as a proxy of dispersal probability has recently been challenged in marine environments, with water mass mixing suggested as a superior alternative (Hernando-Morales *et al.*, 2017). Indeed, further studies explicitly quantifying mixing between waters masses would contribute towards better understanding the role of oceanic fronts in structuring bacterioplankton and protist communities.

3.5.3 Community assembly

The emergent differences between bacterioplankton and protist community structure over the Southland Front system are the result of differences in community assembly processes between these groups. Bacterioplankton were primarily assembled through deterministic processes, whilst protist communities were primarily assembled through stochastic processes (Fig. 3.6). These findings align with a previous study comparing bacterioplankton and protist community assembly in Antarctic marine and freshwater

environments (Logares *et al.*, 2018), but contrast with other work from coastal marine environments which suggested that deterministic processes play a greater role in structuring protist communities as protists are generally less phenotypically plastic than bacterioplankton (Wu *et al.*, 2017a). Furthermore, the dominance of deterministic processes in structuring bacterioplankton communities across the hydrodynamic Southland Front system adds to previous evidence from hyporheic environments demonstrating that deterministic processes remain influential in structuring bacterioplankton communities in hydrodynamically complex and interconnected systems (Graham *et al.*, 2017).

The distinct community assembly processes observed between bacterioplankton and protists may stem from fundamental differences in the community characteristics of these groups. In general, bacterioplankton have smaller cells and larger community sizes (number of individuals) than protists. The relative influence of stochastic processes on community assembly is inversely related to the total number of individuals in the community, as larger community sizes decrease the probability of species loss through ecological drift (Orrock and Watling, 2010). Consequently, stochastic processes should have a lesser effect on bacterioplankton communities, compared with protist communities. Moreover, cell size is inversely related to dispersal ability in passively dispersing aquatic organisms (De Bie *et al.*, 2012; Soininen *et al.*, 2013). Higher dispersal rates increase the effective size of a community, decreasing the influence of stochastic processes on community assembly (Ron *et al.*, 2018). Thus, the smaller cell sizes of bacterioplankton may further contribute to the comparatively weaker influence of stochastic processes when compared with protist communities. Overall, local bacterioplankton communities are seldom influenced by dispersal effects and ecological drift, as the selection pressure of local environmental conditions overwhelms these processes. In contrast, local protist communities are significantly influenced by dispersal limitation and ecological drift as selection pressure is not sufficient to overwhelm these processes (Fig. 3.6).

3.5.4 Bacterioplankton-protist community relationship

The distinct community assembly processes which structure bacterioplankton and protist communities across the Southland Front system highlight the potential decoupling of these communities over hydrodynamic regions such as oceanic fronts. Despite differences in the structure of bacterioplankton and protist communities, the composition of these communities remained well coupled across the Southland Front system (i.e. Fig. A.5a).

Bacterioplankton and protists form important interactions in the marine environment, as symbionts, parasites, and community service providers (Lima-Mendez *et al.*, 2015; Seymour *et al.*, 2017). Indeed, disruption of bacterioplankton-protist interactions across oceanic fronts could have implications for regional primary production and biogeochemical cycling. Interestingly, the coupling of bacterioplankton and protist communities across the Southland Front system highlights the potential of using the region to screen for bacterioplankton-protist interactions which persist through a range of environmental conditions. The importance of bacterioplankton-protist interactions has been increasingly recognised (Lima-Mendez *et al.*, 2015; Seymour *et al.*, 2017) and calls for new approaches towards identifying putative interactions. Oceanic fronts may provide a valuable resource in this context.

3.5.5 Conclusions

In this study, bacterioplankton and protist diversity and community structure was surveyed across the Southland Front system. I found that frontal waters can act as diversity hotspots for bacterioplankton communities but found no evidence of this effect in protist communities. Bacterioplankton and protist communities were both structured according to water masses, though this effect was more pronounced in bacterioplankton communities. Bacterioplankton were primarily assembled through deterministic processes, whilst protist communities were primarily assembled through stochastic processes across the region. I suggest that these distinct community assembly mechanisms are the result different characteristics of bacterioplankton and protist communities, including the total number of individuals in a community, average cell size, and community turnover rates. Overall, these findings contribute to a growing body of evidence demonstrating that sub-mesoscale oceanographic fronts and features play a substantial role in structuring bacterioplankton and protists communities. Consequently, such features should be explicitly considered in attempts to resolve the factors which underpin the abundance and distribution of bacterioplankton and protists through space and time in the marine environment, calling for further exploration of these trends at the interface between physics and biology.

Chapter 4: Bacterial community responses to elevated CO_2 and warming in the oligotrophic South Pacific Gyre

Co-authors of the manuscript: Linn Hoffmann, Cliff Law, Tina Summerfield

Chapter 4: Bacterial community responses to elevated CO_2 and warming in the oligotrophic South Pacific Gyre

4.1 Abstract

Bacteria play a critical role in primary production, carbon cycling, and nutrient cycling in the oligotrophic open ocean. To investigate the effect of elevated CO_2 and warming on the composition and function of bacterial communities in oligotrophic waters, two trace-metal clean deck board incubation experiments were performed during the 2011 New Zealand GEOTRACES transect of the South Pacific Gyre (SPG). High-throughput amplicon sequencing of the 16S rRNA gene revealed that bacterial community composition was distinct between the fringe and ultra-oligotrophic centre of the SPG, and changed consistently between replicates in response to elevated CO_2 at the ultra-oligotrophic centre but not at the fringe of the SPG. Bacterial community composition was not affected consistently between replicates by the combined effects of elevated CO_2 and warming in the SPG, suggesting an antagonistic response in contrast to previous studies. Protein synthesis rates (^{3}H-Leucine incorporation) and bacterial abundance were not affected by elevated CO_2 alone or in combination with warming, whereas DNA synthesis rates (^{3}H-Thymidine incorporation) were enhanced by elevated CO_2 and warming. These data suggest bacterial community responses to elevated CO_2 may be modulated by nutrient regimes, as bacterial communities differed in response between the fringe and the ultra-oligotrophic centre of the SPG.

4.2 Introduction

Oligotrophic subtropical gyres cover approximately 41% of earth's ocean area, and account for 22% of total marine primary production (Hoegh-Guldberg and Poloczanska, 2017). These gyres are expanding globally, as a result of ocean warming, and are likely to play an increasingly important role in marine carbon cycling (Polovina *et al.*, 2008, 2011). The South Pacific Gyre (SPG) is the largest oligotrophic subtropical gyre, and possesses the lowest marine chlorophyll concentrations recorded globally (Claustre and Maritorena, 2003). Primary production in the surface waters of the SPG is limited by the supply of nitrogen and secondarily by the supply of iron (Bonnet *et al.*, 2008; Ellwood *et al.*, 2018), which decrease from the oligotrophic fringe to the ultra-oligotrophic centre of the gyre (Ellwood *et al.*, 2018). The precise role of the SPG in global carbon cycling remains a subject of debate, though in-situ estimates suggest that the region is responsible for significant carbon fixation on a global scale and may act as a net sink for CO_2 (Claustre *et al.*, 2008; Duarte *et al.*, 2013; Williams *et al.*, 2013).

Marine bacteria play a fundamental role in oligotrophic subtropical gyres, and are instrumental in the recycling of carbon and nutrients, where these processes underpin biogeochemical cycles and primary production (Azam and Malfatti, 2007). The cyanobacteria *Prochlorococcus* and *Synechococcus* are the numerically dominant primary producers in these regions, with the vast majority of fixed carbon passing through the microbial loop, where organic matter is recycled through assimilation and respiration by heterotrophic bacteria (Azam *et al.*, 1983; del Giorgio and Duarte, 2002). Only a small proportion of organic matter escapes the microbial loop and is exported to the deep ocean for long-term sequestration (Raven and Falkowski, 1999).

The role of bacterial communities in oligotrophic subtropical gyre carbon cycling is closely related to their taxonomic composition (Guidi *et al.*, 2016). Bacterial community composition (BCC) is predominantly controlled by environmental factors, many of which are in flux as a result of anthropogenic climate change (Hutchins and Fu, 2017). The dissolution of rapidly accumulating atmospheric CO_2 into the ocean has driven a decrease in mean surface ocean pH of 0.1 units since the pre-industrial era, whilst the greenhouse effect of CO_2 has simultaneously increased sea surface temperatures (Hoegh-Guldberg *et al.*, 2014). Further acidification of 0.3 pH units and warming of 3ºC is projected by 2100 under business-as-usual anthropogenic emissions scenarios (Hoegh-Guldberg *et al.*, 2014). Joint *et al.* (2011) hypothesised that bacterial communities would be resistant to elevated

CO_2, due to the variability in marine pH and pCO_2 which they experience across multiple time-scales. In contrast, temperature modulates a range of bacterial processes (Pomeroy and Wiebe, 2001) and is a significant explanatory factor of bacterial biogeography in the SPG (Walsh *et al.*, 2015). As a result, bacterial communities in the SPG may be affected by warming. To date, CO_2 manipulation studies in the Arctic Ocean (Newbold *et al.*, 2012; Roy *et al.*, 2013; Zhang *et al.*, 2013; Oliver *et al.*, 2014; Hartmann *et al.*, 2016; Wang *et al.*, 2016), Ross Sea (Maas *et al.*, 2013), Baltic Sea (Lindh *et al.*, 2013; Bergen *et al.*, 2016), Mediterranean Sea (Baltar *et al.*, 2015a), and Pacific Ocean (Burrell *et al.*, 2017) have found negligible or weak effects of elevated CO_2 on BCC. However, the combined effects of elevated CO_2 and warming have consistently been shown to alter the composition and function of bacterial communities in high-latitude regions (Lindh *et al.* 2013; Bergen *et al.*, 2016).

Despite the prominent role of oligotrophic subtropical gyres in global carbon cycling (Hoegh-Guldberg and Poloczanska, 2017), and their global expansion (Polovina *et al.*, 2008), the effects of elevated CO_2 and warming on BCC remain to be investigated in these regions. pH conditions in the SPG are highly stable (Doney *et al.*, 2009), thus bacterial communities are not exposed to the environmental variability which underpins the hypothesis of resistance posited by Joint *et al.* (2011). Furthermore, marine heterotrophic bacteria are highly diverse and often associated with specific nutrient regimes, making it difficult to generalize responses between ocean regions (Hutchins and Fu, 2017). Indeed, the physiological and functional responses of bacterial communities to elevated CO_2 have previously been shown to be more pronounced under low-nutrient conditions (Bunse *et al.*, 2016; Sala *et al.*, 2016). Consequently, bacterial communities in the SPG may respond differently to elevated CO_2 and warming than those in high-latitude or coastal regions. This represents a significant gap in our understanding of how marine microbial communities are likely to respond to oceanic climate change on a globally relevant scale.

Here, the findings of two deck board incubation experiments which aim to characterise the compositional and functional response of bacterial communities to elevated CO_2 and warming at the oligotrophic fringe and at the ultra-oligotrophic centre of the SPG are reported (Fig. 4.1). In each experiment, surface water was maintained under control (ambient temperature, pH 8.1), high CO_2 (ambient temperature, pH 7.8), and greenhouse (ambient temperature +3°C, pH 7.8) conditions for five days to discriminate between the impacts of ocean acidification alone, and combined with elevated temperature. Importantly, these experiments were performed under trace-metal clean conditions to avoid incidental

iron fertilisation, which can alter bacterial communities in the region (Bonnet *et al.*, 2008; Law *et al.*, 2011). Community composition was investigated using high-throughput amplicon sequencing of the 16S rRNA gene, this data was coupled with flow-cytometry and bacterial secondary production data to investigate the functional response of bacterial communities to these environmental perturbations.

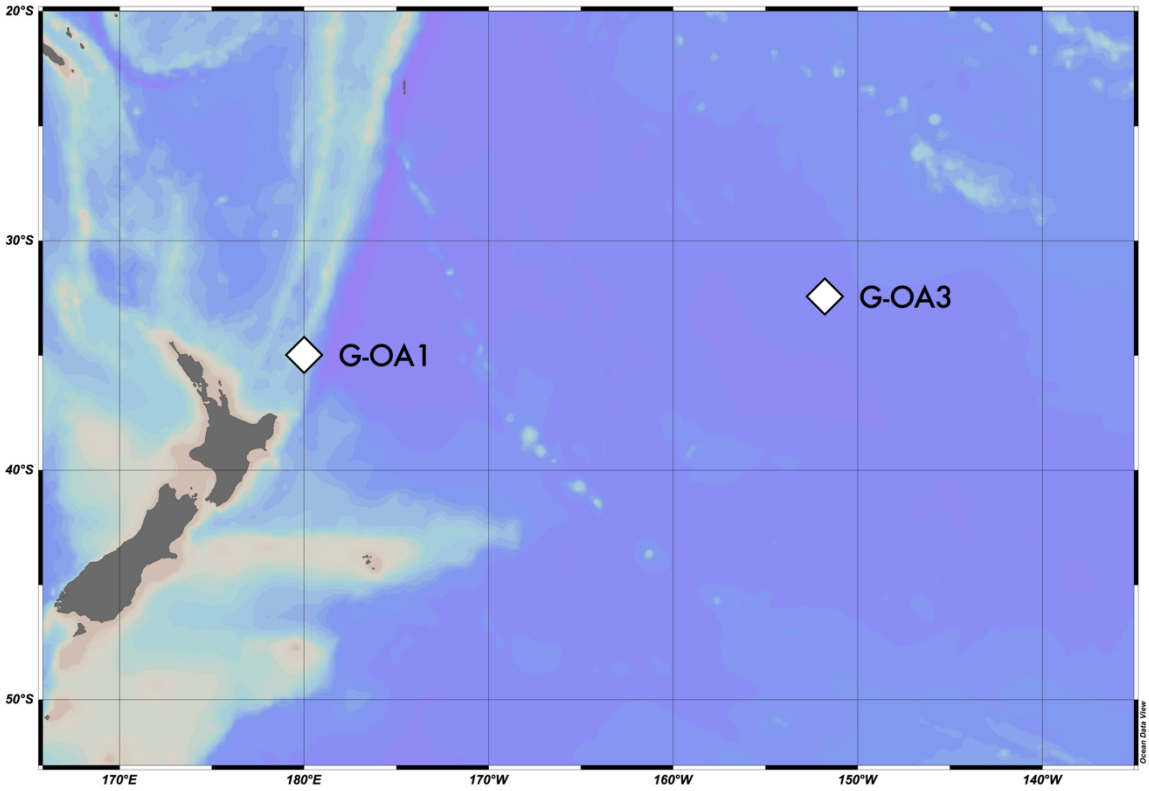

Figure 4.1 The South Pacific Ocean to the east of New Zealand. White diamonds indicate the positions of samples sites at the fringe of the SPG (G-OA1) and the ultra-oligotrophic centre of the SPG (G-OA3).

4.3 Methods

4.3.1 Experimental setup

Two trace-metal clean incubation experiments were performed aboard the *RV Tangaroa* during the New Zealand GEOTRACES transect of the SPG. Seawater for experiment G-OA1 was collected from the oligotrophic fringe of the SPG at 35ºS 180ºW, on 8 June 2011. Seawater for experiment G-OA3 was collected from the ultra-oligotrophic centre of the SPG at 32º 26.4'S 152ºW, on 21 June 2011 (Fig. 4.1). The incubation system setup is described in detail by Law *et al.* (2012). In brief, nine 22 L flexible polyethylene cubitainers were filled with seawater sampled from 25-30 m using a Teflon diaphragm pump. Cubitainers were filled non-sequentially inside a trace-metal clean positive pressure tent, to maximise homogeneity between replicates and prevent trace-metal contamination. After filling, cubitainers were transferred to a thermostatically controlled deck board incubation unit, and maintained at either surface seawater temperature, or surface seawater temperature +3℃ (±0.5 ℃; Table 4.1) to simulate conditions projected in the region at 2100 under 'business as usual' emissions scenarios (Law *et al.*, 2017). Light intensity within the deck board incubation unit was 25% of external PAR. All equipment used in the experimental incubation was acid-washed and thoroughly rinsed with Milli-Q according to standard trace-metal clean practices.

To investigate the effect of elevated CO_2 and warming on bacterial communities, triplicate cubitainers were dedicated to each of three experimental treatments, control, high CO_2, and greenhouse (Table 4.1). Initially, CO_2 concentrations were adjusted by the diffusion of pure CO_2 gas through permeable silicon tubing in each cubitainer (as described in Hoffmann *et al.*, 2013). Pure CO_2 was then substituted for 750 ppmv CO_2 in air to maintain stable target conditions, selected to simulate projected atmospheric CO_2 concentrations in the region at 2100 (Law *et al.*, 2017). pH_T was used as an indicator of pCO_2 and was monitored throughout the experiment using an automated spectrophotometric system (Mcgraw *et al.*, 2010; Law *et al.*, 2012).

Samples were collected from each cubitainer after an 18-24h pH_T adjustment period (Day 1) and at Day 5. Cubitainers were transferred to a laminar flow hood within the trace-metal clean positive pressure tent where sampling was conducted without the introduction of headspace. Cubitainers were then returned to the deck board incubation units. One cubitainer from the greenhouse treatment in experiment G-OA1 was compromised, and subsequently excluded from analysis.

Table 4.1 Details of experiments G-OA1 and G-OA3, including temperature and pH conditions within the cubitainers over the course of the incubation period. Adapted from Law *et al.* (2012).

Experiment	Date	Location	Treatment	Temperature	pH (s.d.)
G-OA1	08/06/2011	35°S 180°W	Control	18.1 °C	8.097 (0.005)
			High CO_2	18.1 °C	7.895 (0.005)
			Greenhouse	21.1 °C	7.864 (0.007)
G-OA3	21/06/2011	32 26.4°S 152°W	Control	19.1 °C	8.120 (0.006)
			High CO_2	19.1 °C	7.877 (0.009)
			Greenhouse	22.1 °C	7.856 (0.006)

4.3.2 DNA sampling, extraction, and PCR

At Day 1 and Day 5 in experiment G-OA1 and G-OA3, 1.5 L water samples were collected from each cubitainer and filtered through 0.2 µm polyethersulfone filters. Filters were immediately snap-frozen in liquid nitrogen and stored in a -80℃ freezer. Prior to DNA extraction, filters were fragmented using a sterile glass rod. Genomic DNA was extracted from each fragmented filter using the DNEasy Plant Mini kit (Qiagen, Valencia, CA, USA) according to the manufacturer's protocol. One filter from the high CO_2 treatment at Day 1 of G-OA3 was lost. The V4 hypervariable region of the 16S rRNA gene was amplified by PCR from genomic DNA using the universal 16S primers 515F (5' GTGCCAGCMGCCGCGGTAA) and 806R (5' GGACTACHVGGGTWTCTAAT) (Caporaso *et al.*, 2011), modified with an overhang region complementary to Illumina sequencing adapters (Griffith *et al.*, 2017). For each sample, triplicate 25 µl PCR reactions mixes were prepared with the HiFi Hotstart PCR kit (KAPA Biosystems, Boston, MA, USA) and contained 1 X KAPA HiFi buffer (2 mM $MgCl_2$), 0.3 mM KAPA dNTP Mix, 0.3 µM of forward and reverse primers, and 0.5 U KAPA HiFi Hotstart DNA Polymerase. PCR reactions were performed using the following protocols: initial denaturation at 95 °C 120 s, followed by 25 cycles of denaturation at 98 °C for 20 s, annealing at 60 °C for 30 s, and extension at 72 °C for 30 s, with a final extension period of 60 s at 72 °C. Resulting triplicate PCR products for each sample were pooled, and subjected to a second round of PCR to attach Illumina sequence adapters and indexes according to the following protocols: initial denaturation at 95 °C for 120 s, followed by 10 cycles of denaturation 98 °C for 20 s, annealing at 60 °C for 20 s, and extension at 72 °C for 20 s, with a final extension period of 60 s at 72 °C. The PCR products were purified after each round of PCR using the Mag-

bind TotalPure NGS kit (OMEGA Bio-tek, Norcross, GA, USA) according to the manufacturer's instructions. After the first round, purified amplicons were quantified using the Qubit dsDNA High Sensitivity Assay (Thermo Fisher Scientific) and diluted to 1 ng μl^{-1} for the second round of PCR. Following the second round of PCR and purification, the amplicons were quantified and pooled for sequencing on the Illumina MiSeq platform using the V2 reagent kit, yielding 2 x 250 bp paired-end reads (Illumina, San Diego, CA, USA).

4.3.3 Sequence processing

From 33 samples, a total of 1,745,501 paired-end reads were returned and processed according to the Bioconductor workflow (Callahan *et al.*, 2016). Paired-end reads were trimmed and truncated to remove primer sequences and low-quality sequences, respectively (forward reads: retained nucleotides corresponding to positions 20-240, reverse reads: retained nucleotides corresponding to positions 19-181). A quality control filter was applied, and reads with more than two expected errors were removed. DADA2 was used to resolve amplicon sequence variants (ASVs) at single nucleotide resolution (Callahan *et al.*, 2016), rather than conventional clustering based on 97% similarity. Exact ASVs resolved by DADA2 increase the accuracy and reproducibility of amplicon sequencing studies (Callahan *et al.*, 2017). Paired-end reads were then merged, and putative ASVs were screened for chimeras. Sequences determined to be chimeric were removed using the *removeBimeraDenovo* function in the 'DADA2' R package. Taxonomic assignment was performed against the SILVA database (version 132; Quast *et al.*, 2013) using the Ribosomal Database Project's naïve Bayesian classifier implemented through the 'DADA2' R package (Wang *et al.*, 2007). 16S rRNA gene amplicon read counts, taxonomic assignments, and associated metadata were combined as an object in the R package 'phyloseq' (McMurdie and Holmes, 2013). ASVs which were not classified as bacteria, or had fewer than 5 reads in a minimum of two samples in either experiment G-OA1 or G-OA3, were excluded. Samples were rarefied to an even depth of 38,691 and 9,819 reads for experiments G-OA1 and G-OA3, respectively. Prior to statistical analyses, data were segregated by experiment and time. All sequence processing was performed in the R environment (R Core Team, 2013) and annotated scripts are available at https://github.com/ro-allen/geotraces_experiment. These sequence data have been submitted to the EMBL database under accession number PRJEB29087.

4.3.4 Bacterial community composition

Analyses of BCC were performed independently for each time point in experiments G-OA1 and G-OA3. To investigate patterns in alpha-diversity, Faith's Phylogenetic Diversity (Faith, 1992) was calculated for each sample. The effect of treatment on Faith's Phylogenetic Diversity was analysed using a one-way ANOVA with Tukey's HSD (α = 0.05). To investigate patterns in beta-diversity, weighted UniFrac (Lozupone and Knight, 2005) was used to calculate a pairwise dissimilarity matrix based on ASV read counts and a maximum-likelihood phylogenetic tree constructed in the R package 'phangorn' (Schliep, 2011). The weighted UniFrac dissimilarity matrix was used as an input for PERMANOVA analyses (Anderson, 2001) implemented using the *adonis* function in the R package 'vegan' (Oksanen *et al.*, 2016), to test differences in BCC between treatments (α = 0.05). Homogeneity of dispersal, a key assumption of PERMANOVA (Anderson and Walsh, 2013), was tested using the *betadisper* function in the R package 'vegan' prior to analysis. There was no significant difference in dispersal between treatments at any time point in either G-OA1 and G-OA3 ($p > 0.05$).

4.3.5 Bacteria and picophytoeukaryote cell density

To determine the cell density of bacteria and picophytoeukaryotes, triplicate 3 ml samples were collected from each cubitainer at Day 1 and Day 5 of experiment G-OA1 and G-OA3 and immediately frozen in liquid nitrogen for later analysis by flow cytometry (Law *et al.*, 2012). To determine total bacterial cell density, the SYBRGreenII nucleic acid stain (Invitrogen, Calsbad, CA, USA) was used with a dark incubation period of 10 minutes to allow bacterial cells to be differentiated from other particles (Maas *et al.*, 2013). Natural chlorophyll *a* fluorescence was used to determined picophytoeukaryote cell density (Maas *et al.*, 2013). The mean cell density derived from triplicate 3 ml samples was carried forward for statistical analysis, to avoid pseudo-replication. Cell density data were analysed using a one-way ANOVA with Tukey's HSD (α= 0.05).

4.3.6 Bacterial secondary production

Bacterial secondary production was determined by ^{3}H-leucine incorporation and ^{3}H-thymidine incorporation using the TCA precipitation and centrifugation methodology described in Knap *et al.* (1996) and Smith and Azam, (1992). ^{3}H-leucine incorporation was used as a proxy for protein synthesis, whilst ^{3}H-thymidine incorporation was used as a proxy for DNA synthesis (Knap *et al.*, 1996). Triplicate incubations were performed under dark conditions simultaneously for each cubitainer for a minimum 3.8-hour period. ^{3}H-thymidine incorporation (mols) was converted to cell number according to Smith and Hall, (1997) estimates of 2.4×10^{18} cells mol^{-1} in open ocean environments. This value was then converted to a carbon value according to 20×10^{-15} g C cell^{-1} (Cho and Azam, 1988). ^{3}H-Leucine incorporation (mols) was converted to bacterial protein production (g) according to the following equation:

$$\text{Bacterial protein production (g)} = \text{Leucine incorporation (mols)} \times 1797 \times 2$$

The resulting value was then multiplied by 0.86 to generate a carbon value (Azam and Simon, 1989). Bacterial secondary production data were analysed using a one-way ANOVA with Tukey's HSD ($\alpha = 0.05$).

4.4 Results

4.4.1 Bacterial community composition

High-throughput amplicon sequencing of part of the 16S rRNA gene was used to characterise BCC at Day 1 and Day 5 of each deck board incubation experiment. At the oligotrophic fringe of the SPG (G-OA1), at Day 1, Bacteroidetes (21.19-38.87%) and Alphaproteobacteria (17.98-34.52%) were dominant across all treatments, followed by Gammaproteobacteria (10.36-15.65%), Cyanobacteria (7.79-15.21%), and Planctomycetes (6.37-12.39%; Fig. 4.2). At the level of specific amplicon sequence variants (ASVs), bacterial communities were dominated by the Alphaproteobacterial *AEGEAN-169_marine_group* asv_2 (4.41-14.53%), whilst a range of ASVs belonging to Bacteroidetes, Cyanobacteria, Planctomycetes, Alphaproteobacteria,

Gammaproteobacteria, and Verrucomicrobia, were also common (> 1%, Fig. 4.3). At Day 5, Bacteroidetes (30.45-42.42%) remained dominant. The relative abundance of Alphaproteobacteria decreased (6.84-11.43%), whilst the proportion of reads classified as Planctomycetes (10.08-28.61%) and Cyanobacteria (11.12-19.43%) increased. *NS2b_marine_group* asv_3 (3.48-13.74%), *CL500-3* asv_4 (3.25-11.89%), and *Prochlorococcus_MIT9313* asv_1 (3.40-7.73%) were the most common ASVs. There was no significant difference in BCC between treatments at either Day 1 or Day 5 in experiment G-OA1 (PERMANOVA, $p > 0.05$, Table A.2; Fig. 4.4).

At the ultra-oligotrophic centre of the SPG (G-OA3), Cyanobacteria (31.46-40.08%), Alphaproteobacteria (17.05-25.44%), and Gammaproteobacteria (10.05-17.31%) displayed the highest relative abundance, followed by Bacteroidetes (6.84-14.95%) and Chloroflexi (5.53-12.62%), across all treatments at Day 1 and Day 5. *Prochlorococcus_MIT9313* asv_1 (16.65-21.76%) was the dominant ASV in all samples, whilst *AEGEAN-169_marine_group* asv_2 (3.39-9.46%), *SAR202_clade* asv_18 (2.74-7.21%), and *Prochlorococcus_MIT9313* asv_24 (3.70-5.06%) were also common. At Day 5 in experiment G-OA3, the relative abundance of Bacteroidetes was higher in the control treatment than in the high CO_2 treatment (control: 13.2 % (±0.42), high CO_2: (7.55% (±0.61), ±1 SD). This difference was influenced by the relative abundance of the Flavobacteriaceae *NS2b_marine_group* asv_3 (control: 2.31% (±0.24), high CO_2: 1.36% (±0.22)) and *NS4_marine_group* asv_10 (control: 1.19% (±0.10), high CO_2: 0.64% (±0.03)). Similarly, the relative abundance of Actinobacteria was higher in the control treatment compared to the high CO_2 treatment (control: 2.43% (±0.60), high CO_2: 1.58% (±0.12)), driven by a lower relative abundance of *Candidatus_Actinomarina* asv_9 (control: 1.67% (±0.27), high CO_2: 1.22% (±0.15)). In contrast to these trends in Bacteroidetes and Actinobacteria, the relative abundance of Cyanobacteria (control: 34.80% (±2.45), high CO_2: 38.91% (±1.30)) and Gammaproteobacteria (control: 13.96% (±0.33), high CO_2: 17.01% (±0.31)) were lower in the control treatment than in the high CO_2 treatment. Trends in Cyanobacteria were driven by *Prochlorococcus_MIT9313* asv_1 (control: 18.91% (±0.98), high CO_2: 21.15% (±0.65)), whilst trends in Gammaproteobacteria were influenced by *SAR86_clade* asv_60 (control: 0.89% (±0.02), high CO_2: 1.42% (±0.14)) and other *SAR86_clade* ASVs. At Day 5 in experiment G-OA3, there was a significant treatment effect on BCC (PERMANOVA, $p = 0.037$, Table A.2; Fig. 4.4). Experimental design precluded pairwise testing; however, principle coordinates analysis (Fig. 4.4D) revealed clear clustering and centroid differentiation between the control and high CO_2 treatments, whilst the greenhouse treatment was highly variable.

Faith's PD, a phylogenetic diversity metric, revealed no significant difference in phylogenetic diversity of bacterial communities between treatments at ether Day 1 or Day 5 in experiment G-OA1 or G-OA3 (Tukey's HSD, $p > 0.05$)

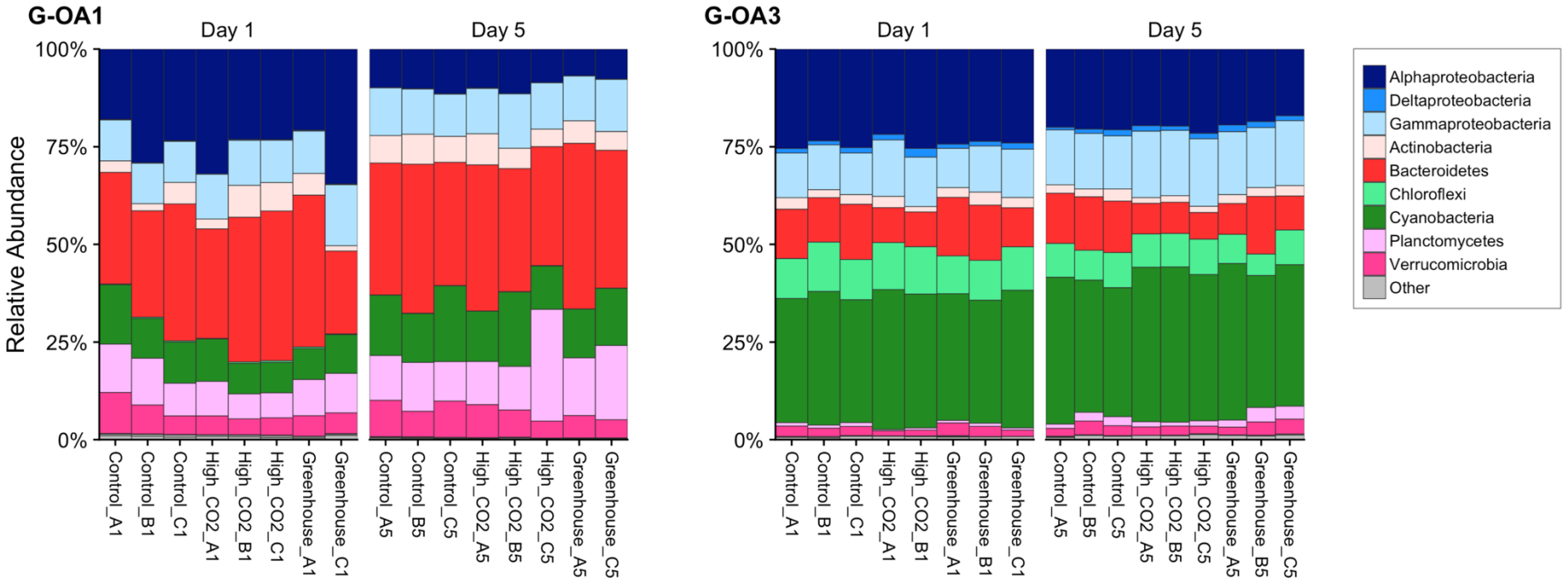

Figure 4.2 Stacked bar plot of bacterial community composition in experiment G-OA1 (left) and G-OA3 (right). Bacteria are grouped by Phylum, except Proteobacteria which are divided into their respective classes. Phyla representing < 1% of total reads are grouped as 'Other'.

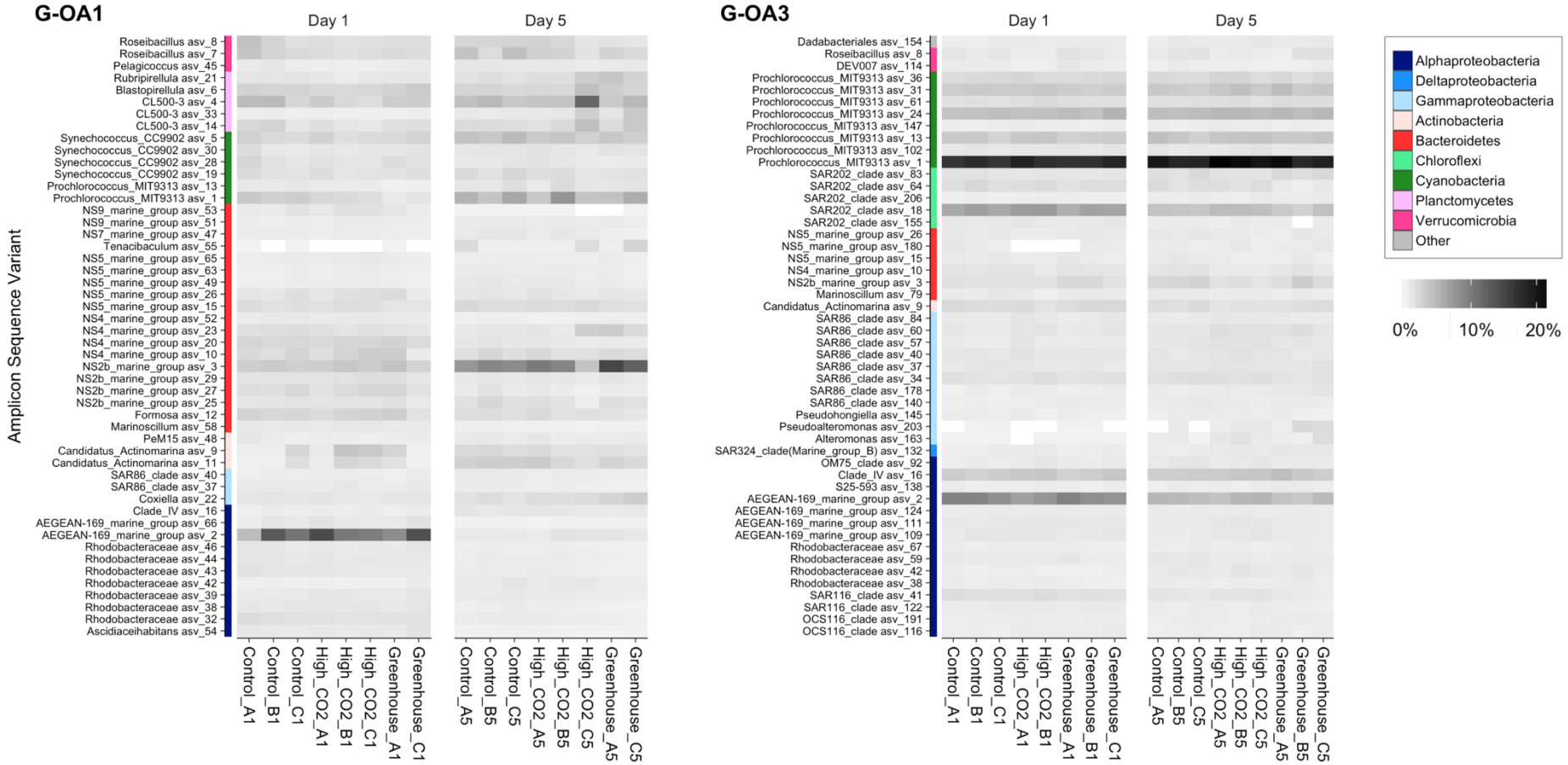

Figure 4.3 Heatmap of the 50 most abundant ASVs in bacterial communities at Day 1 and Day 5 of experiments G-OA1 (left) and G-OA3 (right). Rows correspond to unique ASVs and columns correspond to individual samples. Taxa order is determined according to the neatmap algorithm (Rajaram and Oono, 2010). The colours aligned with the ASV labels indicates the phylum (or Proteobacterial class) of each ASV.

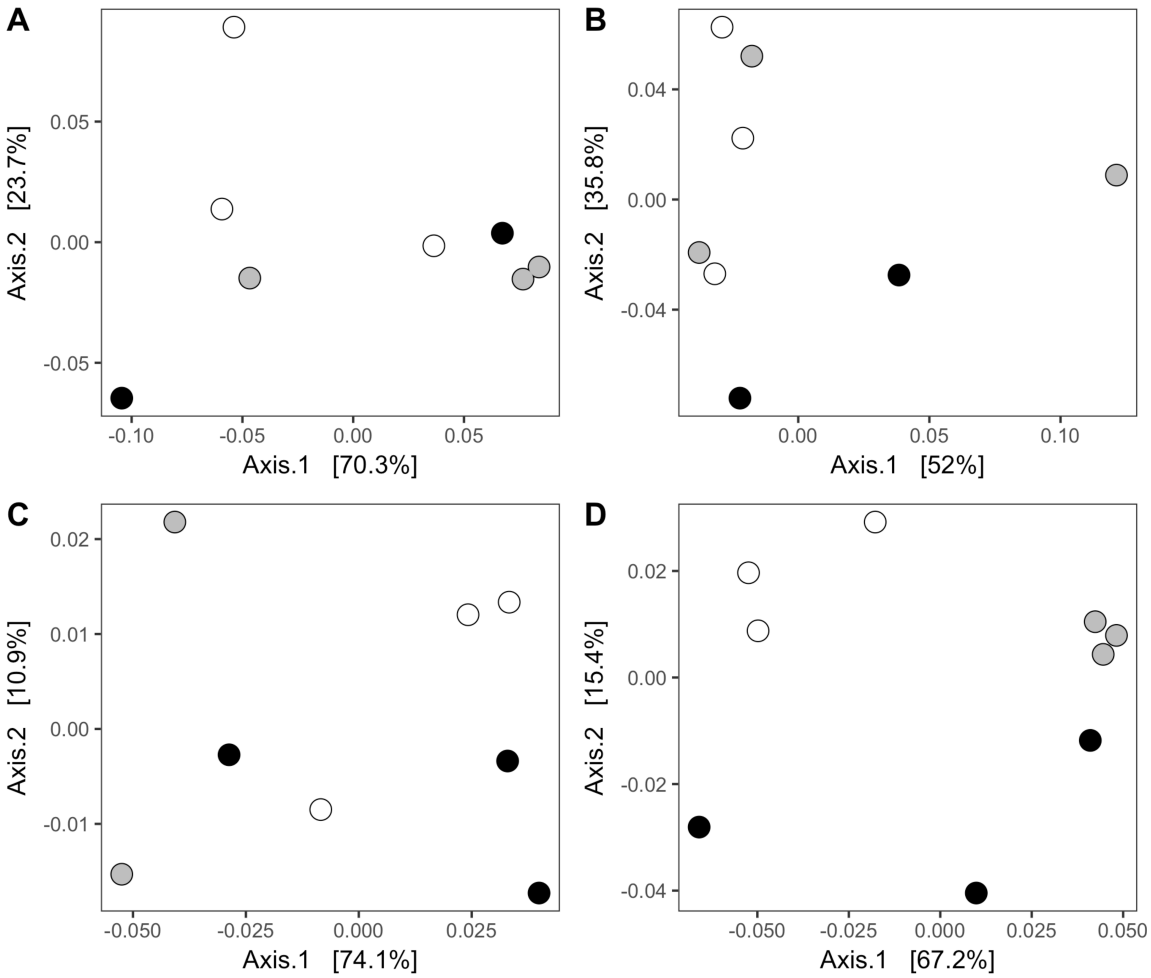

Figure 4.4 Principal coordinates analysis based on weighted UniFrac distance between bacterial communities in control (white), high CO_2 (grey), and greenhouse (black) treatments for G-OA1 Day 1 (A), G-OA1 Day 5 (B), G-OA3 Day 1 (C), and G-OA3 Day 5 (D).

4.4.2 Bacteria and picophytoeukaryote density

Although cell abundance decreased between Day 1 and 5, there was no significant difference in bacteria cell density between treatments in G-OA1 and G-OA3 (Tukey's HSD, $p > 0.05$, Fig. 4.5A). Picophytoeukaryote cell density did not differ between treatments at either time point in G-OA1 (Fig. 4.5B). However, at Day 1 in G-OA3, picophytoeukaryote cell density was significantly greater in the high CO_2 (3,284 (±319) cells ml^{-1}, ±1SD) and greenhouse (3,230 (±101) cells ml^{-1}) treatment compared with the control (2,663 (±134) cells ml^{-1}). At Day 5 in G-OA3, picophytoeukaryote cell density was

significantly greater in the greenhouse (2,214 (±236) cells ml^{-1}) treatment compared with the control (1,612 (±100) cells ml^{-1}).

Comparisons between regions revealed that bacterial cell density was significantly greater in G-OA1 compared to G-OA3 at Day 1 in all treatments (One-way ANOVA, $p < 0.05$). Bacterial cell density was not significantly different between G-OA1 and G-OA3 at Day 5 in any treatment (One-way ANOVA, $p > 0.05$). In contrast, picophytoeukaryote cell density was greater in G-OA1 than G-OA3 in all treatments at Day 1 and Day 5 (One-way ANOVA, $p < 0.05$).

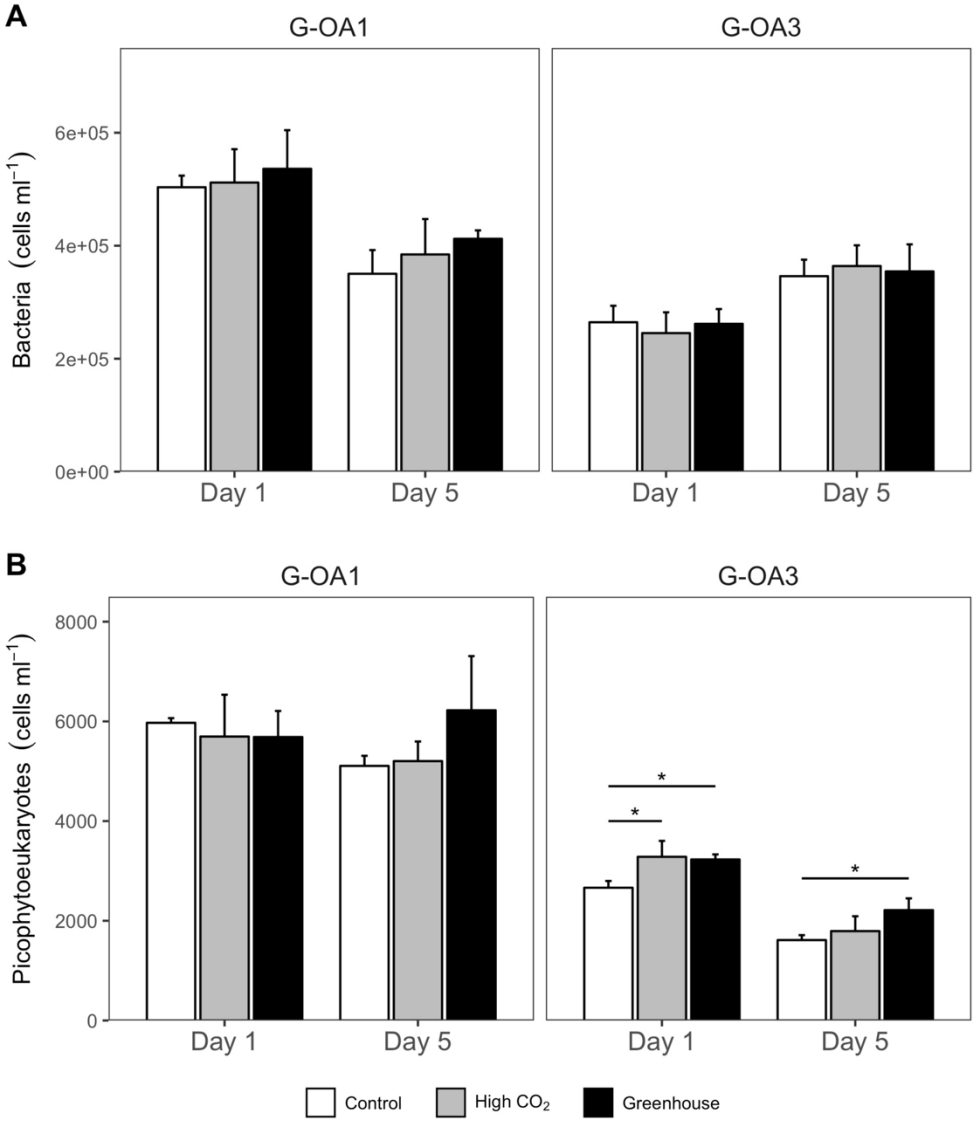

Figure 4.5 Cell density determined by flow-cytometry for bacteria (A) and picophytoeukaryotes (B) in control (white), high CO_2 (grey), and greenhouse (black) treatments at Day 1 and Day 5 in experiments G-OA1 and G-OA3. Error bars represent 1 SD. Horizontal bars indicate significant differences between treatments identified by Tukey's post-hoc test (* $p<0.05$).

4.4.3 Bacterial secondary production

Bacterial secondary production was measured using ^{3}H-Leucine incorporation and ^{3}H-Thymidine incorporation, which act as proxies for protein synthesis and DNA synthesis, respectively. ^{3}H-Leucine incorporation rates decreased between Day 1 and 5 in both experiments, but were not significantly different between treatments at either Day 1 or Day 5 in G-OA1 (Tukey's HSD, $p > 0.05$, Fig. 4.6A, mean 0.20-0.28 µg C l^{-1} d^{-1}), or G-OA3 (Day 1 mean 0.13-0.15 µg C l^{-1} d^{-1}; Day 5 mean 0.09-0.11 µg C l^{-1} d^{-1}). ^{3}H-Thymidine incorporation data was only available for the greenhouse treatment at Day 1 in G-OA1 (0.71 (±0.07) µg C l^{-1} d^{-1}, ±1SD). ^{3}H-Thymidine incorporation increased between Day 1 and 5. In G-OA1 at Day 5, ^{3}H-Thymidine incorporation was significantly higher in the greenhouse (1.80 (±0.19) µg C l^{-1} d^{-1}) compared with the control (0.98 (±0.06) µg C l^{-1} d^{-1}) treatment, whilst the high CO_2 (1.29 (±0.38) µg C l^{-1} d^{-1}) treatment did not differ from either greenhouse or control treatments. In G-OA3, ^{3}H-Thymidine incorporation was significantly higher in the high CO_2 (0.89 (±0.01) µg C l^{-1} d^{-1}) and greenhouse (0.84 (±0.04) µg C l^{-1} d^{-1}) compared with control (0.54 (±0.06) µg C l^{-1} d^{-1}) treatments at Day 1. By Day 5, control (0.72 (±0.16) µg C l^{-1} d^{-1}), high CO_2 (1.13 (±0.34) µg C l^{-1} d^{-1}), and greenhouse (1.43 (±0.33) µg C l^{-1} d^{-1}) treatments were not significantly different, despite a trend of higher incorporation in high CO_2 and greenhouse treatments (Fig. 4.6B).

Comparisons between regions showed that ^{3}H-Leucine incorporation rates were significantly higher in G-OA1 compared with G-OA3 at both Day 1 and Day 5 across all treatments (One-way ANOVA, $p < 0.05$). Whilst it was not possible to compare ^{3}H-Thymidine incorporation rates between experiments at Day 1, at Day 5 ^{3}H-Thymidine incorporation was not significantly different between G-OA1 and G-OA3 in any treatment (One-way ANOVA, $p > 0.05$).

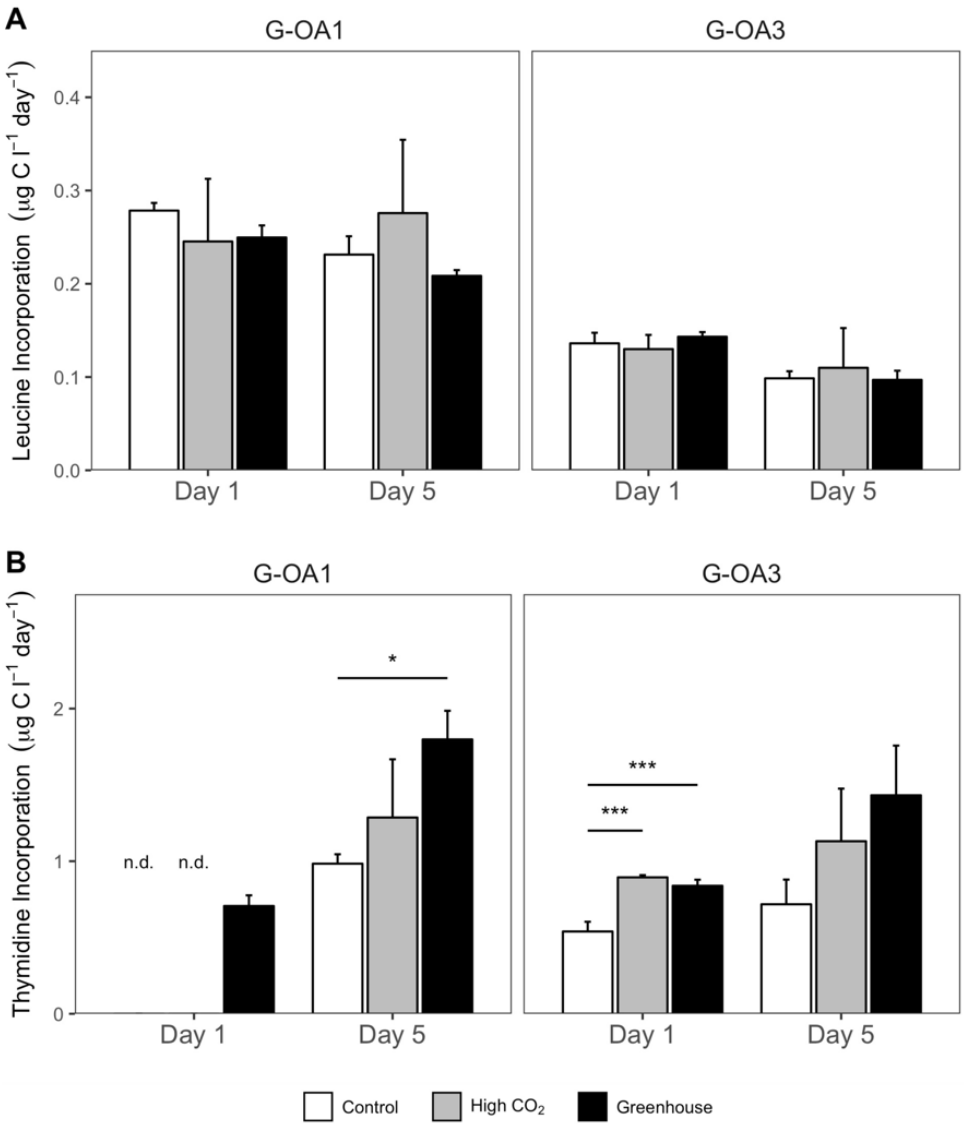

Figure 4.6 Comparison of bacterial secondary production determined by ^{3}H-Leucine incorporation (A) and ^{3}H-Thymidine incorporation (B) in control (white), high CO_2 (grey), and greenhouse (black) treatments at Day 1 and Day 5 in experiments G-OA1 and G-OA3. Error bars represent 1 SD. Horizontal bars indicate significant differences between treatments identified by Tukey's post-hoc test (* $p<0.05$, ** $p<0.01$, *** $p<0.001$).

4.5 Discussion

4.5.1 Bacterial community responses to elevated CO_2 and warming

In this study, the effects of elevated CO_2 and warming on bacterial communities were compared at the oligotrophic fringe and ultra-oligotrophic centre of the SPG. Bacterial community composition was not significantly affected by either high CO_2 or greenhouse conditions at the oligotrophic fringe of the SPG, suggesting some resistance, at least short-term, to these perturbations. In contrast, BCC diverged between the high CO_2 and control treatments after 5 days of incubation at the ultra-oligotrophic centre of the SPG.

The most pronounced difference between the control and high CO_2 treatments at day 5 in the centre of the SPG was a lower relative abundance of the Flavobacteriaceae family (Bacteroidetes) in the high CO_2 treatment (Fig. 4.2; Fig. 4.3). Flavobacteriaceae are commonly associated with phytoplankton blooms in nutrient-replete environments (Buchan *et al.*, 2014) and have previously been shown to be vulnerable to elevated CO_2 in the Arctic Ocean (Zhang *et al.*, 2013), though this trend was not detected in similar experiments in the same region (Newbold *et al.*, 2012; Roy *et al.*, 2013). The relative abundance of Actinobacteria was also lower in the high CO_2 treatment at the centre of the SPG, explained by a lower relative abundance of *Candidatus_Actinomarina* asv_9. These bacteria are amongst the smallest known free-living cells (Ghai *et al.*, 2013). Their adaptation to oligotrophy was revealed by genome assembly, which found extensive evidence of genome streamlining (Mizuno *et al.*, 2015) that reduces cellular nutrient demands (Sela *et al.*, 2016).

In contrast to the responses of Bacteroidetes and Actinobacteria, the relative abundance of Gammaproteobacteria was greater in the high CO_2 treatment at the centre of the SPG (Fig. 4.2). This shift was the result of trends in *SAR86_clade* ASVs. Similarly to *Candidatus Actinomarina*, the SAR86 clade are adapted to oligotrophic environments through streamlined genomes (Dupont *et al.*, 2012), and have previously been reported as abundant in the oligotrophic surface waters of the SPG (West *et al.*, 2016). Notably, the relative abundance of the dominant cyanobacteria *Prochlorococcus* was greater under the high CO_2 treatment at the centre of the SPG. *Prochlorococcus* possess a highly streamlined carbon concentrating mechanism, which is not down-regulated under elevated CO_2 conditions in nutrient-enriched media (Hopkinson *et al.*, 2014). Furthermore, *Prochlorococcus* do not exhibit any growth rate response to elevated CO_2 or temperature in nutrient-enriched monoculture (Fu *et al.*, 2007). This suggests that elevated CO_2 concentrations do not

provide a physiological advantage to the genus under nutrient replete conditions. In contrast, *Prochlorococcus* has been shown to increase in abundance in response to elevated CO_2 in natural communities under low-nutrient conditions (Sala *et al.*, 2016). Thus, the trends in *Prochlorococcus* abundance observed in this study may be the result of indirect effects of elevated CO_2 (e.g. altered competitive interactions) or physiological advantages (e.g. reduced energetic cost of carbon fixation) which are constrained to oligotrophic conditions. Finally, the ubiquitous Alphaproteobacterial SAR11 clade was resistant to elevated CO_2 at the ultra-oligotrophic centre of the SPG, supporting data from high-latitude regions (Hartmann *et al.*, 2016).

Recent metatranscriptomic analysis revealed that different families of heterotrophic bacteria upregulate distinct suites of pH homeostasis-related genes in response to elevated CO_2 under low-nutrient conditions (Bunse *et al.*, 2016). These pH homeostasis mechanisms differ in their energetic demands, which may have taxa specific ramifications for bacterial growth efficiency under elevated CO_2 conditions in the oligotrophic ocean, as heterotrophic bacteria may be energy-limited in these regions (Del Giorgio *et al.*, 2011). Though further research is necessary to characterise the physiological responses of specific bacteria to elevated CO_2, current evidence demonstrates that physiological responses are not consistent between taxa (Bunse *et al.*, 2016). In this study, BCC responses to the elevated CO_2 appeared to be consistent, demonstrated by a high degree of similarity between the high CO_2 replicates at the ultra-oligotrophic centre of the SPG (Fig. 4.4D). The findings of this study are consistent with the notion that physiological differences between bacteria may underpin community responses to elevated CO_2 in ultra-oligotrophic regions.

The most surprising finding of this study is the resistance of BCC to the combined effects of elevated CO_2 and warming (greenhouse treatment) at both the oligotrophic fringe and ultra-oligotrophic centre of the SPG. These findings contrast with previous studies in high-latitude regions which demonstrate significant effects of elevated CO_2 and warming on bacterial community structure and function (Lindh *et al.*, 2013; Bergen *et al.*, 2016). The divergence of the findings of this study and those previously reported may be a result of nutrient limitation in the SPG, which have been shown to supress the metabolic responses of cyanobacteria and heterotrophic bacteria to temperature in laboratory experiments as a result of altered cellular energy budgets and enzyme kinetics (Berggren *et al.*, 2010; Marañón *et al.*, 2018). An important consideration is that this study was performed during the Austral Winter, and the temperature in the greenhouse treatment (+3°C ±0.5) was within the boundaries of annual sea surface temperature (SST) variance in the region

(Signorini and McClain, 2012). Nonetheless, the absence of response observed in the greenhouse treatment cannot be attributed exclusively to annual temperature cycles, as CO_2 concentrations in the greenhouse treatment profoundly exceeded annual variance (Takahashi *et al.*, 2009). Therefore, these data suggest that elevated temperature and CO_2 may act antagonistically on BCC in the SPG.

4.5.2 Differences between the fringe and oligotrophic centre of the SPG

The divergent responses of BCC to elevated CO_2 at the oligotrophic fringe and the ultra-oligotrophic centre of the SPG may be explained by the different nutrient regimes in the respective regions, as the supply of nitrogen and iron is greater at the fringe than in the centre of the SPG (Ellwood *et al.*, 2018). Heterotrophic bacteria can be energy-limited under ultra-oligotrophic conditions (Del Giorgio *et al.*, 2011), thus the energetic ramifications of differential physiological responses to elevated CO_2 may have more pronounced effects on growth efficiency, and therefore community composition, under ultra-oligotrophic conditions compared to regions with greater nutrient supply. Additionally, BCC can vary greatly between nutrient regimes (Hutchins and Fu, 2017). Bacterial communities were profoundly different between the oligotrophic fringe and the ultra-oligotrophic centre of the SPG, reflected in the dominance of Bacteroidetes in G-OA1 and the dominance of Cyanobacteria and Alphaproteobacteria in G-OA3 (Fig. 4.2; Fig. 4.3). Thus, another possible explanation for the different responses of BCC to elevated CO_2 between the fringe and centre of the SPG is that bacterial taxa composing communities at the fringe of the SPG are more tolerant of elevated CO_2 conditions. Nonetheless, these prominent differences suggest that the availability of nitrogen and iron are more influential than elevated CO_2 and warming in structuring bacterial communities in the SPG.

There was a pronounced temporal shift in BCC between day 1 and day 5 at the fringe of the SPG (Fig. 4.3). This may be the result of nutrient depletion over the duration of the experiment, as the incubations were isolated from allochthonous nutrient and iron inputs (e.g. vertical supply of nitrogen and aeolian supply of iron; Ellwood *et al.*, 2018). The temporal shift in BCC at the centre of the SPG was less pronounced (Fig. 4.2; Fig. 4.3). This may reflect the ultra-oligotrophic conditions, where nutrients are predominantly autochthonous and their availability is tightly controlled by bacterial regeneration (Azam and Malfatti, 2007; Bonnet *et al.*, 2008; Raimbault and Garcia, 2008), and so maintained in the G-OA3 incubations. Temporal changes in BCC at both the oligotrophic fringe and

the ultra-oligotrophic centre of the SPG demonstrate the capacity for restructuring of bacterial communities over the timeframe of the investigation. However, it is pertinent to consider that the potential rate of turnover in bacterial communities is related to bacterial growth rates, and may therefore be lower in ultra-oligotrophic environments (Nemergut *et al.*, 2013). Nonetheless, longer incubation periods could enhance potential bottle effects, which have previously been shown to affect the structure and function of bacterioplankton communities under polar and freshwater environments (Massana *et al.*, 2001; Baltar *et al.*, 2012).

4.5.3 Functional responses

^{3}H-Leucine incorporation is a proxy of protein synthesis, whilst ^{3}H-Thymidine incorporation is a proxy of DNA synthesis and therefore cell division (Knap *et al.* 1996). In this study, there was no significant difference in protein synthesis between control, high CO_2, and greenhouse treatments in the SPG. These findings suggest that bacteria possess a community-level physiological tolerance to near-future elevated CO_2 and warming. Although Bunse *et al.* (2016) found that heterotrophic bacterial groups upregulate different suites of pH homeostasis-related genes in response to elevated CO_2, they found that these responses did not affect total community protein synthesis (also derived from ^{3}H-Leucine incorporation rates), in line with the findings of this study. The trend of increased DNA synthesis rates in response to elevated CO_2 and warming suggests that these environmental perturbations may increase rates of bacterial cell division. However, enhanced DNA synthesis rates were not reflected in total bacterial cell density, suggesting top-down control of bacterial populations (e.g. by grazing; Fenchel, 2008; Wambeke *et al.*, 2008). These findings contrast with those of Burrell *et al.* (2017) in nearby mesotrophic waters of the South West Pacific Ocean, where elevated CO_2 conditions did not enhance DNA synthesis rates and interacted antagonistically with temperature, suggesting that the functional responses of bacterial communities to elevated CO_2 and warming can be modulated by nutrient regimes.

Previous studies demonstrate that bacterial recycling of organic matter can be enhanced by elevated CO_2 and warming, which may reduce the export of organic carbon to the deep ocean (Burrell *et al.*, 2017; James *et al.*, 2017). In this study, the effects of elevated CO_2 and warming on bacterial recycling remain unclear, due to inconsistent trends between ^{3}H-Leucine and ^{3}H-Thymidine derived bacterial secondary production rates. However, James

et al. (2017) suggest that increased bacterial respiration rates and altered extracellular enzyme activity may underpin accelerated recycling of organic matter; these parameters were not measured in this study. Picophytoeukaryote cell density was increased by elevated CO_2 and warming, but not elevated CO_2 alone, at the ultra-oligotrophic centre of the SPG (Fig. 4.5B). This contrasts with the findings of previous studies which suggest that picophytoeukaryotes may benefit from elevated CO_2 alone (Sala *et al.*, 2016; Crawfurd *et al.*, 2017; Schulz *et al.*, 2017). Picophytoeukaryotes are major producers of particulate organic carbon in the SPG (Grob *et al.*, 2007), and are closely associated with carbon export in oligotrophic regions (Guidi *et al.*, 2016). Interestingly, post hoc analysis revealed picophytoeukaryote cell density was negatively correlated with bacterial cell density in the ultra-oligotrophic centre of the SPG (Fig. A.7). This suggests that picophytoeukaryotes may be in competition with bacteria for a limiting resource (e.g. nitrate). In contrast, picophytoeukaryote cell density at the fringe of the SPG was positively correlated with bacterial cell density, which could reflect mutualism due to both bacteria benefitting from organic matter production by picophytoeukaryotes, and picophytoeukaryotes benefitting from increased bioavailability of iron due to bacterial production of iron-binding ligands (Boiteau *et al.*, 2016). As a result of inconsistent trends in bacterial secondary production, and greater picophytoeukaryote cell density at the ultra-oligotrophic centre of the SPG, it remains to be resolved how carbon export to the deep ocean will be affected by elevated CO_2 and warming in these regions. The fundamental importance of subtropical gyres in global carbon cycling makes these questions a priority for further investigation (Hoegh-Guldberg and Poloczanska, 2017).

Finally, a previous report from these experiments found no effect of elevated CO_2 and warming on nitrogen fixation in the SPG (Law *et al.*, 2012), which is an important source of nitrogen at the fringe of the SPG but less so at the centre (Law *et al.*, 2011; Ellwood *et al.*, 2018). Though the composition of diazotrophic communities was not explicitly investigated in experiment G-OA1 and G-OA3, communities in the region were thought to be dominated by the cyanobacteria UCYN-A (Halm *et al.*, 2011). However, recent evidence indicates that nitrogen fixing capabilities are present in a wide range of heterotrophic bacteria in the SPG (Delmont *et al.*, 2018). The newly discovered diversity of heterotrophic bacterial diazotrophs may contribute to the resistance of nitrogen fixation rates to elevated CO_2 and warming in these regions.

4.5.4 Conclusions

In conclusion, BCC was modified by elevated CO_2 at the ultra-oligotrophic centre of the SPG, but not at the oligotrophic fringe, suggesting that bacterial community responses to elevated CO_2 can be modulated by nutrient regimes. Responses to elevated CO_2 at the ultra-oligotrophic centre of the SPG were consistent between replicates, and may be underpinned by distinct pH homeostasis responses between bacterial groups under these ultra-oligotrophic conditions (Bunse *et al.*, 2016). Bacterial community resistance to the combined effects of elevated CO_2 and warming contrasts with the findings of previous studies (Lindh *et al.*, 2013; Bergen *et al.*, 2016). This may be the result of nutrient limitation supressing metabolic responses to temperature (Berggren *et al.*, 2010; Marañón *et al.*, 2018). As a result of trends in bacterial secondary production and picophytoeukaryote cell density, it remains uncertain how elevated CO_2 and warming will affect carbon export in the SPG. Long-term manipulation experiments are required to resolve the chronic effects of elevated CO_2 and warming on bacterial community structure and function, whilst further studies in other oligotrophic subtropical gyres are necessary to determine whether these findings can be generalised. Although such studies present logistical challenges in oligotrophic subtropical gyres, they are of paramount importance due to the expansion and role of these regions in global carbon cycling (Polovina *et al.*, 2008, 2011; Hoegh-Guldberg and Poloczanska, 2017).

Chapter 5: Biofilm community responses to ocean acidification at a volcanic CO_2 seep

Co-authors of the manuscript: Tina Summerfield, Ben Harvey, Sylvain Agostini, Jason Hall-Spencer, Linn Hoffmann

Chapter 5: Biofilm community responses to ocean acidification at a volcanic CO_2 seep

5.1 Abstract

Microbial biofilms are important components of coastal marine ecosystems, where they form microhabitats harbouring a wealth of eukaryotic and prokaryotic diversity, in addition to fulfilling key biogeochemical functions and acting as a settlement substrate for habitat forming organisms. Ocean acidification has been shown to affect the structure and function of eukaryotic and prokaryotic biofilm communities, yet little is known about the ecological mechanisms which underpin these responses. In this study, the effect of ocean acidification on the early succession of eukaryotic and prokaryotic microbial biofilms was investigated at a volcanic CO_2 seep system at Shikine-Jima, Japan. Ocean acidification was shown to significantly affect the composition of biofilm communities throughout the early stages of succession, but did not affect the diversity or evenness of these communities. Variability in biofilm community composition was lower under acidification conditions, suggesting that ocean acidification may exert significant selection pressure on both eukaryotic and prokaryotic communities decreasing the influence of stochastic processes on community assembly. The rate of turnover in biofilm community composition between successive time points was not significantly affected by ocean acidification. These findings indicate that species replacement, rather than shifts in diversity, evenness, or successional dynamics, underpin biofilm community responses to ocean acidification.

5.2 Introduction

Biofilms are complex aggregates of microbes occupying surfaces in aquatic environments (Costerton *et al.*, 1995), these biogenic habitats can harbour a wealth of eukaryotic and prokaryotic diversity (Sanli *et al.*, 2015; Flemming *et al.*, 2016). Biofilm microbes exist within a matrix of extracellular polymeric substances (EPS) which facilitate bioadhesion (Flemming and Wingender, 2010). This functionally important EPS matrix acts as a platform for the extracellular breakdown of organic compounds (Pohlon *et al.*, 2010), intercellular communication (De Kievit, 2009), and the storage of excess carbon as polysaccharides (reviewed in Flemming & Wingender 2010). In coastal marine environments, biofilms are a food-source for benthic grazers (Thompson *et al.*, 2004) and are the primary settlement substrate for invertebrates and habitat-forming organisms including scleractinian corals (Tran and Hadfield, 2011; Espinel-Velasco *et al.*, 2018).

Ocean acidification, due to rising atmospheric carbon dioxide (CO_2) concentrations, has driven a decrease in mean surface ocean pH of 0.1 units since the pre-industrial era, and is projected to drive a further decrease of 0.3 units by the end of the century under business-as-usual scenarios (Hoegh-Guldberg *et al.*, 2014). The responses of biofilms to ocean acidification are likely to have ramifications for marine food-webs and biogeochemical cycling. Laboratory studies indicate that ocean acidification has both direct and indirect effects on eukaryotic and prokaryotic biofilm communities (Witt *et al.*, 2011; Krause *et al.*, 2012; Russell *et al.*, 2013; Webster *et al.*, 2013), and that ecosystem level studies in natural environmental settings must necessarily be integrated with laboratory studies to more accurately predict biofilm responses to future ocean acidification (Russell *et al.*, 2013).

Volcanic CO_2 seeps are regions where CO_2 gas is emitted from the seafloor, creating areas of localised acidification comparable to conditions projected by the end of the century (Hall-Spencer *et al.*, 2008; Agostini *et al.*, 2015). These systems provide a lens through which to investigate the ecosystem-level effects of ocean acidification in a setting of chronic exposure and natural realism (Hall-Spencer *et al.*, 2008; Andersson *et al.*, 2015). Studies of eukaryotic biofilm communities at CO_2 seeps have focussed primarily on microalgae (Lidbury *et al.*, 2012; Johnson *et al.*, 2013, 2015), which are expected to be affected by ocean acidification through impacts on their carbon concentrating mechanisms and shifts in competitive interactions due to differences in inorganic carbon utilization (Mackey *et al.*, 2015). These studies have consistently demonstrated that ocean acidification alters the composition of microalgal communities, driving an increase in the

total abundance of diatoms and the relative abundance of large chain-forming diatom species (Johnson *et al.*, 2013, 2015). Despite consistent shifts in community composition, the effect of ocean acidification on eukaryotic biofilm diversity and evenness varies between studies (Lidbury *et al.*, 2012; Johnson *et al.*, 2013, 2015).

Prokaryotic communities are expected to be resilient to ocean acidification due the large fluctuations in pH which these organisms must contend with across spatiotemporal scales (Joint *et al.*, 2011). However, environmental pH can affect processes involved in biofilm formation (Dang and Lovell, 2016). Studies at CO_2 seeps have demonstrated that ocean acidification can significantly alter the composition of prokaryotic biofilm communities settling on artificial substrates over short time periods (Lidbury *et al.*, 2012), though long-term studies suggest that interactions with macro-organisms and other environmental factors may become more important drivers of community structure over time (Hassenrück *et al.*, 2017). Studies of established epilithic and epipelic prokaryotic communities at CO_2 seeps demonstrate consistent compositional shifts driven by an increase in the relative abundance of Bacteroidetes, and decrease in the relative abundance of Gammaproteobacteria and total community diversity, under acidified conditions (Kerfahi *et al.*, 2014; Taylor *et al.*, 2014). Moreover, ocean acidification can alter the composition of planktonic microbial communities at CO_2 seeps, which are the inoculum from which biofilm communities assemble (Burrell *et al.*, 2015; Chauhan *et al.*, 2015).

These compositional shifts in eukaryotic and prokaryotic biofilm communities are associated with shifts in community function, such as enhanced primary production (Lidbury *et al.*, 2012; Johnson *et al.*, 2013, 2015; Russell *et al.*, 2013), and the increased production of uronic acids (Lidbury *et al.*, 2012) which are a proxy of biofilm EPS production (Mojica and Cooney, 2010). While these studies demonstrate that ocean acidification can significantly affect the structure and function of eukaryotic and prokaryotic biofilm communities, successional trends and the ecological mechanisms which underpin biofilm community responses to ocean acidification are yet to be investigated.

The advent of high-throughput amplicon sequencing has revolutionised microbial ecology by facilitating the surveying of eukaryotic and prokaryotic microbial communities in unprecedented depth and resolution (Thompson *et al.*, 2017). Global surveys of marine microbial communities employing high-throughput amplicon sequencing have revealed the vast extent of previously unknown diversity in eukaryotic and prokaryotic marine microbes (de Vargas *et al.*, 2015; Sunagawa *et al.*, 2015; Malviya *et al.*, 2016). These techniques

offer an avenue to investigate the ecology of marine microbial communities, including biofilms (Sanli *et al.*, 2015), in previously unattainable detail.

In this study, the effect of ocean acidification on the composition, diversity, and early successional dynamics of biofilm communities was investigated over 21 days at the Mikama Bay volcanic CO_2 seep system, Shikine-Jima, Japan (Fig. 5.1). High-throughput amplicon sequencing of the 18S rRNA gene (Stoeck *et al.*, 2010; Massana *et al.*, 2015) and 16S rRNA gene (Apprill *et al.*, 2015; Parada *et al.*, 2016) was used to characterise eukaryotic and prokaryotic components of biofilm communities, respectively. To date, these data provide the most detailed assessment of biofilm community composition at CO_2 seeps, and shed new light on the ecological mechanisms which underpin the responses of biofilms to near-future ocean acidification.

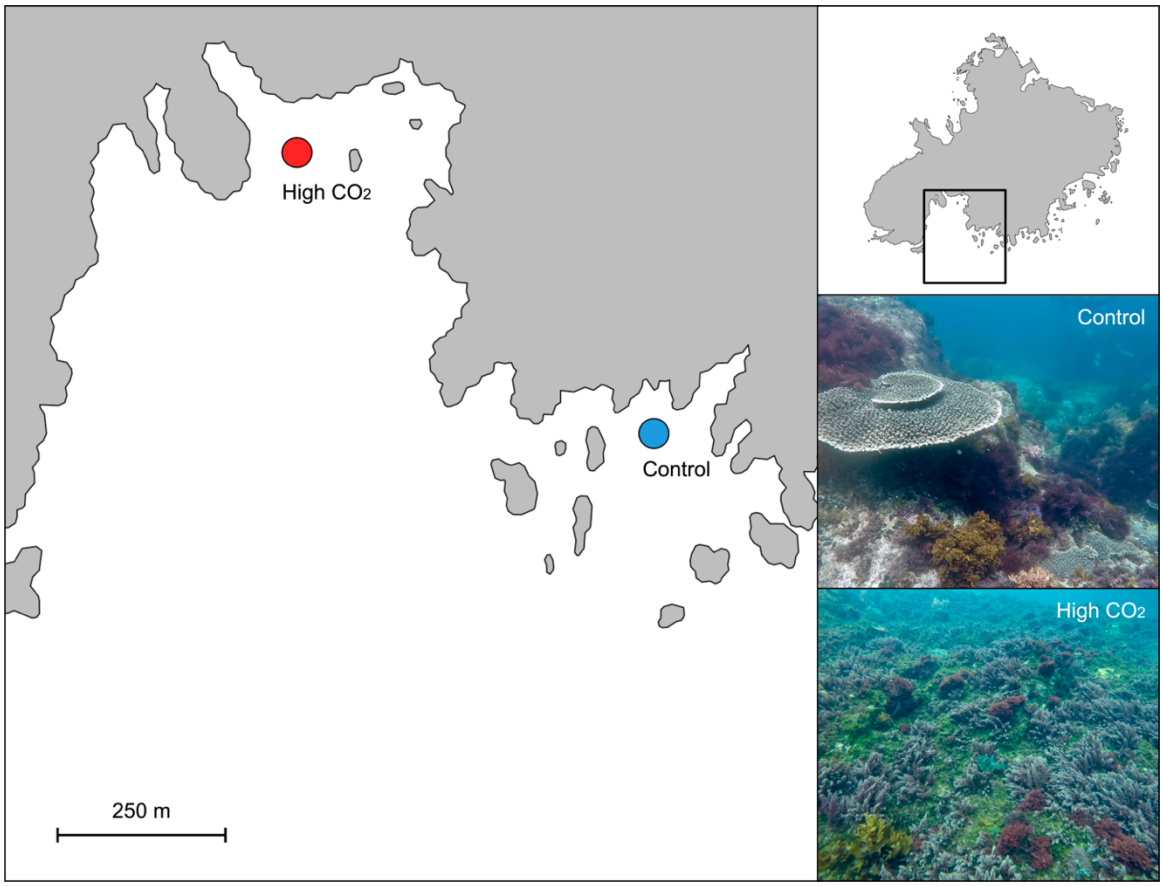

Figure 5.1 Map of Mikama Bay, at Shikine-Jima. Control and high CO_2 sites are indicated by blue and red points, respectively. The inset at the top right shows Shikine-Jima, with a black bounding-box around the Mikama Bay region. The photographic insets at the middle and bottom right show representative seascapes at the control and high CO_2 sites, taken during sampling for this study.

5.3 Methods

5.3.1 Study site and sampling

Shikine-Jima is volcanic island situated approximately 50 km south east of the Shimoda, Japan. The island is at a temperate latitude, but is influenced by the warm Kuroshio current. Consequently, the coastal waters surrounding the island host a diverse range of tropical and temperate organisms including scleractinian corals and canopy-forming macroalgae (Agostini *et al.*, 2018). The island harbours a recently described CO_2 seep system at Mikama Bay where ~98% CO_2 gas percolates through the seafloor creating areas of localised acidification (Agostini *et al.*, 2015), and an adjacent control site unaffected by the CO_2 seep system (Fig. 5.1). The experimental high CO_2 seep site represents a valuable analogue for studying the ecosystem level effects of ocean acidification on coastal marine environments (Agostini *et al.*, 2015, 2018).

Two factory-calibrated Durafet pH sensors (Seafet, Sea-Bird Scientific, Canada) were deployed at the control and high CO_2 sites during the experimental period to record ambient pH_{total} at 15-minute intervals. Data from the Durafet pH sensor deployed at the control site were corrupted upon retrieval and unavailable for the time period of this study. However, Durafet pH sensor data was available from the same period of the previous year, which is reported alongside data from the high CO_2 seep site during the time period of this study (Agostini *et al.*, 2018; Fig. 5.2). Discrete seawater samples were collected from high CO_2 sites (n = 54) for total alkalinity measurements according to methods described in Agostini *et al.* (2018). Carbonate chemistry parameters were estimated for the high CO_2 site using the R package 'seacarb' (Lavigne and Gattuso, 2010), with pH_{total}, total alkalinity, temperature, and salinity as input variables. Due to the corruption of Durafet pH sensor data from the control site, estimated carbonate chemistry parameters are reported from the previous year (Agostini *et al.* 2018; Table 5.1).

To survey the colonisation and early-succession of biofilm communities under control and high CO_2 conditions, 9 rigs were deployed at each site, each holding four 5 cm x 10 cm transparent acrylic slides at a depth of 5-7 m. One slide was collected from each rig by SCUBA divers at 5 days, 10 days , 15 days, and 21 days post-deployment. Acrylic slides were chosen as microalgal settlement is consistent between these artificial substrates and a range of natural substrates (Johnson *et al.*, 2013, 2015).

Following collection, a 30 cm^2 section of biofilm was removed from the upper surface of each slide using a sterile razorblade and transferred into a 2 ml cryovial. Cryovials were immediately transferred to liquid nitrogen prior to DNA extraction. The remaining 20 cm^2 section of biofilm was removed from the upper surface of each slide using a sterile razorblade and transferred to a 2 ml microfuge tube for chlorophyll *a* analysis. Chlorophyll *a* was extracted from biofilm samples in 1 ml of 96% ethanol over a 24-hour period at -20°C. Following this incubation period, each microfuge tube was centrifuged at 8,000 rpm for 5 minutes to remove particulate matter. The supernatant was then used to determined chlorophyll *a* concentration according to spectrophotometric methods described in Jeffrey & Humphrey (1975) using a UV-1280 UV-VIS Spectrophotometer (Shimadzu Corporation, Kyoto, Japan).

Table 5.1 Carbonate chemistry at control and high CO_2 sites at Shikine-Jima, Japan. Data presented for 2016 originate from Agostini *et al.* (2018). Data for 2017 originate from this investigation. Control site data were unavailable for 2017 due to instrument error. Temperature, salinity, pH, and total alkalinity (TA) were measured directly, whilst pCO_2, dissolved inorganic carbon (DIC), bicarbonate (HCO_3^-), carbonate (CO_3^{2-}), calcite saturation state (Ω calcite), and aragonite saturation state (Ω aragonite) were estimated using the R package 'seacarb' with directly measured parameters as input values.

Site	Temp. (ºC)	Salinity (psu)	pH_{total}	TA (µmol kg^{-1})	pCO_2 (µatm)	DIC (µmol kg^{-1})	HCO_3^- (µmol kg^{-1})	CO_3^{2-} (µmol kg^{-1})	Ω calcite	Ω aragonite
Control (2016)	16.5 ± 0.0	34.51 ± 0.03	8.22 ± 0.03	2260 ± 3.00	341.5 ± 26.10	2007.70 ± 14.90	1816.6 ± 22.90	178.8 ± 9.00	4.28 ± 0.22	2.75 ± 0.14
High CO_2 (2016)	19 ± 0.7	34.47 ± 0.06	7.90 ± 0.17	2270 ± 2.00	888.40 ± 471.30	2140.50 ± 61.20	2002.9 ± 78.70	108.00 ± 31.90	2.59 ± 0.76	1.68 ± 0.49
High CO_2 (2017)	22.18 ± 1.94	34.50 ± 0.00	7.77 ± 0.11	2274 ± 6.83	868.28 ± 317.07	2120.81 ± 45.31	1968.03 ± 60.87	126.24 ± 45.31	3.04 ± 0.60	1.98 ± 0.39

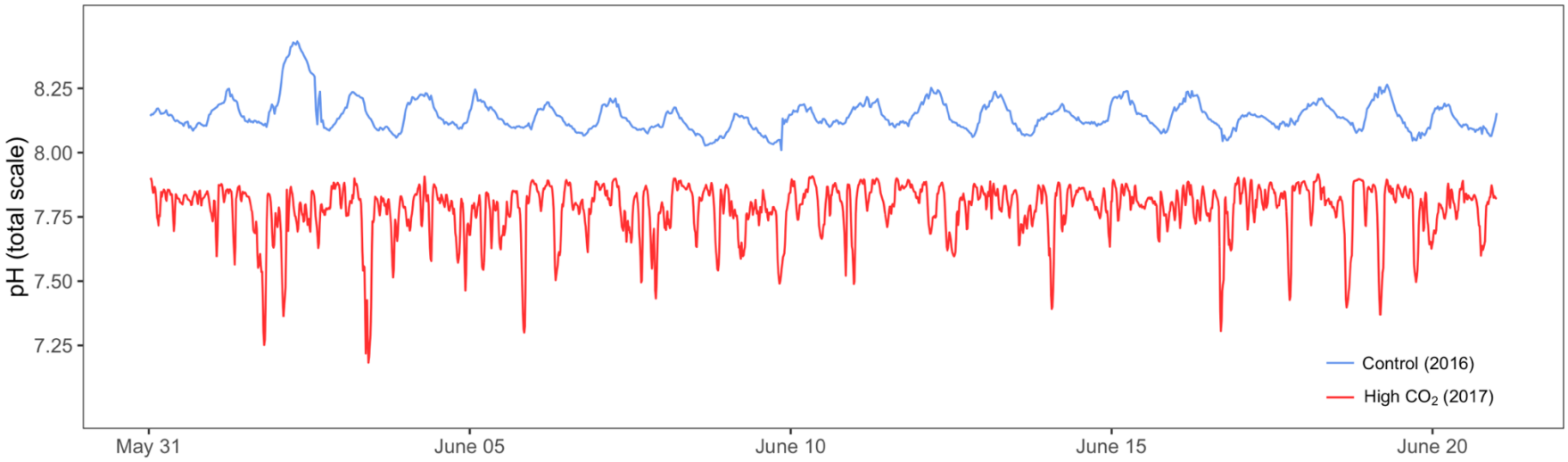

Figure 5.2 Time-series of pH_{total} at control (blue line) and high CO_2 (red line) sites, recording using a Durafet pH sensor during to time period of the study. Durafet pH sensor data from the control site were unavailable during the time period of the study, and consequently, data from the same time period of the previous year are displayed.

3.5.2 Library preparation and sequence processing

Genomic DNA was extracted from each biofilm sample using the Qiagen DNEasy Plant Mini Kit (Qiagen, Valencia, CA, USA) according to the manufacturer's instructions. A two-round PCR protocol was then used to generate paired-end Illumina libraries for 16S and 18S rRNA genes, respectively. In the first round, the V4 region of the 18S rRNA gene was amplified using the TAReuk454FWD1 (5' CCAGCASCYGCGGTAATTCC) and TAReukREV3 (5' ACTTTCGTTCTTGATYRA) primers (Stoeck *et al.*, 2010), and the V4 region of the 16S rRNA gene was amplified using the 515F (5' GTGYCAGCMGCCGCGGTAA) and 806R (5' GGACTACNVGGGTWTCTAAT) primers (Apprill *et al.*, 2015; Parada *et al.*, 2016). Both sets of primers were modified to allow the downstream attachment of Illumina sequencing adapters (Griffith *et al.*, 2017). Triplicate 25 µl PCR mixtures were prepared for each DNA sample using the HiFi Hotstart PCR kit (KAPA Biosystems, Boston, MA, USA) and contained 1 X KAPA HiFi buffer (2 mM $MgCl_2$), 0.3 mM of KAPA dNTP Mix, 0.3 µM of forward and reverse primers, and 0.5 U of KAPA HiFi Hotstart DNA Polymerase. The PCR thermocycler program for the 18S rRNA gene was adapted from Massana *et al.* (2015) and had an initial denaturation step at 95°C for 30 s, followed by 10 cycles of 95°C for 30 s, 53°C for 30 s, and 72°C for 30 s, followed by 15 cycles of 95°C for 30 s, 48 °C for 30 s, and 72°C for 30 s, with a final extension period of 300 s at 72°C. The PCR thermocycler program for the 16S rRNA gene had an initial denaturation step at 95°C for 120 s, followed by 25 cycles of 98°C for 20 s, 60°C for 30 s, and 72°C for 30 s, with a final extension period of 60 s at 72°C. Resulting triplicate PCR products from each sample were pooled and purified using the Mag-bind TotalPure NGS kit (OMEGA Bio-tek, Norcross, GA, USA) according to the manufacturer's instructions. The DNA concentration of the purified PCR products was quantified using the Qubit dsDNA High Sensitivity Assay (Thermo Fisher Scientific, Waltham, MA, USA) according to the manufacturer's instructions. Following quantification, purified PCR products were diluted to a concentration of 1 ng μl^{-1}.

A second round of PCR was performed to attach Illumina sequence adapters and indexes. Each PCR mixture was prepared as described above, and contained 1 µl of diluted first round PCR products. The PCR thermocycler program had an initial denaturation step at 95°C for 120 s, followed by 10 cycles of 98°C for 20 s, 60°C for 20 s, and 72°C for 20 s, with a final extension period of 60 s at 72°C. Second round PCR products were purified, quantified, and pooled to generate libraries for the 18S rRNA gene and 16S rRNA gene,

respectively. Pooled libraries were sequenced on the Illumina MiSeq platform (Illumina, San Diego, CA, USA) using the V3 (2 x 300 bp) and V2 (2 x 250 bp) reagent kits for the 18S rRNA gene and 16S rRNA gene, respectively.

18S rRNA gene and 16S rRNA gene sequences were processed according to the Bioconductor workflow for microbiome data analysis (Callahan *et al.*, 2016). Primers and low-quality sequences were trimmed from the reads, before the DADA2 method (Callahan *et al.*, 2016) was used to infer amplicon sequence variants (ASVs). This method infers ASVs at the single nucleotide resolution, increasing the accuracy and reproducibility of high-throughput amplicon sequencing analyses (Callahan *et al.*, 2017). Chimeric sequences were then removed, and taxonomy was assigned using the RDP Naïve Bayesian classifier (Wang *et al.*, 2007) against the PR2 version 4.10.0 database (Guillou *et al.*, 2013) and SILVA release 132 database (Quast *et al.*, 2013) for 18S rRNA gene and 16S rRNA gene ASVs, respectively. Prior to downstream analysis, 18S rRNA gene ASVs were filtered to remove metazoan sequences. Similarly, 16S rRNA gene ASVs which were not classified as bacteria or archaea, or were classified as chloroplasts or mitochondria, were filtered prior to downstream analysis. Resulting ASV tables, taxonomy tables, and corresponding environmental metadata were assembled as a phyloseq object (McMurdie and Holmes, 2013) for 16S rRNA gene and 18S rRNA gene ASVs, respectively. Sequence reads were then randomly subsampled to an even depth (18S rRNA gene: 11,689 reads, 16S rRNA gene: 18,708), and as a result of this process three 18S rRNA gene samples (control: R6D21; high CO_2: R10D5, R15D5) and three 16S rRNA gene samples (high CO_2: R10D5, R15D5, R15D15) were excluded due to insufficient sequencing depth.

5.3.3 Statistical analyses

A Bray-Curtis dissimilarity matrix was calculated to quantify pairwise dissimilarity between biofilm communities. The Bray-Curtis dissimilarity matrix was then used as an input for PERMANOVA (Anderson, 2001) to test the effect of site (control and high CO_2) and time point (day 5, day 10, day 15, and day 21) on both eukaryotic and prokaryotic biofilm community composition. Pairwise comparisons were then performed between each pair of time points at the control and high CO_2 site, and between control and high CO_2 sites at each time point, respectively. The diversity and evenness of eukaryotic and prokaryotic biofilm communities was quantified using Shannon's Index (H) and the Simpson's index (D), respectively. A two-way ANOVA with Tukey's HSD was then used to test the effects

of site and time point on eukaryotic and prokaryotic biofilm community diversity and evenness.

Variability in eukaryotic and prokaryotic biofilm community composition at each site and time point was quantified using Bray-Curtis dissimilarity. A two-way ANOVA with Tukey's HSD was used to test the effects of site and time point on variability in eukaryotic and prokaryotic biofilm community composition. Turnover in eukaryotic and prokaryotic biofilm community composition was quantified as the Bray-Curtis dissimilarity between successive time points at each rig. A two-way ANOVA with Tukey's HSD was then used to test the effects of site and successive time point on turnover in eukaryotic and prokaryotic biofilm community composition. The coupling of eukaryotic and prokaryotic biofilm communities was investigated using the Mantel test based on Bray-Curtis dissimilarity between pairs of communities, which tests the hypothesis: dissimilarity between pairs of eukaryotic communities is linearly correlated with dissimilarity between corresponding pairs of prokaryotic communities.

Finally, the effect of site and time point on biofilm chlorophyll *a* concentration was compared using a two-way ANOVA with Tukey's HSD, to investigate differences in the standing stock of photosynthetic organisms in total biofilm communities.

5.4 Results

5.4.1 Biofilm community composition

The eukaryotic component of biofilm communities was variable at both the control and high CO_2 site throughout the early-successional stages investigated in this study (Fig. 5.3). At the Division level, Stramenopiles_X, which included Oomycota and Labyrinthulea, represented a significant but highly variable component of biofilms at the control (15.0% ± 15.4; Fig. 5.3) but not the high CO_2 sites (4.5% ± 4.3). Similarly, Ciliophora represented a greater component of biofilms at the control (6.3% ± 4.9) than at the high CO_2 sites (1.8% ± 1.3). In contrast, Rhodophyta represented a greater proportion of biofilm communities in the high CO_2 sites (14.1% ± 9.9) compared to the control sites (3.6% ± 3.3). At day 5, Chlorophyta represented a significant component of eukaryotic biofilm communities at both sites (control: 13.8% ± 5.7, high CO_2: 24.9% ± 5.8), but the relative abundance of Chlorophyta was lower at other time points (control: 2.3% ± 2.0, high CO_2: 0.9% ± 0.64).

From day 10 onwards, Haptophytes had a greater relative abundance at the high CO_2 site (34.9% ± 13.5) than the control site (16.0% ± 10.4).

Generally, trends in eukaryotic biofilm community composition were driven by a small number of highly abundant ASVs (Fig. 5.3). At day 5, control sites were dominated by *Ecotocarpus siliculosus* asv_3 (22.4% ± 14.8), Phaeophyceaea sp. asv_2 (11.6% ± 13.8), and Oomycota sp. asv_6 (22.4% ± 20.1). At the high CO_2 site, Phaeophyceaea sp. asv_2 (15.2% ± 5.6) and Phaeophyceaea sp. asv_12 (16.7% ± 4.0) were the most abundant taxa, whilst *Ecotocarpus siliculosus* asv_3 (1.5% ± 0.4) and Oomycota sp. asv_6 (0.2% ± 0.4) were rare or absent. From day 10 onwards, *Prymnesium sp*. asv_1 (14.3% ± 9.9) and Phaeophyceaea sp. asv_2 (22.0% ± 20.7) had the greatest relative abundance at the control site, whilst *Prymensium sp*. asv_1 (30.8% ± 12.1) dominated the high CO_2 site.

PERMANOVA analysis based on Bray-Curtis dissimilarity revealed that both site (pseudo $F_{1,61}$: 24.15, R^2: 0.18, $p < 0.001$) and time (pseudo $F_{3,61}$: 11.21, R_2: 0.25, $p < 0.001$) significantly affected eukaryotic biofilm community composition, and there was a significant interaction between these factors (pseudo $F_{3,61}$: 4.70, R^2: 0.11, $p < 0.001$). Pairwise comparisons revealed that eukaryotic biofilm communities at control and high CO_2 sites significantly differed at each time point (all $p < 0.001$; Fig. 5.4). At the control site, eukaryotic biofilm communities significantly differed between days 5 and 10 ($p < 0.001$), days 10 and 15 ($p < 0.05$), but not days 15 and 21 ($p > 0.05$). At the high CO_2 site, eukaryotic biofilm communities significantly differed between each successive time point (all $p < 0.05$).

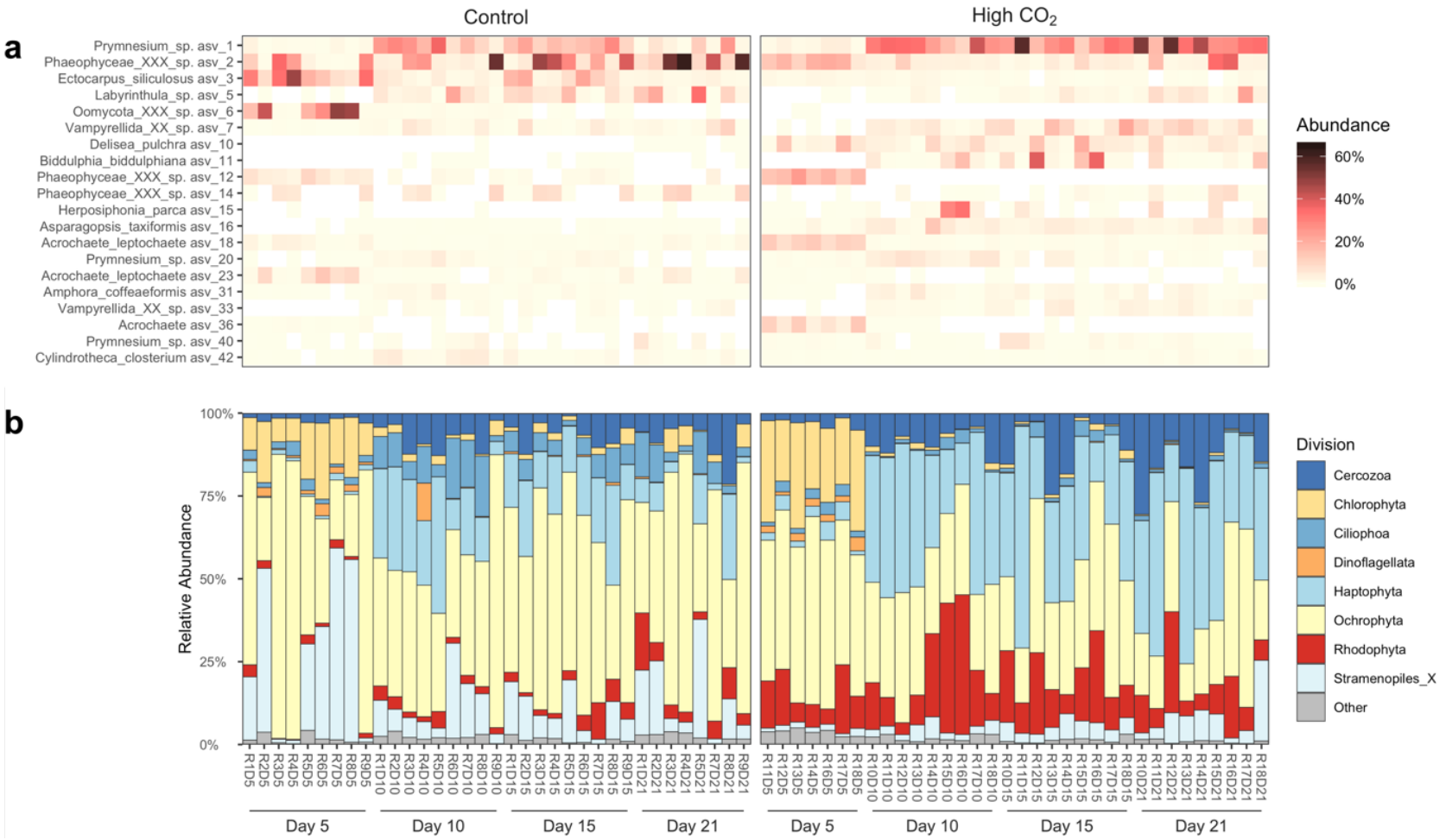

Figure 5.3 (a) Heatmap of the 20 most abundant eukaryotic ASVs in biofilms at control and high CO_2 sites. ASV are ordered according to the neatmap algorithm (Rajaram and Oono, 2010). Colour bar indicates the proportion of reads in each sample attributed to a particular ASV. (b) Division level composition of eukaryotic biofilm communities at control and high CO_2 seep sites.

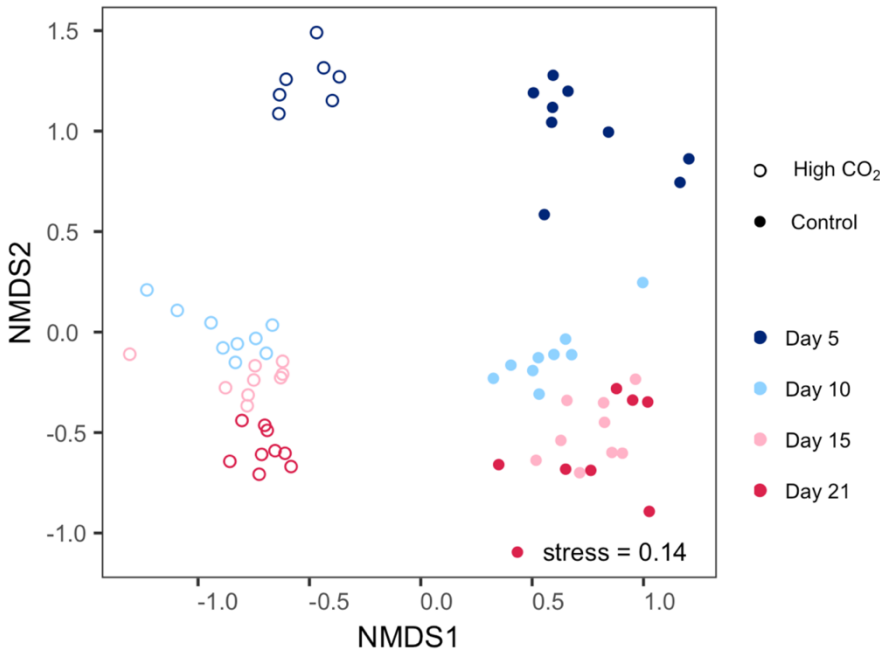

Figure 5.4 Bray-Curtis dissimilarity based nMDS plot of eukaryotic biofilm community composition at control (filled circles) and high CO_2 (open circles) sites at each time point during the study.

At the Phylum and Proteobacterial class level, the prokaryotic component of biofilm communities was dominated by Alphaproteobacteria (control: 41.2% ± 18.5, high CO_2: 43.0% ± 8.2) and Bacteroidetes (control: 37.6% ± 12.3, high CO_2: 34.0% ± 7.4) in both the control and high CO_2 site across all time points during the study (Fig. 5.5). Gammaproteobacteria were a consistent feature of prokaryotic communities at the high CO_2 site (16.1% ± 4.0) but represented a smaller and more variable component of communities at the control site (12.3% ± 6.3). Similarly, Verrucomicrobia were a variable component of prokaryotic communities at the control site (5.7 ± 6.4), but were a smaller and less variable component of prokaryotic communities at the high CO_2 site (3.0 ± 1.8). Trends in prokaryotic biofilm community composition amongst abundant ASVs were subtle at the control site, though Loktanella rosea asv_8, Planktotlea asv_6, and Rubritalea asv_14 sporadically dominated samples (Fig. 5.5). In contrast, at the high CO_2 site, prokaryotic communities displayed clear structuring through time amongst the most abundant ASVs. At the high CO_2 seep site, Planktotalea asv_6 (4.0% ± 0.9), Rhodobacteraceae asv_27 (3.5% ± 0.9), Thalassobius asv_35 (3.1% ± 0.7), and Lentibacter asv_5 (2.9% ± 0.7) had the greatest relative abundance at day 5. By day 21

Cyclobacteriacea asv_9 (3.8% ± 2.1), Tateyamaria asv_17 (3.8% ± 0.8), Glaciecola asv_21 (3.6% ± 2.0), and *Kordia ulvae* asv_13 (3.4% ± 1.2) had the greatest relative abundance. PERMANOVA analysis based on Bray-Curtis dissimilarity revealed that both site (pseudo $F_{1,61}$: 23.95, R^2: 0.18, $p < 0.001$) and time (pseudo $F_{3,61}$: 11.14, R^2: 0.25, $p < 0.001$) significantly affected prokaryotic biofilm community composition, and there was a significant interaction between these factors (pseudo $F_{3,61}$: 4.36, R^2: 0.10, $p < 0.001$). Pairwise comparisons revealed that prokaryotic biofilm communities at control and high CO_2 sites significantly differed at each time point (all $p < 0.001$; Fig. 5.6). Similar to eukaryotic communities, prokaryotic biofilm communities significantly differed between days 5 and 10 ($p < 0.001$), days 10 and 15 ($p < 0.05$), but not days 15 and 21 ($p > 0.05$) at the control site. At the high CO_2 site, prokaryotic communities significantly differed between each successive time point (all $p < 0.001$).

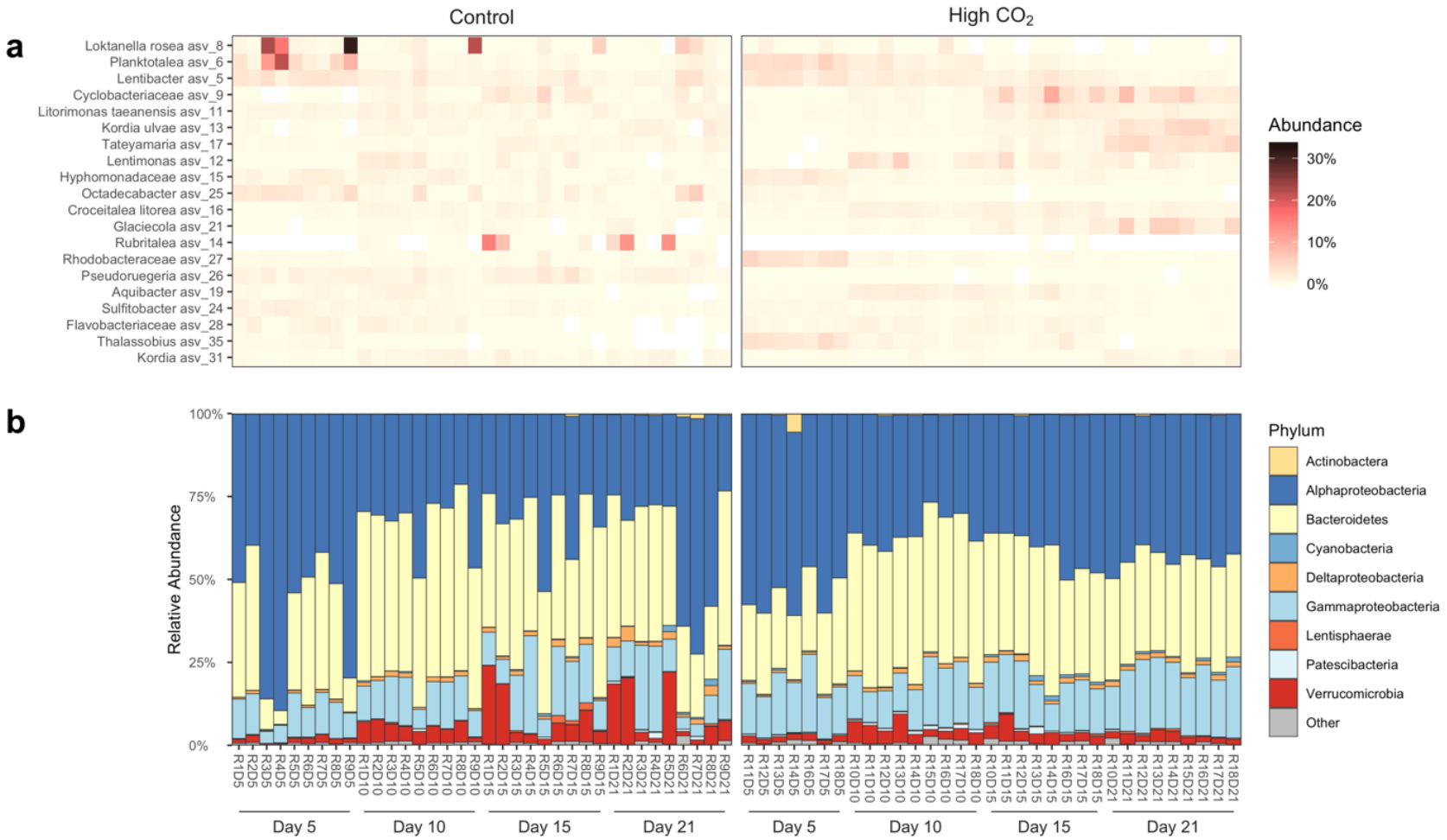

Figure 5.5 (a) Heatmap of the 20 most abundant ASVs in prokaryotic biofilms at control and high CO_2 sites. ASV are ordered according to the neatmap algorithm (Rajaram and Oono, 2010). Colour bar indicates the proportion of reads in each sample attributed to a particular ASV. (b) Phylum level composition of prokaryotic biofilm communities at control and high CO_2 seep sites.

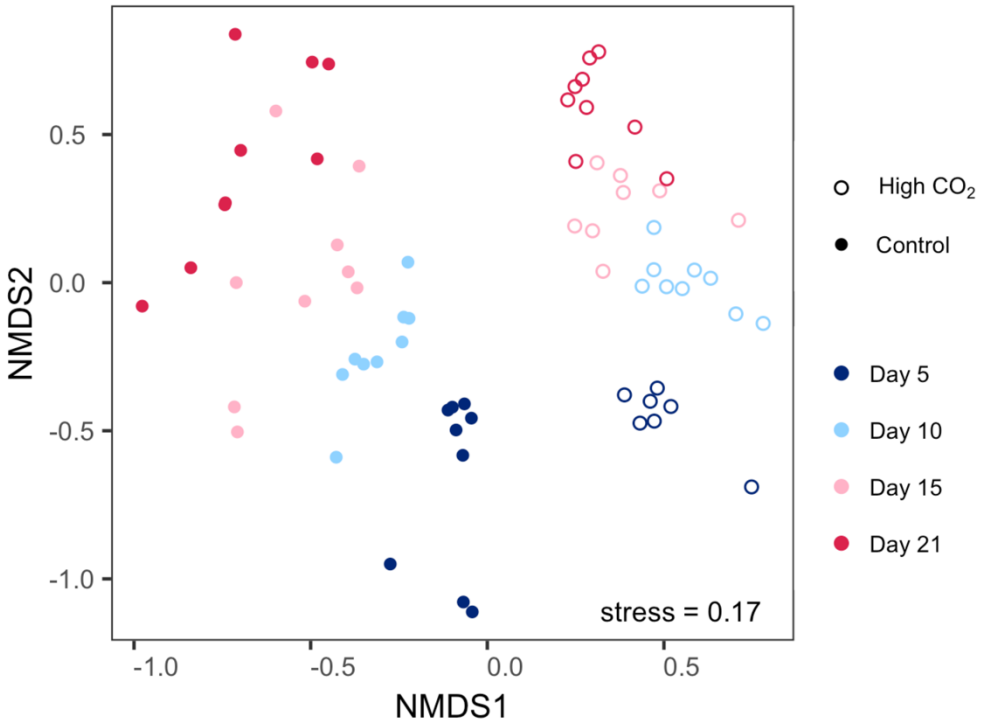

Figure 5.6 Bray-Curtis dissimilarity based nMDS plot of prokaryotic biofilm community composition at control (filled circles) and high CO_2 (open circles) sites at each time point during the study.

5.4.2 Biofilm diversity and evenness

A two-way ANOVA revealed that eukaryotic biofilm diversity (Shannon's index) was significantly affected by time point ($F_{3,61}$: 4.98, $p < 0.01$), but not site ($F_{1,61}$: 0.003, $p > 0.05$), and a significant interaction was present between site and time point ($F_{3,61}$: 4.883, $p < 0.01$). Pairwise comparisons (Tukey's HSD) revealed that eukaryotic biofilm diversity was lower at day 5 than at day 10 in the control site ($p < 0.05$), but did not differ between any other time points in either the control or high CO_2 site (all $p > 0.05$). Moreover, eukaryotic biofilm diversity was lower in the control site than the high CO_2 site at day 5 ($p < 0.05$) but at no other time point (Fig. 5.7a). Prokaryotic biofilm diversity was significantly affected by time point ($F_{3,61}$: 6.30, $p < 0.001$) but not site ($F_{1,61}$: 2.53, $p > 0.05$), with no significant interaction between site and time point ($F_{3,61}$: 0.32, $p > 0.05$). Prokaryotic biofilm diversity was lower at day 5 than at day 10 in the control site ($p < 0.05$), but did not differ between any other time points in either the control or high CO_2 site (all $p > 0.05$; Fig. 5.7b).

Eukaryotic biofilm evenness was significantly affected by time point ($F_{3,61}$: 3.26, $p < 0.05$) but not site ($F_{1,61}$: 0.56, $p > 0.05$) and there was no significant interaction between site and time point ($F_{3,61}$: 2.69, $p > 0.05$). However, pairwise comparisons revealed no significant differences between time points at either the control and high CO_2 sites (all $p > 0.05$; Fig. 5.7c). Prokaryotic biofilm community evenness was significantly affected by site ($F_{1,61}$: 4.727, $p < 0.05$), but not time point ($F_{3,61}$: 2.56, $p > 0.05$), and there was no significant interaction between site and time point ($F_{3,61}$: 1.22, $p > 0.05$). However, pairwise comparisons revealed no significant difference between control and high CO_2 sites at any time point (all $p > 0.05$; Fig. 5.7d).

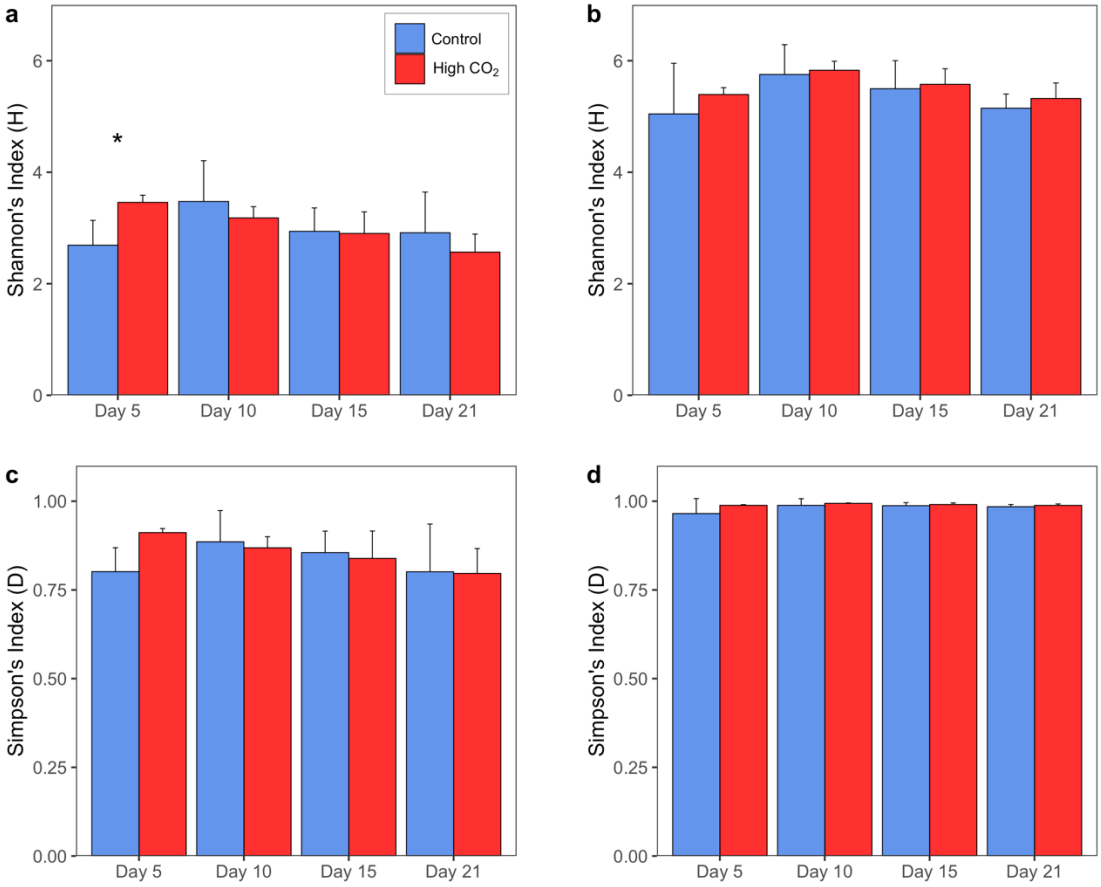

Figure 5.7 (a) Shannon's index diversity of eukaryotic biofilm communities at each time point during the study. (b) Shannon's index diversity of prokaryotic biofilm communities at each time point during the study. (c) Simpson's index evenness of eukaryotic biofilm communities at each time point during the study. (d) Simpson's index evenness of prokaryotic biofilm communities at each time point during the study. Error bars displays standard error. Asterisks denote time points where indexes differed significantly between control and high CO_2 sites (Tukey's HSD, $p < 0.05$).

5.4.3 Biofilm compositional variability

A two-way ANOVA revealed that the compositional variability of eukaryotic biofilm communities was significant affected by site ($F_{1,257}$: 35.51, $p < 0.001$), but not time point ($F_{3,257}$: 2.02, $p > 0.05$), with no significant interaction between the factors ($F_{3,257}$: 2.52, $p > 0.05$). Compositional variability in eukaryotic biofilm communities was greater in the control compared with the high CO_2 site at day 5 ($p < 0.05$; Fig. 5.8a), day 10 ($p < 0.05$), and day 21 ($p < 0.001$), but not at day 15 ($p > 0.05$). The compositional variability of prokaryotic biofilm communities was significant affected by both site ($F_{1,257}$: 103.88, $p < 0.001$) and time point ($F_{3,257}$: 27.34, $p < 0.001$) and a significant interaction was present between these factors ($F_{3,257}$: 7.71, $p < 0.001$). Pairwise comparisons revealed that compositional variability in prokaryotic communities at the control site at day 5 and day 10 was significantly lower than at day 15 and day 21 (all $p > 0.01$). At the high CO_2 site, variability in prokaryotic biofilm communities at day 5 was lower than at day 15 ($p < 0.05$), though no significant differences were observed between other time points ($p > 0.05$). Compositional variability in prokaryotic biofilm communities differed between control and high CO_2 sites at day 5 ($p < 0.01$; Fig. 5.8b), day 15 ($p < 0.001$), and day 21 ($p < 0.001$) but not at day 10 ($p > 0.05$).

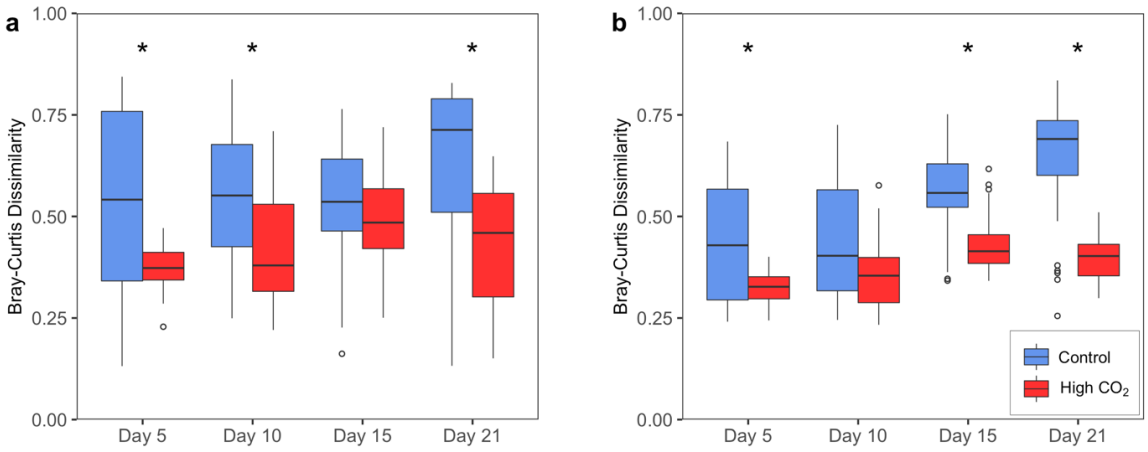

Figure 5.8 Boxplot of compositional variability (Bray-Curtis dissimilarity) in (a) eukaryotic and (b) prokaryotic biofilm communities at control and high CO_2 sites at each time point during the study. Horizontal bars represent the median value, the box represents the interquartile range, and the whiskers represent the minimum and maximum values excluding outliers. Outliers are represented by open circles. Asterisks denote time points where Bray-Curtis dissimilarity differs significantly between sites (Tukey's HSD, $p < 0.05$).

5.4.4 Biofilm succession

A two-way ANOVA revealed that successive time point ($F_{2,45}$: 42.44, $p < 0.001$), but not site ($F_{1,45}$: 0.93, $p > 0.05$), significantly affected turnover in the composition of eukaryotic biofilm communities (Fig. 5.9a), and there was no significant interaction between these factors ($F_{2,45}$: 0.004, $p > 0.05$). Pairwise comparisons revealed that at both the control and high CO_2 sites, turnover in eukaryotic biofilms was greater between day 5 and day 10, than between day 10 and day 15 ($p < 0.001$), and day 15 and day 21 ($p < 0.001$). Similar to eukaryotic communities, time point ($F_{2,44}$: 5.16, $p < 0.01$), but not site ($F_{1,44}$: 0.006, $p > 0.05$), affected significantly turnover in the composition of prokaryotic biofilm communities (Fig 5.9b), and there was no significant interaction between these factors ($F_{2,44}$: 1.049, $p > 0.05$). However, pairwise comparisons revealed no significant difference between pairs of successive time points in either the control or high CO_2 site (all $p < 0.05$).

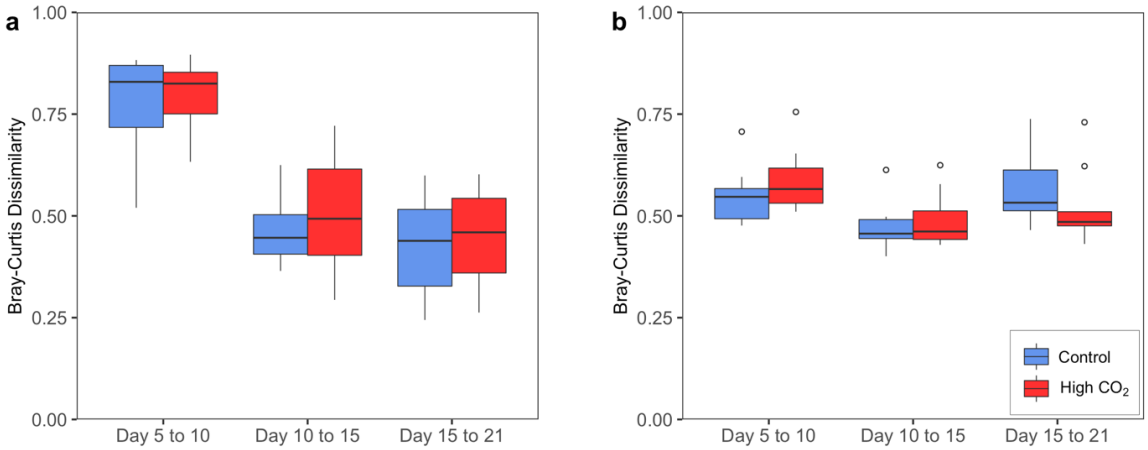

Figure 5.9 Boxplot of compositional turnover (Bray-Curtis dissimilarity) in (a) eukaryotic and (b) prokaryotic biofilm communities at each rig between successive time points at control and high CO_2 sites. Horizontal bars represent the median value, the box represents the interquartile range, and the whiskers represent the minimum and maximum values excluding outliers. Outliers are represented by open circles.

5.4.5 Eukaryotic-prokaryotic biofilm community coupling

Coupling between eukaryotic and prokaryotic communities, based on Bray-Curtis dissimilarity, was measured using the Mantel test. The composition of eukaryotic and prokaryotic communities was significantly related at both the control (r: 0.513, $p < 0.001$) and high CO_2 (r: 0.716, $p < 0.001$) sites (Fig. 5.10). However, the strength of this relationship was much greater at the high CO_2 seep site, demonstrating stronger coupling between eukaryotic and prokaryotic communities under these conditions.

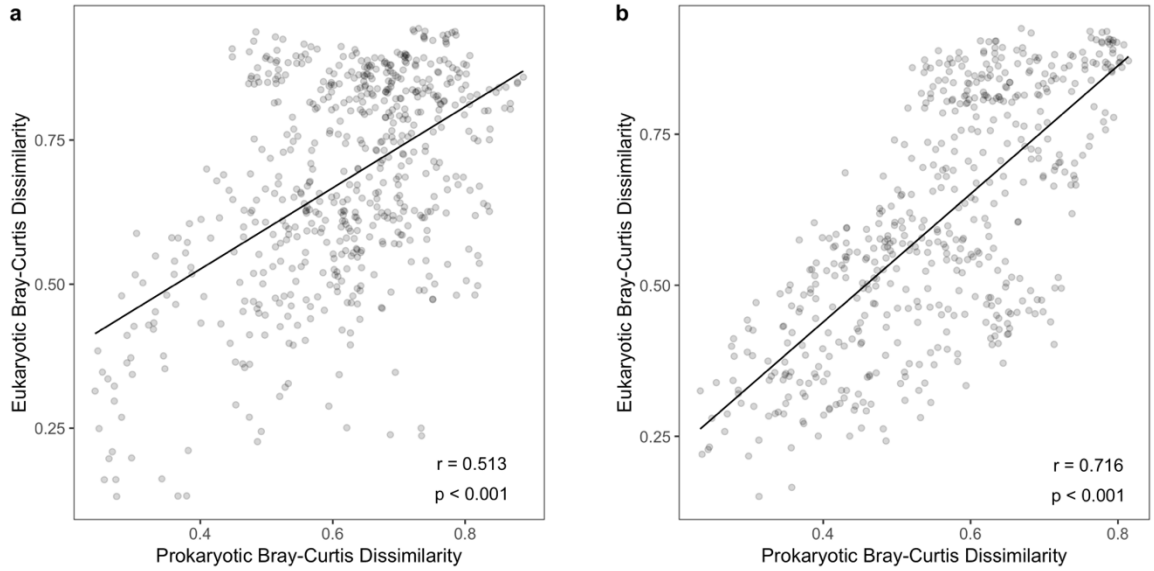

Figure 5.10 The relationship between eukaryotic and prokaryotic biofilm community composition at (a) control and (b) high CO_2 sites during the study, investigated using the Mantel test.

5.4.6 Biofilm chlorophyll

A two-way ANOVA revealed that chlorophyll *a* concentration was significantly affected by time point ($F_{3,64}$: 18.67, $p < 0.001$), but not site ($F_{1,64}$: 0.18, $p > 0.05$), and there was no significant interaction between these factors ($F_{3,64}$: 0.76, $p > 0.05$). Chlorophyll *a* concentrations at both the control and high CO_2 site were greater at day 10, day 15, and day 21, when compared with day 5 (all $p < 0.001$), but did not significantly differ between any other time points (Fig. 5.11).

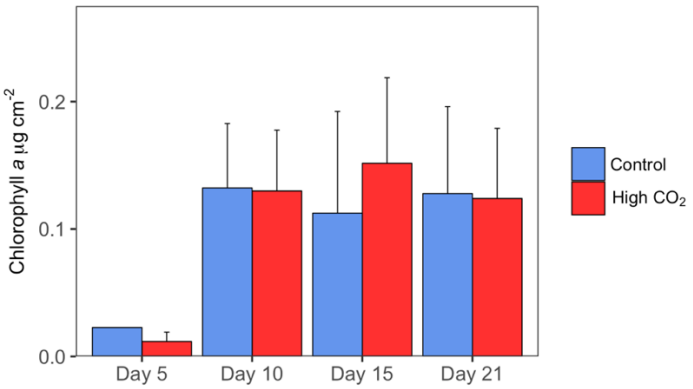

Figure 5.11 Concentrations of chlorophyll a in total biofilms colonising slides at each time point during the study. Error bars displays standard error.

5.5 Discussion

5.5.1 Eukaryotic community composition

The eukaryotic biofilm community composition at high CO_2 sites differed from control sites at all time points during the investigation (Fig. 5.4), supporting the findings of previous CO_2 seep studies investigating biofilms on both artificial (Lidbury *et al.*, 2012; Johnson *et al.*, 2013) and natural substrates (Johnson *et al.*, 2015). The rate of succession (compositional turnover between successive timepoints at each rig) in eukaryotic biofilm community composition did not significantly differ between control and high CO_2 seep sites, indicating that the successional dynamics of eukaryotic biofilm communities are not affected by ocean acidification (Fig. 5.9a).

From day 10 onwards, eukaryotic biofilm communities at the high CO_2 site were dominated by *Prymnesium sp.* (Fig. 5.3). *Prymnesium* is a genus of mixotrophic golden algae responsible for the production of prymnesins, compounds with allelopathic and toxic effects (Manning and La Claire, 2010). These golden algae can form harmful blooms resulting in large-scale fish kills with significant socioeconomic implications (Roelke *et al.*, 2016). *Prymnesium sp.* consume microbes affected by their toxins (Roelke *et al.*, 2016), whilst the allelopathic nature of prymnesins can reduce grazing pressure and suppress competition from other microalgae (Fistarol *et al.*, 2003; Roelke *et al.*, 2016). These factors simultaneously increase the fitness of *Prymnesium sp.* and decrease the fitness of

competitors (Roelke *et al.*, 2016). Prosser *et al.* (2012) found that low pH conditions, comparable to those at the high CO_2 site in this study, supress bloom formation in *Prymnesium parvum*. However, their study manipulated pH through sulfuric acid addition rather than CO_2 addition, and consequently is not directly comparable. *Prymnesium sp.* may be able to capitalise on increased CO_2 concentrations, which have previously been shown to increase toxin production in other microalgae (Hall-Spencer & Allen, 2015, Riebesell *et al.,* 2018), allowing them to dominate the eukaryotic component of biofilms at the high CO_2 site. These findings add to a previous report by Riebesell *et al.* (2018), which showed that some toxic microalgae are consistently able to capitalise on projected near-future CO_2 concentrations at the ecosystem-level. Due to the potential socioeconomic impacts of *Prymnesium sp.*, physiological studies are warranted to further explore the responses of *Pyrmnesium sp.* and the production of prymnesins to ocean acidification through CO_2 manipulation experiments.

The large chain-forming diatom *Biddulphia biddulphiana* sporadically colonized slides at the high CO_2 site, but not the control site (Fig. 5.3). These diatoms can form thick mats that overgrow corals and macroalgae, smothering the benthos (Galland and Pennebaker, 2012). However, little is known about the environmental conditions which induce such events (Galland and Pennebaker, 2012). The findings of this study demonstrate that *Biddulphia biddulphiana* are able to rapidly colonise available substrate under high CO_2 conditions, suggesting that CO_2 concentrations may be an important environmental factor in the formation of benthic blooms of *Biddulphia biddulphiana.* These data align with previous reports from CO_2 seeps in Italy, which show that large chain-forming diatom species may benefit from high CO_2 conditions (Johnson *et al.*, 2013, 2015).

Eukaryotic biofilm community diversity was enhanced at the high CO_2 site at day 5 in this study, but at no other time point (Fig. 5.7a). This initial greater diversity at the high CO_2 site may be driven by accelerated colonisation of slides by algae which can benefit from the increase availability of CO_2. However, eukaryotic biofilm diversity did not differ between sites beyond day 5, in contrast to the findings of previous CO_2 seep studies in Italy (Johnson *et al.*, 2013, 2015). Eukaryotic biofilm evenness did not significantly differ between control and high CO_2 sites at any time point, but has been shown to decrease under high CO_2 conditions in other studies as a smaller cohort of taxa become dominant (Johnson *et al.*, 2013, 2015). Whilst previous studies have focussed on the photosynthetic component of biofilm communities (Lidbury *et al.*, 2012; Johnson *et al.*, 2013, 2015), this study considers the complete community of microbial eukaryotes and finds no prolonged effect of ocean acidification on diversity or evenness. Moreover, previous studies demonstrate

that elevated CO_2 conditions interact with other environmental variables, including light, to affect eukaryotic biofilm diversity (Lidbury et al. 2012). Consequently, it is unsurprising that reports of the responses of eukaryotic biofilm diversity to ocean acidification across different biogeographic regions and different settlement substrates present contrasting results.

5.5.2 Prokaryotic community composition

Similar to eukaryotic community composition, the prokaryotic community composition of biofilms was distinct between control and high CO_2 sites at all time points during the investigation (Fig. 5.6). These findings align with previous reports from CO_2 seep studies investigating epilithic biofilms (Taylor *et al.*, 2014), epipelic prokaryotic communities (Kerfahi *et al.*, 2014), and biofilms settling on artificial substrates (Lidbury *et al.*, 2012). The rate of succession in prokaryotic biofilm communities did not significant differ between control and high CO_2 sites, indicating that ocean acidification does not alter the successional dynamics of prokaryotic biofilm communities (Fig. 5.9b).

Previous studies of prokaryotic communities at CO_2 seeps found that ocean acidification can enhance the relative abundance of Bacteroidetes (Kerfahi *et al.*, 2014; Taylor *et al.*, 2014). This effect was suggested to emerge from enhanced productivity of biofilms under high CO_2 conditions, resulting in a greater supply of organic matter to Bacteroidetes, and in particular Flavobacteria, which possess a wide range of mechanisms for utilising organic carbon and are associated with productive marine environments (Fernández-Gómez *et al.*, 2013; Buchan *et al.*, 2014). In this study, the relative abundance of Bacteroidetes did not differ between control and high CO_2 sites (Fig. 5.5), potentially due to the lack of significant differences in chlorophyll *a* concentration between biofilms at control and high CO_2 sites which indicates that the standing stock of primary producers does not differ between the two sites. Previous studies of prokaryotic communities at CO_2 seep sites report an decrease in the relative abundance of Gammaproteobacteria (Kerfahi *et al.*, 2014; Taylor *et al.*, 2014). In this study, the relative abundance of Gammaproteobacteria was greater at the high CO_2 site (Fig. 5.5). Interestingly, Cyanobacteria represented a very small component of biofilm communities at both control and high CO_2 sites during this study (Fig. 5.5), contrasting with reports from previous characterisations of marine biofilms in other regions (Sanli *et al.*, 2015; Hassenrück *et al.*, 2017). These findings indicate that eukaryotic microalgae are the dominant primary producers in biofilms in the region.

The diversity and evenness of prokaryotic biofilm communities did not significantly differ between control and high CO_2 sites at any time point during the study (Fig. 5.7b). Previous CO_2 seep studies have reported conflicting effects of ocean acidification on prokaryotic community composition. Kerfahi *et al.* (2014) showed that prokaryotic diversity in epipelic communities is greater under high CO_2 conditions. Similarly, Lidbury *et al.* (2012) found that prokaryotic diversity can be enhanced under high CO_2 conditions, but that these effects are modulated by light conditions. In contrast, Taylor *et al.* (2014) demonstrated that prokaryotic diversity in epilithic biofilms is lower under high CO_2 conditions. Whilst this study provides greater taxonomic resolution and depth than previous reports, it is apparent that the effects of ocean acidification on prokaryotic biofilm community composition are not consistent between studies, suggesting that environmental factors other than the CO_2 may be more influential determinants of prokaryotic diversity (Hassenrück *et al.*, 2017).

5.5.3 Biofilm compositional variability

Quantifying changes in the compositional variability (within-group dissimilarity) of biofilm communities can provide insights into the ecological mechanisms which underpin community responses to environmental stressors, such as ocean acidification. The compositional variability of both eukaryotic and prokaryotic biofilm communities was lower at the high CO_2 site than at the control site (Fig. 5.8). This suggests that the influence of stochastic (i.e. neutral) processes on biofilm assembly was lower under high CO_2 conditions (Evans *et al.*, 2017). Macroecological studies demonstrate that environmental stressors can decrease the influence of stochasticity on community assembly (Chase, 2007), as is observed here. More recently, environmental stress has been shown to decrease the influence of stochastic processes in microbial community assembly (Valverde *et al.*, 2014). These findings, combined with the clear compositional differences between biofilms at control and high CO_2 sites, demonstrate that biofilms respond in a directional manner to ocean acidification by shifting to new, less variable, deterministic configuration (Fig. 5.4; Fig; 5.6; Fig. 5.8).

The assembly of prokaryotic communities in aquatic environments has previously been shown to be dominated by deterministic processes (Chapter 2; Logares *et al.* 2018), whilst stochastic processes appear to be comparatively more influential in the assembly of eukaryotic microbial communities (Chapter 3; Logares *et al.* 2018). Although both eukaryotic and prokaryotic biofilm communities are assembled through a greater influence

of deterministic processes and lesser influence of stochastic processes at high CO_2 sites, a trend of greater compositional variability in eukaryotic communities compared with prokaryotic communities was observed at both sites (Fig. 5.8). These data broadly support the notion that prokaryotic community assembly is comparatively more deterministic than eukaryotic community assembly in aquatic environments (Chapter 3; Logares *et al.* 2018). Significant compositional variation in both eukaryotic and prokaryotic biofilm communities occurred at all time points during the study (Fig. 5.8). Hassenrück *et al.* (2017) reported high levels of compositional variability in prokaryotic biofilm communities settling on artificial substrates across a gradient of acidification at two CO_2 seep systems in Papua New Guinea. Biofilms are characterised by sharp physicochemical gradients across microscales leading to patchiness in the distribution of taxa throughout the biofilm matrix (Flemming *et al.*, 2016), extending to the centimetre scale (Cordero and Datta, 2016). The scale of sampling employed in this study (30 cm^2 area) and by Hassenrück *et al.* (2017; 4 cm^2 area) may not be sufficient to overwhelm the influence of microscale variability, and may contribute to the significant compositional variability observed in biofilm communities. Indeed, sampling of larger sections of homogenised biofilms may reveal more consistent trends in community composition facilitating more general conclusions regarding the responses of marine biofilms to ocean acidification.

5.5.4 Eukaryotic-prokaryotic biofilm community coupling

The composition of eukaryotic and prokaryotic biofilm communities was more closely coupled under high CO_2 conditions (Fig. 5.10). These findings indicate that the strength of ecological interactions between eukaryotes and prokaryotes may be enhanced by ocean acidification. In this instance, the closer coupling of eukaryotic and prokaryotic communities may emerge from the consistent dominance of *Prymnesium sp.* under high CO_2 conditions. As discussed above, these mixotrophic algae produce toxic and allelopathic prymensins which can exert controls on the composition of both eukaryotic and prokaryotic communities. Moreover, previous studies demonstrate the ocean acidification can enhance the production of EPS in biofilm communities (Lidbury *et al.*, 2012), which may further contribute to the development of a more closely coupled eukaryotic and prokaryotic biofilm community.

5.5.5 Invertebrate settlement

Differences in the composition of eukaryotic and prokaryotic biofilm communities between control and high CO_2 sites are likely to affect the recruitment of invertebrates and habitat-forming organisms, which has previously been shown to be impacted by ocean acidification at CO_2 seeps (Cigliano *et al.*, 2010; Fabricius *et al.*, 2015; Allen *et al.*, 2016). In particular, the dominance of *Prymnesium sp.* at high CO_2 sites may have profound implications for the recruitment of invertebrates and other habitat forming organisms, due to the toxic and allelopathic properties of prymnesins, as discussed above. Fabricius *et al.* (2017) recently demonstrated that the recruitment of keystone invertebrate species, such as scleractinian corals, is more severely affected by ocean acidification associated shifts in substrate composition than by the direct effects of seawater chemistry. Moreover, Espinel-Velasco *et al.* (2018) reviewed the effects of ocean acidification on invertebrate settlement and metamorphosis, highlighting the fundamental importance of substrate composition, and in particular biofilm community composition, in modulating the effects of ocean acidification on invertebrate recruitment. The findings of this study demonstrate clear shifts in biofilm community composition under high CO_2 conditions, which may have severe consequences across multiple trophic levels, in addition to effects on the composition of the biofilms themselves. Indeed, these shifts in biofilm community composition and consequent effects on the recruitment of invertebrates and habitat-forming organisms may contribute significantly to the restructuring of coastal marine environments under elevated CO_2 conditions observed at CO_2 seep sites globally (Hall-Spencer *et al.*, 2008; Fabricius *et al.*, 2011; Agostini *et al.*, 2018).

5.5.6 Summary

In summary, this study shows that the composition eukaryotic and prokaryotic biofilm communities differ deterministically between control and high CO_2 sites, whilst the diversity and evenness these communities was unaffected by high CO_2 conditions. Both eukaryotic and prokaryotic biofilm communities displayed less compositional variability at high CO_2 sites, indicating that the influence of stochastic processes may be lower under high CO_2 conditions, in line with macroecological theory suggesting that stochastic processes are less influential under environmentally stressful conditions (Chase, 2007). Furthermore, the successional trajectory and rate of turnover between biofilm communities

appears unaffected by ocean acidification and is not a mechanism through which the composition of these communities is affected by ocean acidification across short timeframes. These data indicate that species replacement, rather than shifts in diversity, evenness, or successional dynamics, underpin biofilm community responses to ocean acidification. Furthermore, the dominance of the toxin-producing golden algae genera *Prymnesium* under high CO_2 conditions builds on concerns that ocean acidification may systematically favour harmful algal species (Hall-Spencer and Allen, 2015; Riebesell *et al.*, 2018). The findings of this study unveil the ecological mechanisms which underpin biofilm community responses to ocean acidification at the Shikine-Jima CO_2 seep system, representing a significant contribution to our understanding of how these critical marine resources may respond to ocean acidification in the near future. However, further studies employing high-resolution molecular techniques are warranted in different regions to establish whether these findings can be generalized.

Chapter 6: Discussion

Chapter 6: Discussion

6.1 Marine microbial community assembly

6.1.1 Prokaryotic community assembly

To date, numerous studies have investigated the ecological processes which underpin prokaryotic community assembly across a range of systems (Stegen *et al.*, 2013; Martínez *et al.*, 2015; Graham *et al.*, 2017; Griffin and Wells, 2017; Tripathi *et al.*, 2018). These studies indicate that deterministic processes (homogeneous selection and variable selection; Table 2.1) are the predominant drivers of prokaryotic community assembly in freshwater, terrestrial, industrial, and host-associated environments. Studies of marine sediments show that prokaryotic community assembly is highly deterministic; this is unsurprising due to the sharp physicochemical gradients occurring across short vertical spatial scales in these environments (Meyerhof *et al.*, 2016; Petro *et al.*, 2017; Starnawski *et al.*, 2017). Studies of pelagic marine environments display less consistent results. Vergin *et al.* (2017) and Logares *et al.* (2018) demonstrate that deterministic processes dominate prokaryotic community assembly in the Atlantic Ocean and Antarctic marine and freshwater lakes, respectively. In contrast, Wu *et al.* (2017a) and Mo *et al.* (2018) report a more balanced influence of stochastic and deterministic processes on community assembly in the East China Sea. Differences in community assembly processes between sediment and pelagic environments may result from sharper physicochemical gradients in sediment versus pelagic environments, exerting stronger abiotic selection pressures across shorter spatial scales.

Chapter 2 of this thesis demonstrated that deterministic processes dominate prokaryotic community assembly across horizontal spatial scales in the oligotrophic SPG (Fig. 2.5). These findings are sensical in the oligotrophic SPG, as the region is characterised by severe nutrient limitation and stable environmental conditions across horizontal spatial scales of over 2,000 km (Ellwood *et al.*, 2018). Consequently, homogeneity in prokaryotic community composition, driven by homogeneous selection, was observed across the region. Importantly, these findings indicate that homogeneous selection was able to

overwhelm the influence of dispersal effects and ecological drift across vast spatial distances in the surface waters of the oligotrophic SPG. The findings of Chapter 2 significantly expand our understanding of prokaryotic biogeography in the under-sampled oligotrophic SPG (Sunagawa *et al.,* 2015) and illustrate that homogeneous selection drives homogeneity in prokaryotic community composition across horizontal spatial scales exceeding 2,000 km in the region (Fig. 2.2). Similarly, Chapter 3 demonstrated that prokaryotic community assembly is highly deterministic across short spatial scales in the Southland Front system (Fig. 3.6). These data indicate that selection pressure was sufficient to overwhelm dispersal effects and ecological drift across the region. These findings align with evidence from hyporheic environments which demonstrate that selection pressure can overwhelm dispersal effects and ecological drift even in highly connected aquatic environments (Graham *et al.*, 2017).

While deterministic processes dominated prokaryotic community assembly across horizontal spatial scales in both the oligotrophic SPG and the Southland Front system, stochastic processes (specifically dispersal limitation) were comparatively more influential across vertical spatial scales in the highly stratified oligotrophic SPG (Fig. 2.5, Table 2.2). The surface waters of the oligotrophic SPG are separated from the nutrient-rich deep waters by a density gradient (Ellwood *et al.*, 2018), suggesting that minimal mixing occurs between these water masses. As a result, connectivity between these environments is limited, allowing these communities to diverge through ecological drift acting with a degree of independence on communities in the surface waters and the deep waters (i.e. dispersal limitation). These findings highlight that although deterministic processes dominate prokaryotic community assembly in the marine environment, stochastic processes can still play a role in structuring prokaryotic communities between contiguous water masses.

Overall, the findings of this thesis contribute to the notion that prokaryotic communities are assembled through predominantly deterministic processes, suggesting that differences in the environmental niches of prokaryotic ASVs underpin their distribution through space and time in the marine environment. Consequently, changes in abiotic or biotic environmental conditions which exert selection pressure may have profound implications for the structure of prokaryotic communities in a future ocean.

6.1.2 Protist community assembly

The substantial role of dispersal limitation and ecological drift (undominated scenario) in protist community assembly was eluded to by the emergence of strong distance-decay relationships in global-scale surveys of eukaryotic marine plankton communities (de Vargas *et al.*, 2015). A study of Antarctic lakes, ranging from freshwater to marine, found that dispersal limitation and ecological drift underpinned protist community assembly (Logares *et al.*, 2018). Furthermore, studies of planktonic picoeukaryotes in the East China Sea showed that dispersal limitation dominated community assembly in abundant taxa, while abiotic selection had minimal influence (Wu *et al.*, 2017b). These findings correspond with evidence from the Southern Ocean indicating that abiotic selection has a minimal influence on protist community composition across short spatial scales, and the dispersal effects and ecological drift explained a large proportion of variation in community structure (Moreno-Pino *et al.*, 2016).

Chapter 3 found that dispersal limitation and ecological drift dominated protist community assembly in the Southland Front system (Fig. 3.6). These data align with previous evidence suggesting that stochastic processes underpin protist community assembly across short spatial scales in marine environments (Moreno-Pino *et al.*, 2016). Moreover, these data corroborate previous evidence suggesting that dispersal limitation may be important in structuring protist communities between contiguous water masses (Monier *et al.*, 2015). Inferences about the broader implications of these findings should be considered with caution, as I only present data from a single region during a single sampling day. Nonetheless, the results of Chapter 3 contribute to a growing body of evidence indicating that marine protist communities respond to broad-scale rather than fine-scale environmental conditions and are more strongly influenced by dispersal effects and ecological drift across short spatial scales when environmental gradients are not dramatic (Monier *et al.*, 2015; Moreno-Pino *et al.*, 2016; Wu *et al.*, 2017b).

The large influence of stochastic processes on protist community assembly, particularly at the sub-mesoscale, may distort our ability to predict the responses of marine protist communities to environmental change. This is because trait-independent (stochastic) processes are important drivers of protist community composition. Thus, to develop a deeper understanding of how environmental change, including ocean acidification, may affect marine protist communities, it is important to explicitly consider the influence of

stochastic processes and the interaction between environmental change and the balance between stochastic and deterministic community assembly processes.

6.1.3 Prokaryotic versus protist community assembly

Chapter 3 represents the first integrated study of prokaryotic and protist community composition across a sub-mesoscale oceanic front using high-throughput amplicon sequencing. These data facilitated the direct comparison of prokaryotic and protist community structure and assembly across a convergence of four water masses. The findings of Chapter 3 demonstrated that deterministic processes underpin prokaryotic community assembly, while stochastic processes underpin protist community assembly across the Southland Front system. These findings align well with previous studies comparing prokaryotic and protist community assembly in aquatic environments (Moreno-Pino *et al.*, 2016; Logares *et al.*, 2018). Differences in community assembly processes between prokaryotic and protist communities may emerge from differences in the community level traits of these groups.

The average cell size of protists is larger than the average cell size of prokaryotes (Zinger *et al.*, 2018). Cell size is inversely related to dispersal ability in passively dispersing aquatic organisms (De Bie *et al.*, 2012; Soininen *et al.*, 2013). The ecological processes of dispersal limitation (i.e. ecological drift acting independently on local communities between which dispersal is limited) plays a more significant role in community assembly when dispersal rates are lower (Evans *et al.*, 2017). Global surveys of eukaryotic plankton communities indicate that larger plankton were more strongly influenced by dispersal effects and ecological drift, supporting this narrative (de Vargas *et al.*, 2015). In Chapter 3, I demonstrate that dispersal limitation is a key process in protist community assembly but is inconsequential in prokaryotic community assembly (Fig. 3.6).

The size of prokaryotic communities (number of individuals) is greater than the size of protist communities in the marine environment. For example, a single microliter of seawater can contain up to 20 protists but up to 1,000 heterotrophic bacteria (Azam and Malfatti, 2007). The influence of stochastic processes on community assembly is inversely related to community size, as the probability of species loss through ecological drift is lower in larger communities (Orrock and Watling, 2010). Furthermore, this effect interacts with dispersal ability, as greater dispersal ability increases the effective size of a

community, and subsequently decreases the influence of stochastic processes on community assembly (Ron *et al.*, 2018).

Finally, in contrast to classic metabolic theory which predicts that growth rates will be highest for the smallest organisms (Brown *et al.*, 2004), the average turnover time of phytoplankton communities in natural marine environments is estimated to be an order of magnitude greater than the turnover time of heterotrophic bacteria (Kirchman, 2016). The faster turnover rate of protist communities may contribute to the enhanced effect of stochastic processes on community assembly. Under environmental conditions which do not exert strong selection pressure, higher turnover rates increase the rate at which dispersal limitation and ecological drift can affect a community. This proposed mechanism is more controversial than the effects of average cell size and community size, as under intense selection pressure faster community turnover rates would be expected to enhance the influence of deterministic processes on community assembly. Nonetheless, the role of turnover rate in protist and prokaryotic community assembly warrants further investigation in the marine environment.

6.2 Marine microbial community responses to ocean acidification

6.2.1 Bacterioplankton community responses

Previous studies investigating the responses of planktonic prokaryotic communities (bacterioplankton) to ocean acidification have demonstrated either minor effects on community composition or no statistically significant effects across a range of ocean basins (Newbold *et al.*, 2012; Zhang *et al.*, 2013; Lindh *et al.*, 2013; Maas *et al.*, 2013; Roy *et al.*, 2013; Oliver *et al.*, 2014; Baltar *et al.*, 2015a; Bergen *et al.*, 2016; Wang *et al.*, 2016; Hartmann *et al.*, 2016; Sala *et al.*, 2016; Burrell *et al.*, 2017). These findings broadly support the hypothesis proposed by Joint *et al.* (2011) that marine prokaryotes would be resilient to ocean acidification as they must already contend with significant fluctuations in pH across a range of spatiotemporal scales and consequently possess sufficient physiological plasticity to tolerate projected decreases in mean surface ocean pH.

Chapter 4 investigated the effect of ocean acidification and warming on bacterioplankton communities in the SPG under trace-metal clean conditions for the first time. Despite the biogeochemical importance of oligotrophic subtropical gyres (Hoegh-Guldberg and

Poloczanska, 2017), the responses of bacterioplankton communities to ocean acidification remain poorly investigated in these region. Chapter 4 showed that ocean acidification altered prokaryotic community structure at the ultra-oligotrophic centre of the SPG but not at the fringe of the SPG, suggesting that nutrient regimes and ocean acidification may interact to affect prokaryotic community composition. These findings align with previous indications that the prevailing nutrient regime may modulate the effect of ocean acidification on prokaryotic communities (Sala *et al.*, 2016). Although ocean acidification significantly affected prokaryotic community composition at the ultra-oligotrophic centre of the SPG, these effects were subtle (Fig. 4.3) and it is challenging to infer whether such minor compositional shifts are of ecological or biogeochemical relevance. Indeed, the resilience of prokaryotic communities to ocean acidification at the fringe of the SPG, and the subtle effects observed at the ultra-oligotrophic centre of the SPG do not deviate from the narrative that ocean acidification has relatively minor impacts on the composition of prokaryotic communities (Joint *et al.*, 2011).

As a growing body of evidence indicates that deterministic processes dominate prokaryotic community assembly in the marine environment, shifts in environmental conditions may be expected to have significant effects on prokaryotic community composition. However, the minimal influence of near-future CO_2 concentrations on prokaryotic community composition suggests that these environmental perturbations exert relatively weak selection pressure on prokaryotic communities in pelagic environments.

This investigation would have benefitted significantly from greater replication, and a full factorial design to allow the effect of temperature and the interaction between temperature and ocean acidification to be resolved. The limited replication of this study reduces the statistical power of analyses, and the potential to identify the actual effects of ocean acidification on prokaryotic community composition. However, significant logistical challenges surrounding trace-metal clean deckboard incubation experiments constrained these ambitions. Consequently, the data from Chapter 4 form the basis for the hypothesis that the composition of prokaryotic communities in the ultra-oligotrophic centre of the SPG may be vulnerable to ocean acidification over the next century. However, significant further investigation is necessary before firm conclusions can be drawn.

6.2.2 Biofilm community responses

Early laboratory studies indicated that ocean acidification can alter the composition of biofilm communities through short-term experiments (Witt *et al.*, 2011; Krause *et al.*, 2012). More recently, CO_2 seeps have been employed to investigate the effects of ocean acidification in the context of natural communities, where recruitment dynamics and biofilm formation may be more realistic than in laboratory experiments. Studies at CO_2 seeps have investigated the effects of ocean acidification on biofilm communities forming on artificial substrates (Lidbury *et al.*, 2012; Johnson *et al.*, 2013; Hassenrück *et al.*, 2017), intertidal rock surfaces (Taylor *et al.*, 2014; Johnson *et al.*, 2015), sand surfaces (Johnson *et al.*, 2015), and sediment surfaces (Kerfahi *et al.*, 2014; Johnson *et al.*, 2015). These studies have consistently demonstrated shifts in the composition of both eukaryotic (Lidbury *et al.*, 2012; Johnson *et al.*, 2013, 2015) and prokaryotic (Lidbury *et al.*, 2012; Kerfahi *et al.*, 2014; Taylor *et al.*, 2014) biofilm communities under elevated CO_2 conditions. However, the effect of elevated CO_2 conditions on community diversity and evenness varies between studies. For example, Lidbury *et al.*, (2012) found no effect of elevated CO_2 conditions on eukaryotic community diversity, while Johnson *et al.* (2013, 2015) found a decrease in the diversity of photosynthetic eukaryotes under these conditions. Kerfahi *et al.* (2014) found increased prokaryotic community diversity under elevated CO_2 conditions. Similarly, Lidbury *et al.* (2012) found greater prokaryotic community diversity under elevated CO_2 conditions in low light environments. In contrast, Taylor *et al.* (2014) found decreased prokaryotic diversity under elevated CO_2 conditions. The conflicting findings of these studies are challenging to reconcile due to the different molecular techniques employed by the respective investigations, and the various substrates which these experiments investigated. To date, studies of biofilm community responses to ocean acidification at natural CO_2 seep systems have been almost exclusively performed at the Vulcano CO_2 seep system in the Mediterranean Sea (Lidbury *et al.*, 2012; Johnson *et al.*, 2013, 2015; Kerfahi *et al.*, 2014; Taylor *et al.*, 2014), excluding a single study at Upa Upasina in Papua New Guinea (Hassenrück *et al.*, 2017). Moreover, these studies employ a single time point design (excluding Hassenrück *et al.*, 2017), and offer limited insights into the effect ocean acidification on successional dynamics or the ecological mechanisms which underpin community responses to ocean acidification.

Chapter 5 investigated the effects of ocean acidification on eukaryotic and prokaryotic biofilm community diversity, composition, and succession, at the Shikine-Jima CO_2 seep system in Japan. The study found that elevated CO_2 conditions drive clear directional shifts

in the composition of both eukaryotic and prokaryotic communities throughout the early stages of biofilm succession (Fig. 5.4., Fig. 5.6). The diversity and evenness of both eukaryotic and prokaryotic biofilm communities were unaffected by elevated CO_2 conditions (Fig. 5.7). Furthermore, the rate of succession in both eukaryotic and prokaryotic biofilm communities was unaffected by elevated CO_2 conditions (Fig. 5.9), in contrast to speculation that faster growth rates of certain marine algae may accelerate biofilm succession under elevated CO_2 conditions (Dutkiewicz *et al.*, 2015; Mackey *et al.*, 2015). These findings indicate that both eukaryotic and prokaryotic biofilm communities respond to ocean acidification through shifts in the relative abundance of constituent ASVs and the replacement of ASVs sensitive to ocean acidification with ASVs tolerant of ocean acidification. These compositional shifts are not associated with any effect on community diversity, evenness, or successional dynamics, and are more representative of a simple species replacement mechanism.

To date, Chapter 5 of this thesis represents the most detailed investigation of the responses of eukaryotic and prokaryotic biofilm communities to ocean acidification. The study employed high-throughput sequencing of the 16S and 18S rRNA genes across 66 samples at four time points, offering greater replication, temporal resolution, and taxonomic resolution than previous investigations. These findings support the consensus of previous literature indicating that near-future ocean acidification can significantly alter the composition of both eukaryotic and prokaryotic biofilm communities, in addition to offering new insights into the ecological mechanisms which underpin these responses.

Biofilms are a basal component of coastal marine food webs, as subtidal benthic microalgae fix approximately 135 g C m^{-2} y^{-1}, which is marginally greater than estimated phytoplankton productivity in coastal environments (Beardall and Light, 1994). Furthermore, biofilms act as a settlement substrate for invertebrates and habitat-forming organisms (Qian *et al.*, 2007; Hadfield, 2011). Biofilm community composition directly affects invertebrate settlement as invertebrate larvae respond to the presence of specific bacterial taxa (Hadfield, 2011). Indeed, shifts in the composition of biofilm communities are a likely driver of changes in invertebrate settlement and recruitment associated with ocean acidification (Espinel-Velasco *et al.*, 2018). Studies performed at CO_2 seeps indicate that ocean acidification may cause significant remodelling of coastal marine environments (Hall-Spencer *et al.*, 2008; Fabricius *et al.*, 2011; Agostini *et al.*, 2018), and I speculate that changes in biofilm community composition may initiate these effects.

6.2.3 Effects of ocean acidification on harmful algae

Toxin-producing algae are expected to benefit physiologically from elevated CO_2 concentrations (Fu *et al.*, 2012; Hall-Spencer and Allen, 2015). Laboratory studies indicate that the growth rate of toxin-producing diatoms (Sun *et al.*, 2011), dinoflagellates (Tatters *et al.*, 2013; Errera *et al.*, 2014; Hattenrath-Lehmann *et al.*, 2015; Ou *et al.*, 2017; Pang *et al.*, 2017), and haptophytes (Wang *et al.*, 2010) can be enhanced under elevated CO_2 conditions. These toxin-producing algae appear to benefit more consistently from ocean acidification than microalgae considered more broadly (Dutkiewicz *et al.*, 2015). Moreover, the cellular toxicity of these algae can increase under elevated CO_2 conditions (Sun *et al.*, 2011; Tatters *et al.*, 2012, 2013; Pang *et al.*, 2017) as excess carbon due to increased photosynthetic activity is shunted to toxin production (Fu *et al.*, 2012).

Despite evidence from laboratory experiments indicating that the growth rate and cellular toxicity of toxin-producing algae can be enhanced by ocean acidification, few studies have linked these physiological effects to ecological advantages at an ecosystem level. Riebesell *et al.* (2018) demonstrated that the toxin-producing algae *Vicicitus globosus* consistently benefitted from elevated CO_2 concentrations in a large-scale mesocosm experiment, providing some of the first *in-situ* evidence of the proliferation of toxin-producing algae as a result of ocean acidification. In Chapter 5, I show that the relative abundance of the toxin-producing golden algal genus *Prymnesium* is enhanced in biofilm communities under elevated CO_2 conditions at the Shikine-Jima CO_2 seep (Fig. 5.3). The results of Chapter 5 represent the second demonstration of the proliferation of toxin-producing algae under elevated CO_2 conditions in an ecosystem level investigation.

While predicting the occurrence of harmful algal blooms under future ocean acidification scenarios remains a significant challenge (Hallegraeff, 2010; Fu *et al.*, 2012), it is feasible that the enhanced relative abundance of toxin-producing algae in biofilm communities may act as a seed population from which planktonic blooms can form. Indeed, *Prymnesium sp.* are associated with large scale regional fish kills, and blooming events are likely to have widespread socioeconomic ramifications (Roelke *et al.*, 2016). Furthermore, toxin-producing algae can disrupt the flow of carbon through marine food webs, leading to a significant decline in carbon export from pelagic environments (Riebesell *et al.*, 2018), potentially creating a positive feedback loop with rising atmospheric CO_2 concentrations. Indeed, the disruption of carbon flow through marine food webs may also contribute to the trophic simplification and reduction of diversity observed at high CO_2 seep sites in Shikine-Jima, Japan (Agostini *et al.*, 2018). While observations of these ecosystem level trends

remain in their infancy, they represent a significant cause for concern due to the dramatic socioeconomic consequences of harmful algal blooms on a global scale (Berdalet *et al.*, 2016).

In addition to the dominance of the toxin-producing algae genera *Prymnesium*, the relative abundance of the mat-forming diatom *Biddulphia biddulphiana* was higher at the high CO_2 site than at the control site at Shikine-Jima. *Biddulphia biddulphiana* mats can completely smother benthic environments and represent a significant threat to habitat-forming organisms as they bypass competition for space, contributing significantly to the reduction of habitat complexity observed under elevated CO_2 conditions (Agostini *et al.*, 2018). Although the environmental factors which induce the formation of such mats are poorly understood (Galland and Pennebaker, 2012), it is apparent that elevated CO_2 concentrations contribute to this behaviour. Mat-forming behaviour was observed on biofilm settlement slides at the high CO_2 site (Fig. 6.1) but did not form with sufficient voracity to smother the benthos surrounding the experimental site. However, at nearby sites of extreme seeping, where CO_2 concentration exceeded end-of-century projections (Hoegh-Guldberg *et al.*, 2014), *Biddulphia biddulphiana* mats completely smothered the benthos leading to an ecosystem-level reconfiguration of these coastal marine environments (Fig. 6.1). Previous reports that similar *Biddulphia biddulphiana* mats have formed outside CO_2 seep sites (Galland and Pennebaker, 2012) suggest that other environmental factors may be important in modulating this behaviour, raising concerns that potential interactions between ocean acidification and these latent environment variables could lead to the proliferation of *Biddulphia biddulphiana* mats in the near future.

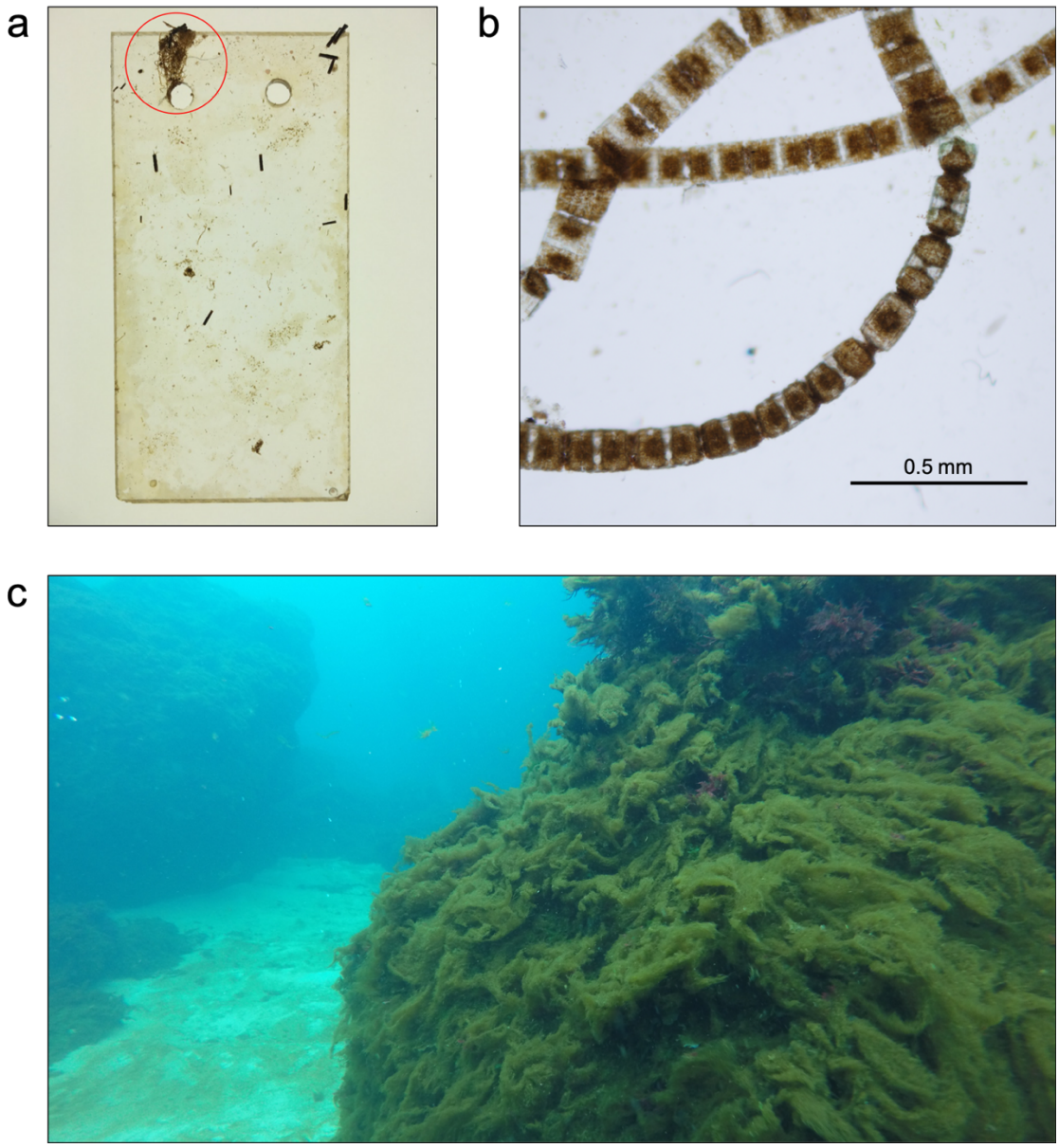

Figure 6.1 (a) *Biddulphia biddulphiana* mat-forming behavior observed on slide collected from high CO_2 site after day 15. Red circle indicates the initiation of a *Biddulphia biddulphiana* mat. (b) Isolated *Biddulphia biddulphiana* chains observed using a light microscope. (c) *Biddulphia bidduphiana* mats smothering the benthos at extreme CO_2 sites.

6.2.4 Effects of ocean acidification on community assembly

While the effect of ocean acidification on community assembly processes was not explicitly quantified in this thesis, patterns in community structure observed in both Chapter 4 and Chapter 5 indicate that ocean acidification may increase the influence of deterministic processes on both prokaryotic and eukaryotic community assembly. In prokaryotic communities at the ultra-oligotrophic centre of the SPG, and in both prokaryotic and eukaryotic biofilm communities at Shikine-Jima, elevated CO_2 conditions resulted in lower within-group distance in community composition when compared with ambient CO_2 conditions (Fig. 5.8). A higher degree of similarity between replicates can emerge from either a greater influence of homogenising dispersal or homogenous selection. In the context of these experiments, dispersal is not expected to differ substantively between treatments, as water flow is similar at control and high CO_2 sites in Shikine-Jima (Agostini *et al.*, 2015) and cubitainers in Chapter 4 act as absolute dispersal barriers between replicates. Consequently, the congruence between communities under elevated CO_2 conditions observed in both of these experiments may emerge from homogenous selection. These findings indicate that elevated CO_2 conditions exert consistent selection pressure on prokaryotic and eukaryotic communities (though this selection pressure is relatively weak in pelagic environments), driving a deterministic directional shift in community composition. Indeed, in both macro-ecology and microbial ecology, the presence of abiotic stressors decreases the role of stochasticity in community assembly as a result of increased selection pressure, leading to congruence in community composition (Chase, 2007; Valverde *et al.*, 2014).

6.3 Limitations of high-throughput sequencing studies

Though high-throughput amplicon sequencing has made an enormous contribution to our understanding of marine microbial ecology (Salazar and Sunagawa, 2017), it is essential to consider the nuances of these data. The first of these considerations is the potential for primer biases. The original Earth Microbiome Project primers (Caporaso *et al.*, 2011) were found to underestimate the relative abundance of SAR11 clade Alphaoproteobacteria, which are amongst the most abundant bacteria in the marine environment (Apprill *et al.*, 2015). These primers were subsequently modified to more accurately represent the relative

abundance of SAR11 (Apprill *et al.*, 2015), but the presence of other primer biases cannot be completely ruled out. A second consideration is that the number of 16S or 18S rRNA gene copies in prokaryotes (Louca, Doebeli, *et al.*, 2018) and protists (Zhu *et al.*, 2005; Weber and Pawlowski, 2013) vary between species. In prokaryotic communities, differences in 16S rRNA gene copy number between taxa are relatively minor, and databases are being developed with the goal of normalising high-throughput amplicon sequencing profiles against the gene copy numbers of constituent taxa (Louca, Doebeli, *et al.*, 2018). In protists, 18S rRNA gene copy number can differ by at least three orders of magnitude between species (Zhu *et al.*, 2005). However, 18S rRNA gene copy number correlates well with cell length (Zhu *et al.*, 2005) and biovolume (Godhe *et al.*, 2008) in the marine environment, and profiles of protist community composition inferred from high-throughput amplicon sequencing are closely aligned with profiles obtained through microscopy analysis (Piredda *et al.*, 2017, 2018). A third consideration is that high-throughput amplicon sequencing data are compositional (Gloor *et al.*, 2017), meaning that the relative abundance of taxa in a community lack independence from one another. However, extensive benchmarking studies demonstrate that these data accurately identify patterns in microbial beta-diversity and remain suitable for studying microbial ecology at the community level (Weiss *et al.*, 2017; Knight *et al.*, 2018). Despite these nuances, high-throughput amplicon sequencing offers unprecedented depth, coverage, and taxonomic resolution for the profiling of microbial communities, and is an essential tool for marine microbial ecologists (Salazar and Sunagawa, 2017).

6.4 Future research directions

6.4.1 Marine microbial community assembly

In this thesis, I investigated the ecological processes which underpin both prokaryotic and protist community assembly in the marine environment. The findings of this thesis aligned well with previous reports indicating that deterministic processes predominantly underpin prokaryotic community assemble, while stochastic processes predominantly underpin protist community assembly (Moreno-Pino *et al.*, 2016; Logares *et al.*, 2018). However, investigations of the relative importance of stochastic and deterministic processes are likely to vary across spatiotemporal scales and interact with hydrographic features such as oceanic

fronts. Consequently, significant further work is warranted to resolve the contribution of these processes to community assembly across different regions and different environmental contexts. Importantly, the relative influence of stochastic and deterministic processes has seldom been considered in the context of phytoplankton bloom events, despite significant research effort allocated to resolving the dynamics of prokaryotic and protist communities during these periods (Needham and Fuhrman, 2016). Moreover, studies allowing the direct comparison of prokaryotic and protist community assembly may help elucidate the traits which underpin differences in community assembly between these groups.

6.4.2 Incorporating community assembly into ocean acidification studies

The findings of Chapter 4 and Chapter 5 indicate that ocean acidification may alter the relative importance of stochastic and deterministic processes in prokaryotic and eukaryotic community assembly. Most community and ecosystem level investigations of microbial community responses to ocean acidification have focussed exclusively on quantifying the impact of abiotic environmental variables on community composition. However, in this thesis, I highlight the critical role of stochastic ecological processes in community assembly, particularly in protist communities (Fig. 3.6). I suggest that further efforts to quantify the impact of ocean acidification on community assembly processes and the explicit consideration of these processes in future investigations may help to reconcile discrepancies between studies and act as a platform for developing a deeper understanding of how ocean acidification may restructure both prokaryotic and protist communities. Indeed, novel conceptual frameworks for the investigation of microbial community dynamics have been developed and may benefit ocean acidification research (Stegen *et al.*, 2018).

6.4.3 Linking community structure, function, and activity: a multi-omics approach

A central goal of marine microbial ecologists is to link the structure, function, and activity of communities. High-throughput amplicon sequencing is a DNA based technique providing significant insights into the composition of both prokaryotic and protist

communities (de Vargas *et al.*, 2015; Sunagawa *et al.*, 2015) but offers limited information towards the function or activity of these communities.

RNA-based high-throughput amplicon sequencing can be performed by extracting RNA from environmental samples and using this RNA as a template to produce complementary DNA, which can then be processed according to the same protocols as DNA-based high-throughput amplicon sequencing. This RNA-based method isolates the metabolically active component of microbial communities and has the potential to return more meaningful profiles of microbial community composition with minimal distortion from metabolically inactive (dormant) taxa (Lennon and Jones, 2011; Salazar and Sunagawa, 2017). Consequently, these techniques may more accurately capture the effect of abiotic environmental conditions on prokaryotic and protist community composition. RNA-based profiling of prokaryotic community composition has already provided key insights into the seasonal dynamics (Salter *et al.*, 2015), bloom dynamics (Klindworth *et al.*, 2014; Wemheuer *et al.*, 2014), and sediment community responses to elevated CO_2 conditions in the marine environment (Yanagawa *et al.*, 2013).

Metagenomics investigates the total genomic composition of microbial communities to infer its metabolic potential and can contribute towards bridging the gap between community structure and function in marine environments (Sanli *et al.*, 2015). Galand *et al.* (2018) combined metagenomics and high-throughput amplicon sequencing to highlight that functional diversity and taxonomic diversity of marine prokaryotes are well correlated in the marine environment, suggesting low levels of functional redundancy in these communities. Moreover, metagenomics has assisted in the discovery of novel functions in uncultured bacterial groups (Delmont *et al.*, 2018).

Metatranscriptomics investigates the active genomic composition (i.e. gene expression) of microbial communities to infer metabolic activity. Metatranscriptomics have already been applied to ocean acidification research, revealing distinct pH-homeostasis mechanisms and consequently distinct sensitivities of marine bacteria to elevated CO_2 conditions (Bunse *et al.*, 2016). Moreover, metatranscriptomics has significantly advanced our understanding of marine protist communities (Caron *et al.*, 2016). For example, by demonstrating the metabolic underpinnings of diatom responses to iron fertilization (Marchetti *et al.*, 2012), the level of functional variation within diatom communities (Pearson *et al.*, 2015), and the interactions between marine protists and their associated viruses (Moniruzzaman *et al.*, 2017).

Combining the techniques mentioned above promises to provide more profound insights into the dynamics of marine microbial communities and how they respond to environmental changes such as ocean acidification (Fig. 6.2; Salazar and Sunagawa, 2017).

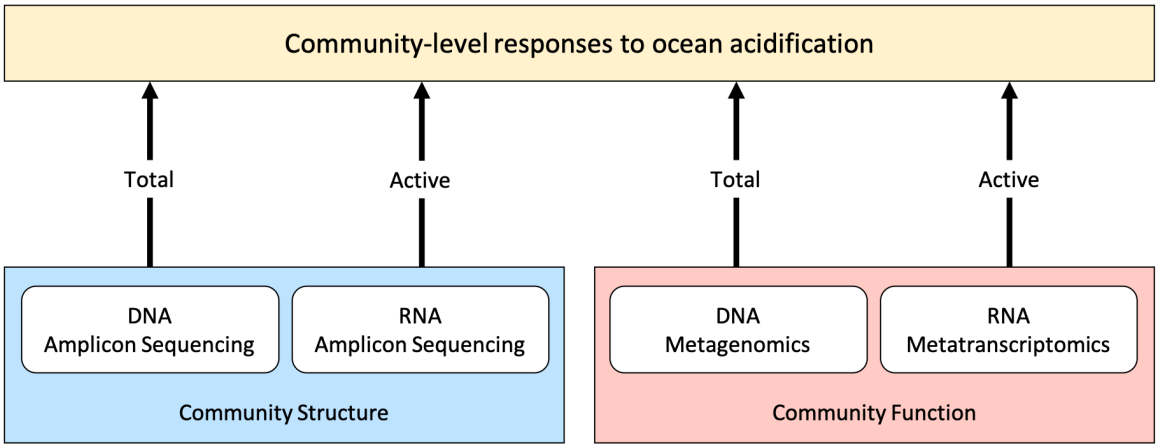

Figure 6.2 Representation DNA-based and RNA-based multi-omics approaches to advance our understanding of microbial community responses to ocean acidification by partitioning total and active components of community structure and function.

6.4.5 Harmful algae: from physiology to ecology

Greater efforts to link the physiological responses of harmful algae and the ecosystem level manifestations of these responses are necessary. These could include further investigations at CO_2 seeps or in large-scale mesocosms, in addition to environmental monitoring studies. Further investigations at CO_2 seeps should aim to quantify the toxicity of biofilms, rather than the relative abundance of toxin-producing ASVs. The responses of *Prymensium* growth rate and toxin production under elevated CO_2 conditions have not been investigated, despite the ease of culturing, the precedent for elevated CO_2 concentrations to enhance toxic algal growth and toxicity, and the sizeable socioeconomic impact of the genus (Roelke *et al.*, 2016). Indeed, these factors highlight *Prymnesium* as a critical target for future physiological investigations of harmful algal responses to elevated CO_2.

References

Aberle, N., Schulz, K.G., Stuhr, A., Malzahn, A.M., Ludwig, A., and Riebesell, U. (2013) High tolerance of microzooplankton to ocean acidification in an Arctic coastal plankton community. *Biogeosciences* **10**: 1471–1481.

Agostini, S., Harvey, B.P., Wada, S., Kon, K., Milazzo, M., Inaba, K., and Hall-Spencer, J.M. (2018) Ocean acidification drives community shifts towards simplified non-calcified habitats in a subtropical−temperate transition zone. *Sci. Rep.* **8**: 11354.

Agostini, S., Wada, S., Kon, K., Omori, A., Kohtsuka, H., Fujimura, H., et al. (2015) Geochemistry of two shallow CO_2 seeps in Shikine Island (Japan) and their potential for ocean acidification research. *Reg. Stud. Mar. Sci.* **2**: 45–53.

Allen, R., Foggo, A., Fabricius, K., Balistreri, A., and Hall-Spencer, J.M. (2016) Tropical CO_2 seeps reveal the impact of ocean acidification on coral reef invertebrate recruitment. *Mar. Pollut. Bull.* **124**: 607–613.

Alonso-Sáez, L., Gasol, J.M., Arístegui, J., Vilas, J.C., Vaqué, D., Duarte, C.M., and Agustí, S. (2007) Large-scale variability in surface bacterial carbon demand and growth efficiency in the subtropical northeast Atlantic Ocean. *Limnol. Oceanogr.* **52**: 533–546.

Anderson, M.J. (2001) A new method for non-parametric multivariate analysis of variance. *Austral Ecol.* **26**: 32–46.

Anderson, M.J. and Walsh, D.C.I. (2013) PERMANOVA, ANOSIM, and the Mantel test in the face of heterogeneous dispersions: What null hypothesis are you testing? *Ecol. Monogr.* **83**: 557–574.

Andersson, A., Kline, D., Edmunds, P., Archer, S., Bednaršek, N., Carpenter, R., et al. (2015) Understanding Ocean Acidification Impacts on Organismal to Ecological Scales. *Oceanography* **25**: 16–27.

Apprill, A., Mcnally, S., Parsons, R., and Weber, L. (2015) Minor revision to V4 region SSU rRNA 806R gene primer greatly increases detection of SAR11 bacterioplankton. *Aquat. Microb. Ecol.* **75**: 129–137.

Arrigo, K.R., Robinson, D.H., Worthen, D.L., Dunbar, R.B., DiTullio, G.R., VanWoert,

M., and Lizotte, M.P. (1999) Phytoplankton community structure and the drawdown of nutrients and CO_2 in the Southern Ocean. *Science* **283**: 365–367.

Azam, F., Fenchel, T., Field, J.G., Gray, J.S., Meyerreil, L.A., and Thingstad, F. (1983) The ecological role of water column microbes in the sea. *Mar. Ecol. Prog. Ser.* **10**: 257–263.

Azam, F. and Malfatti, F. (2007) Microbial structuring of marine ecosystems. *Nat. Rev. Microbiol.* **5**: 782–791.

Azam, F. and Simon, M. (1989) Protein content and protein synthesis rates of planktonic marine bacteria. *Mar. Ecol. Prog. Ser.* **51**: 201–213.

Bach, L.T., Mackinder, L.C.M., Schulz, K.G., Wheeler, G., Schroeder, D.C., Brownlee, C., and Riebesell, U. (2013) Dissecting the impact of CO_2 and pH on the mechanisms of photosynthesis and calcification in the coccolithophore Emiliania huxleyi. *New Phytol.* **199**: 121–134.

Bach, L.T., Taucher, J., Boxhammer, T., Ludwig, A., Achterberg, E.P., Algueró-Muñiz, M., et al. (2016) Influence of Ocean Acidification on a Natural Winter-to-Summer Plankton Succession: First Insights from a Long-Term Mesocosm Study Draw Attention to Periods of Low Nutrient Concentrations. *PLoS One* **11**: e0159068.

Baltar, F. and Arístegui, J. (2017) Fronts at the Surface Ocean Can Shape Distinct Regions of Microbial Activity and Community Assemblages Down to the Bathypelagic Zone: The Azores Front as a Case Study. *Front. Mar. Sci.* **4**: 1–13.

Baltar, F., Currie, K., Stuck, E., Roosa, S., and Morales, S.E. (2016) Oceanic fronts: transition zones for bacterioplankton community composition. *Environ. Microbiol. Rep.* **8**: 132–138.

Baltar, F., Lindh, M. V., Parparov, A., Berman, T., and Pinhassi, J. (2012) Prokaryotic community structure and respiration during long-term incubations. *MicrobiologyOpen* **1**: 214–224.

Baltar, F., Palovaara, J., Vila-Costa, M., Salazar, G., Calvo, E., Pelejero, C., et al. (2015) Response of rare, common and abundant bacterioplankton to anthropogenic perturbations in a Mediterranean coastal site. *FEMS Microbiol. Ecol.* **91**: 1–12.

Baltar, F., Stuck, E., Morales, S., and Currie, K. (2015) Bacterioplankton carbon cycling along the Subtropical Frontal Zone off New Zealand. *Prog. Oceanogr.* **135**: 168–175.

Beardall, J. and Light, B. (1994) Biomass, productivity and nutrient requirements of microphytobenthos CSIRO Institute for Natural Resources and Environment.

Beaufort, L., Probert, I., de Garidel-Thoron, T., Bendif, E.M., Ruiz-Pino, D., Metzl, N., et al. (2011) Sensitivity of coccolithophores to carbonate chemistry and ocean

acidification. *Nature* **476**: 80–83.

Behrenfeld, M.J., Randerson, J.T., McClain, C.R., Feldman, G.C., Los, S.O., Tucker, C.J., et al. (2001) Biospheric primary production during an ENSO transition. *Science* **291**: 2594–2597.

Belkin, I.M., Cornillon, P.C., and Sherman, K. (2009) Fronts in Large Marine Ecosystems. *Prog. Oceanogr.* **81**: 223–236.

Beltrán-Heredia, E., Aksnes, D.L., and Cao, F.J. (2017) Phytoplankton size scaling with nutrient concentration. *Mar. Ecol. Prog. Ser.* **571**: 59–64.

Bender, S.J., Moran, D.M., McIlvin, M.R., Zheng, H., McCrow, J.P., Badger, J., et al. (2018) Colony formation in *Phaeocystis antarctica*: Connecting molecular mechanisms with iron biogeochemistry. *Biogeosciences* **15**: 4923–4942.

Berdalet, E., Fleming, L.E., Gowen, R., Davidson, K., Hess, P., Backer, L.C., et al. (2016) Marine harmful algal blooms, human health and wellbeing: challenges and opportunities in the 21st century. *J. Mar. Biol. Assoc. United Kingdom* **96**: 61–91.

Bergen, B., Endres, S., Engel, A., Zark, M., Dittmar, T., Sommer, U., and Jürgens, K. (2016) Acidification and warming affect prominent bacteria in two seasonal phytoplankton bloom mesocosms. *Environ. Microbiol.* **18**: 4579–4595.

Berggren, M., Laudon, H., Jonsson, A., and Jansson, M. (2010) Nutrient constraints on metabolism affect the temperature regulation of aquatic bacterial growth efficiency. *Microb. Ecol.* **60**: 894–902.

Berthelot, H., Duhamel, S., L'Helguen, S., Maguer, J.F., Wang, S., Cetinić, I., and Cassar, N. (2018) NanoSIMS single cell analyses reveal the contrasting nitrogen sources for small phytoplankton. *ISME J.* **13**: 651-662.

Le Bescot, N., Mahé, F., Audic, S., Dimier, C., Garet, M.J., Poulain, J., et al. (2016) Global patterns of pelagic dinoflagellate diversity across protist size classes unveiled by metabarcoding. *Environ. Microbiol.* **18**: 609–626.

Biard, T., Bigeard, E., Audic, S., Poulain, J., Gutierrez-Rodriguez, A., Pesant, S., et al. (2017) Biogeography and diversity of Collodaria (Radiolaria) in the global ocean. *ISME J.* **11**: 1331–1344.

Biard, T., Stemmann, L., Picheral, M., Mayot, N., Vandromme, P., Hauss, H., et al. (2016) In situ imaging reveals the biomass of giant protists in the global ocean. *Nature* **532**: 504–507.

De Bie, T., De Meester, L., Brendonck, L., Martens, K., Goddeeris, B., Ercken, D., et al. (2012) Body size and dispersal mode as key traits determining metacommunity structure of aquatic organisms. *Ecol. Lett.* **15**: 740–747.

Biller, S.J., Berube, P.M., Lindell, D., and Chisholm, S.W. (2014) Prochlorococcus: the structure and function of collective diversity. *Nat. Rev. Microbiol.* **13**: 13–27.

Blais, M., Ardyna, M., Gosselin, M., Dumont, D., Bélanger, S., Tremblay, J.É., et al. (2017) Contrasting interannual changes in phytoplankton productivity and community structure in the coastal Canadian Arctic Ocean. *Limnol. Oceanogr.* **62**: 2480–2497.

Blondeau-Patissier, D., Gower, J.F.R., Dekker, A.G., Phinn, S.R., and Brando, V.E. (2014) A review of ocean color remote sensing methods and statistical techniques for the detection, mapping and analysis of phytoplankton blooms in coastal and open oceans. *Prog. Oceanogr.* **123**: 23–144.

Boiteau, R.M., Mende, D.R., Hawco, N.J., McIlvin, M.R., Fitzsimmons, J.N., Saito, M.A., et al. (2016) Siderophore-based microbial adaptations to iron scarcity across the eastern Pacific Ocean. *Proc. Natl. Acad. Sci.* **113**: 14237–14242.

Bonnet, S., Guieu, C., Bruyant, F., Pr, O., Wambeke, F. Van, Raimbault, P., et al. (2008) Nutrient limitation of primary productivity in the Southeast Pacific (BIOSOPE cruise). *Biogeosciences* **5**: 215–225.

Boyd, P.W., Dillingham, P.W., McGraw, C.M., Armstrong, E.A., Cornwall, C.E., Feng, Y. -y., et al. (2016) Physiological responses of a Southern Ocean diatom to complex future ocean conditions. *Nat. Clim. Chang.* **6**: 207–213.

Brown, J.H., Gillooly, J.F., Allen, A.P., Savage, V.M., and West, G.B. (2004) Toward a metabolic theory of ecology. *Ecology* **85**: 1771–1789.

Bryson, S., Li, Z., Chavez, F., Weber, P.K., Pett-Ridge, J., Hettich, R.L., et al. (2017) Phylogenetically conserved resource partitioning in the coastal microbial loop. *ISME J.* **11**: 2781–2792.

Buchan, A., LeCleir, G.R., Gulvik, C.A., and González, J.M. (2014) Master recyclers: features and functions of bacteria associated with phytoplankton blooms. *Nat. Rev. Microbiol.* **12**: 686–698.

Bunse, C., Lundin, D., Karlsson, C.M.G., Akram, N., Vila-Costa, M., Palovaara, J., et al. (2016) Response of marine bacterioplankton pH homeostasis gene expression to elevated CO_2. *Nat. Clim. Chang.* **6**: 483–487.

Burrell, T.J., Maas, E.W., Hulston, D.A., and Law, C.S. (2015) Bacterial abundance, processes and diversity responses to acidification at a coastal CO_2 vent. *FEMS Microbiol. Lett.* **362**: fnv154.

Burrell, T.J., Maas, E.W., Hulston, D.A., and Law, C.S. (2017) Variable response to warming and ocean acidification by bacterial processes in different plankton communities. *Aquat. Microb. Ecol.* **79**: 49–62.

Caldeira, K. and Wickett, M.E. (2003) Oceanography: Anthropogenic carbon and ocean pH. *Nature* **425**: 365.

Callahan, B.J., McMurdie, P.J., and Holmes, S.P. (2017) Exact sequence variants should replace operational taxonomic units in marker-gene data analysis. *ISME J.* **11**: 2639–2643.

Callahan, B.J., McMurdie, P.J., Rosen, M.J., Han, A.W., Johnson, A.J.A., and Holmes, S.P. (2016) DADA2: High-resolution sample inference from Illumina amplicon data. *Nat. Methods* **13**: 581–583.

Callahan, B.J., Sankaran, K., Fukuyama, J.A., McMurdie, P.J., and Holmes, S.P. (2016) Bioconductor Workflow for Microbiome Data Analysis: from raw reads to community analyses. *F1000Research* **5**: 1492.

Caporaso, J.G., Lauber, C.L., Walters, W.A., Berg-Lyons, D., Huntley, J., Fierer, N., et al. (2012) Ultra-high-throughput microbial community analysis on the Illumina HiSeq and MiSeq platforms. *ISME J.* **6**: 1621–1624.

Caporaso, J.G., Lauber, C.L., Walters, W.A., Berg-Lyons, D., Lozupone, C.A., Turnbaugh, P.J., et al. (2011) Global patterns of 16S rRNA diversity at a depth of millions of sequences per sample. *Proc. Natl. Acad. Sci.* **108**: 4516–4522.

Caron, D.A., Alexander, H., Allen, A.E., Archibald, J.M., Armbrust, E.V., Bachy, C., et al. (2016) Probing the evolution, ecology and physiology of marine protists using transcriptomics. *Nat. Rev. Microbiol.* **15**: 6–20.

Caron, D.A. and Hu, S.K. (2018) Are We Overestimating Protistan Diversity in Nature? *Trends Microbiol.* **27**: 197–205.

Chao, A. (1984) Nonparametric estimation of the number of classes in a population. *Scand. J. Stat.* 265–270.

Chase, J.M. (2007) Drought mediates the importance of stochastic community assembly. *Proc. Natl. Acad. Sci.* **104**: 17430–17434.

Chase, J.M. (2010) Stochastic Community Assembly Causes Higher Biodiversity in More Productive Environments. *Science* **328**: 1388–1391.

Chase, J.M., Kraft, N.J.B., Smith, K.G., Vellend, M., and Inouye, B.D. (2011) Using null models to disentangle variation in community dissimilarity from variation in α-diversity. *Ecosphere* **2**: 24.

Chase, J.M. and Leibold, M.A. (2003) Ecological niches: linking classical and contemporary approaches University of Chicago Press.

Chase, J.M. and Myers, J.A. (2011) Disentangling the importance of ecological niches from stochastic processes across scales. *Philos. Trans. R. Soc. London B Biol. Sci.* **366**:

2351–2363.

Chassot, E., Bonhommeau, S., Dulvy, N.K., Mélin, F., Watson, R., Gascuel, D., and Le Pape, O. (2010) Global marine primary production constrains fisheries catches. *Ecol. Lett.* **13**: 495–505.

Chauhan, A., Pathak, A., Rodolfo-Metalpa, R., Milazzo, M., Green, S.J., and Hall-Spencer, J.M. (2015) Metagenomics Reveals Planktonic Bacterial Community Shifts across a Natural CO_2 Gradient in the Mediterranean Sea. *Genome Announc.* **3**: 2–3.

Cho, B.C. and Azam, F. (1988) Major role of bacteria in biogeochemical fluxes in the ocean's interior. *Nature* **332**: 441.

Cigliano, M., Gambi, M.C., Rodolfo-Metalpa, R., Patti, F.P., and Hall-Spencer, J.M. (2010) Effects of ocean acidification on invertebrate settlement at volcanic CO_2 vents. *Mar. Biol.* **157**: 2489–2502.

Claustre, H., Huot, Y., Obernosterer, I., Gentili, B., Tailliez, D., and Lewis, M. (2008) Gross community production and metabolic balance in the South Pacific Gyre, using a non intrusive bio-optical method. *Biogeosciences* **5**: 463–474.

Claustre, H. and Maritorena, S. (2003) The many shades of ocean blue. *Science* **302**: 1514–1515.

Clayton, S., Dutkiewicz, S., Jahn, O., and Follows, M.J. (2013) Dispersal, eddies, and the diversity of marine phytoplankton. *Limnol. Oceanogr. Fluids Environ.* **3**: 182–197.

Clayton, S., Lin, Y.-C., Follows, M.J., and Worden, A.Z. (2017) Co-existence of distinct Ostreococcus ecotypes at an oceanic front. *Limnol. Oceanogr.* **62**: 75–88.

Clayton, S., Nagai, T., and Follows, M.J. (2014) Fine scale phytoplankton community structure across the Kuroshio Front. *J. Plankton Res.* **36**: 1017–1030.

Cole, J.R., Wang, Q., Fish, J.A., Chai, B., McGarrell, D.M., Sun, Y., et al. (2014) Ribosomal Database Project: Data and tools for high throughput rRNA analysis. *Nucleic Acids Res.* **42**: 633–642.

Cordero, O.X. and Datta, M.S. (2016) Microbial interactions and community assembly at microscales. *Curr. Opin. Microbiol.* **31**: 227–234.

Costerton, J.W., Lewandowski, Z., Caldwell, D.E., Korber, D.R., and Lappin-Scott, H.M. (1995) Microbial biofilms. *Annu. Rev. Microbiol.* **49**: 711–745.

Crawfurd, Katharine J., Alvarez-Fernandez, S., Mojica, K.D.A., Riebesell, U., and Brussaard, C.P.D. (2017) Alterations in microbial community composition with increasing fCO_2: a mesocosm study in the eastern Baltic Sea. *Biogeosciences* **14**: 3831–3849.

Currie, K.I., Reid, M.R., and Hunter, K.A. (2011) Interannual variability of carbon dioxide

drawdown by subantarctic surface water near New Zealand. *Biogeochemistry* **104**: 23–34.

Dandonneau, Y., Deschamps, P.Y., Nicolas, J.M., Loisel, H., Blanchot, J., Montel, Y., et al. (2004) Seasonal and interannual variability of ocean color and composition of phytoplankton communities in the North Atlantic, equatorial Pacific and South Pacific. *Deep. Res. Part II Top. Stud. Oceanogr.* **51**: 303–318.

Dang, H. and Lovell, C.R. (2016) Microbial Surface Colonization and Biofilm Development in Marine Environments. *Microbiol. Mol. Biol. Rev.* **80**: 91–138.

Davidson, E.A. and Janssens, I.A. (2006) Temperature sensitivity of soil carbon decomposition and feedbacks to climate change. *Nature* **440**: 165.

De'ath, G. (2002) Multivariate Regression Trees: A New Technique for Modeling Species-Environment Relationships. *Ecology* **83**: 1105–1117.

Decelle, J., Romac, S., Stern, R.F., Bendif, E.M., Zingone, A., Audic, S., et al. (2015) PhytoREF: A reference database of the plastidial 16S rRNA gene of photosynthetic eukaryotes with curated taxonomy. *Mol. Ecol. Resour.* **15**: 1435–1445.

Delmont, T.O., Quince, C., Shaiber, A., Esen, Ö.C., Lee, S.T., Rappé, M.S., et al. (2018) Nitrogen-fixing populations of Planctomycetes and Proteobacteria are abundant in surface ocean metagenomes. *Nat. Microbiol.* **3**: 804–813.

DeSantis, T.Z., Hugenholtz, P., Larsen, N., Rojas, M., Brodie, E.L., Keller, K., et al. (2006) Greengenes, a chimera-checked 16S rRNA gene database and workbench compatible with ARB. *Appl. Environ. Microbiol.* **72**: 5069–5072.

Dini-Andreote, F., Stegen, J.C., van Elsas, J.D., and Salles, J.F. (2015) Disentangling mechanisms that mediate the balance between stochastic and deterministic processes in microbial succession. *Proc. Natl. Acad. Sci.* **112**: E1326–E1332.

Djurhuus, A., Boersch-Supan, P.H., Mikalsen, S., and Rogers, A.D. (2017) Microbe biogeography tracks water masses in a dynamic oceanic frontal system. *R. Soc. Open Sci.* **4**: 170033.

Donahue, K., Klaas, C., Dillingham, P.W., and Hoffmann, L.J. (2019) Combined effects of ocean acidification and increased light intensity on natural phytoplankton communities from two Southern Ocean water masses. *J. Plankton Res.* **41**: 30–45.

Doney, S.C., Fabry, V.J., Feely, R. a, and Kleypas, J. a (2009) Ocean acidification: the other CO_2 problem. *Ann. Rev. Mar. Sci.* **1**: 169–92.

Duarte, C.M., Regaudie-de-Gioux, A., Arrieta, J.M., Delgado-Huertas, A., and Agustí, S. (2013) The oligotrophic ocean is heterotrophic. *Ann. Rev. Mar. Sci.* **5**: 551–69.

Dunne, J.P., Sarmiento, J.L., and Gnanadesikan, A. (2007) A synthesis of global particle

export from the surface ocean and cycling through the ocean interior and on the seafloor. *Global Biogeochem. Cycles* **21**: GB4006.

Dupont, C.L., Rusch, D.B., Yooseph, S., Lombardo, M.J., Alexander Richter, R., Valas, R., et al. (2012) Genomic insights to SAR86, an abundant and uncultivated marine bacterial lineage. *ISME J.* **6**: 1186–1199.

Dutkiewicz, S., Morris, J.J., Follows, M.J., Scott, J., Levitan, O., Dyhrman, S.T., and Berman-Frank, I. (2015) Impact of ocean acidification on the structure of future phytoplankton communities. *Nat. Clim. Chang.* **5**: 1002–1006.

Eggers, S.L., Lewandowska, A.M., Barcelos e Ramos, J., Blanco-Ameijeiras, S., Gallo, F., and Matthiessen, B. (2014) Community composition has greater impact on the functioning of marine phytoplankton communities than ocean acidification. *Glob. Chang. Biol.* **20**: 713–723.

Ehrenreich, A. (2006) DNA microarray technology for the microbiologist: An overview. *Appl. Microbiol. Biotechnol.* **73**: 255–273.

Ellwood, M.J., Bowie, A.R., Baker, A., Gault-Ringold, M., Hassler, C., Law, C.S., et al. (2018) Insights Into the Biogeochemical Cycling of Iron, Nitrate, and Phosphate Across a 5,300 km South Pacific Zonal Section (153°E-150°W). *Global Biogeochem. Cycles* **32**: 187–207.

Errera, R.M., Yvon-Lewis, S., Kessler, J.D., and Campbell, L. (2014) Reponses of the dinoflagellate Karenia brevis to climate change: pCO_2 and sea surface temperatures. *Harmful Algae* **37**: 110–116.

Espinel-Velasco, N., Hoffmann, L., Agüera, A., Byrne, M., Dupont, S., Uthicke, S., et al. (2018) Effects of ocean acidification on the settlement and metamorphosis of marine invertebrate and fish larvae: a review. *Mar. Ecol. Prog. Ser.* **606**: 237–257.

Evans, S., Martiny, J.B.H., and Allison, S.D. (2017) Effects of dispersal and selection on stochastic assembly in microbial communities. *ISME J.* **11**: 176–185.

Fabricius, K.E., Kluibenschedl, A., Harrington, L., Noonan, S., and De'ath, G. (2015) In situ changes of tropical crustose coralline algae along carbon dioxide gradients. *Sci. Rep.* **5**: 9537.

Fabricius, K.E., Langdon, C., Uthicke, S., Humphrey, C., Noonan, S., De'ath, G., et al. (2011) Losers and winners in coral reefs acclimatized to elevated carbon dioxide concentrations. *Nat. Clim. Chang.* **1**: 165–169.

Fabricius, K.E., Noonan, S.H.C., Abrego, D., Harrington, L., and De'Ath, G. (2017) Low recruitment due to altered settlement substrata as primary constraint for coral communities under ocean acidification. *Proc. R. Soc. B Biol. Sci.* **284**: 20171536.

Faith, D.P. (1992) Conservation evaluation and phylogentic diversity. *Biol. Conserv.* **61**: 1–10.

Farrant, G.K., Doré, H., Cornejo-Castillo, F.M., Partensky, F., Ratin, M., Ostrowski, M., et al. (2016) Delineating ecologically significant taxonomic units from global patterns of marine picocyanobacteria. *Proc. Natl. Acad. Sci.* **113**: E3365–E3374.

Faure, E., Not, F., Benoiston, A.-S., Labadie, K., Bittner, L., and Ayata, S.-D. (2019) Mixotrophic protists display contrasted biogeographies in the global ocean. *ISME J.* **13**: 1072-1083.

Fenchel, T. (2008) The microbial loop - 25 years later. *J. Exp. Mar. Bio. Ecol.* **366**: 99–103.

Feng, Y., Hare, C.E., Rose, J.M., Handy, S.M., DiTullio, G.R., Lee, P.A., et al. (2010) Interactive effects of iron, irradiance and CO_2 on Ross Sea phytoplankton. *Deep. Res. Part I Oceanogr. Res. Pap.* **57**: 368–383.

Fernández-Gómez, B., Richter, M., Schüler, M., Pinhassi, J., Acinas, S.G., González, J.M., and Pedrós-Alió, C. (2013) Ecology of marine bacteroidetes: A comparative genomics approach. *ISME J.* **7**: 1026–1037.

Field, C.B. (1998) Primary Production of the Biosphere: Integrating Terrestrial and Oceanic Components. *Science* **281**: 237–240.

Fisher, M.M. and Triplett, E.W. (1999) Automated approach for ribosomal intergenic spacer analysis of microbial diversity and its application to freshwater bacterial communities. *Appl. Environ. Microbiol.* **65**: 4630–4636.

Fistarol, G.O., Legrand, C., and Granéli, E. (2003) Allelopathic effect of Prymnesium parvum on a natural plankton community. *Mar. Ecol. Prog. Ser.* **255**: 115–125.

Flemming, H.C., Wingender, J., Szewzyk, U., Steinberg, P., Rice, S.A., and Kjelleberg, S. (2016) Biofilms: an emergent form of bacterial life. *Nat. Rev. Microbiol.* **14**: 563–575.

Flemming, H.C. and Wingender, J. (2010) The biofilm matrix. *Nat. Rev. Microbiol.* **8**: 623–633.

Flombaum, P., Gallegos, J.L., Gordillo, R.A., Rincón, J., Zabala, L.L., and Jiao, N. (2013) Present and future global distributions of the marine Cyanobacteria Prochlorococcus and Synechococcus. *Proc. Natl. Acad. Sci.* **110**: 9824–9829.

Fu, F.-X., Warner, M.E., Zhang, Y., Feng, Y., and Hutchins, D.A. (2007) Effects of increased temperature and CO_2 on photosynthesis, growth, and elemental ratios in marine Synechococcus and Prochlorococcus (Cyanobacteria). *J. Phycol.* **43**: 485–496.

Fu, F.X., Tatters, A.O., and Hutchins, D. a. (2012) Global change and the future of harmful algal blooms in the ocean. *Mar. Ecol. Prog. Ser.* **470**: 207–233.

Fuhrman, J. (2009) Microbial community structure and its functional implications. *Nature* **459**: 193–9.

Galand, P.E., Pereira, O., Hochart, C., Auguet, J.C., and Debroas, D. (2018) A strong link between marine microbial community composition and function challenges the idea of functional redundancy. *ISME J.* **10**: 2470-2478.

Galland, G. and Pennebaker, S. (2012) A benthic diatom bloom in the Gulf of California, Mexico. *BioInvasions Rec.* **1**: 65–69.

Ghai, R., Mizuno, C.M., Picazo, A., Camacho, A., and Rodriguez-Valera, F. (2013) Metagenomics uncovers a new group of low GC and ultra-small marine Actinobacteria. *Sci. Rep.* **3**: 2471.

Gildor, H., Fredj, E., Steinbuck, J., and Monismith, S. (2009) Evidence for Submesoscale Barriers to Horizontal Mixing in the Ocean from Current Measurements and Aerial Photographs. *J. Phys. Oceanogr.* **39**: 1975–1983.

Del Giorgio, P.A. and Cole, J.J. (1998) Bacterial growth efficiency in natural aquatic systems. *Annu. Rev. Ecol. Syst.* **29**: 503–541.

Del Giorgio, P.A., Condon, R., Bouvier, T., Longnecker, K., Bouvier, C., Sherr, E., and Gasol, J.M. (2011) Coherent patterns in bacterial growth, growth efficiency, and leucine metabolism along a northeastern Pacific inshore-offshore transect. *Limnol. Oceanogr.* **56**: 1–16.

Del Giorgio, P.A. and Duarte, C.M. (2002) Respiration in the open ocean. *Nature* **420**: 379–384.

Giovannoni, S.J. (2017) SAR11 Bacteria: The Most Abundant Plankton in the Oceans. *Ann. Rev. Mar. Sci.* **9**: 231–255.

Gloor, G.B., Macklaim, J.M., Pawlowsky-Glahn, V., and Egozcue, J.J. (2017) Microbiome Datasets Are Compositional: And This Is Not Optional. *Front. Microbiol.* **8**: 2224.

Godhe, A., Asplund, M.E., Härnström, K., Saravanan, V., Tyagi, A., and Karunasagar, I. (2008) Quantification of diatom and dinoflagellate biomasses in coastal marine seawater samples by real-time PCR. *Appl. Environ. Microbiol.* **74**: 7174–7182.

Graham, E.B., Crump, A.R., Resch, C.T., Fansler, S., Arntzen, E., Kennedy, D.W., et al. (2017) Deterministic influences exceed dispersal effects on hydrologically-connected microbiomes. *Environ. Microbiol.* **19**: 1552–1567.

Graham, E.B. and Stegen, J.C. (2017) Dispersal-Based Microbial Community Assembly Decreases Biogeochemical Function. *Processes* **5**: 65.

Griffin, J.S. and Wells, G.F. (2017) Regional synchrony in full-scale activated sludge bioreactors due to deterministic microbial community assembly. *ISME J.* **11**: 500–

511.

Griffith, J.C., Lee, W.G., Orlovich, D.A., and Summerfield, T.C. (2017) Contrasting bacterial communities in two indigenous Chionochloa (Poaceae) grassland soils in New Zealand. *PLoS One* **12**: e0179652.

Grob, C., Ulloa, O., Claustre, H., Huot, Y., Alarcón, G., and Marie, D. (2007) Contribution of picoplankton to the total particulate organic carbon concentration in the eastern South Pacific. *Biogeosciences* **4**: 837–852.

Grossmann, L., Beisser, D., Bock, C., Chatzinotas, A., Jensen, M., Preisfeld, A., et al. (2016) Trade-off between taxon diversity and functional diversity in European lake ecosystems. *Mol. Ecol.* **25**: 5876–5888.

Guidi, L., Chaffron, S., Bittner, L., Eveillard, D., Larhlimi, A., Roux, S., et al. (2016) Plankton networks driving carbon export in the oligotrophic ocean. *Nature* **532**: 465–470.

Guillou, L., Bachar, D., Audic, S., Bass, D., Berney, C., Bittner, L., et al. (2013) The Protist Ribosomal Reference database (PR2): A catalog of unicellular eukaryote Small Sub-Unit rRNA sequences with curated taxonomy. *Nucleic Acids Res.* **41**: 597–604.

Gutierrez-Rodriguez, A., Stukel, M.R., Lopes dos Santos, A., Biard, T., Scharek, R., Vaulot, D., et al. (2018) High contribution of Rhizaria (Radiolaria) to vertical export in the California Current Ecosystem revealed by DNA metabarcoding. *ISME J.* **13**: 964-976.

Hadfield, M.G. (2011) Biofilms and Marine Invertebrate Larvae: What Bacteria Produce That Larvae Use to Choose Settlement Sites. *Ann. Rev. Mar. Sci.* **3**: 453–470.

Hall-Spencer, J.M. and Allen, R. (2015) The impact of CO_2 emissions on 'nuisance' marine species. *Res. Reports Biodivers. Stud.* 4: 33-46.

Hall-Spencer, J.M., Rodolfo-Metalpa, R., Martin, S., Ransome, E., Fine, M., Turner, S.M., et al. (2008) Volcanic carbon dioxide vents show ecosystem effects of ocean acidification. *Nature* **454**: 96–99.

Hall, E.K., Dzialowski, A.R., Stoxen, S.M., and Cotnera, J.B. (2009) The effect of temperature on the coupling between phosphorus and growth in lacustrine bacterioplankton communities. *Limnol. Oceanogr.* **54**: 880–889.

Hall, E.K., Neuhauser, C., and Cotner, J.B. (2008) Toward a mechanistic understanding of how natural bacterial communities respond to changes in temperature in aquatic ecosystems. *ISME J.* **2**: 471–481.

Hallegraeff, G.M. (2010) Ocean climate change, phytoplankton community responses, and harmful algal blooms: A formidable predictive challenge. *J. Phycol.* **46**: 220–235.

Halm, H., Lam, P., Ferdelman, T.G., Lavik, G., Dittmar, T., Laroche, J., et al. (2011) Heterotrophic organisms dominate nitrogen fixation in the South Pacific Gyre. *ISME J.* **6**: 1238–1249.

Hancock, A.M., Davidson, A.T., McKinlay, J., McMinn, A., Schulz, K.G., and Van Den Enden, R.L. (2018) Ocean acidification changes the structure of an Antarctic coastal protistan community. *Biogeosciences* **15**: 2393–2410.

Hanson, C.A., Fuhrman, J.A., Horner-Devine, M.C., and Martiny, J.B.H. (2012) Beyond biogeographic patterns: Processes shaping the microbial landscape. *Nat. Rev. Microbiol.* **10**: 497–506.

Hartmann, M., Hill, P.G., Tynan, E., Achterberg, E.P., Leakey, R.J.G., and Zubkov, M. V. (2016) Resilience of SAR11 bacteria to rapid acidification in the high-latitude open ocean. *FEMS Microbiol. Ecol.* **92**: fiv161.

Hassenrück, C., Tegetmeyer, H.E., Ramette, A., and Fabricius, K.E. (2017) Minor impacts of reduced pH on bacterial biofilms on settlement tiles along natural pH gradients at two CO_2 seeps in Papua New Guinea. *ICES J. Mar. Sci.* **74**: 978–987.

Hattenrath-Lehmann, T.K., Smith, J.L., Wallace, R.B., Merlo, L.R., Koch, F., Mittelsdorf, H., et al. (2015) The effects of elevated CO_2 on the growth and toxicity of field populations and cultures of the saxitoxin-producing dinoflagellate, Alexandrium fundyense. *Limnol. Oceanogr.* **60**: 198–214.

Hernando-Morales, V., Ameneiro, J., and Teira, E. (2017) Water mass mixing shapes bacterial biogeography in a highly hydrodynamic region of the Southern Ocean. *Environ. Microbiol.* **19**: 1017–1029.

Hoegh-Guldberg, O., Poloczanska, E., Brewer, P., Sundby, S., Hilmi, K., Fabry, V., and Jung, S. (2014) The Ocean. In, *Climate Change 2014: Impacts, Adaptation, and Vulnerability. Part A: Global and Sectoral Aspects. Contribution of Working Group II to the Fifth Assessment Report of the Intergovernmental Panel on Climate Change*. Cambridge, United Kingdom, and New York, NY, USA, pp. 1655–1731.

Hoegh-Guldberg, O. and Poloczanska, E.S. (2017) Editorial: The Effect of Climate Change across Ocean Regions. *Front. Mar. Sci.* **4**: 361.

Hoffmann, L.J., Breitbarth, E., McGraw, C.M., Law, C.S., Currie, K.I., and Hunter, K.A. (2013) A trace-metal clean, pH-controlled incubator system for ocean acidification incubation studies. *Limnol. Oceanogr. Methods* **11**: 53–61.

Hopkinson, B.M., Dupont, C.L., Allen, A.E., and Morel, F.M.M. (2011) Efficiency of the CO_2-concentrating mechanism of diatoms. *Proc. Natl. Acad. Sci.* **108**: 3830–3837.

Hopkinson, B.M., Young, J.N., Tansik, A.L., and Binder, B.J. (2014) The Minimal CO_2-

Concentrating Mechanism of Prochlorococcus spp. MED4 Is Effective and Efficient. *Plant Physiol.* **166**: 2205–2217.

Hoppe, C.J.M., Hassler, C.S., Payne, C.D., Tortell, P.D., Rost, B., and Trimborn, S. (2013) Iron Limitation Modulates Ocean Acidification Effects on Southern Ocean Phytoplankton Communities. *PLoS One* **8**: e79890.

Hoppe, C.J.M., Wolf, K.K.E., Schuback, N., Tortell, P.D., and Rost, B. (2018) Compensation of ocean acidification effects in Arctic phytoplankton assemblages. *Nat. Clim. Chang.* **8**: 529–533.

Hu, C., Lee, Z., and Franz, B. (2012) Chlorophyll a algorithms for oligotrophic oceans: A novel approach based on three-band reflectance difference. *J. Geophys. Res. Ocean.* **117**: C01011.

Hubbell, S.P. (2001) The unified neutral theory of species abundance and diversity. *Princet. Univ. Press. Princeton, NJ. Hubbell, SP Q. Rev. Biol.* **79**: 96–97.

Hugerth, L.W. and Andersson, A.F. (2017) Analysing microbial community composition through amplicon sequencing: From sampling to hypothesis testing. *Front. Microbiol.* **8**: 1–22.

Hughes, J.B., Hellmann, J.J., Ricketts, T.H., and Bohannan, B.J. (2001) Counting the uncountable: statistical approaches to estimating microbial diversity. *Appl. Environ. Microbiol.* **67**: 4399–406.

Hutchins, D.A. and Fu, F. (2017) Microorganisms and ocean global change. *Nat. Microbiol.* **2**: 17058.

Irwin, A.J. and Oliver, M.J. (2009) Are ocean deserts getting larger? *Geophys. Res. Lett.* **36**: L18609.

Iversen, M.H. and Ploug, H. (2010) Ballast minerals and the sinking carbon flux in the ocean: Carbon-specific respiration rates and sinking velocity of marine snow aggregates. *Biogeosciences* **7**: 2613–2624.

James, A.K., Passow, U., Brzezinski, M.A., Parsons, R.J., Trapani, J.N., and Carlson, C.A. (2017) Elevated pCO_2 enhances bacterioplankton removal of organic carbon. *PLoS One* **12**: e0173145.

Jeffrey, S.W. t and Humphrey, G.F. (1975) New spectrophotometric equations for determining chlorophylls a, b, c1 and c2 in higher plants, algae and natural phytoplankton. *Biochem. und Physiol. der Pflanz.* **167**: 191–194.

Jillett, J.B. (1969) Seasonal hydrology of waters off the Otago Peninsula, south-eastern New Zealand. *New Zeal. J. Mar. Freshw. Res.* **3**: 349–375.

Johnson, V., Brownlee, C., Milazzo, M., and Hall-Spencer, J. (2015) Marine

Microphytobenthic Assemblage Shift along a Natural Shallow-Water CO_2 Gradient Subjected to Multiple Environmental Stressors. *J. Mar. Sci. Eng.* **3**: 1425–1447.

Johnson, V.R., Brownlee, C., Rickaby, R.E.M., Graziano, M., Milazzo, M., and Hall-Spencer, J.M. (2013) Responses of marine benthic microalgae to elevated CO_2. *Mar. Biol.* **160**: 1813–1824.

Joint, I., Doney, S.C., and Karl, D.M. (2011) Will ocean acidification affect marine microbes? *ISME J.* **5**: 1–7.

Jones, K.N., Currie, K.I., McGraw, C.M., and Hunter, K.A. (2013) The effect of coastal processes on phytoplankton biomass and primary production within the near-shore Subtropical Frontal Zone. *Estuar. Coast. Shelf Sci.* **124**: 44–55.

Keeling, P.J. and del Campo, J. (2017) Marine Protists Are Not Just Big Bacteria. *Curr. Biol.* **27**: R541–R549.

Kembel, S.W., Cowan, P.D., Helmus, M.R., Cornwell, W.K., Morlon, H., Ackerly, D.D., et al. (2010) Picante: R tools for integrating phylogenies and ecology. *Bioinformatics* **26**: 1463–1464.

Kemp, A.E.S. and Villareal, T.A. (2018) The case of the diatoms and the muddled mandalas: Time to recognize diatom adaptations to stratified waters. *Prog. Oceanogr.* **167**: 138–149.

Kerfahi, D., Hall-Spencer, J.M., Tripathi, B.M., Milazzo, M., Lee, J., and Adams, J.M. (2014) Shallow Water Marine Sediment Bacterial Community Shifts Along a Natural CO_2 Gradient in the Mediterranean Sea Off Vulcano, Italy. *Microb. Ecol.* **67**: 819–828.

De Kievit, T.R. (2009) Quorum sensing in Pseudomonas aeruginosa biofilms. *Environ. Microbiol.* **11**: 279–288.

Kirchman, D.L. (2016) Growth Rates of Microbes in the Oceans. *Ann. Rev. Mar. Sci.* **8**: 285–309.

Klindworth, A., Mann, A.J., Huang, S., Wichels, A., Quast, C., Waldmann, J., et al. (2014) Diversity and activity of marine bacterioplankton during a diatom bloom in the North Sea assessed by total RNA and pyrotag sequencing. *Mar. Genomics* **18**: 185–192.

Knap, A.H., Michaels, A., Close, A.R., Ducklow, H., and Dickson, A.G. (1996) Protocols for the joint global ocean flux study (JGOFS) core measurements.

Knight, R., Vrbanac, A., Taylor, B.C., Aksenov, A., Callewaert, C., Debelius, J., et al. (2018) Best practices for analysing microbiomes. *Nat. Rev. Microbiol.* **16**: 410–422.

Krause, E., Wichels, A., Giménez, L., Lunau, M., Schilhabel, M.B., and Gerdts, G. (2012) Small Changes in pH Have Direct Effects on Marine Bacterial Community

Composition: A Microcosm Approach. *PLoS One* **7**: e47035.

Landa, M., Blain, S., Christaki, U., Monchy, S., and Obernosterer, I. (2016) Shifts in bacterial community composition associated with increased carbon cycling in a mosaic of phytoplankton blooms. *ISME J.* **10**: 39–50.

Langer, G., Nehrke, G., Probert, I., Ly, J., and Ziveri, P. (2009) Strain-specific responses of Emiliania huxleyi to changing seawater carbonate chemistry. *Biogeosciences Discuss.* **6**: 4361–4383.

Lauro, F.M., McDougald, D., Thomas, T., Williams, T.J., Egan, S., Rice, S., et al. (2009) The genomic basis of trophic strategy in marine bacteria. *Proc. Natl. Acad. Sci.* **106**: 15527–15533.

Lavigne, H. and Gattuso, J. (2010) seacarb: seawater carbonate chemistry with R.

Law, C.S., Bell, J.J., Bostock, H.C., Cornwall, C.E., Cummings, V.J., Currie, K., et al. (2017) Ocean acidification in New Zealand waters: trends and impacts. *New Zeal. J. Mar. Freshw. Res.* **8330**: 1–41.

Law, C.S., Breitbarth, E., Hoffmann, L.J., McGraw, C.M., Langlois, R.J., LaRoche, J., et al. (2012) No stimulation of nitrogen fixation by non-filamentous diazotrophs under elevated CO_2 in the South Pacific. *Glob. Chang. Biol.* **18**: 3004–3014.

Law, C.S., Woodward, E.M.S., Ellwood, M.J., Marriner, A., Bury, S.J., and Safi, K.A. (2011) Response of surface nutrient inventories and nitrogen fixation to a tropical cyclone in the southwest Pacific. *Limnol. Oceanogr.* **56**: 1372–1385.

Leblanc, K., Quéguiner, B., Diaz, F., Cornet, V., Michel-Rodriguez, M., Durrieu de Madron, X., et al. (2018) Nanoplanktonic diatoms are globally overlooked but play a role in spring blooms and carbon export. *Nat. Commun.* **9**: 953.

Lee, Z., Marra, J., Perry, M.J., and Kahru, M. (2015) Estimating oceanic primary productivity from ocean color remote sensing: A strategic assessment. *J. Mar. Syst.* **149**: 50–59.

Leibold, M.A., Holyoak, M., Mouquet, N., Amarasekare, P., Chase, J.M., Hoopes, M.F., et al. (2004) The metacommunity concept: a framework for multi-scale community ecology. *Ecol. Lett.* **7**: 601–613.

Lennon, J.T. and Jones, S.E. (2011) Microbial seed banks: The ecological and evolutionary implications of dormancy. *Nat. Rev. Microbiol.* **9**: 119–130.

Lévy, M., Franks, P.J.S., and Smith, K.S. (2018) The role of submesoscale currents in structuring marine ecosystems. *Nat. Commun.* **9**: 4758.

Lewis, S.L. and Maslin, M.A. (2015) Defining the Anthropocene. *Nature* **519**: 171–180.

Li, Y., Zhuang, S., Wu, Y., Ren, H., Cheng, F., Lin, X., et al. (2015) Ocean acidification

modulates expression of genes and physiological performance of a marine diatom. *Biogeosciences Discuss.* **12**: 15809–15833.

Liao, J., Cao, X., Zhao, L., Wang, J., Gao, Z., Wang, M.C., and Huang, Y. (2016) The importance of neutral and niche processes for bacterial community assembly differs between habitat generalists and specialists. *FEMS Microbiol. Ecol.* **92**: fiw174.

Lidbury, I., Johnson, V., Hall-Spencer, J.M., Munn, C.B., and Cunliffe, M. (2012) Community-level response of coastal microbial biofilms to ocean acidification in a natural carbon dioxide vent ecosystem. *Mar. Pollut. Bull.* **64**: 1063–1066.

Lima-Mendez, G., Faust, K., Henry, N., Decelle, J., Colin, S., Carcillo, F., et al. (2015) Determinants of community structure in the global plankton interactome. *Science* **348**: 1262073.

Lindh, M. V., Riemann, L., Baltar, F., Romero-Oliva, C., Salomon, P.S., Granéli, E., and Pinhassi, J. (2013) Consequences of increased temperature and acidification on bacterioplankton community composition during a mesocosm spring bloom in the Baltic Sea. *Environ. Microbiol. Rep.* **5**: 252–262.

Liu, J., Weinbauer, M.G., Maier, C., Dai, M., and Gattuso, J.P. (2010) Effect of ocean acidification on microbial diversity and on microbe-driven biogeochemistry and ecosystem functioning. *Aquat. Microb. Ecol.* **61**: 291–305.

Liu, W., Marsh, T.L., Cheng, H., and Forney, L.J. (1997) Characterization of microbial diversity by determining terminal restriction fragment length polymorphisms of genes encoding 16S rRNA. *Appl. Environ. Microbiol.* **63**: 4516–4522.

Logares, R., Tesson, S.V.M., Canbäck, B., Pontarp, M., Hedlund, K., and Rengefors, K. (2018) Contrasting prevalence of selection and drift in the community structuring of bacteria and microbial eukaryotes. *Environ. Microbiol.* **20**: 2231–2240.

Louca, S., Doebeli, M., and Parfrey, L.W. (2018) Correcting for 16S rRNA gene copy numbers in microbiome surveys remains an unsolved problem. *Microbiome* **6**: 41.

Louca, S., Parfrey, L.W., and Doebeli, M. (2016) Decoupling function and taxonomy in the global ocean microbiome. *Science* **353**: 1272–1277.

Louca, S., Polz, M.F., Mazel, F., Albright, M.B.N., Huber, J.A., O'Connor, M.I., et al. (2018) Function and functional redundancy in microbial systems. *Nat. Ecol. Evol.* **2**: 936–943.

Lovejoy, C., Massana, R., and Pedros-Alio, C. (2006) Diversity and Distribution of Marine Microbial Eukaryotes in the Arctic Ocean and Adjacent Seas. *Appl. Environ. Microbiol.* **72**: 3085–3095.

Lozupone, C. and Knight, R. (2005) UniFrac: a New Phylogenetic Method for Comparing

Microbial Communities. *Appl. Environ. Microbiol.* **71**: 8228–8235.

Lüthi, D., Le Floch, M., Bereiter, B., Blunier, T., Barnola, J.M., Siegenthaler, U., et al. (2008) High-resolution carbon dioxide concentration record 650,000-800,000 years before present. *Nature* **453**: 379–382.

Maas, E., Law, C., Hall, J., Pickmere, S., Currie, K., Chang, F., et al. (2013) Effect of ocean acidification on bacterial abundance, activity and diversity in the Ross Sea, Antarctica. *Aquat. Microb. Ecol.* **70**: 1–15.

Mackey, K.R.M., Morris, J.J., Morel, F.M.M., and Kranz, S.A. (2015) Response of Photosynthesis to Ocean Acidification. *Oceanography* **25**: 74-91.

Malviya, S., Scalco, E., Audic, S., Vincent, F., Veluchamy, A., Poulain, J., et al. (2016) Insights into global diatom distribution and diversity in the world's ocean. *Proc. Natl. Acad. Sci.* **113**: E1516–E1525.

Manning, S.R. and La Claire, J.W. (2010) Prymnesins: Toxic metabolites of the golden alga, Prymnesium parvum Carter (Haptophyta). *Mar. Drugs* **8**: 678–704.

Marañón, E., Lorenzo, M.P., Cermeño, P., and Mouriño-Carballido, B. (2018) Nutrient limitation suppresses the temperature dependence of phytoplankton metabolic rates. *ISME J.* **12**: 1836–1845.

Marchetti, A., Schruth, D.M., Durkin, C.A., Parker, M.S., Kodner, R.B., Berthiaume, C.T., et al. (2012) Comparative metatranscriptomics identifies molecular bases for the physiological responses of phytoplankton to varying iron availability. *Proc. Natl. Acad. Sci.* **109**: E317–E325.

Martínez, I., Stegen, J.C., Maldonado-Gómez, M.X., Eren, M.A., Siba, P.M., Greenhill, A.R., and Walter, J. (2015) The Gut Microbiota of Rural Papua New Guineans: Composition, Diversity Patterns, and Ecological Processes. *Cell Rep.* **11**: 527–538.

Martiny, J.B.H. (2015) Microbiomes in light of traits: A phylogenetic perspective. *Science* **350**: aac9323.

Massana, R., Gobet, A., Audic, S., Bass, D., Bittner, L., Boutte, C., Chambouvet, A., Christen, R., Claverie, J.-M., Decelle, J., Dolan, J.R., Dunthorn, M., Edvardsen, B., Forn, I., Forster, D., Guillou, L., Jaillon, O., Kooistra, Wiebe H C F, et al. (2015) Marine protist diversity in European coastal waters and sediments as revealed by high-throughput sequencing. *Environ. Microbiol.* **17**: 4035–4049.

Massana, R., Gobet, A., Audic, S., Bass, D., Bittner, L., Boutte, C., Chambouvet, A., Christen, R., Claverie, J.-M., Decelle, J., Dolan, J.R., Dunthorn, M., Edvardsen, B., Forn, I., Forster, D., Guillou, L., Jaillon, O., Kooistra, Wiebe H. C. F., et al. (2015) Marine protist diversity in European coastal waters and sediments as revealed by high-

throughput sequencing. *Environ. Microbiol.* **17**: 4035–4049.

Massana, R., Pedrós-Alió, C., Casamayor, E.O., and Gasol, J.M. (2001) Changes in marine bacterioplankton phylogenetic composition during incubations designed to measure biogeochemically significant parameters. *Limnol. Oceanogr.* **46**: 1181–1188.

Mayot, N., D'Ortenzio, F., Uitz, J., Gentili, B., Ras, J., Vellucci, V., et al. (2017) Influence of the Phytoplankton Community Structure on the Spring and Annual Primary Production in the Northwestern Mediterranean Sea. *J. Geophys. Res. Ocean.* **122**: 9918–9936.

Mccoy, S.J. (2013) Morphology of the crustose coralline alga Pseudolithophyllum muricatum (Corallinales, Rhodophyta) responds to 30 years of ocean acidification in the Northeast Pacific. *J. Phycol.* **49**: 830–837.

Mcgraw, C.M., Cornwall, C.E., Reid, M.R., Currie, K.I., Hepburn, C.D., Boyd, P., et al. (2010) An automated pH-controlled culture system for laboratory-based ocean acidification experiments. *Limnol. Oceanogr. Methods* **8**: 686–694.

McMurdie, P.J. and Holmes, S. (2013) phyloseq: An R Package for Reproducible Interactive Analysis and Graphics of Microbiome Census Data. *PLoS One* **8**: e61217.

Mestre, M., Ruiz-González, C., Logares, R., Duarte, C.M., Gasol, J.M., and Sala, M.M. (2018) Sinking particles promote vertical connectivity in the ocean microbiome. *Proc. Natl. Acad. Sci.* **115**: E6799–E6807.

Meyer, J. and Riebesell, U. (2014) Responses of coccolithophores to ocean acidification: a meta-analysis. *Biogeosciences Discuss.* **11**: 14857–14887.

Meyerhof, M.S., Wilson, J.M., Dawson, M.N., and Michael Beman, J. (2016) Microbial community diversity, structure and assembly across oxygen gradients in meromictic marine lakes, Palau. *Environ. Microbiol.* **18**: 4907–4919.

Mizuno, C.M., Rodriguez-Valera, F., and Ghai, R. (2015) Genomes of Planktonic Acidimicrobiales : Widening Horizons for Marine Actinobacteria by Metagenomics. *MBio* **6**: e02083-14.

Mo, Y., Zhang, W., Yang, J., Lin, Y., Yu, Z., and Lin, S. (2018) Biogeographic patterns of abundant and rare bacterioplankton in three subtropical bays resulting from selective and neutral processes. *ISME J.* **12**: 2198–2210.

Mojica, K. and Cooney, M. (2010) The uronic acids assay: a method for the determination of chemical activity on biofilm EPS. *Biofouling* **26**: 301–312.

Monier, A., Comte, J., Babin, M., Forest, A., Matsuoka, A., and Lovejoy, C. (2015) Oceanographic structure drives the assembly processes of microbial eukaryotic communities. *ISME J.* **9**: 990–1002.

Moniruzzaman, M., Wurch, L.L., Alexander, H., Dyhrman, S.T., Gobler, C.J., and Wilhelm, S.W. (2017) Virus-host relationships of marine single-celled eukaryotes resolved from metatranscriptomics. *Nat. Commun.* **8**: 16054.

Moore, C.M., Mills, M.M., Arrigo, K.R., Berman-Frank, I., Bopp, L., Boyd, P.W., et al. (2013) Processes and patterns of oceanic nutrient limitation. *Nat. Geosci.* **6**: 701-710.

Morales, S.E., Meyer, M., Currie, K., and Baltar, F. (2018) Are oceanic fronts ecotones? Seasonal changes along the subtropical front show fronts as bacterioplankton transition zones but not diversity hotspots. *Environ. Microbiol. Rep.* **10**: 184–189.

Moreira, D. and López-García, P. (2002) The molecular ecology of microbial eukaryotes unveils a hidden world. *Trends Microbiol.* **10**: 31–38.

Moreno-Pino, M., De la Iglesia, R., Valdivia, N., Henríquez-Castilo, C., Galán, A., Díez, B., and Trefault, N. (2016) Variation in coastal Antarctic microbial community composition at sub-mesoscale: Spatial distance or environmental filtering? *FEMS Microbiol. Ecol.* **92**: fiw088.

Mousing, E.A., Richardson, K., Bendtsen, J., Cetinić, I., and Perry, M.J. (2016) Evidence of small-scale spatial structuring of phytoplankton alpha- and beta-diversity in the open ocean. *J. Ecol.* **104**: 1682–1695.

Müller, M.N., Trull, T.W., and Hallegraeff, G.M. (2015) Differing responses of three Southern Ocean Emiliania huxleyi ecotypes to changing seawater carbonate chemistry. *Mar. Ecol. Prog. Ser.* **531**: 81–90.

Muyzer, G., de Waal, E., and Uitterlinden, A.G. (1993) Profiling of complex microbial populations by denaturing gradient gel electrophoresis analysis of polymerase chain. *Appl. Environ. Microbiol.* **59**: 695–700.

Nedashkovskaya, O.I., Kukhlevskiy, A.D., Zhukova, N. V., and Kim, S.B. (2016) Amylibacter ulvae sp. nov., a new alphaproteobacterium isolated from the Pacific green alga Ulva fenestrata. *Arch. Microbiol.* **198**: 251–256.

Needham, D.M. and Fuhrman, J.A. (2016) Pronounced daily succession of phytoplankton , archaea and bacteria following a spring bloom. *Nat. Microbiol.* **1**: 16005.

Nemergut, D., Shade, A., and Violle, C. (2014) When, where and how does microbial community composition matter? *Front. Microbiol.* **5**: 2012–2014.

Nemergut, D.R., Schmidt, S.K., Fukami, T., O'Neill, S.P., Bilinski, T.M., Stanish, L.F., et al. (2013) Patterns and Processes of Microbial Community Assembly. *Microbiol. Mol. Biol. Rev.* **77**: 342–356.

Newbold, L.K., Oliver, A.E., Booth, T., Tiwari, B., Desantis, T., Maguire, M., et al. (2012) The response of marine picoplankton to ocean acidification. *Environ. Microbiol.* **14**:

2293–2307.

Oksanen, J., Blanchet, F.G., Friendly, M., Kindt, R., Legendre, P., McGlinn, D., et al. (2016) vegan: Community Ecology Package.

Oliver, A.E., Newbold, L.K., Whiteley, A.S., and van der Gast, C.J. (2014) Marine bacterial communities are resistant to elevated carbon dioxide levels. *Environ. Microbiol. Rep.* **6**: 574–582.

Orr, J.C., Fabry, V.J., Aumont, O., Bopp, L., Doney, S.C., Feely, R.A., et al. (2005) Anthropogenic ocean acidification over the twenty-first century and its impact on calcifying organisms. **437**: 681–686.

Orrock, J.L. and Watling, J.I. (2010) Local Community size mediates ecological drift and competition in metacommunities. *Proc. R. Soc. B Biol. Sci.* **277**: 2185–2191.

Ou, G., Wang, H., Si, R., and Guan, W. (2017) The dinoflagellate Akashiwo sanguinea will benefit from future climate change: The interactive effects of ocean acidification, warming and high irradiance on photophysiology and hemolytic activity. *Harmful Algae* **68**: 118–127.

Palenik, B., Grimwood, J., Aerts, A., Rouzé, P., Salamov, A., Putnam, N., et al. (2007) The tiny eukaryote Ostreococcus provides genomic insights into the paradox of plankton speciation. *Proc. Natl. Acad. Sci.* **104**: 7705–7710.

Pang, M., Xu, J., Qu, P., Mao, X., Wu, Z., Xin, M., et al. (2017) Effect of CO_2 on growth and toxicity of Alexandrium tamarense from the East China Sea, a major producer of paralytic shellfish toxins. *Harmful Algae* **68**: 240–247.

Parada, A.E., Needham, D.M., and Fuhrman, J.A. (2016) Every base matters: assessing small subunit rRNA primers for marine microbiomes with mock communities, time series and global field samples. *Environ. Microbiol.* **18**: 1403–1414.

Passow, U. and Carlson, C.A. (2012) The biological pump in a high CO_2 world. *Mar. Ecol. Prog. Ser.* **470**: 249–271.

Pearson, G.A., Lago-Leston, A., Cánovas, F., Cox, C.J., Verret, F., Lasternas, S., et al. (2015) Metatranscriptomes reveal functional variation in diatom communities from the Antarctic Peninsula. *ISME J.* **9**: 2275-2289.

Pedrós-Alió, C. (2006) Marine microbial diversity: can it be determined? *Trends Microbiol.* **14**: 257–263.

Petro, C., Starnawski, P., Schramm, A., and Kjeldsen, K.U. (2017) Microbial community assembly in marine sediments. *Aquat. Microb. Ecol.* **79**: 177–195.

Piredda, R., Claverie, J., Decelle, J., de Vargas, C., Dunthorn, M., Edvardsen, B., et al. (2018) Diatom diversity through HTS-metabarcoding in coastal European seas. *Sci.*

Rep. **8**: 18059.

Piredda, R., Tomasino, M.P., D'Erchia, A.M., Manzari, C., Pesole, G., Montresor, M., et al. (2017) Diversity and temporal patterns of planktonic protist assemblages at a Mediterranean Long Term Ecological Research site. *FEMS Microbiol. Ecol.* **93**: fiw200.

Pohlon, E., Marxsen, J., and Küsel, K. (2010) Pioneering bacterial and algal communities and potential extracellular enzyme activities of stream biofilms. *FEMS Microbiol. Ecol.* **71**: 364–373.

Polovina, J.J., Dunne, J.P., Woodworth, P.A., and Howell, E.A. (2011) Projected expansion of the subtropical biome and contraction of the temperate and equatorial upwelling biomes in the North Pacific under global warming. *ICES J. Mar. Sci.* **68**: 986–995.

Polovina, J.J., Howell, E.A., and Abecassis, M. (2008) Ocean's least productive waters are expanding. *Geophys. Res. Lett.* **35**: 2–6.

Pomeroy, L.R. (1974) The ocean's food web, a changing paradigm. *Bioscience* **24**: 499–504.

Pomeroy, L.R. and Wiebe, W.J. (2001) Temperature and substrates as interactive limiting factors for marine heterotrophic bacteria. *Aquat. Microb. Ecol.* **23**: 187–204.

Prosser, K.N., Valenti, T.W., Hayden, N.J., Neisch, M.T., Hewitt, N.C., Umphres, G.D., et al. (2012) Low pH preempts bloom development of a toxic haptophyte. *Harmful Algae* **20**: 156–164.

Qian, P.Y., Lau, S.C.K., Dahms, H.U., Dobretsov, S., and Harder, T. (2007) Marine biofilms as mediators of colonization by marine macroorganisms: Implications for antifouling and aquaculture. *Mar. Biotechnol.* **9**: 399–410.

Quast, C., Pruesse, E., Yilmaz, P., Gerken, J., Schweer, T., Yarza, P., et al. (2013) The SILVA ribosomal RNA gene database project: Improved data processing and web-based tools. *Nucleic Acids Res.* **41**: 590–596.

Raes, E.J., Bodrossy, L., van de Kamp, J., Bissett, A., Ostrowski, M., Brown, M. V., et al. (2018) Oceanographic boundaries constrain microbial diversity gradients in the South Pacific Ocean. *Proc. Natl. Acad. Sci.* **115**: E8266–E8275.

Raimbault, P. and Garcia, N. (2008) Evidence for efficient regenerated production and dinitrogen fixation in nitrogen-deficient waters of the South Pacific Ocean: impact on new and export production estimates. *Biogeosciences* **5**: 323–338.

Raimbault, P., Garcia, N., and Cerutti, F. (2008) Distribution of inorganic and organic nutrients in the South Pacific Ocean-evidence for long-term accumulation of organic matter in nitrogen-depleted waters. *Biogeosciences* **5**: 281–298.

Rajaram, S. and Oono, Y. (2010) NeatMap - non-clustering heat map alternatives in R. *BMC Bioinformatics* **11**: 45.

Raven, J.A. and Falkowski, P.G. (1999) Oceanic sinks for atmospheric CO_2. *Plant, Cell Environ.* **22**: 741–755.

Reinfelder, J.R. (2011) Carbon concentrating mechanisms in eukaryotic marine phytoplankton. *Ann. Rev. Mar. Sci.* **3**: 291–315.

Reinthaler, T. and Herndl, G.J. (2005) Seasonal dynamics of bacterial growth efficiencies in relation to phytoplankton in the southern North Sea. *Aquat. Microb. Ecol.* **39**: 7–16.

Reinthaler, T., Winter, C., and Herndl, G.J. (2005) Relationship between bacterioplankton richness, respiration, and production in the southern North Sea. *Appl. Environ. Microbiol.* **71**: 2260–2266.

Reintjes, G., Arnosti, C., Fuchs, B., and Amann, R. (2018) Selfish, sharing and scavenging bacteria in the Atlantic Ocean: a biogeographical study of bacterial substrate utilisation. *ISME J.* **13**: 1119-1132.

Ribalet, F., Marchetti, A., Hubbard, K.A., Brown, K., Durkin, C.A., Morales, R., et al. (2010) Unveiling a phytoplankton hotspot at a narrow boundary between coastal and offshore waters. *Proc. Natl. Acad. Sci.* **107**: 16571–16576.

Riebesell, U., Aberle-Malzahn, N., Achterberg, E.P., Algueró-Muñiz, M., Alvarez-Fernandez, S., Arístegui, J., et al. (2018) Toxic algal bloom induced by ocean acidification disrupts the pelagic food web. *Nat. Clim. Chang.* **8**: 1082–1086.

Roelke, D.L., Barkoh, A., Brooks, B.W., Grover, J.P., Hambright, K.D., LaClaire, J.W., et al. (2016) A chronicle of a killer alga in the west: ecology, assessment, and management of Prymnesium parvum blooms. *Hydrobiologia* **764**: 29–50.

Roemmich, D., Gilson, J., Sutton, P., and Zilberman, N. (2016) Multidecadal Change of the South Pacific Gyre Circulation. *J. Phys. Oceanogr.* **46**: 1871–1883.

Ron, R., Fragman-Sapir, O., and Kadmon, R. (2018) Dispersal increases ecological selection by increasing effective community size. *Proc. Natl. Acad. Sci.* **115**: 11280–11285.

Rousseaux, C. and Gregg, W. (2013) Interannual Variation in Phytoplankton Primary Production at A Global Scale. *Remote Sens.* **6**: 1–19.

Roy, A.S., Gibbons, S.M., Schunck, H., Owens, S., Caporaso, J.G., Sperling, M., et al. (2013) Ocean acidification shows negligible impacts on high-latitude bacterial community structure in coastal pelagic mesocosms. *Biogeosciences* **10**: 555–566.

Russell, B.D., Connell, S.D., Findlay, H.S., Tait, K., Widdicombe, S., and Mieszkowska,

N. (2013) Ocean acidification and rising temperatures may increase biofilm primary productivity but decrease grazer consumption. *Philos. Trans. R. Soc. Lond. B. Biol. Sci.* **368**: 20120438.

Sabine, C.L., Feely, R.A., Gruber, N., Key, R.M., Bullister, J.L., Wanninkhof, R., et al. (2004) The Oceanic Sink for Anthropogenic CO_2. *Science* **305**: 367–371.

Sala, M.M., Aparicio, F.L., Balagué, V., Boras, J.A., Borrull, E., Cardelús, C., et al. (2016) Contrasting effects of ocean acidification on the microbial food web under different trophic conditions. *ICES J. Mar. Sci.* **73**: 670–679.

Salazar, G. and Sunagawa, S. (2017) Marine microbial diversity. *Curr. Biol.* **27**: R489–R494.

Salter, I., Galand, P.E., Fagervold, S.K., Lebaron, P., Obernosterer, I., Oliver, M.J., et al. (2015) Seasonal dynamics of active SAR11 ecotypes in the oligotrophic Northwest Mediterranean Sea. *ISME J.* **9**: 347–360.

Sanli, K., Bengtsson-Palme, J., Nilsson, R.H., Kristiansson, E., Alm Rosenblad, M., Blanck, H., and Eriksson, K.M. (2015) Metagenomic sequencing of marine periphyton: taxonomic and functional insights into biofilm communities. *Front. Microbiol.* **6**: 1192.

Santoro, A.E., Richter, R.A., and Dupont, C.L. (2019) Planktonic Marine Archaea. *Ann. Rev. Mar. Sci.* **11**: 131–158.

Schliep, K.P. (2011) phangorn: Phylogenetic analysis in R. *Bioinformatics* **27**: 592–593.

Schlitzer, R., Anderson, R.F., Dodas, E.M., Lohan, M., Geibert, W., Tagliabue, A., et al. (2018) The GEOTRACES Intermediate Data Product 2017. *Chem. Geol.* **493**: 210–223.

Schmidt, M.L., White, J.D., and Denef, V.J. (2016) Phylogenetic conservation of freshwater lake habitat preference varies between abundant bacterioplankton phyla. *Environ. Microbiol.* **18**: 1212–1226.

Schulz, K.G., Bach, L.T., Bellerby, R.G.J., Bermúdez, R., Büdenbender, J., Boxhammer, T., et al. (2017) Phytoplankton Blooms at Increasing Levels of Atmospheric Carbon Dioxide: Experimental Evidence for Negative Effects on Prymnesiophytes and Positive on Small Picoeukaryotes. *Front. Mar. Sci.* **4**: 64.

Schulz, K.G., Bellerby, R.G.J., Brussaard, C.P.D., Büdenbender, J., Czerny, J., Engel, A., et al. (2013) Temporal biomass dynamics of an Arctic plankton bloom in response to increasing levels of atmospheric carbon dioxide. *Biogeosciences* **10**: 161–180.

Seeleuthner, Y., Mondy, S., Lombard, V., Carradec, Q., Pelletier, E., Wessner, M., et al. (2018) Single-cell genomics of multiple uncultured stramenopiles reveals

underestimated functional diversity across oceans. *Nat. Commun.* **9**: 310.

Sela, I., Wolf, Y.I., and Koonin, E. V. (2016) Theory of prokaryotic genome evolution. *Proc. Natl. Acad. Sci.* **113**: 11399–11407.

Seymour, J.R., Amin, S.A., Raina, J.-B., and Stocker, R. (2017) Zooming in on the phycosphere: the ecological interface for phytoplankton–bacteria relationships. *Nat. Microbiol.* **2**: 17065.

Shade, A., Dunn, R.R., Blowes, S.A., Keil, P., Bohannan, B.J.M., Herrmann, M., et al. (2018) Macroecology to Unite All Life, Large and Small. *Trends Ecol. Evol.* **33**: 731–744.

Siegel, D.A., Buesseler, K.O., Behrenfeld, M.J., Benitez-Nelson, C.R., Boss, E., Brzezinski, M.A., et al. (2016) Prediction of the Export and Fate of Global Ocean Net Primary Production: The EXPORTS Science Plan. *Front. Mar. Sci.* **3**: 22.

Signorini, S.R. and McClain, C.R. (2012) Subtropical gyre variability as seen from satellites. *Remote Sens. Lett.* **3**: 471–479.

Silva, P.C. (2008) Historical Review of Attempts to Decrease Subjectivity in Species Identification, with Particular Regard to Algae. *Protist* **159**: 153–161.

Smayda, T.J. (2011) Cryptic planktonic diatom challenges phytoplankton ecologists. *Proc. Natl. Acad. Sci.* **108**: 4269–4270.

Smetacek, V. (2018) Seeing is Believing: Diatoms and the Ocean Carbon Cycle Revisited. *Protist* **169**: 791–802.

Smith, D.C. and Azam, F. (1992) A simple, economical method for measuring bacterial protein synthesis rates in seawater using ^{3}H-leucine. *Mar. Microb. Food Webs* **6**: 107–114.

Smith, R. and Hall, J. (1997) Bacterial abundance and production in different water masses around South Island, New Zealand. *New Zeal. J. Mar. Freshw. Res.* **31**: 515–524.

Smith, T.B. (1997) A Role for Ecotones in Generating Rainforest Biodiversity. *Science* **276**: 1855–1857.

Sogin, M.L., Morrison, H.G., Huber, J.A., Welch, D.M., Huse, S.M., Neal, P.R., et al. (2006) Microbial diversity in the deep sea and the underexplored "rare biosphere". *Proc. Natl. Acad. Sci.* **103**: 12115–12120.

Soininen, J., Korhonen, J.J., and Luoto, M. (2013) Stochastic species distributions are driven by organism size. *Ecology* **94**: 660–670.

Starnawski, P., Bataillon, T., Ettema, T.J.G., Jochum, L.M., Schreiber, L., Chen, X., et al. (2017) Microbial community assembly and evolution in subseafloor sediment. *Proc. Natl. Acad. Sci.* **114**: 2940–2945.

Stegen, J.C., Bottos, E.M., and Jansson, J.K. (2018) A unified conceptual framework for prediction and control of microbiomes. *Curr. Opin. Microbiol.* **44**: 20–27.

Stegen, J.C., Lin, X., Fredrickson, J.K., Chen, X., Kennedy, D.W., Murray, C.J., et al. (2013) Quantifying community assembly processes and identifying features that impose them. *ISME J.* **7**: 2069–2079.

Stegen, J.C., Lin, X., Fredrickson, J.K., and Konopka, A.E. (2015) Estimating and mapping ecological processes influencing microbial community assembly. *Front. Microbiol.* **6**: 370.

Stocker, T. (2014) Climate change 2013: the physical science basis: Working Group I contribution to the Fifth assessment report of the Intergovernmental Panel on Climate Change Cambridge University Press.

Stoeck, T., Bass, D., Nebel, M., Christen, R., Jones, M.D.M., Breiner, H.W., and Richards, T.A. (2010) Multiple marker parallel tag environmental DNA sequencing reveals a highly complex eukaryotic community in marine anoxic water. *Mol. Ecol.* **19**: 21–31.

Strassert, J.F.H., Karnkowska, A., Hehenberger, E., Del Campo, J., Kolisko, M., Okamoto, N., et al. (2018) Single cell genomics of uncultured marine alveolates shows paraphyly of basal dinoflagellates. *ISME J.* **12**: 304–308.

Suffrian, K., Simonelli, P., Nejstgaard, J.C., Putzeys, S., Carotenuto, Y., and Antia, A.N. (2008) Microzooplankton grazing and phytoplankton growth in marine mesocosms with increased CO_2 levels. *Biogeosciences* **5**: 1145–1156.

Sun, J., Hutchins, D. a., Feng, Y., Seubert, E.L., Caron, D. a., and Fu, F.-X. (2011) Effects of changing pCO_2 and phosphate availability on domoic acid production and physiology of the marine harmful bloom diatom Pseudo-nitzschia multiseries. *Limnol. Oceanogr.* **56**: 829–840.

Sunagawa, S., Coelho, L.P., Chaffron, S., Kultima, J.R., Labadie, K., Salazar, G., et al. (2015) Structure and function of the global ocean microbiome. *Science* **348**: 1261359.

Sutton, P.J.H. (2003) The Southland Current: a subantarctic current. *New Zeal. J. Mar. Freshw. Res.* **37**: 645–652.

Takahashi, T., Sutherland, S.C., Wanninkhof, R., Sweeney, C., Feely, R.A., Chipman, D.W., et al. (2009) Climatological mean and decadal change in surface ocean pCO_2, and net sea-air CO_2 flux over the global oceans. *Deep. Res. Part II Top. Stud. Oceanogr.* **56**: 554–577.

Talaber, I., Francé, J., Flander-Putrle, V., and Mozetič, P. (2018) Primary production and community structure of coastal phytoplankton in the Adriatic Sea: Insights on taxon-specific productivity. *Mar. Ecol. Prog. Ser.* **604**: 65–81.

Tatters, A.O., Flewelling, L.J., Fu, F., Granholm, A.A., and Hutchins, D.A. (2013) High CO_2 promotes the production of paralytic shellfish poisoning toxins by Alexandrium catenella from Southern California waters. *Harmful Algae* **30**: 37–43.

Tatters, A.O., Fu, F.X., and Hutchins, D. a. (2012) High CO_2 and silicate limitation synergistically increase the toxicity of pseudo-nitzschia fraudulenta. *PLoS One* **7**: e32116.

Taylor, A.G., Goericke, R., Landry, M.R., Selph, K.E., Wick, D.A., and Roadman, M.J. (2012) Sharp gradients in phytoplankton community structure across a frontal zone in the California Current Ecosystem. *J. Plankton Res.* **34**: 778–789.

Taylor, J.D., Ellis, R., Milazzo, M., Hall-Spencer, J.M., and Cunliffe, M. (2014) Intertidal epilithic bacteria diversity changes along a naturally occurring carbon dioxide and pH gradient. *FEMS Microbiol. Ecol.* **89**: 670–678.

R Core Team (2013) R: A language and environment for statistical computing.

Teeling, H., Fuchs, B.M., Becher, D., Klockow, C., Gardebrecht, A., Bennke, C.M., et al. (2012) Substrate-Controlled Succession of Marine Bacterioplankton Populations Induced by a Phytoplankton Bloom. *Science* **336**: 608–611.

Thompson, L.R., Sanders, J.G., McDonald, D., Amir, A., Ladau, J., Locey, K.J., et al. (2017) A communal catalogue reveals Earth's multiscale microbial diversity. *Nature* **551**: 457–463.

Thompson, R.C., Norton, T.A., and Hawkins, S.J. (2004) Physical stress and biological control regulate the producer–consumer balance in intertidal biofilms. *Ecology* **85**: 1372–1382.

Tran, C. and Hadfield, M.G. (2011) Larvae of Pocillopora damicornis (Anthozoa) settle and metamorphose in response to surface-biofilm bacteria. *Mar. Ecol. Prog. Ser.* **433**: 85–96.

Tréguer, P., Bowler, C., Moriceau, B., Dutkiewicz, S., Gehlen, M., Aumont, O., et al. (2018) Influence of diatom diversity on the ocean biological carbon pump. *Nat. Geosci.* **11**: 27–37.

Trimborn, S., Brenneis, T., Hoppe, C.J.M., Laglera, L.M., Norman, L., Santos-Echeandía, J., et al. (2017) Iron sources alter the response of Southern Ocean phytoplankton to ocean acidification. *Mar. Ecol. Prog. Ser.* **578**: 35–50.

Tripathi, B.M., Stegen, J.C., Kim, M., Dong, K., Adams, J.M., and Lee, Y.K. (2018) Soil pH mediates the balance between stochastic and deterministic assembly of bacteria. *ISME J.* **12**: 1072–1083.

Turley, C.M. and Stutt, E.D. (2000) Depth-related cell-specific bacterial leucine

incorporation rates on particles and its biogeochemical significance in the Northwest Mediterranean. *Limnol. Oceanogr.* **45**: 419–425.

Vallina, S.M., Follows, M.J., Dutkiewicz, S., Montoya, J.M., Cermeno, P., and Loreau, M. (2014) Global relationship between phytoplankton diversity and productivity in the ocean. *Nat. Commun.* **5**: 4299.

Valverde, A., Makhalanyane, T.P., and Cowan, D.A. (2014) Contrasting assembly processes in a bacterial metacommunity along a desiccation gradient. *Front. Microbiol.* **5**: 668.

de Vargas, C., Audic, S., Henry, N., Decelle, J., Mahe, F., Logares, R., et al. (2015) Eukaryotic plankton diversity in the sunlit ocean. *Science* **348**: 1261605–1261605.

Vellend, M. (2010) Conceptual Synthesis in Community Ecology. *Q. Rev. Biol.* **85**: 183–206.

Vellend, M., Srivastava, D.S., Anderson, K.M., Brown, C.D., Jankowski, J.E., Kleynhans, E.J., et al. (2014) Assessing the relative importance of neutral stochasticity in ecological communities. *Oikos* **123**: 1420–1430.

Vergin, K.L., Done, B., Carlson, C.A., and Giovannoni, S.J. (2013) Spatiotemporal distributions of rare bacterioplankton populations indicate adaptive strategies in the oligotrophic ocean. *Aquat. Microb. Ecol.* **71**: 1–13.

Vergin, K.L., Jhirad, N., Dodge, J., Carlson, C.A., and Giovannoni, S.J. (2017) Marine bacterioplankton consortia follow deterministic, non-neutral community assembly rules. *Aquat. Microb. Ecol.* **79**: 165–175.

Walsh, E.A., Smith, D.C., Sogin, M.L., and D'Hondt, S. (2015) Bacterial and archaeal biogeography of the deep chlorophyll maximum in the South Pacific Gyre. *Aquat. Microb. Ecol.* **75**: 1–13.

Van Wambeke, F., Bonnet, S., Moutin, T., Raimbault, P., Alarcón, G., and Guieu, C. (2008) Factors limiting heterotrophic bacterial production in the southern Pacific Ocean. *Biogeosciences* **5**: 833–845.

Wang, J., Shen, J., Wu, Y., Tu, C., Soininen, J., Stegen, J.C., et al. (2013) Phylogenetic beta diversity in bacterial assemblages across ecosystems: Deterministic versus stochastic processes. *ISME J.* **7**: 1310–1321.

Wang, Q., Garrity, G.M., Tiedje, J.M., and Cole, J.R. (2007) Naïve Bayesian classifier for rapid assignment of rRNA sequences into the new bacterial taxonomy. *Appl. Environ. Microbiol.* **73**: 5261–5267.

Wang, Y., Smith, W.O., Wang, X., and Li, S. (2010) Subtle biological responses to increased CO_2 concentrations by Phaeocystis globosa Scherffel, a harmful algal bloom

species. *Geophys. Res. Lett.* **37**: L09604.

Wang, Y., Zhang, R., Zheng, Q., Deng, Y., Van Nostrand, J.D., Zhou, J., and Jiao, N. (2016) Bacterioplankton community resilience to ocean acidification: evidence from microbial network analysis. *ICES J. Mar. Sci.* **73**: 865–875.

Ward, C.S., Yung, C.M., Davis, K.M., Blinebry, S.K., Williams, T.C., Johnson, Z.I., and Hunt, D.E. (2017) Annual community patterns are driven by seasonal switching between closely related marine bacteria. *ISME J.* **11**: 1412–1422.

Webb, C.O., Ackerly, D.D., and Kembel, S.W. (2008) Phylocom: software for the analysis of phylogenetic community structure and trait evolution. *Bioinformatics* **24**: 2098-2100.

Weber, A.A.-T. and Pawlowski, J. (2013) Can Abundance of Protists Be Inferred from Sequence Data: A Case Study of Foraminifera. *PLoS One* **8**: e56739.

Webster, N.S., Negri, A.P., Flores, F., Humphrey, C., Soo, R., Botte, E.S., et al. (2013) Near-future ocean acidification causes differences in microbial associations within diverse coral reef taxa. *Environ. Microbiol. Rep.* **5**: 243–251.

Weiss, S., Xu, Z.Z., Peddada, S., Amir, A., Bittinger, K., Gonzalez, A., et al. (2017) Normalization and microbial differential abundance strategies depend upon data characteristics. *Microbiome* **5**: 27.

Wemheuer, B., Güllert, S., Billerbeck, S., Giebel, H.A., Voget, S., Simon, M., and Daniel, R. (2014) Impact of a phytoplankton bloom on the diversity of the active bacterial community in the southern North Sea as revealed by metatranscriptomic approaches. *FEMS Microbiol. Ecol.* **87**: 378–389.

West, N.J., Lepère, C., Manes, C.L. de O., Catala, P., Scanlan, D.J., and Lebaron, P. (2016) Distinct spatial patterns of SAR11, SAR86, and Actinobacteria diversity along a transect in the ultra-oligotrophic South Pacific Ocean. *Front. Microbiol.* **7**: 234.

Whitman, W.B., Coleman, D.C., and Wiebe, W.J. (1998) Prokaryotes: the unseen majority. *Proc. Natl. Acad. Sci.* **95**: 6578–83.

Wilkins, D., van Sebille, E., Rintoul, S.R., Lauro, F.M., and Cavicchioli, R. (2013) Advection shapes Southern Ocean microbial assemblages independent of distance and environment effects. *Nat. Commun.* **4**: 2457.

Williams, P.J. le B., Quay, P.D., Westberry, T.K., and Behrenfeld, M.J. (2013) The Oligotrophic Ocean Is Autotrophic. *Ann. Rev. Mar. Sci.* **5**: 535–549.

Witt, V., Wild, C., Anthony, K.R.N., Diaz-Pulido, G., and Uthicke, S. (2011) Effects of ocean acidification on microbial community composition of, and oxygen fluxes through, biofilms from the Great Barrier Reef. *Environ. Microbiol.* **13**: 2976–2989.

Worden, A.Z., Follows, M.J., Giovannoni, S.J., Wilken, S., Zimmerman, A.E., and Keeling, P.J. (2015) Rethinking the marine carbon cycle: Factoring in the multifarious lifestyles of microbes. *Science* **347**: 1257594.

Wu, W., Logares, R., Huang, B., and Hsieh, C.H. (2017) Abundant and rare picoeukaryotic sub-communities present contrasting patterns in the epipelagic waters of marginal seas in the northwestern Pacific Ocean. *Environ. Microbiol.* **19**: 287–300.

Wu, W., Lu, H.-P., Sastri, A., Yeh, Y.-C., Gong, G.-C., Chou, W.-C., and Hsieh, C.-H. (2017) Contrasting the relative importance of species sorting and dispersal limitation in shaping marine bacterial versus protist communities. *ISME J.* **12**: 485–494.

Wu, Y., Campbell, D.A., Irwin, A.J., Suggett, D.J., and Finkel, Z. V (2014) Ocean acidification enhances the growth rate of larger diatoms. *Limnol. Ocean.* **59**: 1027–1034.

Yanagawa, K., Morono, Y., De Beer, D., Haeckel, M., Sunamura, M., Futagami, T., et al. (2013) Metabolically active microbial communities in marine sediment under high-CO_2 and low-pH extremes. *ISME J.* **7**: 555–567.

Yung, C.M., Vereen, M.K., Herbert, A., Davis, K.M., Yang, J., Kantorowska, A., et al. (2015) Thermally adaptive tradeoffs in closely related marine bacterial strains. *Environ. Microbiol.* **17**: 2421–2429.

Zhang, C., Dang, H., Azam, F., Benner, R., Legendre, L., Passow, U., et al. (2018) Evolving paradigms in biological carbon cycling in the ocean. *Natl. Sci. Rev.* **5**: 481–499.

Zhang, R., Xia, X., Lau, S.C.K., Motegi, C., Weinbauer, M.G., and Jiao, N. (2013) Response of bacterioplankton community structure to an artificial gradient of pCO_2 in the Arctic Ocean. *Biogeosciences* **10**: 3679–3689.

Zhou, J. and Ning, D. (2017) Stochastic community assembly: does it matter in microbial ecology? *Microbiol. Mol. Biol. Rev.* **81**: e00002-17.

Zhu, F., Massana, R., Not, F., Marie, D., and Vaulot, D. (2005) Mapping of picoeucaryotes in marine ecosystems with quantitative PCR of the 18S rRNA gene. *FEMS Microbiol. Ecol.* **52**: 79–92.

Zinger, L., Taberlet, P., Schimann, H., Bonin, A., Boyer, F., De Barba, M., et al. (2018) Body size determines soil community assembly in a tropical forest. *Mol. Ecol.* **28**: 528-543.

Appendix

Supplementary figures

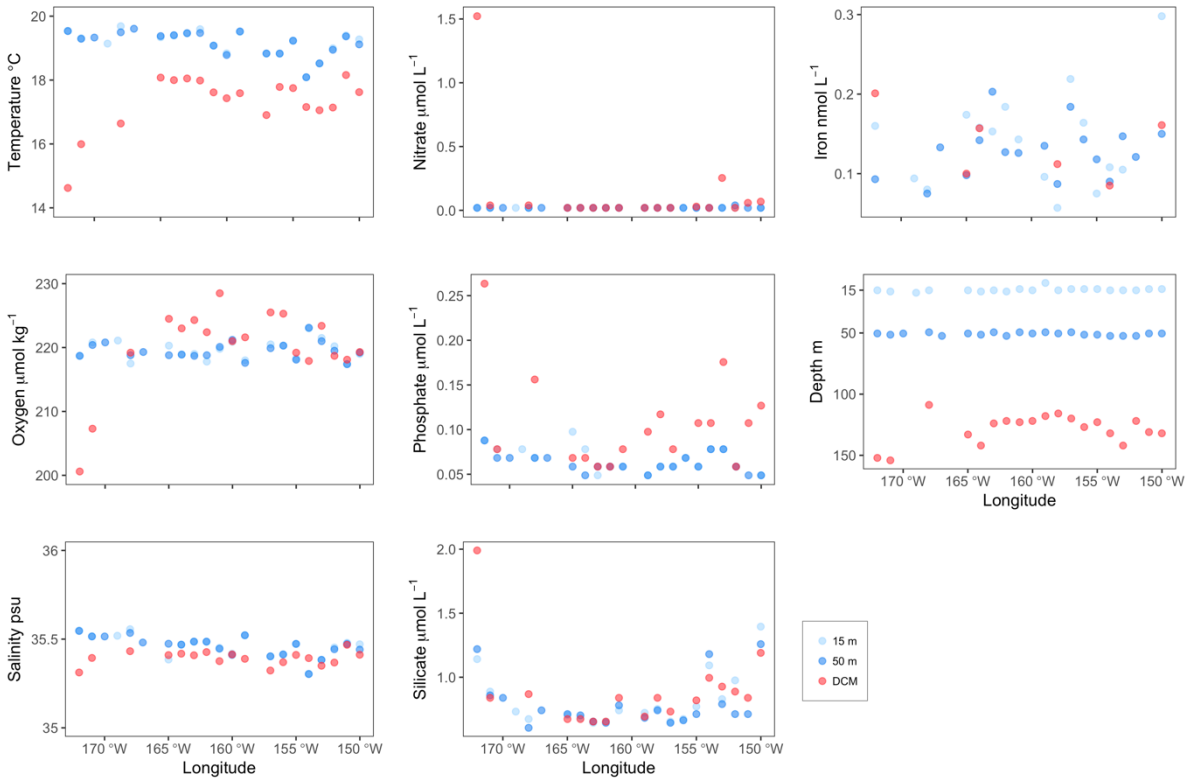

Figure A.1 Physical and chemical environmental conditions at 15 m, 50 m, and the DCM at sampled stations in the oligotrophic South Pacific Gyre. Sampling was conducted according to methods reported in Ellwood *et al.* (Ellwood *et al.*, 2018).

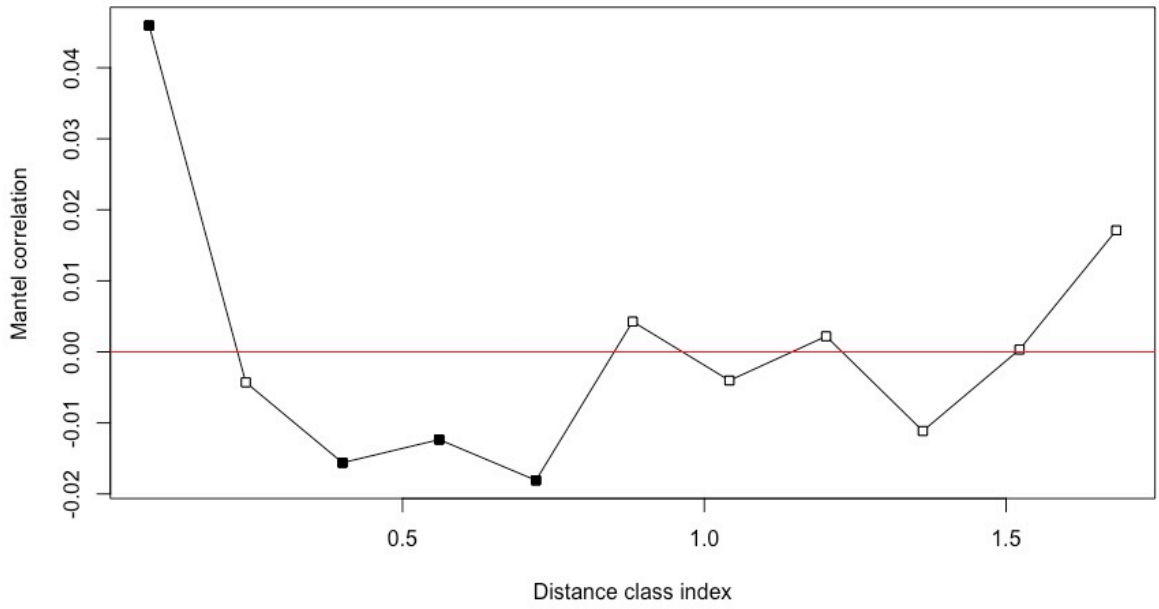

Figure A.2 Phylogenetic signal in microbial communities of the SPG. Phylogenetic signal was quantified first by calculating the relative abundance-weighted mean for a subset of physicochemical parameters (temperature, salinity, oxygen, depth) for each ASV. From these values, I calculated a Euclidean distance matrix to represent the relative ecological niches of each ASV. A corresponding matrix representing phylogenetic distance between ASVs was calculated from the maximum-likelihood tree using the *cophenetic.phylo* function in the R package 'picante' (Kembel *et al.*, 2010). A Mantel correlogram was used to quantify the relationship between ecological niche distance and phylogenetic distance. Ecological niche distance was well correlated with phylogenetic distance amongst closely related taxa, but this relationship quickly decomposed with more phylogenetically distant taxa. This suggests that closely related taxa share similar niche preferences with regards to the environmental parameters considered. Consequently, phylogenetic turnover within and between communities was quantified among closest relatives (Stegen *et al.*, 2013). Closed squares represent significant correlations, open squares represent non-significant correlations.

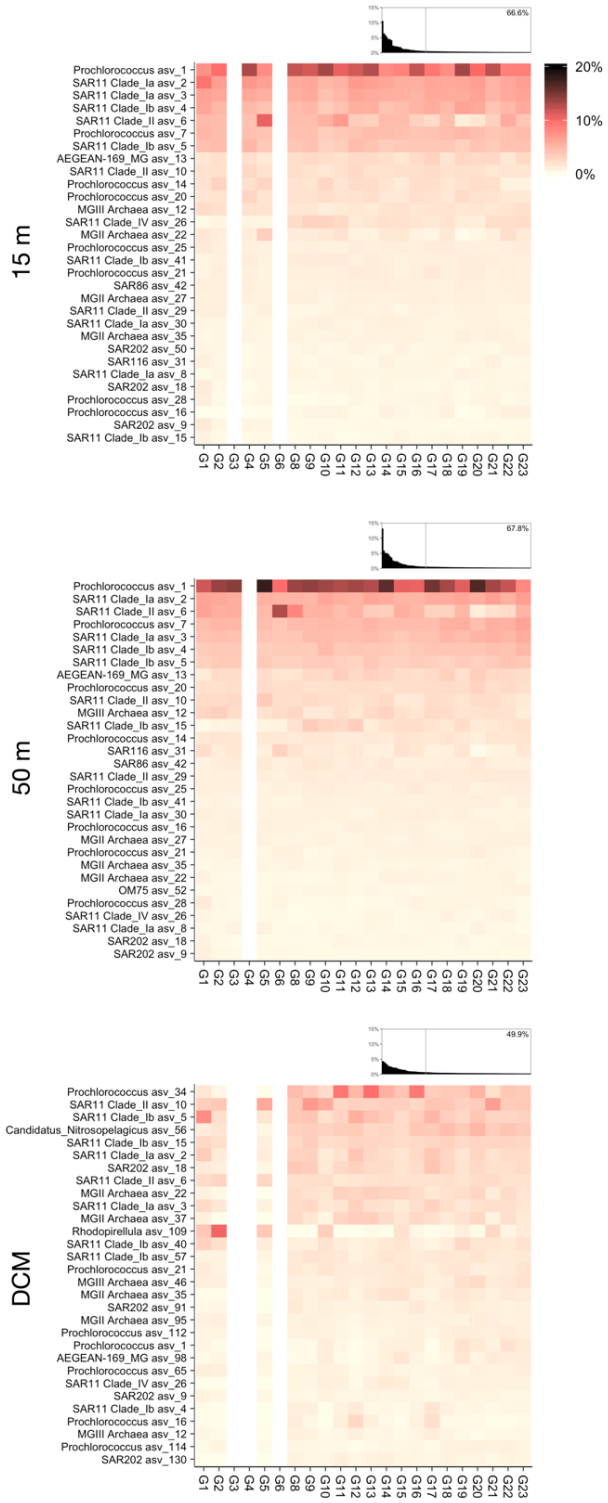

Figure A.3 Microbial community composition in the oligotrophic South Pacific Gyre based on 16S rRNA gene read abundance. Heatmaps display the 30 most abundant taxa at each depth (15 m, 50 m, DCM) in descending order, calculated based on the sums of total reads pooled across all samples. Rank-abundance plots above each heatmap display the proportion of total reads represented by each of the 100 most abundant taxa at each depth, in descending order. The grey vertical lines on the rank-abundance plots marks the cut-off for the 30 most abundant taxa, and the proportion of total reads represented by these taxa (and consequently displayed on the heatmap) are displayed in the top right corner.

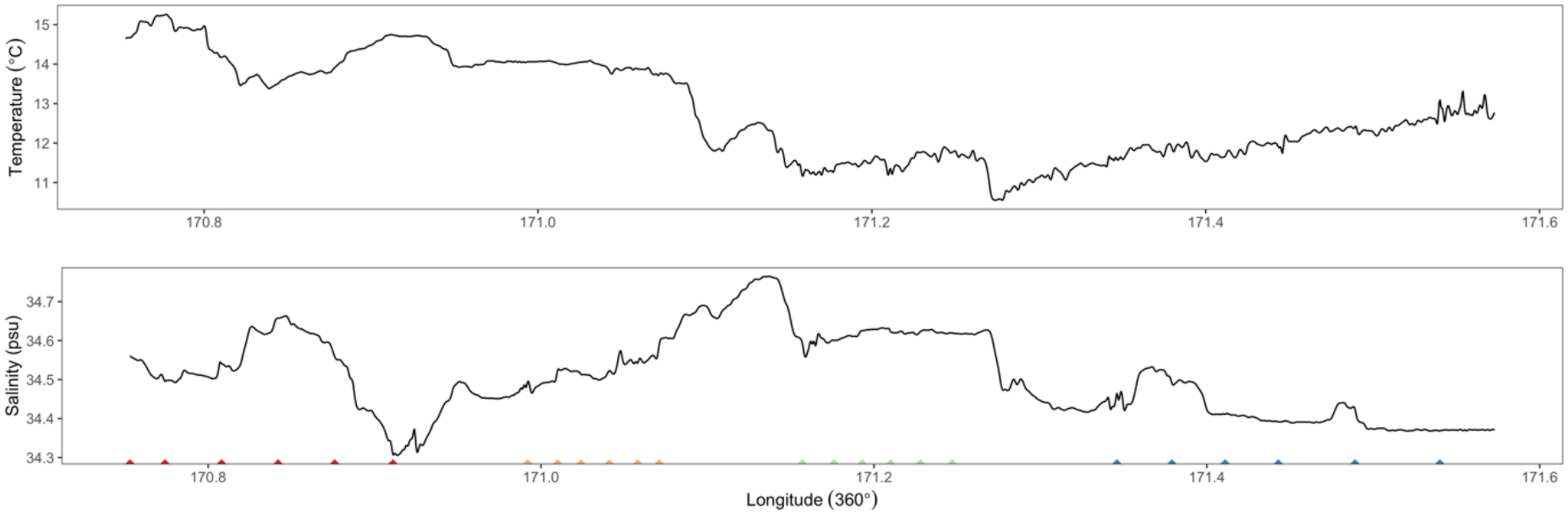

Figure A.4 Temperature and salinity profiles obtained from the RV Polaris II continuous underway sampling system during the sampling voyage of the Munida Time Series Transect. Triangles indicate the longitudinal position of sampling stations (red: coastal waters, orange: subtropical waters, green: frontal waters, blue: subantarctic waters).

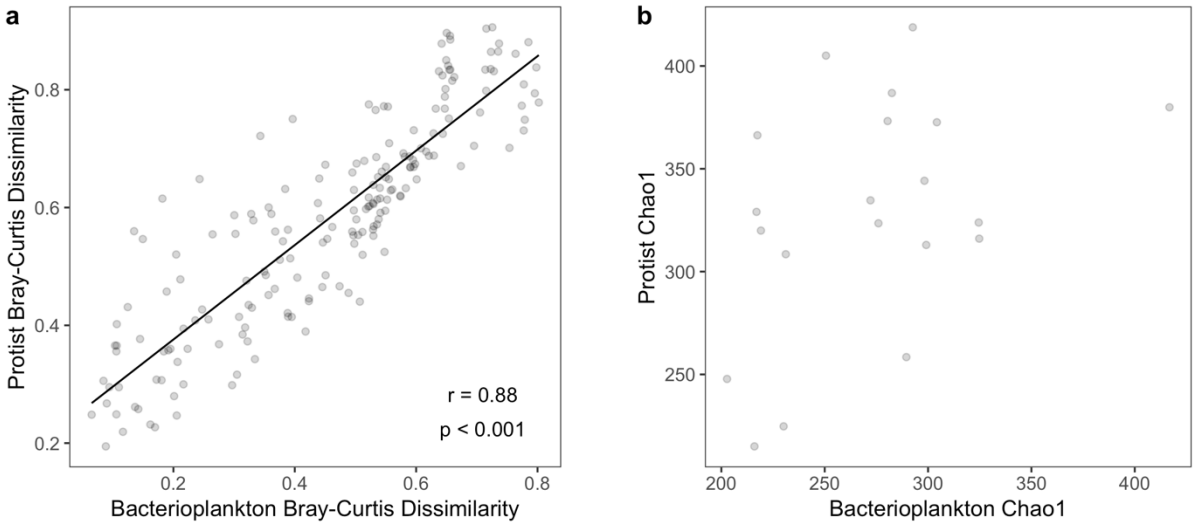

Figure A.5 (a) The relationship between protist and bacterioplankton community dissimilarity, mantel statistic and significance are displayed. (b) The relationship between protist and bacterioplankton ASV richness, estimated using Chao1, analysed using a linear model.

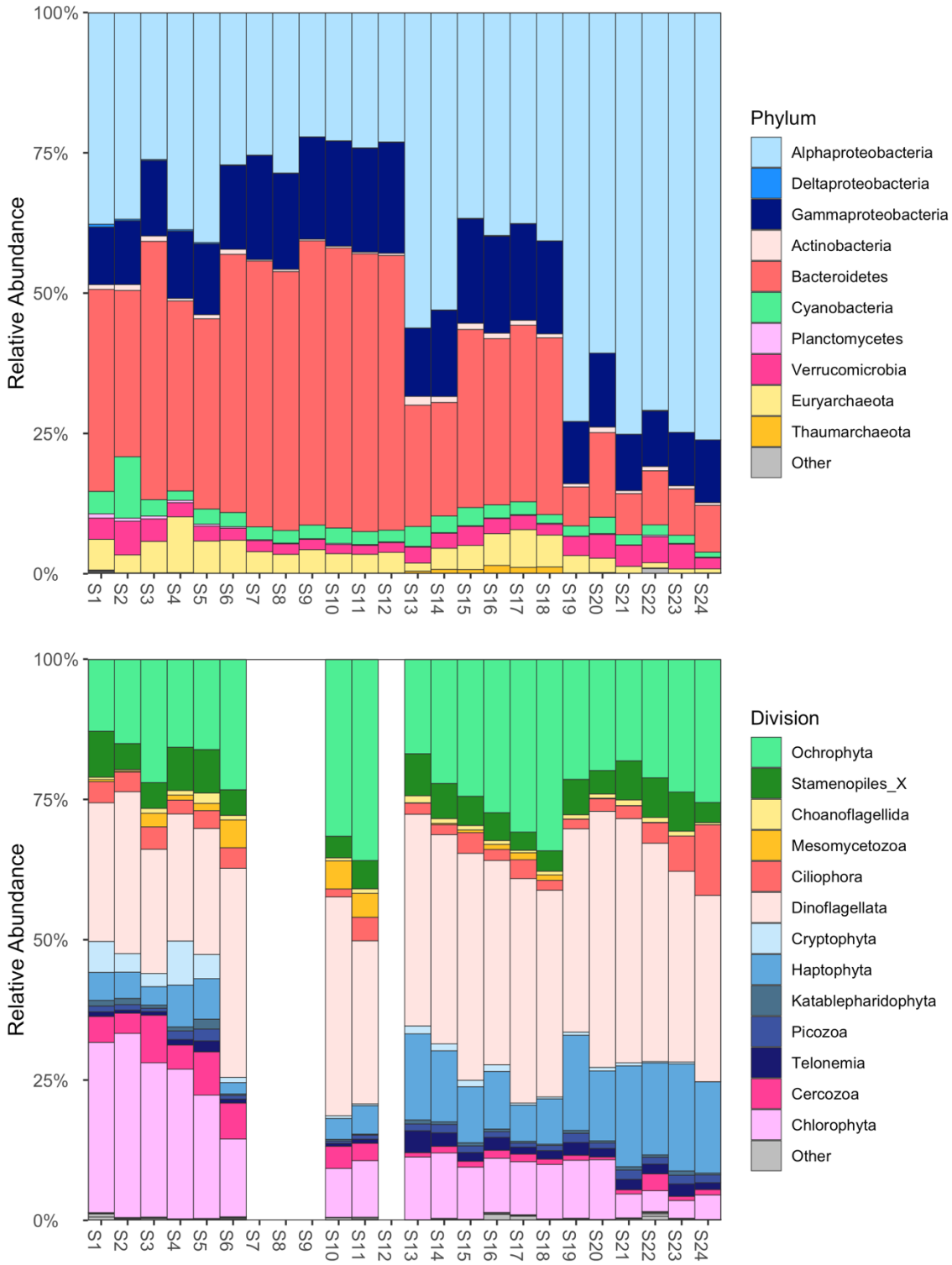

Figure A.6 *Top*: Stacked bar plot of bacterioplankton community composition across the Southland Front system. Bars represent phylum level classification of taxa, except for Proteobacteria which are subdivided into classes. *Bottom:* Stacked bar plot of protist community composition across the Southland Front system at the Division level. Blank bars represent samples which were removed due to the dominance of metazoan sequences.

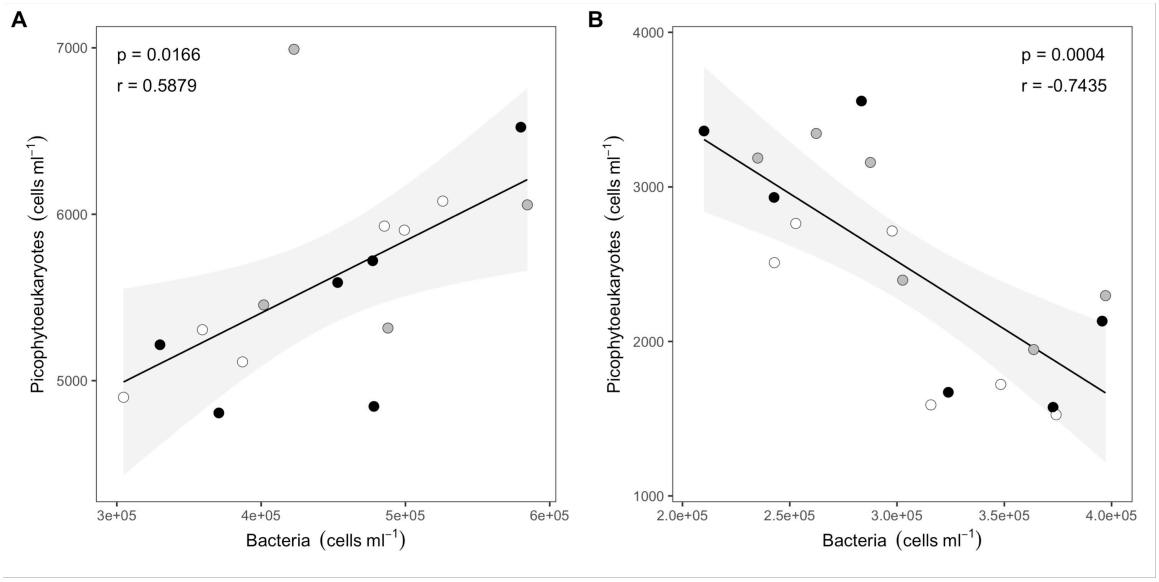

Figure A.7 The relationship between bacterial cell density and picophytoeukaryote cell density during experiment G-OA1 (A) and experiment G-OA3 (B) in control (white), high CO_2 (grey) and greenhouse (black) treatments. Shaded area represents 95% confidence interval.

Supplementary tables

Table A.1 Environmental conditions at each samples station across the Southland Front system (n.d. = no data, d.l. = below detection limit).

Water Mass	Station	Temperature (°C)	Salinity (psu)	Chlorophyll *a* (mg l^{-1})	Nitrate (µmol l^{-1})	Phosphate (µmol l^{-1})	Ammonia (µmol l^{-1})	Silicate (µmol l^{-1})
Coastal	S1	14.64	34.56	0.53	0.11	0.06	0.62	2.19
	S2	15.23	34.49	0.24	0.03	0.03	0.49	2.22
	S3	14.29	34.55	0.31	0.01	0.02	0.40	1.58
	S4	13.43	34.66	0.42	0.13	0.05	0.93	1.88
	S5	13.82	34.56	0.42	0.04	0.03	0.51	1.97
	S6	14.75	34.32	0.68	0.00	0.03	0.20	2.50
Subtropical	S7	14.03	34.49	1.08	0.12	0.03	0.21	1.95
	S8	14.05	34.51	*n.d.*	0.07	0.03	0.20	1.38
	S9	14.03	34.52	0.91	0.08	0.03	0.10	1.90
	S10	13.88	34.52	0.89	0.11	0.03	0.00	1.91
	S11	13.9	34.54	0.58	0.17	0.03	0.18	1.39
	S12	13.75	34.6	0.91	0.28	0.04	0.19	1.30
Frontal	S13	11.48	34.59	0.05	2.08	0.18	0.07	3.33
	S14	11.36	34.6	0.15	2.01	0.16	0.08	3.04
	S15	11.45	34.62	0.42	1.79	0.16	0.18	3.40
	S16	11.36	34.63	*d.l.*	2.00	0.17	0.19	3.96
	S17	11.71	34.62	*d.l.*	1.71	0.16	0.28	3.73
	S18	11.83	34.62	0.39	2.04	0.18	0.15	4.64
Subantarctic	S19	11.57	34.46	0.19	2.46	0.21	0.18	3.90
	S20	11.96	34.5	*d.l.*	2.25	0.19	0.23	4.16
	S21	11.73	34.41	0.04	2.38	0.20	0.33	4.22
	S22	12.02	34.39	*d.l.*	2.48	0.22	0.21	3.14
	S23	12.41	34.42	*d.l.*	2.43	0.22	0.22	2.80
	S24	12.58	34.37	*d.l.*	2.54	0.23	0.26	1.93

Table A.2 Summary of permutational analysis of variance (PERMANOVA) statistics, based on weighted UniFrac distance, to test treatment effects on overall bacterial community composition.

			Df	Sums Of Sqs	Mean Sqs	F Model	R^2	p
G-OA1	Day 1							
		Treatment	2	0.015035	0.0075177	0.95307	0.27601	0.3964
		Residuals	5	0.03944	0.0078879	0.72399		
		Total	7	0.054475	1			
	Day 5							
		Treatment	2	0.011508	0.0057542	1.015	0.28877	0.4776
		Residuals	5	0.028345	0.005669	0.71123		
		Total	7	0.039853	1			
G-OA3	Day 1							
		Treatment	2	0.0064386	0.0032193	2.4261	0.4925	0.1558
		Residuals	5	0.0066347	0.0013269	0.5075		
		Total	7	0.0130733	1			
	Day 5							
		Treatment	2	0.014588	0.0072938	3.6938	0.55182	**0.0374**
		Residuals	6	0.011848	0.0019746	0.44818		
		Total	8	0.026435	1			

Leaders of the world, you must lead. The continuation of our civilisations, and the natural world on which we depend, is in your hands.

- David Attenborough